Chapter 3

CKM ELEMENTS FROM TREE-LEVEL B DECAYS AND LIFETIMES

Conveners: E. Barberio, L. Lellouch, K.R. Schubert
Contributors: M. Artuso, M. Battaglia, C. Bauer, D. Becirevic, M. Beneke, I. Bigi, T. Brandt, D. Cassel, M. Calvi, M. Ciuchini, A. Dighe ,K. Ecklund, P. Gagnon, P. Gambino, S. Hashimoto, A. Hoang, T. Hurth, A. Khodjamirian, C.S. Kim, A. Kronfeld, A. Lenz, A. Le Yaouanc, Z. Ligeti, V. Lubicz, D. Lucchesi, T. Mannel, M. Margoni, G. Martinelli, D. Melikhov, V. Morénas, H.G. Moser, L. Oliver, O. Pène, J.-C. Raynal, P. Roudeau, C. Schwanda, B. Serfass, M. Smizanska, J. Stark, B. Stech, A. Stocchi, N. Uraltsev, A. Warburton, L.H. Wilden.

Tree level semileptonic (s.l.) decays of B mesons are crucial for determining the $|V_{ub}|$ and $|V_{cb}|$ elements of the CKM matrix. In this Chapter we review our present understanding of inclusive and exclusive s.l. B decays and give an overview of the experimental situation. The second part of the Chapter is devoted to B mesons lifetimes, whose measurement are important for several reasons. Indeed, these lifetimes are necessary to extract the s.l. widths, while the B^0 lifetime differences and the ratios of lifetimes of individual species provide a test of the OPE.

After a brief introduction to the main concepts involved in theoretical analysis of the inclusive decays, we discuss the determination of the relevant parameters — b quark mass and non-perturbative parameters of the Operator Product Expansion (OPE) — and underlying assumption of quark-hadron duality. We then review the inclusive determination of $|V_{ub}|$ and $|V_{cb}|$. The extraction of these two CKM elements from exclusive s.l. B decays is discussed in the two following sections, after which we review the theoretical framework and the measurements of the lifetimes and lifetime differences.

1. Theoretical tools

1.1. The Operator Product Expansion for inclusive decays

Sometimes, instead of identifying all particles in a decay, it is convenient to be ignorant about some details. For example, we might want to specify the energy of a charged lepton or a photon in the final state, without looking at the specific accompanying hadron. These decays are inclusive in the sense that we sum over final states which can be produced as a result of a given short distance interaction. Typically, we are interested in a quark-level transition, such as $b \to c\ell\bar{\nu}$, $b \to s\gamma$, etc., and we would like to extract the corresponding short distance parameters, $|V_{cb}|$, $C_7(m_b)$, etc., from the data. To do this, we

need to be able to model independently relate the quark-level operators to the experimentally accessible observables.

In the large m_b limit, we have $M_W \gg m_b \gg \Lambda_{\rm QCD}$ and we can hope to use this hierarchy to organize an expansion in $\Lambda_{\rm QCD}/m_b$, analogous to the one in $1/M_W$ introduced in Chapter 1, already based on the OPE. Since the energy released in the decay is large, a simple heuristic argument shows that the inclusive rate may be modelled simply by the decay of a free b quark. The b quark decay mediated by weak interactions takes place on a time scale that is much shorter than the time it takes the quarks in the final state to form physical hadronic states. Once the b quark has decayed on a time scale $t \ll \Lambda_{\rm QCD}^{-1}$, the probability that the final states will hadronize somehow is unity, and we need not know the probability of hadronization into specific final states. Moreover, since the energy release in the decay is much larger than the hadronic scale, the decay is largely insensitive to the details of the initial state hadronic structure. This intuitive picture is formalized by the OPE, which expresses the inclusive rate as an expansion in inverse powers of the heavy quark mass, with the leading term corresponding to the free quark decay [1,2] (for a pedagogical introduction to the OPE and its applications, see [3,4]).

Let us consider, as an example, the inclusive s.l. $b \to c$ decay, mediated by the operator $O_{\rm sl} = -4G_F/\sqrt{2}\, V_{cb}\, (J_{bc})^\alpha\, (J_{\ell\nu})_\alpha$, where $J^\alpha_{bc} = (\overline{c}\,\gamma^\alpha P_L\, b)$ and $J^\beta_{\ell\nu} = (\overline{\ell}\,\gamma^\beta P_L\, \nu)$. The decay rate is given by the square of the matrix element, integrated over phase space and summed over final states,

$$\Gamma(\mathrm{B} \to X_c \ell \bar\nu) \sim \sum_{X_c} \int \mathrm{d[PS]}\, |\langle X_c \ell \bar\nu | O_{\rm sl} | \mathrm{B}\rangle|^2 \,. \tag{1}$$

Since the leptons have no strong interaction, it is convenient to factorize the phase space into $\mathrm{B} \to X_c W^*$ and a perturbatively calculable leptonic part, $W^* \to \ell\bar\nu$. The nontrivial part is the hadronic tensor,

$$\begin{aligned} W^{\alpha\beta} &\sim \sum_{X_c} \delta^4(p_B - q - p_{X_c})\, |\langle \mathrm{B}|\mathrm{J}^{\alpha\dagger}_{\rm bc}|\mathrm{X_c}\rangle\, \langle \mathrm{X_c}|\mathrm{J}^{\beta}_{\rm bc}|\mathrm{B}\rangle|^2 \\ &\sim \mathrm{Im} \int \mathrm{d}x\, e^{-iq\cdot x}\, \langle \mathrm{B}|\, \mathrm{T}\{\mathrm{J}^{\alpha\dagger}_{\rm bc}(\mathrm{x})\, \mathrm{J}^{\beta}_{\rm bc}(0)\}\, |\mathrm{B}\rangle \,, \end{aligned} \tag{2}$$

where the second line is obtained using the optical theorem, and T denotes the time ordered product of the two operators. This is convenient because the time ordered product can be expanded in local operators in the $m_b \gg \Lambda_{\rm QCD}$ limit. In this limit the time ordered product is dominated by short distances, $x \ll \Lambda_{\rm QCD}^{-1}$, and one can express the nonlocal hadronic tensor $W^{\alpha\beta}$ as a sum of local operators. Schematically,

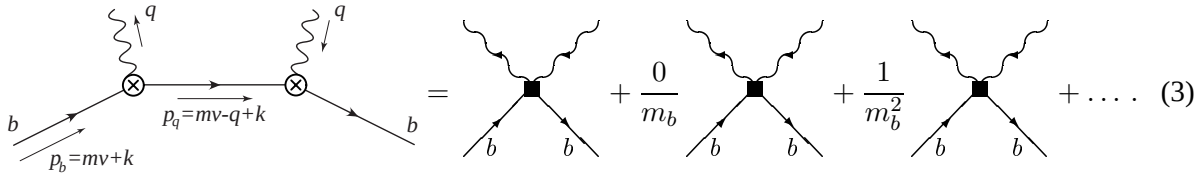

(3)

At leading order the decay rate is determined by the b quark content of the initial state, while subleading effects are parametrized by matrix elements of operators with increasing number of derivatives that are sensitive to the structure of the B meson. There are no $O(\Lambda_{\rm QCD}/m_b)$ corrections, because the B meson matrix element of any dimension-4 operator vanishes. As the coefficients in front of each operator are calculable in perturbation theory, this leads to a simultaneous expansion in powers of the strong coupling constant $\alpha_s(m_b)$ and inverse powers of the heavy b quark mass (more precisely, of $m_b - m_q$). The leading order of this expansion is the parton model s.l. width

$$\Gamma_0 = \frac{G_F^2 |V_{cb}|^2 m_b^5}{192\pi^3} \left(1 - 8\rho + 8\rho^3 - \rho^4 - 12\rho^2 \ln\rho\right) \,, \tag{4}$$

where $\rho = m_q^2/m_b^2$. Non-perturbative corrections are suppressed by at least two powers of m_b [2]. The resulting expression for the total rate of the s.l. $\mathrm{B} \to X_c \ell \bar{\nu}$ has the form

$$\Gamma^{b\to c} = \Gamma_0 \left[1 + A \left[\frac{\alpha_s}{\pi} \right] + B \left[\left(\frac{\alpha_s}{\pi} \right)^2 \beta_0 \right] + 0 \left[\frac{\Lambda}{m_b} \right] + C \left[\frac{\Lambda^2}{m_b^2} \right] + O\left(\alpha_s^2, \frac{\Lambda^3}{m_b^3}, \frac{\alpha_s}{m_b^2} \right) \right] , \qquad (5)$$

where the coefficients A, B, C depend on the quark masses $m_{c,b}$. The perturbative corrections are known up to order $\alpha_s^2\beta_0$. Non-perturbative corrections are parameterized by matrix elements of local operators. The $O(\Lambda^2/m_b^2)$ corrections are given in terms of the two matrix elements

$$\begin{aligned} \lambda_1 &= \frac{1}{2M_B} \left\langle \mathrm{B} | \bar{h}_v (iD)^2 h_v | \mathrm{B} \right\rangle , \\ \lambda_2 &= \frac{1}{6M_B} \left\langle \mathrm{B} \left| \bar{h}_v \frac{g}{2} \sigma_{\mu\nu} G^{\mu\nu} h_v \right| \mathrm{B} \right\rangle . \end{aligned} \qquad (6)$$

The dependence on these matrix elements is contained in the coefficient $C \equiv C(\lambda_1, \lambda_2)$. Up to higher-order corrections, the connection to an alternative notation is $\lambda_1 = -\mu_\pi^2$ and $\lambda_2 = \mu_G^2/3$. At order $1/m_b^3$ there are two additional matrix elements. Thus, the total decay rate depends on a set of non-perturbative parameters, including the quark masses, with the number of such parameters depending on the order in $\Lambda_{\mathrm{QCD}}/m_b$ one is working.

Similar results can be derived for differential distributions, as long as the distributions are sufficiently inclusive. To quantify this last statement, it is crucial to remember that the OPE does not apply to fully differential distributions but requires that such distributions be smeared over enough final state phase space. The size of the smearing region Δ introduces a new scale into the expressions for differential rates and can lead to non-perturbative corrections being suppressed by powers of $\Lambda_{\mathrm{QCD}}^n/\Delta^n$ rather than $\Lambda_{\mathrm{QCD}}^n/m_b^n$. Thus, a necessary requirement for the OPE to converge is $\Delta \gg \Lambda_{\mathrm{QCD}}$, although a quantitative understanding of how experimental cuts affect the size of smearing regions is difficult.

1.2. Heavy Quark Effective Theory

The bound state problem for exclusive decays of hadrons composed of a heavy quark Q and light degrees of freedom simplifies in the limit $m_Q \gg \Lambda_{QCD}$. The size of such heavy-light hadrons is $\sim 1/\Lambda_{QCD}$ and hence, the typical momenta exchanged between the heavy and light degrees of freedom are of order Λ_{QCD}. Such momenta do not permit the light constituents to resolve the quantum numbers of the heavy quark, whose Compton wavelength is $\sim 1/m_Q$. It follows that the light constituents of hadrons which differ only by the flavour or spin of their heavy quark have the same configuration. For N_Q heavy-quark flavours, this invariance results in an $SU(2N_Q)_v$ symmetry which acts on the spin and flavour components of the heavy-quark multiplet and under which the strong interactions are invariant at energies much smaller than m_Q [5,6,7,8,9]. The subscript v on $SU(2N_Q)_v$ labels the velocity of the heavy quark on which the configuration of the light constituents obviously depends.

The spin-flavour symmetry leads to many interesting relations between the properties of hadrons containing a heavy quark. The most immediate consequences concern the spectra of these states [9]. Indeed, since the spin of the heavy quark decouples, states occur in mass-degenerate doublets corresponding to the two possible orientations of the heavy-quark spin.* Examples are the meson doublets $(\mathrm{B}, \mathrm{B}^*)$ and $(\mathrm{D}, \mathrm{D}^*)$ or the baryon doublets (Σ_b, Σ_b^*) and (Σ_c, Σ_c^*). Moreover, the flavour symmetry implies that the energy carried by the light constituents in a heavy-light hadron must be the same whether the heavy quark is a beauty or a charm. Thus, in the symmetry limit, we have relations such as $M_{\Lambda_b} - M_B = M_{\Lambda_c} - M_D$ and $M_{B_s} - M_B = M_{D_s} - M_D$. All of these relations are satisfied experimentally to the expected accuracy, that is up to terms of order Λ_{QCD}/m_b or Λ_{QCD}/m_c, depending on whether the charm quark is present.

*An exception to this rule are the ground state baryons Λ_b and Λ_c: their light constituents carry no angular momentum.

Another set of consequences of heavy quark symmetry concerns current matrix elements and, in particular, $\mathrm{B} \to \mathrm{D}^{(*)}$ transitions [7,8,9]. Consider the matrix element of the b-number current between B meson states of given velocities:

$$\langle \mathrm{B}(v')|\bar{b}\gamma^\mu b|\mathrm{B}(v)\rangle = M_B(v+v')^\mu F_B(t_{BB}) \tag{7}$$

with $t_{BB} = M_B^2(v-v')^2 = 2M_B^2(1-w)$, where $w = v\cdot v'$. $F_B(t_{BB})$ simply measures the overlap of the wave-function of light constituents around a b quark of velocity v with that of light constituents around a b quark of velocity v'. In the heavy-quark limit, flavour symmetry implies that this same form factor describes the matrix element obtained by replacing one or both of the beauty quarks by a charm quark of same velocity. The spin symmetry implies that this form factor parametrizes matrix elements in which the initial and/or final pseudo-scalar meson is replaced by the corresponding vector meson. It further requires the same form factor to parametrize matrix elements in which a vector current such as $\bar{c}\gamma^\mu b$ is replaced by any other $b \to c$ current. This means that in the heavy-quark limit, the s.l. decays $\mathrm{B} \to \mathrm{D}\ell\nu$ and $\mathrm{B} \to \mathrm{D}^*\ell\nu$, which are governed by the hadronic matrix elements, $\langle \mathrm{D}^{(*)}|\bar{c}\gamma^\mu(\gamma^5)b|\mathrm{B}\rangle$, are described by a single form factor, $\xi(w) = F_B(t_{BB}(w)) + O(1/m_b)$, instead of the six form factors allowed by Lorentz invariance. Moreover, this form factor, known as the Isgur-Wise function, is normalized to one at zero-recoil, i.e. $\xi(1) = 1$ for $v = v'$ or $w = 1$, because the b-number current is conserved.

The normalization imposed by heavy quark symmetry is the basis for the measurement of $|V_{cb}|$ from exclusive s.l. B decays described in Sec. 3.. Symmetry is used to the same effect elsewhere in the determination of CKM matrix elements: isospin symmetry normalizes the form factor in β decays, yielding $|V_{ud}|$, and $SU(3)$ flavour symmetry of light quarks approximatively normalizes the form factor in K_{l3} decays, yielding $|V_{us}|$.

In order to explore the consequences of heavy quark symmetry more systematically and compute corrections to the symmetry limit, which are essential for reaching the accuracies required for precise determinations of CKM parameters, it is convenient to construct an effective field theory which displays this symmetry explicitly and gives a simplified description of QCD at low energies [10]. The idea behind effective theories is a separation of scales such that the effective theory correctly reproduces the long-distance physics of the underlying theory. For the case at hand, we are after a theory which duplicates QCD on scales below a cutoff μ such that:

$$\Lambda_{QCD} \ll \mu \ll m_Q \; . \tag{8}$$

The construction of heavy quark effective theory (HQET)[†] begins with the observation that the heavy quark bound inside a heavy-light hadron is nearly on-shell and that its four-velocity is approximately the hadron's velocity, v. Its momentum can thus be written

$$p^\mu = m_Q v^\mu + k^\mu \; , \tag{9}$$

where the components of the residual momentum k^μ are much smaller than m_Q and where $v^2 = 1$. The heavy-quark field is then decomposed into its "particle" and "anti-particle" components, h_v and H_v, as

$$Q(x) = e^{-im_Q v\cdot x}\left[\frac{1+\not{v}}{2}h_v(x) + \frac{1-\not{v}}{2}H_v(x)\right] \; . \tag{10}$$

This decomposition shifts the zero of four-momentum in such a way that the heavy-quark degrees of freedom become massless while the anti-quark degrees of freedom acquire a mass $2m_Q$.[‡] The latter are the heavy degrees of freedom which are integrated out in the construction of the effective theory.

[†]There exist many reviews of heavy quark effective theory. See for instance [11–13].

[‡]A description of heavy anti-quarks is obtained by performing a shift in four-momentum of opposite sign.

Performing this operation in the path integral and expanding the result in powers of terms of order $1/2m_Q$, one finds the following leading order effective Lagrangian:

$$\mathcal{L}_{eff} = \mathcal{L}_0 + O\left(\frac{1}{2m_Q}\right) = \bar{h}_v iv \cdot D h_v + O\left(\frac{1}{2m_Q}\right) . \tag{11}$$

At subleading order it becomes:

$$\mathcal{L}_{eff} = \mathcal{L}_0 + \mathcal{L}_1 + O\left(\frac{1}{4m_Q^2}\right) = \mathcal{L}_0 + \frac{1}{2m_Q}\bar{h}_v (iD_\perp)^2 h_v + \frac{g}{2m_Q}\bar{h}_v \sigma_{\mu\nu} G^{\mu\nu} h_v + O\left(\frac{1}{4m_Q^2}\right) , \tag{12}$$

with $D_\perp^\mu = D - v^\mu v \cdot D$.

The absence of Dirac structure and of masses in $\mathcal{L}_0$ signals the existence of the heavy quark spin-flavour symmetry. This symmetry is broken at order $1/m_Q$. In Eq. (12), the first correction corresponds to the gauge-invariant extension of the kinetic energy arising from the residual motion of the heavy quark and breaks only the flavour component of the symmetry. The second term describes the colour-magnetic coupling of the heavy-quark spin to the gluons and breaks both the spin and the flavour components of the symmetry.

In order to incorporate the weak interactions of heavy quarks, one must also consider the expansion of weak operators in powers of $1/2m_Q$. Introducing a source in the path integral for the quark field, $Q(x)$, one finds that this source couples to

$$\begin{aligned} Q(x) &= e^{-im_Q v\cdot x}\left[1 + \frac{1}{iv\cdot D + 2m_Q} i\not{D}_\perp\right] h_v(x) \\ &= e^{-im_Q v\cdot x}\left[1 + \frac{i\not{D}_\perp}{2m_Q} + O(1/4m_Q^2)\right] h_v(x) , \end{aligned} \tag{13}$$

once the substitution of Eq. (10) and the integral over the "anti-quark" mode H_v are performed. Thus, the expansion of weak currents involving heavy quarks in powers of $1/2m_Q$ is obtained by replacing occurrences of $Q(x)$ by the expansion of Eq. (13).

The construction described up until now correctly reproduces the long-distance physics of QCD, (below μ of Eq. (8)). However, this procedure does not take into account the effects of hard gluons whose virtual momenta can be of the order of the heavy-quark mass, or even larger [6]. Such gluons can resolve the flavour and the spin of the heavy quark and thus induce symmetry breaking corrections. Schematically, the relation between matrix elements of an operator $\mathcal{O}$ in the full and in the effective theory is

$$\langle \mathcal{O}(\mu)\rangle_{QCD} = C_0(\mu,\bar{\mu})\langle \bar{\mathcal{O}}_0(\bar{\mu})\rangle_{HQET} + \frac{C_1(\mu,\bar{\mu})}{2m_Q}\langle \bar{\mathcal{O}}_1(\bar{\mu})\rangle_{HQET} , \tag{14}$$

where $\bar{\mu} \sim \mu$ and where we have assumed, for simplicity, that only one HQET operator appears at leading and at sub-leading order in the $1/2m_Q$ expansion. The short-distance coefficients $C_i(\mu,\bar{\mu})$ are defined by this equation, and should be accurately calculable order by order in perturbation theory because α_s is small in the region between μ and m_Q. One typically obtains $C_i = 1 + O(\alpha_s)$. The way in which these virtual processes break the heavy quark symmetry is by inducing a logarithmic dependence of the C_i on m_Q and by causing mixing with operators which have a different spin structure (not shown here).

Since the effective theory is constructed to reproduce the low-energy behaviour of QCD, the matching procedure must be independent of long-distance effects such as infrared singularities or the nature of the external states used. It is therefore possible and convenient to perform the matching using external on-shell quark states. Furthermore, if the logarithms of m_Q/μ which appear in the short-distance coefficients are uncomfortably large, it is possible to resum them using renormalization group techniques.

It is important to note that the matrix elements in the effective theory, such as $\langle\bar{\mathcal{O}}_0(\bar{\mu})\rangle_{HQET}$ and $\langle\bar{\mathcal{O}}_1(\bar{\mu})\rangle_{HQET}$ in Eq. (14), involve long-distance strong-interaction effects and therefore require non-perturbative treatment. It is also important to note that the separation between short-distance perturbative and long-distance non-perturbative contributions is ambiguous, though these ambiguities must cancel in the calculation of physical observables. These ambiguities require one to be careful in combining results for short-distant coefficients and for the non-perturbative HQET matrix elements. In particular, one has to make sure that these coefficients are combined with matrix elements which are defined at the same order and, of course, in the same renormalization scheme.

2. Inclusive semileptonic *b* decays

2.1. Bottom and charm quark mass determinations

In the framework of B physics the bottom quark mass parameter is particularly important because theoretical predictions of many quantities strongly depend on m_b. Thus, uncertainties on m_b can affect the determination of other parameters. However, due to confinement and the non-perturbative aspect of the strong interaction the concept of quark masses cannot be tied to an intuitive picture of the weight or the rest mass of a particle, such as for leptons, which are to very good approximation insensitive to the strong interactions. Rather, quark masses have to be considered as couplings of the Standard Model Lagrangian that have to be determined from processes that depend on them. As such, the bottom quark mass is a scheme-dependent, renormalized quantity. For recent reviews on the determination of the b quark mass, see [14].

2.1.1. Quark mass definitions in perturbation theory

In principle, any renormalization scheme, or definition for quark masses is possible. In the framework of QCD perturbation theory the difference between two mass schemes can be determined as a series in powers of α_s. Therefore, higher-order terms in the perturbative expansion of a quantity that depends on quark masses are affected by which scheme is employed. There are schemes that are more appropriate and more convenient for some purposes than others. In this section we review the prevalent perturbative quark mass definitions, focusing on the case of the bottom quark.

Pole mass

The bottom quark pole mass m_b is defined as the solution to

$$\not{p} - m_b - \Sigma(p, m_b)\Big|_{p^2=m_b^2} = 0\,, \tag{15}$$

where $\Sigma(p, m_b)$ is the bottom quark self energy. The pole mass definition is gauge-invariant and infrared-safe [15] to all orders in perturbation theory and has been used as the standard mass definition of many perturbative computations in the past. By construction, the pole mass is directly related to the concept of the mass of a free quark, which is, however, problematic because of confinement. In practical applications the pole mass has the disadvantage that the perturbative series relating it to physical quantities are in general quite badly behaved, due to a strong sensitivity of the pole mass definition itself to infrared gluons [16].

There is nothing wrong to use the pole mass as an intermediate quantity, as long as it is used in a consistent way. In particular, the presence of a renormalon ambiguity [16] requires considering the numerical value of the pole mass as an order-dependent quantity. Because this makes estimates of uncertainties difficult, the pole mass definition should be avoided for analyses where quark mass uncertainties smaller than $\Lambda_{\rm QCD}$ are necessary. The problems of the pole mass definition can be avoided if one uses quark mass definitions that are less sensitive to small momenta and do not have an ambiguity

of order $\Lambda_{\rm QCD}$. Such quark mass definitions are generically called "short-distance" masses. They have a parametric ambiguity or order $\Lambda_{\rm QCD}^2/m_b$ or smaller.

$\overline{\rm MS}$ mass

The most common short-distance mass parameter is the $\overline{\rm MS}$ mass $\overline{m}_b(\mu)$, which is defined by regulating QCD with dimensional regularization and subtracting the divergences in the $\overline{\rm MS}$ scheme. Since the subtractions do not contain any infrared sensitive terms, the $\overline{\rm MS}$ mass is only sensitive to scales of order or larger than m_b. The relation between the pole mass and the $\overline{\rm MS}$ mass is known to $\mathcal{O}(\alpha_s^3)$ [17,18] and reads ($\bar\alpha_s \equiv \alpha_s^{(n_l=4)}(\overline{m}_b(\overline{m}_b))$)

$$\frac{m_{b,\rm pole}}{\overline{m}_b(\overline{m}_b)} = 1 + \frac{4\bar\alpha_s}{3\pi} + \left(\frac{\bar\alpha_s}{\pi}\right)^2 \left(13.44 - 1.04\,n_f\right) + \left(\frac{\bar\alpha_s}{\pi}\right)^3 \left(190.8 - 26.7\,n_f + 0.65\,n_f^2\right) + \dots \,. \quad (16)$$

The bottom quark $\overline{\rm MS}$ mass arises naturally in processes where the bottom quark is far off-shell. The scale μ in the $\overline{\rm MS}$ mass is typically chosen of the order of the characteristic energy scale of the process under consideration since perturbation theory contains logarithmic terms $\sim \alpha_s(\mu)^n \ln(Q^2/\mu^2)$ that would be large otherwise. Using the renormalization group equation for $\overline{m}_b(\mu)$ the value of the $\overline{\rm MS}$ mass for different μ can be related to each other. The $\overline{\rm MS}$ mass definition is less useful for processes where the bottom quark is close to its mass-shell, i.e. when the bottom quark has non-relativistic energies.

Threshold masses

The shortcomings of the pole and the $\overline{\rm MS}$ masses in describing non-relativistic bottom quarks can be resolved by so-called threshold masses [19]. The threshold masses are free of an ambiguity of order $\Lambda_{\rm QCD}$ and, at the same time, are defined through subtractions that contain contributions that are universal for the dynamics of non-relativistic quarks. Since the subtractions are not unique, an arbitrary number of threshold masses can be constructed. In the following the threshold mass definitions that appear in the literature are briefly reviewed.

Kinetic mass

The kinetic mass is defined as [20,21]

$$m_{b,\rm kin}(\mu_{\rm kin}) \;=\; m_{b,\rm pole} - \left[\bar\Lambda(\mu_{\rm kin})\right]_{\rm pert} - \left[\frac{\mu_\pi^2(\mu_{\rm kin})}{2m_{b,\rm kin}(\mu_{\rm kin})}\right]_{\rm pert} + \dots \,, \quad (17)$$

where $\left[\bar\Lambda(\mu_{\rm kin})\right]_{\rm pert}$ and $\left[\mu_\pi^2(\mu_{\rm kin})\right]_{\rm pert}$ are perturbative evaluations of HQET matrix elements that describe the difference between the pole and the B meson mass.

The relation between the kinetic mass and the $\overline{\rm MS}$ mass is known to $\mathcal{O}(\alpha_s^2)$ and $\mathcal{O}(\alpha_s^3\beta_0)$ [22,33]. The formulae for $[\bar\Lambda(\mu_{\rm kin})]_{\rm pert}$ and $[\mu_\pi^2(\mu_{\rm kin})]_{\rm pert}$ at $\mathcal{O}(\alpha_s^2)$ read [33]

$$\left[\bar\Lambda(\mu)\right]_{\rm pert} \;=\; \frac{4}{3}C_F\mu_{\rm kin}\frac{\alpha_s(\bar m)}{\pi}\left\{1 + \frac{\alpha_s}{\pi}\left[\left(\frac{4}{3} - \frac{1}{2}\ln\frac{2\mu_{\rm kin}}{\bar m}\right)\beta_0 - C_A\left(\frac{\pi^2}{6} - \frac{13}{12}\right)\right]\right\}, \quad (18)$$

$$\left[\mu_\pi^2(\bar m)\right]_{\rm pert} \;=\; C_F\mu^2\frac{\alpha_s(\bar m)}{\pi}\left\{1 + \frac{\alpha_s}{\pi}\left[\left(\frac{13}{12} - \frac{1}{2}\ln\frac{2\mu_{\rm kin}}{\bar m}\right)\beta_0 - C_A\left(\frac{\pi^2}{6} - \frac{13}{12}\right)\right]\right\}. \quad (19)$$

where $\bar m = \overline{m}_b(\overline{m}_b)$, $C_F = 4/3$, and $\beta_0 = 11 - \frac{2}{3}\,n_f$. For $\mu_{\rm kin} \to 0$ the kinetic mass reduces to the pole mass.

Potential-subtracted mass

The potential-subtracted (PS) mass is similar to the kinetic mass, but arises considering the static energy of a bottom-antibottom quark pair in NRQCD [23].The PS mass is known to $\mathcal{O}(\alpha_s^3)$ and its relation to the pole mass reads

$$m_{b,\rm PS}(\mu_{\rm PS}) \,=\, m_{b,\rm pole} - \frac{C_F\alpha_s(\mu)}{\pi}\,\mu_{\rm PS}\Bigg[1 + \frac{\alpha_s(\mu)}{4\pi}\left(a_1 - \beta_0\left(\ln\frac{\mu_{\rm PS}^2}{\mu^2} - 2\right)\right) \\ + \left(\frac{\alpha_s(\mu)}{4\pi}\right)^2\left(a_2 - (2a_1\beta_0 + \beta_1)\left(\ln\frac{\mu_{\rm PS}^2}{\mu^2} - 2\right) + \beta_0^2\left(\ln^2\frac{\mu_{\rm PS}^2}{\mu^2} - 4\ln\frac{\mu_{\rm PS}^2}{\mu^2} + 8\right)\right)\Bigg], \tag{20}$$

where $\beta_0 = 11 - \frac{2}{3}\,n_f$ and $\beta_1 = 102 - \frac{38}{3}\,n_f$ are the one- and two-loop beta functions, and $a_1 = \frac{31}{3} - \frac{10}{9}\,n_f$, $a_2 = 456.749 - 66.354\,n_f + 1.235\,n_f^2$ (see Refs. [24]). For $\mu_{\rm PS} \to 0$ the PS mass reduces to the pole mass.

1S mass

The kinetic and the potential-subtracted mass depend on an explicit subtraction scale to remove the universal infrared sensitive contributions associated with the non-relativistic heavy quark dynamics. The 1S mass [25,26] achieves the same task without a factorization scale, since it is directly related to a physical quantity. The bottom 1S mass is defined as one half of the perturbative contribution to the mass of the $n = 1$, $^{2s+1}L_j = {}^3S_1$ quarkonium bound state in the limit $m_b \gg m_b v \gg m_b v^2 \gg \Lambda_{\rm QCD}$. To three loop order the 1S mass is defined as

$$\frac{m_{b,\rm 1S}}{m_{b,\rm pole}} \;=\; 1 - \frac{(C_F\alpha_s(\mu))^2}{8}\Bigg\{1 + \Big(\frac{\alpha_s(\mu)}{\pi}\Big)\left[\beta_0\left(L+1\right) + \frac{a_1}{2}\right] \\ + \Big(\frac{\alpha_s(\mu)}{\pi}\Big)^2\left[\beta_0^2\left(\frac{3}{4}L^2 + L + \frac{\zeta_3}{2} + \frac{\pi^2}{24} + \frac{1}{4}\right) + \beta_0\,\frac{a_1}{2}\left(\frac{3}{2}\,L + 1\right)\right. \\ \left. + \frac{\beta_1}{4}\left(L+1\right) + \frac{a_1^2}{16} + \frac{a_2}{8} + \left(C_A - \frac{C_F}{48}\right)C_F\pi^2\right]\Bigg\}, \tag{21}$$

where $L \equiv \ln(\mu/(C_F\alpha_s(\mu)\,m_{b,\rm pole}))$ and $\zeta_3 = 1.20206$. The expression for the 1S mass is derived in the framework of the non-relativistic expansion, where powers of the bottom quark velocity arise as powers of α_s in the 1S mass definition. Thus, to achieve the renormalon cancellation for B decays in the 1S mass scheme it is mandatory to treat terms of order α_s^{n+1} in Eq. (21) as being of order α_s^n. This prescription is called "upsilon expansion" [25] and arises because of the difference between the non-relativistic power counting and the usual counting in numbers of loops of powers of α_s.

Renormalon-subtracted mass

The renormalon-subtracted mass [27] is defined as the perturbative series that results from subtracting all non-analytic pole terms from the Borel transform of the pole-$\overline{\rm MS}$ mass relation at $u = 1/2$ with a fixed choice for the renormalization scale $\mu = \mu_{\rm RS}$. The scale $\mu_{\rm RS}$ is then kept independent from the renormalization scale used for the computation of the quantities of interest. To order α_s the relation between RS mass and pole mass reads,

$$M_{\rm RS}(\mu_{\rm RS}) \;=\; m_{\rm pole} - c\,\alpha_s\,\mu_{\rm RS} \,+\, \ldots\,, \tag{22}$$

where the constant c depends on the number of light quark species and has an uncertainty because the residue at $u = 1/2$ in the Borel transform of the pole-$\overline{\rm MS}$ mass relation is known only approximately.

In Table 3.1 the various b quark mass parameters are compared numerically taking the $\overline{\rm MS}$ mass $\overline{m}_b(\overline{m}_b)$ as a reference value for different values for the strong coupling. Each entry corresponds to the mass using the respective 1-loop/2-loop/3-loop relations.

$\overline{m}_b(\overline{m}_b)$	$m_{b,\rm pole}$	$m_{b,\rm kin}(1\,\text{GeV})$	$m_{b,\rm PS}(2\,\text{GeV})$	$m_{b,\rm 1S}$
$\alpha_s^{(5)}(m_Z) = 0.116$				
4.10	4.48/4.66/4.80	4.36/4.42/4.45 *	4.29/4.37/4.40	4.44/4.56/4.60
4.15	4.53/4.72/4.85	4.41/4.48/4.50 *	4.35/4.42/4.45	4.49/4.61/4.65
4.20	4.59/4.77/4.90	4.46/4.53/4.56 *	4.40/4.48/4.51	4.54/4.66/4.71
4.25	4.64/4.83/4.96	4.52/4.59/4.61 *	4.46/4.53/4.56	4.60/4.72/4.76
4.30	4.69/4.88/5.01	4.57/4.64/4.67 *	4.51/4.59/4.62	4.65/4.77/4.81
$\alpha_s^{(5)}(m_Z) = 0.118$				
4.10	4.49/4.69/4.84	4.37/4.44/4.46 *	4.30/4.38/4.41	4.45/4.57/4.62
4.15	4.55/4.74/4.89	4.42/4.49/4.52 *	4.36/4.43/4.47	4.50/4.63/4.67
4.20	4.60/4.80/4.94	4.47/4.55/4.57 *	4.41/4.49/4.52	4.55/4.68/4.73
4.25	4.65/4.85/5.00	4.52/4.60/4.63 *	4.46/4.54/4.58	4.61/4.73/4.78
4.30	4.71/4.91/5.05	4.58/4.66/4.69 *	4.52/4.60/4.63	4.66/4.79/4.84
$\alpha_s^{(5)}(m_Z) = 0.120$				
4.10	4.51/4.72/4.88	4.37/4.45/4.48 *	4.31/4.39/4.43	4.46/4.59/4.64
4.15	4.56/4.77/4.93	4.43/4.51/4.54 *	4.36/4.45/4.48	4.51/4.64/4.70
4.20	4.61/4.83/4.99	4.48/4.56/4.59 *	4.42/4.50/4.54	4.56/4.70/4.75
4.25	4.67/4.88/5.04	4.54/4.62/4.65 *	4.47/4.56/4.59	4.62/4.75/4.80
4.30	4.72/4.94/5.10	4.59/4.67/4.71 *	4.53/4.61/4.65	4.67/4.81/4.86

Table 3.1: *Numerical values of b quark masses in units of GeV for a given* $\overline{\rm MS}$ *mass for* $\overline{m}_b(\overline{m}_b)$ *for* $\mu = m_b(m_b)$, $n_l = 4$ *and three values of* $\alpha_s^{(5)}(m_Z)$. *Flavor matching was carried out at* $\mu = \overline{m}_b(\overline{m}_b)$. *Numbers with a star are given in the large-*β_0 *approximation.*

2.1.2. Bottom quark mass from spectral sum rules

The spectral sum rules for $\sigma(e^+e^- \to b\bar{b})$ start from the correlator of two electromagnetic bottom quark currents

$$(g_{\mu\nu}\, q^2 - q_\mu\, q_\nu)\, \Pi(q^2) \;\; = \;\; -\, i \int dx\, e^{i\, qx}\, \langle\, 0\,|\, T\, j^b_\mu(x)\, j^b_\nu(0)\,|\, 0\,\rangle\,, \tag{23}$$

where $j^b_\mu(x) \equiv \bar{b}(x)\gamma_\mu b(x)$. Using analyticity and the optical theorem one can relate theoretically calculable derivatives of Π at $q^2 = 0$ to moments of the total cross section $\sigma(e^+e^- \to b\bar{b})$,

$$\mathcal{M}_n \;=\; \frac{12\,\pi^2\, Q_b^2}{n!} \left(\frac{d}{dq^2}\right)^n \Pi(q^2)\Big|_{q^2=0} \;=\; \int \frac{ds}{s^{n+1}}\, R(s)\,, \tag{24}$$

where $R = \sigma(e^+e^- \to b\bar{b})/\sigma(e^+e^- \to \mu^+\mu^-)$. From Eq. (24) it is possible to determine the bottom quark mass [28]. From the theoretical point of view n cannot be too large because the effective energy range contributing to the moment becomes of order or smaller than $\Lambda_{\rm QCD}$ and non-perturbative effects become uncontrollable. Since the effective range of $\sqrt{s}$ contributing to the spectral integral is of order m_b/n one finds the range

$$n \lesssim 10\,, \tag{25}$$

author		$\overline{m}_b(\overline{m}_b)$	other mass	comments, Ref.
spectral sum rules				
Voloshin	95		$m_{\rm pole} = 4.83 \pm 0.01$	$8 < n < 20$, NLO; no theo.uncert. [29]
Kühn	98		$m_{\rm pole} = 4.78 \pm 0.04$	$10 < n < 20$, NLO [30]
Penin	98		$m_{\rm pole} = 4.78 \pm 0.04$	$10 < n < 20$, NNLO [31]
Hoang	98		$m_{\rm pole} = 4.88 \pm 0.13$	$4 < n < 10$, NLO [32]
Hoang	98		$m_{\rm pole} = 4.88 \pm 0.09$	$4 < n < 10$, NNLO [32]
Melnikov	98	4.20 ± 0.10	$M_{\rm kin}^{\rm 1GeV} = 4.56 \pm 0.06$	$x < n < x$, NNLO [33]
Penin	98		$m_{\rm pole} = 4.80 \pm 0.06$	$8 < n < 12$, NNLO [31]
Jamin	98	4.19 ± 0.06		$7 < n < 15$ [34]
Hoang	99	4.20 ± 0.06	$M_{\rm 1S} = 4.71 \pm 0.03$	$4 < n < 10$, NNLO [35]
Beneke	99	4.26 ± 0.09	$M_{\rm PS}^{\rm 2GeV} = 4.60 \pm 0.11$	$6 < n < 10$, NNLO [36]
Hoang	00	4.17 ± 0.05	$M_{\rm 1S} = 4.69 \pm 0.03$	$4 < n < 10$, NNLO, $m_c \neq 0$ [37]
Kühn	01	4.21 ± 0.05		$1 < n < 4$, $\mathcal{O}(\alpha_s^2)$ [38]
Erler	02	4.21 ± 0.03		$\mathcal{O}(\alpha_s^2)$ [39]
Eidemüller	02	4.24 ± 0.10	$M_{\rm PS}^{\rm 2GeV} = 4.56 \pm 0.11$	$3 < n < 12$ [40]
Bordes	02	4.19 ± 0.05		$\mathcal{O}(\alpha_s^2)$ [41]
Corcella	02	4.20 ± 0.09		$1 < n < 3$, $\mathcal{O}(\alpha_s^2)$ [42]
$\Upsilon(1{\rm S})$ mass				
Pineda	97		$m_{\rm pole} = 5.00^{+0.10}_{-0.07}$	NNLO [43]
Beneke	99	4.24 ± 0.09	$M_{\rm PS}^{\rm 2GeV} = 4.58 \pm 0.08$	NNLO [36]
Hoang	99	4.21 ± 0.07	$M_{\rm 1S} = 4.73 \pm 0.05$	NNLO [44]
Pineda	01	4.21 ± 0.09	$M_{\rm RS}^{\rm 2GeV} = 4.39 \pm 0.11$	NNLO [27]
Brambilla	01	4.19 ± 0.03		NNLO, pert. th. only [45]

Table 3.2: *Collection in historical order in units of GeV of recent bottom quark mass determinations from spectral sum rules and the $\Upsilon(1S)$ mass. Only results where α_s was taken as an input are shown. The uncertainties quoted in the respective references have been added quadratically. All numbers have been taken from the respective publications.*

where a reliable extraction of the bottom quark mass is feasible. In this range one can distinguish two regions. In the large-n region, $4 \lesssim n \lesssim 10$, the $b\bar{b}$-dynamics is predominantly non-relativistic and threshold masses are the suitable mass parameters that can be determined. In the small-n region, $1 \leq n \lesssim 4$, the $b\bar{b}$ dynamics is predominantly relativistic and the $\overline{\rm MS}$ mass is the appropriate mass parameter. In the following the advantages and disadvantages of the two types of sum rules are reviewed. Results for bottom quark masses obtained in recent sum rule analyses have been collected in Table 3.2.

Non-relativistic sum rules

The large-n sum rules have the advantage that the experimentally unknown parts of the $\bar{b}b$ continuum cross section above the Υ resonance region are suppressed. A crude model for the continuum cross section is sufficient and causes an uncertainty in the b quark mass below the 10 MeV level. Depending on which moment is used the overall experimental uncertainties in the b quark mass are between 15 and 20 MeV. Over the past years there has been a revived interest in non-relativistic sum rules because new

theoretical developments allowed for the systematic determination of $\mathcal{O}(v^2)$ (NNLO) corrections to the spectral moments [31–33,35–37]. All analyses found that the NNLO corrections were as large or even larger than the NLO corrections and various different methods were devised to extract numerical values for the bottom quark mass. In Refs. [33,35–37] threshold masses were implemented accounting for the renormalon problem. This removed one source of the bad perturbative behaviour, but it was found that a considerable theoretical uncertainty remained, coming from the theoretical description of the production and annihilation probability of the $b\bar{b}$ pair. In Refs. [33] and [36] the kinetic and the PS mass were determined from fits of individual moments. It was found that the NLO and NNLO results for the bottom mass differ by about 200 MeV. In Ref. [33] it was argued that the results form an alternating series and a value of $m_{b,\mathrm{kin}}(1\,\mathrm{GeV}) = 4.56 \pm 0.06(\mathrm{ex,th})$ GeV was determined. In Ref. [36] only the NNLO results were accounted based on consistency arguments with computations of the $\Upsilon(1\mathrm{S})$ mass and the result $m_{b,\mathrm{PS}}(2\,\mathrm{GeV}) = 4.60 \pm 0.02(\mathrm{ex}) \pm 0.10(\mathrm{th})$ GeV was obtained. In Ref. [35] the 1S mass was employed and a χ^2-fit based on four different moments was carried out. It was found that the large normalization uncertainties drop out at NLO and NNLO and that the results for the mass at NLO and NNLO showed good convergence. The result was $m_{b,\mathrm{1S}} = 4.71 \pm 0.02(\mathrm{ex}) \pm 0.02(\mathrm{th})$ GeV. A subsequent analysis [37] which included the effects of the nonzero charm mass yielded $m_{b,\mathrm{1S}} = 4.69 \pm 0.02(\mathrm{ex}) \pm 0.02(\mathrm{th})$ GeV.

Relativistic sum rules

The small-n sum rules have the disadvantage that the unknown parts of the $b\bar{b}$ continuum cross section above the Υ resonance region constitute a substantial contribution to the spectral moments. The advantage is that the computation of the theoretical moments is less involved since usual perturbation theory in powers of α_s can be employed. In Ref. [38] the theoretical moments were determined at order $\mathcal{O}(\alpha_s^2)$ and it was found that the perturbative behaviour of the theoretical moments is quite good. For the bottom quark mass determination it was assumed that the unknown experimental continuum cross section agrees with the perturbation theory prediction and subsequently the result $\overline{m}_b(\overline{m}_b) = 4.21 \pm 0.05$ GeV was determined. A more conservative analysis in Ref. [42] obtained the result $\overline{m}_b(\overline{m}_b) = 4.20 \pm 0.09$ GeV.

2.1.3. Bottom quark mass from the mass of the $\Upsilon(1\mathrm{S})$

Among the earliest values of the b quark mass were determinations that were based on analysis of the observed spectrum of the Υ mesons. However, since these determinations used potential models to describe the $b\bar{b}$ dynamics they have little value for present analyses in B physics. The same conceptual advances that led to the progress in the determination of the $\mathcal{O}(v^2)$ corrections to the spectral moments also allowed to systematically determine $\mathcal{O}(v^2)$ corrections to the spectrum of quark-antiquark bound states, which provides another method to determine a bottom quark threshold mass. The disadvantage of this method is that the theoretical tools only apply to the case in which the binding energy $\sim m_b\, v^2$ is larger than Λ_{QCD}, which is unlikely for higher radial excitations and questionable for the ground state. As such, also the theoretical methods to determine the effects of non-perturbative corrections, which are based on Shifman et al. [46], could be unreliable. In recent analyses (see Tab. 3.2) only the $\Upsilon(1\mathrm{S})$ mass has been used for a bottom mass extraction. The uncertainty is completely dominated by the estimate of the non-perturbative effects.

2.1.4. Summary of m_b *determinations from sum rules*

Comparing the results from the recent bottom quark mass determinations (see Tab. 3.2) one finds a remarkable consistency among the various analyses. However, the impression could be misleading because all methods have problematic issues. Therefore, it is prudent to adopt a more conservative view in averaging and interpreting the results. For the workshop is was agreed that the $\overline{m}_b(\overline{m}_b)$ shall be used as reference mass and that the respective threshold masses shall be determined from it. This leads to an enhancement of the theoretical error in the threshold masses, due to their dependence on α_s. An averaging

prescription for the results in Tab. 3.2 has not been given, and it was agreed on the value

$$\boxed{\overline{m}_b(\overline{m}_b) \;=\; 4.21 \pm 0.08 \text{ GeV}.} \tag{26}$$

Future work should aim to reduce the uncertainty to a level of 50 MeV.

2.1.5. Charm quark mass from sum rules

The charm mass plays a less important role than m_b in applications related to the CKM determination, although it certainly is a fundamental parameter. Perhaps because of that, the determination of m_c from $e^+e^- \to$ hadrons has so far received less attention than that of m_b and has not reached the same level of maturity; we will not discuss the subject here. The most recent analyses can be found in [40,47,38]. Typical results for the $\overline{\rm MS}$ mass $\overline{m}_c(\overline{m}_c)$ range between 1.19 and 1.37 GeV, with uncertainties varying between 30 and 110 MeV.

2.1.6. Charm and bottom quark masses from Lattice QCD

The determination of both heavy and light quark masses is one of the most important field of activity of lattice QCD simulations. Two major theoretical advances have allowed to increase the accuracy of these determinations. The first one has been the development of non-perturbative renormalization techniques. The renormalized quark mass $m_q(\mu)$, in a given renormalization scheme, is related to the bare quark mass $m_q(a)$, which is a function of the lattice spacing a, through a multiplicative renormalization constant,

$$m_q(\mu) = Z_m(\mu\, a)\, m_q(a)\,. \tag{27}$$

The bare quark mass $m_q(a)$ (with $q = u,\, d,\, s,\, c, \ldots$) is a free parameter of the QCD Lagrangian. It can be computed on the lattice by requiring the mass of some physical hadron (π, K, D, B, ...), determined from the numerical simulation, to be equal to the corresponding experimental value. Therefore, one experimental input is needed to fix the value of the quark mass for each flavour of quark.

The quark mass renormalization constant, $Z_m(\mu\, a)$, can be computed in principle in perturbation theory. Its perturbative expansion, however, is known only at one loop and the corresponding theoretical uncertainty is therefore rather large. The non-perturbative renormalization techniques allow to compute Z_m in a non-perturbative way directly from a numerical simulation, with an accuracy which is at the level of few per cent. The two most important non-perturbative renormalization methods developed so far are based on the so called RI/MOM [48] and Schrödinger functional [49] schemes.

The other important theoretical progress, in lattice QCD calculations, has been the introduction of improved actions and operators, which allow to reduce discretization errors (finite cut-off effects) from $\mathcal{O}(a)$ to $\mathcal{O}(a^2)$. This improvement has been particularly relevant for the lattice determination of the charm quark mass. Typical values of the lattice cut-off, in current numerical simulations, are in the range $a^{-1} \sim 3 - 4$ GeV. With these values, leading discretization effects proportional to $m_c\, a$ can be of the order of 30% or larger, and they would represent the major source of systematic uncertainty in lattice determinations of the charm quark mass. The use of improved actions, combined with the extrapolation to the continuum limit $(a \to 0)$ of the results obtained at fixed lattice spacing, allows to reduce discretization errors well below the 10% level.

Two lattice determinations of the charm quark mass, which use both non-perturbative renormalization and a non-perturbatively improved action, have been performed so far. The results, in the $\overline{\rm MS}$ scheme, read [50,51]

$$\begin{aligned} \overline{m}_c(\overline{m}_c) &= 1.26 \pm 0.04 \pm 0.12\text{GeV} \\ \overline{m}_c(\overline{m}_c) &= 1.301 \pm 0.034\text{GeV}\,. \end{aligned} \tag{28}$$

The first of these results has been obtained at a fixed value of the lattice spacing, corresponding to $a^{-1} \simeq 2.7$ GeV. The second one also involves an extrapolation to the continuum limit, and therefore the prediction is more accurate in this case. At fixed value of the lattice spacing the two calculations are in very good agreement. The only uncertainty which is not quoted in Eq. (28) is due to the use of the quenched approximation. For the b-quark mass the quenching effect has been found to be very small, of the order of 1–2% [52,53], while determinations of this effect for light quarks are more uncertain, lying in the range between 10 and 25%. In order to account for the quenching error in the case of the charm quark mass, a (probably conservative) estimate consists in adding a systematic uncertainty of the order of 10% to the result of Eq. (28). This gives, as best lattice estimate for the charm quark mass, the value

$$\overline{m}_c(\overline{m}_c) = 1.30 \pm 0.03 \pm 0.15\text{GeV} \,. \tag{29}$$

Lattice determinations of the b-quark mass have reached, at present, a very high level of both statistical and systematic accuracy. Since the mass of the b quark is larger than the UV cut-off (the inverse of the lattice spacing) used in current lattice calculations, the b quark cannot be simulated directly on the lattice. Therefore, one is led to use an effective theory, like HQET or NRQCD, in which the heavy degrees of freedom associated with the b quark are integrated out. Within the effective theory, the pole mass of the b quark is related to the B meson mass M_B through the relation

$$M_B = m_b^{\rm pole} + \varepsilon - \delta m \,, \tag{30}$$

which is valid up to $\mathcal{O}(1/m_b^2)$ corrections. In Eq. (30), ε is the so called binding energy and δm is a mass counterterm induced by radiative corrections. Neither ε nor δm are real physical quantities, and indeed they are separately power divergent. The binding energy ε is the quantity which is directly measured in the numerical simulations of the effective theory on the lattice. At the same time, an accurate determination of δm is necessary in order to achieve a precise estimate of the b-quark mass.

The most accurate determination of the b-quark mass on the lattice has been obtained with the HQET [53]. It relies on the NNLO perturbative calculation of the residual mass performed in Ref. [54]. The final unquenched ($N_f = 2$) result for the b-quark mass in the $\overline{\rm MS}$ scheme reads

$$\overline{m}_b(\overline{m}_b) = 4.26 \pm 0.06 \pm 0.07\text{GeV} \,, \tag{31}$$

in which the combined statistical and systematic uncertainty is at the level of 2%. Other lattice determinations of the b-quark mass have been also obtained by using NRQCD [55]. Since the systematic is rather different in the latter case, it is quite reassuring to find that the lattice-NRQCD results are in very good agreement with the prediction of Eq. (31).

The lattice determinations of the b-quark mass can be further improved. In the quenched case, the residual mass δm has been computed at $\mathcal{O}(\alpha_s^3)$ by implementing the so called numerical stochastic perturbation theory [56]. The same NNNLO accuracy could be achieved also for the unquenched theory. More recently, a completely non-perturbative approach to the calculation of δm has been proposed. The corresponding (preliminary) quenched result for the b-quark mass is $\overline{m}_b(\overline{m}_b) = 4.53(5)(7)$GeV [57], which is larger than the lattice determination of Eq. (31) and than the non-lattice estimates reviewed in the previous subsection. Since the approach of Ref. [57] is new, it deserves further investigations. On the other hand, being completely non-perturbative, it is quite promising for future and even more accurate lattice determinations of the b-quark mass.

2.2. Extraction of heavy-quark parameters from semileptonic moments

Important information on the parameters of the OPE can be extracted from the moments of the differential distributions in s.l. and radiative B decays, which encode the shape of these spectra. Recently, the first few moments of the hadronic, leptonic, and photonic spectra in s.l. and radiative B decays have been

measured by several experiments [58,59,60]. We define the moments of the leptonic energy distribution as

$$M_1^\ell = \frac{1}{\Gamma}\int dE_\ell\, E_\ell \frac{d\Gamma}{dE_\ell}; \qquad M_n^\ell = \frac{1}{\Gamma}\int dE_\ell \left(E_\ell - M_1^\ell\right)^n \frac{d\Gamma}{dE_\ell} \quad (n>1), \tag{32}$$

and the moments of the distribution of M_X, the invariant hadronic mass, as

$$M_1^X = \frac{1}{\Gamma}\int dM_X^2\, (M_X^2 - \bar{M}_D^2)\frac{d\Gamma}{dM_X^2}; \qquad M_n^X = \frac{1}{\Gamma}\int dM_X^2\, (M_X^2 - \langle M_X^2\rangle)^n \frac{d\Gamma}{dM_X^2} \ (n>1), \tag{33}$$

where $\bar{M}_D = 1.973$ GeV is the spin averaged D meson mass and Γ is the total s.l. width. In general, n can also be fractional. Some experiments apply a lower cut on the lepton energy. In that case two truncated leptonic moments, originally suggested by Gremm *et al.* [61] and defined as

$$R_0 = \frac{\int_{1.7}(d\Gamma_{sl}/dE_l)dE_l}{\int_{1.5}(d\Gamma_{sl}/dE_l)dE_l} \quad \text{and} \quad R_1 = \frac{\int_{1.5} E_l(d\Gamma_{sl}/dE_l)dE_l}{\int_{1.5}(d\Gamma_{sl}/dE_l)dE_l}, \tag{34}$$

are often used in the experimental analysis. The theoretical framework to interpret these data has long been known and is based on the OPE. Different formulations exist, depending on the way the quark masses are treated. For instance, the m_b and m_c masses can be taken as independent parameters or subject to a constraint on $m_b - m_c$, imposed from the measured $\mathrm{B}^{(*)}$ and $D^{(*)}$ meson masses. The second choice introduces a $1/m_c$ expansion. Another option concerns the normalization scheme used for quark masses and non-perturbative parameters. As explained in the previous section, one can use short-distance masses, such as the low-scale running masses, or pole masses.

The moments M_n^ℓ, R_i, and M_n^X are highly sensitive to the quark masses and to the non-perturbative parameters of the OPE. For instance, the hadronic moments M_n^X vanish at the parton level and are generated only by real gluon emission at $O(\alpha_s)$ and by non-perturbative effects suppressed by powers of the b quark mass. The OPE expresses lepton moments through quark masses as a double expansion in α_s and $1/m_b$:

$$M_n^\ell = \left(\frac{m_b}{2}\right)^n \left[\varphi_n(r) + \bar{a}_n(r)\frac{\alpha_s}{\pi} + \bar{b}_n(r)\,\frac{\mu_\pi^2}{m_b^2} + \bar{c}_n(r)\,\frac{\mu_G^2}{m_b^2} + \bar{d}_n(r)\,\frac{\rho_D^3}{m_b^3} + \bar{s}_n(r)\,\frac{\rho_{LS}^3}{m_b^3} + ...\right], \tag{35}$$

where $r = (m_c/m_b)^2$. Analogous expressions hold for the truncated moments R_i. The higher coefficient functions $\bar{b}(r)$, $\bar{c}(r)$, ... are also perturbative series in α_s. The functions φ_n in Eq. (35) are well-known parton expressions, given e.g. in [62]. The expectation values of only two operators contribute to $O(1/m_b^3)$: the Darwin term ρ_D^3 and the spin-orbital term ρ_{LS}^3. Due to the kinematic definition of the hadronic invariant mass M_X^2, the general expression for the hadronic moments includes M_B explicitly, but it is otherwise similar to Eq. (35):

$$\begin{aligned} M_n^X \;=\; m_b^{2n}\sum_{l=0}\left[\frac{M_B - m_b}{m_b}\right]^l \Bigg(& E_{nl}(r) + a_{nl}(r)\frac{\alpha_s}{\pi} + b_{nl}(r)\frac{\mu_\pi^2}{m_b^2} + c_{nl}(r)\frac{\mu_G^2}{m_b^2} \\ & + d_{nl}(r)\frac{\rho_D^3}{m_b^3} + s_{nl}(r)\frac{\rho_{LS}^3}{m_b^3} + ...\Bigg). \end{aligned} \tag{36}$$

It is possible to re-express the heavy quark masses, m_Q, in the above equations, in terms of the meson masses, M_{H_Q}, through the relation [21]:

$$M_{H_Q} = m_Q + \bar{\Lambda} + \frac{\mu_\pi^2 - a_{H_Q}\mu_G^2}{2m_Q} + \frac{\rho_D^3 + a_{H_Q}\rho_{LS}^3 - \rho_{nl}^3}{4m_Q^2} + \mathcal{O}\left(\frac{1}{m_Q^3}\right), \tag{37}$$

where $a_{H_Q} = 1$ and $-1/3$ for pseudo-scalar and vector mesons, respectively. The use of these expressions introduces an explicit dependence on the non-local correlators contributing to ρ_{nl}^3. In the notation of [63], ρ_{nl}^3 corresponds to linear combinations of $\mathcal{T}_{1-4}$.

	φ_n	$\bar{a}_n$	$\bar{b}_n$	$\bar{c}_n$	$\bar{d}_n$	$\bar{s}_n$
M_1^ℓ	0.6173	0.015	0.31	-0.73	-3.7	0.2
$M_2^\ell\ (\times 10)$	0.3476	0.026	1.7	-1.0	-10.2	-0.9
$M_3^\ell\ (\times 10^2)$	-0.3410	0.066	3.4	1.3	-23	-4.2

Table 3.3: *Numerical values of the coefficients in Eq.(35) evaluated at r=0.06 and $m_{b,\rm kin}(1\,{\rm GeV}) = 4.6\,{\rm GeV}$ and without a lepton energy cut.*

i	E_{i1}	E_{i2}	E_{i3}	a_{i0}	a_{i1}	b_{i0}	b_{i1}	c_{i0}	c_{i1}	d_{i0}	s_{i0}
1	0.839	1	0	0.029	0.013	-0.58	-0.58	0.31	0.87	3.2	-0.4
2	0	0.021	0	- 0.001	-0.002	0.16	0.34	0	-0.05	-0.8	0.05
3	0	0	-0.0011	0.0018	0.0013	0	0.034	0	0	0.15	0

Table 3.4: *Numerical values of the coefficients in Eq.(36) evaluated at r=0.06 and $m_{b,\rm kin}(1\ {\rm GeV})$ = 4.6 GeV and without a lepton energy cut.*

The moments of the photon spectrum in inclusive radiative B decays, $\mathrm{B} \to X_s\gamma$, are also useful to constrain the non-perturbative parameters. The relevant formulae can be found in [65] and Refs. therein.

Of all the possible formalisms we discuss here only two extreme cases.[§] The first formalism is based on the kinetic running masses, $m_Q(\mu)$, and non-perturbative parameters, introduced in [20,66]. No charm mass expansion is assumed. The second formalism employs quark pole masses and the $\mathrm{B}^{(*)}$ and $D^{(*)}$ meson mass relations. Contributions through $O(\alpha_s^2\beta_0)$ [67,68] and $O(1/m_b^3)$ [1,2,62,63,69,61,70] to the moments are available. Depending on the formulation adopted, the number of parameters involved at this order ranges from six to nine. Some of these parameters, like m_b and $\lambda_2 \simeq \mu_G^2/3$, are relatively well known. Others, notably those which appear at $O(1/m_b^3)$, are virtually unknown.

2.2.1. The $m_{b,\rm kin}(\mu)$, $m_{c,\rm kin}(\mu)$ and $\mu_\pi^2(\mu)$ formalism

The quark masses are here identified by the running kinetic quark masses $m_{b,\rm kin}(\mu)$ and $m_{c,\rm kin}(\mu)$, and since no relation like Eq. (37) is used, they are two independent parameters. Apart from $\mu_\pi^2(\mu)$ and $\mu_G^2(\mu)$, defined here as expectation values in the actual B meson, there are two $1/m_b^3$ parameters, ρ_D^3 and ρ_{LS}^3. The effect of ρ_{LS}^3 turns out to be numerically small. In Eqs. (35) and (36) the mass ratio r is given by $(m_{c,\rm kin}(\mu)/m_{b,\rm kin}(\mu))^2$, and the b quark mass is understood as $m_{b,\rm kin}(\mu)$. The perturbative coefficients additionally depend on μ/m_b and the mass normalization scale μ is set at $\mu = 1$ GeV. To illustrate the size of different contributions to M_n^ℓ, we give the relevant coefficients for the first three moments in the case without a cut on the lepton energy in Table 3.3, using $m_{b,\rm kin}$(1 GeV) = 4.6 GeV and $r = 0.06$ [71] (the $O(\alpha_s^2\beta_0)$ corrections are also available [68]). In the case of hadronic moments, keeping terms up to $1/m_b^3$, we discard in Eq. (36) coefficients b_{nl}, c_{nl} with $l>1$, and d_{nl}, s_{nl} with $l>0$. The only non-vanishing E_{i0} coefficient is $E_{10} = r - \bar{M}_D^2/m_b^2$. The value of the other coefficients, at $r = 0.06$ and again without a cut on the hadron energy, are listed in Table 3.4. The $O(\alpha_s^2\beta_0)$ corrections to hadronic moments are not yet available in this scheme.

[§] A few different possibilities are considered in [65].

2.2.2. The $\bar{\Lambda}$ and λ_1 formalism

This widely used scheme results from the combination of the OPE with the HQET. Following the notation of Ref. [70], the moments are expressed in the following general form:

$$M_n = M_B^k \left[a_0 + a_1 \frac{\alpha_s(\overline{M}_B)}{\pi} + a_2 \beta_0 \frac{\alpha_s^2}{\pi^2} + b_1 \frac{\bar{\Lambda}}{\overline{M}_B} + b_2 \frac{\alpha_s}{\pi} \frac{\bar{\Lambda}}{\overline{M}_B} + \frac{c_1\,\lambda_1 + c_2\,\lambda_2 + c_3\,\bar{\Lambda}^2}{{\overline{M}_B}^2} \right.$$
$$\left. + \frac{1}{\overline{M}_B^3} \left(d_1\,\lambda_1 \bar{\Lambda} + d_2\,\lambda_2 \bar{\Lambda} + d_3\,\bar{\Lambda}^3 + d_4\,\rho_1 + d_5\,\rho_2 + \sum_{i=1,4} d_{5+i} \mathcal{T}_i \right) + O\left(\frac{\Lambda_{QCD}^4}{m_Q^4} \right) \right], \quad (38)$$

where $k = n$ and $k = 2n$ for leptonic and hadronic moments, respectively, while $a_0 = 0$ for hadronic moments. Analogous expressions hold for the truncated moments. $\overline{M}_B = 5.3135$ GeV is the spin-averaged B meson mass, and $\beta_0 = 11 - 2/3 n_f$, with $n_f = 3$. The terms $O(\alpha_s^2\beta_0)$ and $O(\alpha_s\bar{\Lambda})$ are not known in the case of the third hadronic moment. The coefficients a_i, b_i, c_i, d_i for the first three leptonic, $M_{1,2,3}^{\ell}$, and hadronic moments, $M_{1,2,3}^{X}$, without a cut on the lepton energy are given in [71]. The coefficients for $i = 1, 2$ with a cut on the lepton energy and for $R_{0,1}$ can be found in [65]. The non-perturbative parameters in Eq.(38) are related to those in Sec. 2.2.1. by the following relations, valid up to $\mathcal{O}(\alpha_s)$:

$$\mu_\pi^2 = -\lambda_1 - \frac{\mathcal{T}_1 + 3\mathcal{T}_2}{m_b}; \quad \mu_G^2 = 3\lambda_2 + \frac{\mathcal{T}_3 + 3\mathcal{T}_4}{m_b}; \quad \rho_D^3 = \rho_1\,; \quad \rho_{LS}^3 = 3\rho_2\,. \quad (39)$$

Perturbative corrections introduce a significant numerical difference between the parameters in the two schemes. At $\mu = 1$ GeV:

$$\bar{\Lambda} \simeq M_B - m_{b,\mathrm{kin}}(1\ \mathrm{GeV}) - \frac{\mu_\pi^2 - \mu_G^2}{2m_b} - 0.26\ \mathrm{GeV}\,; \qquad -\lambda_1 \simeq \mu_\pi^2(1\ \mathrm{GeV}) - 0.17\ \mathrm{GeV}^2\,. \quad (40)$$

As anticipated in the previous Section, the use of the ill-defined pole quark mass induces in this formalism large perturbative corrections, which are however expected to cancel in the relation between physical observables, as long as all observables involved in the analysis are computed at the same order in α_s. We also note that, as a consequence of the HQET mass relations for the mesons, the intrinsic expansion parameter in Eq.(38) is $1/M_D$, rather than $1/M_B$. The convergence of this expansion has been questioned, in view of indications [72,73] that the matrix elements $\mathcal{T}_i$ of some non-local operators could be larger than that expected from dimensional estimates.

Higher moments are generally more sensitive to the $1/m_b^3$ corrections, but the uncertainty due to unknown perturbative and non-perturbative higher orders prevents a precision determination of the related parameters. Higher moments contain nonetheless useful information: as we will see below, they have been employed in the first analyses based on multi-parameter fits [65,71].

Measurements of the moments and non-perturbative parameters

The study of moments in B meson s.l. decays and $\mathrm{B} \to X_s\gamma$ allows to perform several independent determinations of the non-perturbative parameters and is now pursued by different experiments. Here we summarize the measurements performed by the CLEO collaboration, taking data at the CESR e^+e^- collider, and by the DELPHI Collaboration at LEP. Measurements of the first hadronic moment in $\mathrm{B} \to X_c\ell\bar{\nu}$ with different minimum charged lepton momentum have also been reported by the BaBar Collaboration [78].

CLEO and BaBar measurements have been performed at the $\Upsilon(4S)$ resonance. While there is an obvious advantage in measuring the spectra in events where the decaying B rest frame almost coincides with the laboratory frame, low energy particles cannot be identified there. It is thus necessary to rely on models for extrapolating the lepton energy spectrum to zero energy or to resort to computations for a truncated spectrum. On the other hand, performing the analysis at energies around the Z^0 peak, the

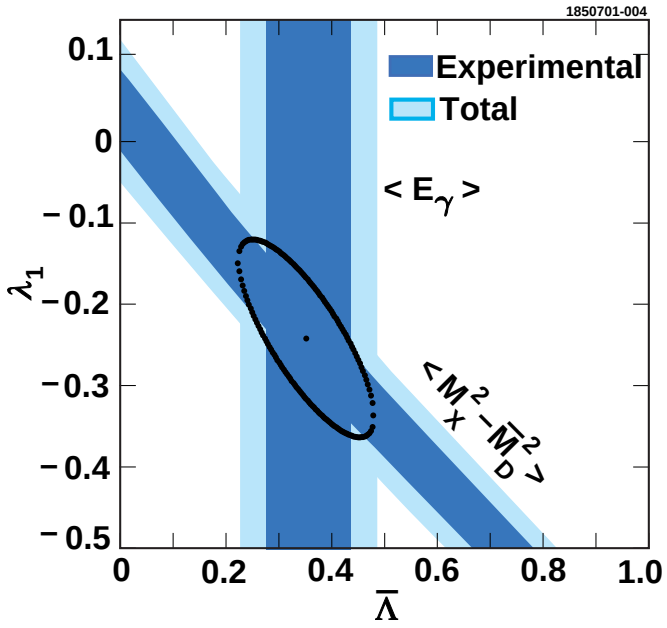

Fig. 3.1: *Constraints on $\bar{\Lambda}$ (GeV), λ_1 (GeV^2) from the first hadronic moment and the first moment of the photon energy spectrum in $b \to s\gamma$ [58,74]. The inner bands show the experimental error bands. The light gray extensions show the theoretical errors.*

large momentum of the b-hadrons ensures sensitivity to almost the full lepton spectrum, thus reducing modelling assumptions. The main challenge put by the higher energy is the accurate determination of the B rest frame.

2.2.3. Moments of hadronic mass and $b \to s\gamma$ photon energy spectra at CLEO

The first experimental determination of the HQE parameters based on the shape variables was performed by the CLEO collaboration [58]. The analysis was based on the measurement of the photon spectrum above 2.0 GeV in $b \to s\gamma$ inclusive decays [74] and on s.l. inclusive decays. CLEO measured the first two moments of the photon spectrum in radiative decays,

$$\langle E_\gamma \rangle = 2.346 \pm 0.032 \pm 0.011 \text{ GeV} \text{ and } \langle E_\gamma^2 \rangle - \langle E_\gamma \rangle^2 = 0.0226 \pm 0.0066 \pm 0.0020 \text{ GeV}^2$$

the first of which is related to half the value of the b quark pole mass, and thus to $\overline{\Lambda}$, of course up to $1/M_B^3$ corrections. The parameter λ_1 was then extracted from a measurement of the first moment, M_1^X, of the mass of the hadronic system recoiling against the ℓ-$\bar{\nu}$ pair in s.l. decays. This measurement takes advantage of the ability of the CLEO experiment to reconstruct the ν 4-momentum with high efficiency and resolution, by virtue of the hermeticity of the detector and the simplicity of the initial state in $\Upsilon(4S) \to B\bar{B}$. CLEO applied a 1.5 GeV/c lower cut on the charged lepton momentum. The explicit relation between M_1^X and the HQE parameters $\overline{\Lambda}$, λ_1, etc. is given in that case in [58]. CLEO found

$$M_1^X = 0.251 \pm 0.023 \pm 0.062 \text{ GeV}^2 \quad \text{and} \quad M_2^X = 0.576 \pm 0.048 \pm 0.163 \text{ GeV}^4,$$

where the first error is statistical and the second is systematic. From M_1^X and $\langle E_\gamma \rangle$, CLEO extracted $\overline{\Lambda}$ and λ_1, obtaining $\overline{\Lambda} = 0.35 \pm 0.07 \pm 0.10$ GeV , and $\lambda_1 = -0.236 \pm 0.071 \pm 0.078$ GeV^2 . Here, the first error is governed by the experimental measurements of the moments, and the second error reflects theoretical uncertainties, and in particular those related to $O(1/m_b^3)$ contributions. Figure 3.1 shows the bands corresponding to these two constraints as well as the $\Delta\chi^2 = 1$ ellipse in the $\overline{\Lambda}, \lambda_1$ plane.

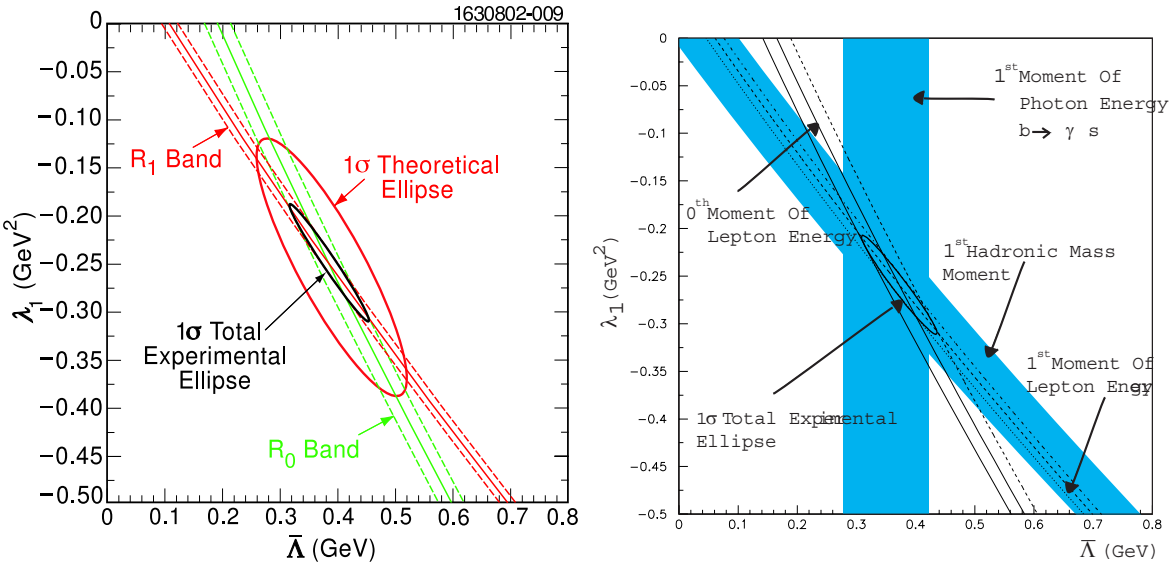

Fig. 3.2: *Left: constraints from combined electron and muon $R_{0,1}$ moments, with $\Delta\chi^2 = 1$ contours for total experimental and theoretical uncertainties [75]. Right: comparison of the same constraints with those in Fig. 3.1. λ_1 and $\bar{\Lambda}$ are computed in the $\overline{MS}$ scheme to order $1/M_B^3$ and $\beta_0\alpha_s^2$.*

2.2.4. Moments of the leptonic spectrum at CLEO

A recent CLEO analysis [75] reports the measurement of the truncated moments of the lepton spectrum, with a momentum cut of $p_\ell \geq 1.5$ GeV/c in the B meson rest frame [75]. This choice for the lepton momentum cut decreases the sensitivity of the measurement to the secondary leptons from the cascade decays ($b \to c \to s/d\ell\bar{\nu}$). The small contribution coming from charmless s.l. decays $b \to u\ell\bar{\nu}$ is included by adding the contribution from $d\Gamma_u/dE_\ell$, scaled by $|V_{ub}/V_{cb}|^2$ [61,64]. CLEO results for $R_{0,1}$ are given in Table 3.5. The values of the HQE parameters and their experimental uncertainties are obtained by calculating the χ^2 from the measured moments R_0^{exp} and R_1^{exp} and the covariance matrix $\mathrm{E}_{R_0R_1}$. The theoretical uncertainties on the HQE parameters are determined by varying, with flat distributions, the input parameters within their respective errors: $|\frac{V_{ub}}{V_{cb}}| = 0.09 \pm 0.02$, $\alpha_s = 0.22 \pm 0.027$, $\lambda_2 = 0.128 \pm 0.010$ GeV^2, $\rho_1 = \frac{1}{2}(0.5)^3 \pm \frac{1}{2}(0.5)^3$ GeV^3, $\rho_2 = 0 \pm (0.5)^3$ GeV^3, and $\mathcal{T}_i = 0.0 \pm (0.5)^3$ GeV^3. The contour that contains 68% of the probability is shown in Fig. 3.2. This procedure for evaluating the theoretical uncertainty from the unknown expansion parameters that enter at order $1/M_B^3$ is similar to that used by Gremm and Kapustin [63] and Bauer and Trott [64], but different from the procedure used in the CLEO analysis discussed above [58]. The dominant theoretical uncertainty is related to the $1/M_B^3$ terms in the non-perturbative expansion discussed before. Ref. [65] has explored the convergence of the perturbative and non-perturbative series appearing in the expressions for the moments described in the previous Section. The most conservative estimate gives a truncation error of at most 20%. The theoretical

	R_0^{exp}	R_1^{exp}
$e^\pm$	$0.6184 \pm 0.0016 \pm 0.0017$	$1.7817 \pm 0.0008 \pm 0.0010$
$\mu^\pm$	$0.6189 \pm 0.0023 \pm 0.0020$	$1.7802 \pm 0.0011 \pm 0.0011$
Combined	$0.6187 \pm 0.0014 \pm 0.0016$	$1.7810 \pm 0.0007 \pm 0.0009$

Table 3.5: *Measured truncated lepton moments for $e^\pm$ and $\mu^\pm$, and for the sum.*

uncertainties presented in this CLEO analysis do not include this truncation error. The extracted λ_1 and $\bar{\Lambda}$ are given in Table 3.6. The rhs in Fig. 3.2 shows a comparison of these CLEO results with the ones in Ref. [58]. The errors shown correspond to the experimental errors only: the agreement is good, although the theoretical uncertainties do not warrant a very precise comparison.

	λ_1(GeV^2)	$\bar{\Lambda}$(GeV)
$e^{\pm}$	$-0.28 \pm 0.03\vert_{stat} \pm 0.06\vert_{syst} \pm 0.14\vert_{th}$	$0.41 \pm 0.04\vert_{stat} \pm 0.06\vert_{syst} \pm 0.12\vert_{th}$
$\mu^{\pm}$	$-0.22 \pm 0.04\vert_{stat} \pm 0.07\vert_{syst} \pm 0.14\vert_{th}$	$0.36 \pm 0.06\vert_{stat} \pm 0.08\vert_{syst} \pm 0.12\vert_{th}$
$\ell^{\pm}$	$-0.25 \pm 0.02\vert_{stat} \pm 0.05\vert_{syst} \pm 0.14\vert_{th}$	$0.39 \pm 0.03\vert_{stat} \pm 0.06\vert_{syst} \pm 0.12\vert_{th}$

Table 3.6: *Values λ_1 and $\bar{\Lambda}$ extracted from CLEO measurement of $R_{0,1}$, including statistical, systematic, and theoretical errors. The last row shows the results obtained combining $e^{\pm}$ and $\mu^{\pm}$ samples.*

CLEO also performed an analysis of the truncated leptonic moments in terms of the short distance m_b^{1S} mass instead of the pole mass scheme implicit in the $\lambda_1, \overline{\Lambda}$ formalism. The results in Ref. [64] are used to extract m_b^{1S}, or rather $\bar{\Lambda}^{1S} \equiv \bar{M}_B - m_b^{1S}$. Table 3.7 summarizes the values of $\bar{\Lambda}^{1S}$ and m_b^{1S} extracted from $R_{0,1}$ for electrons and muons samples separately, and for their sum. The final result $m_b^{1S} = (4.82 \pm 0.07\vert_{exp} \pm 0.11\vert_{th})\mathrm{GeV}/c^2$ is in good agreement with the estimates of m_b^{1S} [35,76] discussed in Sec. 2.1.

	$\bar{\Lambda}^{1S}$(GeV)	m_b^{1S}(GeV/c^2)
$e^{\pm}$	$0.52 \pm 0.04\vert_{stat} \pm 0.06\vert_{syst} \pm 0.11\vert_{th}$	$4.79 \pm 0.07\vert_{exp} \pm 0.11\vert_{th}$
$\mu^{\pm}$	$0.46 \pm 0.05\vert_{stat} \pm 0.08\vert_{syst} \pm 0.11\vert_{th}$	$4.85 \pm 0.09\vert_{exp} \pm 0.11\vert_{th}$
Combined	$0.49 \pm 0.03\vert_{stat} \pm 0.06\vert_{syst} \pm 0.11\vert_{th}$	$4.82 \pm 0.07\vert_{exp} \pm 0.11\vert_{th}$

Table 3.7: *Values of $\bar{\Lambda}^{1S}$ and m_b^{1S} extracted from $R_{0,1}$. The quoted errors reflect statistical, systematic, and theoretical uncertainties, respectively.*

We have mentioned in the previous Section that one can also consider fractional moments. Bauer and Trott [64] have explored different lepton energy moments, by varying the exponent of the energy in the integrands and the lower limits of integration. In particular, they identify several moments that provide constraints for m_b^{1S} and λ_1 that are less sensitive to higher order terms in the non-perturbative expansion. The shape of the truncated lepton spectrum recently measured by CLEO [77] allows to measure the following ones

$$\mathrm{R}_a^{(3)} = \frac{\int_{1.7} E_l^{0.7} (d\Gamma_{sl}/dE_l) dE_l}{\int_{1.5} E_l^2 (d\Gamma_{sl}/dE_l) dE_l}, \quad \mathrm{R}_b^{(3)} = \frac{\int_{1.6} E_l^{0.9} (d\Gamma_{sl}/dE_l) dE_l}{\int_{1.7} (d\Gamma_{sl}/dE_l) dE_l}, \tag{41}$$

$$\mathrm{R}_a^{(4)} = \frac{\int_{1.6} E_l^{0.8} (d\Gamma_{sl}/dE_l) dE_l}{\int_{1.7} (d\Gamma_{sl}/dE_l) dE_l}, \quad \mathrm{R}_b^{(4)} = \frac{\int_{1.6} E_l^{2.5} (d\Gamma_{sl}/dE_l) dE_l}{\int_{1.5} E_l^{2.9} (d\Gamma_{sl}/dE_l) dE_l}. \tag{42}$$

Tables 3.8 and 3.9 summarize the measured values, as well as the statistical and systematic errors. Fig. 3.3 shows the values of $\bar{\Lambda}^{1S}$ and λ_1 extracted from these two sets of observables, as well as the constraints derived from the moments R_0 and R_1. Although these results confirm that the $1/M_B^3$ terms induce much smaller uncertainties using $R_{a,b}^{(3,4)}$, the experimental errors are larger in this case because of the similar slopes for the two constraints. However, the different relative importance of experimental and theoretical errors makes these results complementary to the previous ones reported.

	$R_a^{(3)}(\mathrm{GeV}^{-1.3})$	$R_b^{(3)}(\mathrm{GeV}^{0.9})$
$e^{\pm}$	$0.3013 \pm 0.0006\|_{stat} \pm 0.0005\|_{syst}$	$2.2632 \pm 0.0029\|_{stat} \pm 0.0026\|_{syst}$
$\mu^{\pm}$	$0.3019 \pm 0.0009\|_{stat} \pm 0.0007\|_{syst}$	$2.2611 \pm 0.0042\|_{stat} \pm 0.0020\|_{syst}$
$\ell^{\pm}$	$0.3016 \pm 0.0005\|_{stat} \pm 0.0005\|_{syst}$	$2.2621 \pm 0.0025\|_{stat} \pm 0.0019\|_{syst}$

Table 3.8: *Measured truncated lepton moments $R_{a,b}^{(3)}$ for $e^{\pm}$, $\mu^{\pm}$, and their weighted average.*

	$R_a^{(4)}(\mathrm{GeV}^{0.8})$	$R_b^{(4)}(\mathrm{GeV}^{-0.4})$
$e^{\pm}$	$2.1294 \pm 0.0028\|_{stat} \pm 0.0027\|_{syst}$	$0.6831 \pm 0.0005\|_{stat} \pm 0.0007\|_{syst}$
$\mu^{\pm}$	$2.1276 \pm 0.0040\|_{stat} \pm 0.0015\|_{syst}$	$0.6836 \pm 0.0008\|_{stat} \pm 0.0014\|_{syst}$
$\ell^{\pm}$	$2.1285 \pm 0.0024\|_{stat} \pm 0.0018\|_{syst}$	$0.6833 \pm 0.0005\|_{stat} \pm 0.0006\|_{syst}$

Table 3.9: *Measured truncated $R_{4a,b}$ moments for $e^{\pm}$, $\mu^{\pm}$, and their weighted average.*

Bauer and Trott [64] also identify moments that are insensitive to m_b^{1S} and λ_1. They suggest that a comparison between a theoretical evaluations of these "duality moments" and their experimental values may provide useful constraints on possible quark-hadron duality violations in s.l. processes. CLEO measures two such "duality moments", defined as

$$\mathrm{D}_3 = \frac{\int_{1.6} E_l^{0.7}(d\Gamma_{sl}/dE_l)dE_l}{\int_{1.5} E_l^{1.5}(d\Gamma_{sl}/dE_l)dE_l}, \quad \mathrm{D}_4 = \frac{\int_{1.6} E_l^{2.3}(d\Gamma_{sl}/dE_l)dE_l}{\int_{1.5} E_l^{2.9}(d\Gamma_{sl}/dE_l)dE_l}. \tag{43}$$

The theoretical predictions from Ref. [64] are compared with the measured $D_{3,4}$ from the combined lepton sample in Table 3.10. The agreement is excellent and thus no internal inconsistency of the theory is uncovered in this analysis.

	Experimental	Theoretical
D_3	$0.5193 \pm 0.0008\|_{exp}$	$0.5195 \pm 0.0006\|_{\lambda_1,\bar{\Lambda}^{1S}} \pm 0.0003\|_{th}$
D_4	$0.6036 \pm 0.0006\|_{exp}$	$0.6040 \pm 0.0006\|_{\lambda_1,\bar{\Lambda}^{1S}} \pm 0.0005\|_{th}$

Table 3.10: *Measured duality moments and theoretical predictions using the values λ_1 and $\bar{\Lambda}^{1S}$ [77]. The errors reflect the experimental uncertainties in these parameters and the theoretical errors, respectively.*

2.2.5. Moments of leptonic and hadronic mass spectra at DELPHI

Results obtained by the DELPHI collaboration for the first three moments of the lepton energy and the hadronic mass spectra have been presented at ICHEP02 [59]. The analyses were based on b-hadron s.l. decays into electrons and muons, selected from a sample of about 3×10^6 $e^+e^- \to Z^0 \to q\bar{q}$ events recorded with the DELPHI detector at LEP. Electrons and muons were required to have a momentum greater than 2-3 GeV/c in the laboratory frame. For the lepton energy spectrum measurement an inclusive reconstruction of the secondary vertex of the charm hadron decay was performed. The energy of the B hadron was estimated as the energy sum of the identified lepton, the secondary hadronic system and the neutrino energy, evaluated from the event missing energy. The identified lepton was then boosted back to the reconstructed B rest frame and its energy E_ℓ re-computed in this frame. Results for the first three

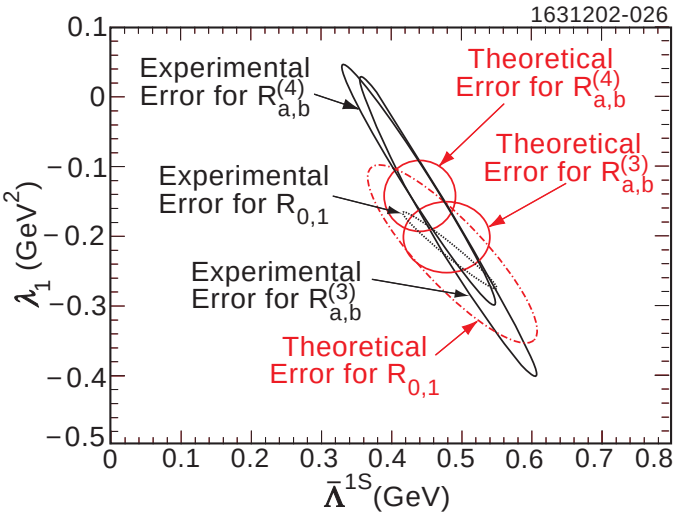

Fig. 3.3: *Constraints on the HQE parameters λ_1 and $\bar{\Lambda}^{1S}$ from different CLEO measured spectral moments.*

moments are summarized in Table 3.11. In order to study the hadronic mass distribution the exclusive reconstruction of $\bar{B}^0_d \to D^{**}\ell\bar{\nu}$ states was performed and the total D^{**} production in b-hadron s.l. decays was determined. Moments of the hadronic mass distribution were measured for D^{**} candidates and moments of the hadronic mass distribution in inclusive b-hadron s.l. decays, M_X, were derived including $b \to D$ and $D^*\ell^-\overline{\nu}_\ell$ channels. Results for the first three moments are summarized in Table 3.11. As we will discuss in the next subsection, the DELPHI results have been used in [71] as inputs of a multi-parameter fit to determine the heavy quark masses and non-perturbative parameters of the HQE. The use of higher moments guarantees a sensitivity to the $1/m_b^3$ parameters and the simultaneous use of the hadronic and leptonic spectra ensures that a larger number of parameters can be kept free in the fit.

Moment	Result	(stat)	(syst)	
$M_1(E_\ell)$	(1.383	$\pm$ 0.012	$\pm$0.009)	GeV
$M_2(E_\ell)$	(0.192	$\pm$ 0.005	$\pm$0.008)	GeV^2
$M_3(E_\ell)$	(-0.029	$\pm$ 0.005	$\pm$0.006)	GeV^3
$M_1(M_X)$	(0.534	$\pm$ 0.041	$\pm$ 0.074)	GeV^2
$M_2(M_X)$	(1.226	$\pm$ 0.158	$\pm$ 0.152)	GeV^4
$M_3(M_X)$	(2.970	$\pm$ 0.673	$\pm$ 0.478)	GeV^6

Table 3.11: *DELPHI results for the first three leptonic and hadronic moments.*

2.2.6. Multi-parameter fits of heavy-quark parameters and outlook

A recent and promising development, in view of the greater precision expected at the B-factories, consists in combining leptonic and hadronic moments in a multi-parameter fit to determine not just m_b and $\lambda_1 \sim -\mu_\pi^2$ but also the dominant $O(1/m_b^3)$ parameters. The first comprehensive analyses that employ this approach [65,71] have shown that present data are consistent with each other (with the possible exception of the preliminary BaBar data [78]) and with our theoretical understanding, most notably with the underlying assumption of quark-hadron duality.

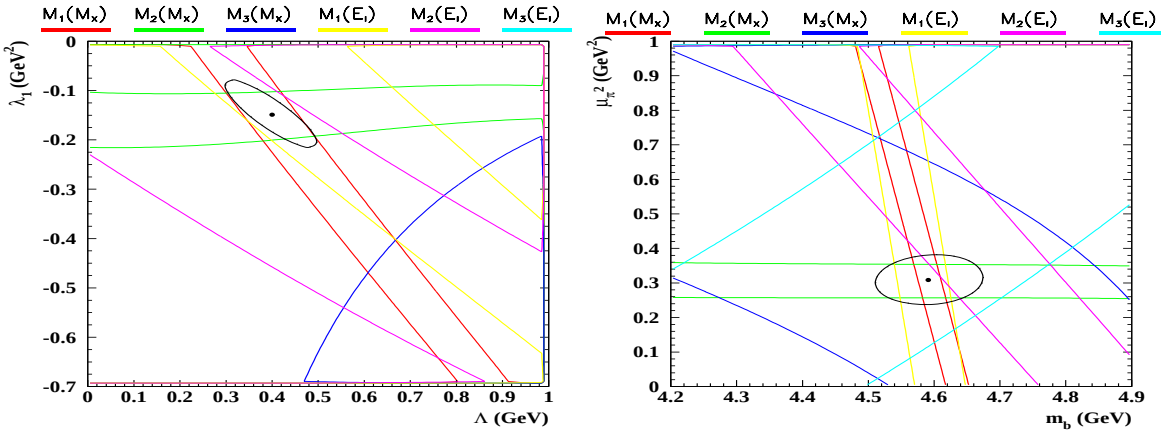

Fig. 3.4: *Projection of the constraints from the six DELPHI moments on the ($m_b(1\ \mathrm{GeV})$, μ_π^2) and ($\overline{\Lambda}$, λ_1) planes [71]. The bands correspond to the total experimental error and given keeping all the other parameters at their central values. The ellipses represent the 1σ contour.*

The analysis of [71] is based solely on the DELPHI data in Table 3.11, and performed in the two theoretical framework described above in Secs. 2.2.1. and 2.2.2. The projection of the various constraints on the ($m_{b,\mathrm{kin}}(1\ \mathrm{GeV})$, μ_π^2) and ($\overline{\Lambda}$, λ_1) planes are given in Fig. 3.4, which shows very good consistency. The results of the fits are shown in Tables 3.12 and 3.13. In the framework of Sec. 2.2.1. the charm mass is a free parameter of the fit, though strongly correlated to the bottom mass. Given a precise determination $\delta m_{b,\mathrm{kin}}(1\ \mathrm{GeV}) \sim 50$ MeV, the charm mass could therefore be extracted with $\delta m_c \sim 90$ MeV, a competitive determination [71] (Cfr. Sec. 2.1.).

Fit Parameter	Fit Values	Fit Uncertainty	Syst. Uncertainty	
$m_{b,\mathrm{kin}}$ (1 GeV)	4.59	$\pm$ 0.08	$\pm$ 0.01	GeV
$m_{c,\mathrm{kin}}$ (1 GeV)	1.13	$\pm$ 0.13	$\pm$ 0.03	GeV
μ_π^2 (1 GeV)	0.31	$\pm$ 0.07	$\pm$ 0.02	GeV^2
ρ_D^3	0.05	$\pm$ 0.04	$\pm$ 0.01	GeV^3

Table 3.12: *Results of fits to the moments of Table 3.11 for the $m_b(\mu)$, $m_c(\mu)$ and $\mu_\pi^2(\mu)$ formalism [71].*

The analysis of Ref. [65] includes the first two hadronic moments measured by CLEO and DELPHI, $R_{0,1}$ measured by CLEO, the first two leptonic DELPHI moments, and the first two moments of the photon spectrum in $\mathrm{B} \to X_s\gamma$. The results in one of the formalisms adopted are shown in Table 3.14. They are in good agreement with both CLEO and DELPHI analyses mentioned above. The preferred ranges for the heavy quark masses and for the non-perturbative parameters in Tables 3.12, 3.13, and 3.14 are in agreement with theoretical expectations and with each other, although the analyses [65,71] differ in several respects (data employed, additional constraints, scheme adopted, treatment of theoretical errors).

In summary, the experimental information appears so far consistent with the theoretical framework, with the possible exception of the preliminary BaBar result. The emerging experimental information from the B factories will eventually lead to a more complete assessment of our present understanding of inclusive s.l. decays.

Fit Parameter	Fit Values	Fit Uncertainty	Syst. Uncertainty	
$\overline{\Lambda}$	0.40	$\pm$ 0.10	$\pm$ 0.02	GeV
λ_1	-0.15	$\pm$ 0.07	$\pm$ 0.03	GeV^2
λ_2	0.12	$\pm$ 0.01	$\pm$ 0.01	GeV^2
ρ_1	-0.01	$\pm$ 0.03	$\pm$ 0.03	GeV^3
ρ_2	0.03	$\pm$ 0.03	$\pm$ 0.01	GeV^3

Table 3.13: *Results of fit to the moments of Table 3.11 for the $\bar{\Lambda} - \lambda_1$ formalism [71].*

Fit Parameter	Fit Values	Fit Uncertainty	
m_b^{1S}	4.74	$\pm$ 0.10	GeV
$\lambda_1 + \frac{\mathcal{T}_1+3\mathcal{T}_3}{m_b}$	-0.31	$\pm$ 0.17	GeV^2
ρ_1	0.15	$\pm$ 0.12	GeV^3
ρ_2	-0.01	$\pm$ 0.11	GeV^3

Table 3.14: *Results of fit for the m_b^{1S}-λ_1 formalism [65].*

2.3. Parton–hadron duality in B decays

Parton-hadron duality [¶] – or duality for short – is invoked to connect quantities evaluated on the quark-gluon level to the (observable) world of hadrons. It is used all the time, often without explicit reference to it. A striking example of the confidence high-energy physicists have in the asymptotic validity of duality was provided by the discussion of the width $\Gamma(Z^0 \to H_b H_b' X)$. There was about a 2% difference between the predicted and measured decay width, which lead to lively debates on its significance vis-a-vis the *experimental* error, before disappearing when the analysis was improved. No concern was expressed about the fact that the Z^0 width was calculated on the quark-gluon level, yet measured for hadrons. Likewise the strong coupling $\alpha_{\rm s}(\rm M_Z)$ is routinely extracted from the perturbatively computed hadronic Z^0 width with a stated theoretical uncertainty of 0.003 which translates into a theoretical error in $\Gamma_{had}(Z^0)$ of about 0.1%.

There are, however, several different versions and implementations of the concept of duality. The problem with invoking duality implicitly is that it is very often unclear which version is used. In B physics – in particular when determining $|V_{cb}|$ and $|V_{ub}|$ – the measurements have become so precise that theory can no longer hide behind experimental errors. To estimate theoretical uncertainties in a meaningful way one has to give clear meaning to the concept of duality; only then can one analyse its limitations. In response to the demands of B physics a considerable literature has been created on duality over the last few years, which we summarize here. Technical details can be found in the references.

Duality for processes involving time-like momenta was first addressed theoretically in the late '70's in references [79] and [80]. Using the optical theorem, the cross section for $e^+e^- \to \rm hadrons$ at

[¶] This name might be more appropriate than the more frequently used *quark*-hadron duality since gluonic effects have to be included as well into the theoretical expressions.

leading order in α_{em} can be expressed as

$$\sigma(s) = \frac{16\pi^2\alpha_{em}}{s}\mathrm{Im}\ \Pi(s) \tag{44}$$

where $\Pi(s)$ is defined through the correlator of electromagnetic currents:

$$T_{\mu\nu}(q^2) = i\int d^4x\, e^{iqx}\,\langle 0|T\left(J_\mu(x)J_\nu(0)\right)|0\rangle = (g_{\mu\nu}q^2 - q_\mu q_\nu)\Pi(q^2)\ . \tag{45}$$

One might be tempted to think that by invoking QCD's asymptotic freedom one can compute $\sigma(\mathrm{e^+e^-} \to \mathrm{hadrons})$ for large c.m. energies $\sqrt{s} \gg \Lambda_{QCD}$ in terms of quarks (and gluons) since it is shaped by short distance dynamics. However production thresholds like those for charm induce singularities that vitiate such a straightforward computation. Under such circumstances, duality between the QCD-inferred cross section and the observed one looks problematic. It was suggested in [79] that the equality between the two would be restored after averaging or "smearing" over an energy interval:

$$\langle T_{\mu\nu}^{hadronic}\rangle_w \simeq \langle T_{\mu\nu}^{partonic}\rangle_w \tag{46}$$

where $\langle ...\rangle_w$ denotes the smearing which is an average using a smooth weight function $w(s)$:

$$\langle ...\rangle_w = \int ds\, ...\, w(s) \tag{47}$$

The degree to which $\langle T_{\mu\nu}^{partonic}\rangle_w$ can be trusted as a theoretical description of the observable $\langle T_{\mu\nu}^{hadronic}\rangle_w$ depends on the weight function, in particular its width. It can be broad compared to the structures that may appear in the hadronic spectral function, or it could be quite narrow, as an extreme case even $w(s) \sim \delta(s - s_0)$. It has become customary to refer to the first and second scenarios as *global* and *local* duality, respectively. Other authors use different names, and one can argue that this nomenclature is actually misleading. Below these items are described in more detail without attempting to impose a uniform nomenclature.

Irrespective of names, a fundamental distinction concerning duality is often drawn between s.l. and non-leptonic widths. Since the former necessarily involves smearing with a smooth weight function due to the integration over neutrino momenta, it is often argued that predictions for the former are fundamentally more trustworthy than for the latter. However, such a categorical distinction is overstated and artificial. Of much more relevance is the differentiation between distributions and fully integrated rates.

No real progress beyond the more qualitative arguments of Refs. [79] and [80] occurred for many years. For as long as one has very limited control over non-perturbative effects, there is little meaningful that can be said about duality violation. Yet this has changed for heavy flavour physics with the development of heavy quark expansions, since within this OPE framework we can assess non-perturbative effects as well as duality violation.

2.3.1. What is parton–hadron duality?

In order to discuss possible violations of duality one has to give first a more precise definition of this notion, which requires the introduction of some theoretical tools. Here the arguments given in the extensive reviews of Ref. [81] and [82][‖] are followed closely.

The central ingredient in the definition of duality that will be used here is the method of the Wilsonian OPE frequently used in field theory to perform a separation of scales. In practical terms this means that we can write

$$i\int d^4x\, e^{iqx}\,\langle A|T\left(J^\mu(x)J^\nu(0)\right)|A\rangle \simeq \sum_n \left(\frac{1}{Q^2}\right)^n c_n^{\mu\nu}(Q^2;\lambda)\langle A|\mathcal{O}_n|A\rangle_\lambda \tag{48}$$

[‖] It can be noted that even the authors of Ref. [81] and [82] – although very close in the substance as well as the spirit of their discussion – do not use exactly the same terminology concerning different aspects of duality.

for $Q^2 = -q^2 \to \infty$. The following notation has been used: $|A\rangle$ denotes a state that could be the vacuum – as for $e^+e^- \to hadrons$ considered above – or a B meson when describing s.l. beauty decays. J^μ denote electro-magnetic and weak current operators ($b \to c$ or u) for the former and the latter processes, respectively; for other decays like non-leptonic or radiative ones one employs different $\Delta B = 1$ operators; the $\mathcal{O}_n$ are local operators of increasing dimension. The operator of lowest dimension yields the leading contribution. In e^+e^- annihilation it is the unit operator $\mathcal{O}_0 = 1$, for B decays $\mathcal{O}_0 = \bar{b}b$. As we have seen in Sec. 1.1., they lead (among other things) to the naive partonic results. Yet the OPE allows us to systematically improve the naive partonic result. The coefficients $c_n^{\mu\nu}$ contain the contributions from short distance dynamics calculated perturbatively based on QCD's asymptotic freedom. Following Wilson's prescription a mass scale λ has been introduced to separate long and short distance dynamics; both the coefficients and the matrix elements depend on it, but their product does not.

The perturbative expansion takes the form

$$c_n^{\mu\nu} = \sum_i \left(\frac{\alpha_s(Q^2)}{\pi} \right)^i a_{n,i}^{\mu\nu} \tag{49}$$

and is performed in terms of quarks and gluons. The expectation values for the local operators provide the gateways through which non-perturbative dynamics enters.

The crucial point is that the OPE result is obtained in the Euclidean domain, far from any singularities induced by hadronic thresholds, and has to be continued analytically into the Minkowskian regime relating the OPE result to observable hadronic quantities. As long as QCD is the theory of the strong interactions, it does not exhibit unphysical singularities in the complex Q^2 plane, and the analytical continuation will not induce additional contributions. To conclude: *duality between* $\langle T_{\mu\nu}^{hadronic} \rangle_w$ *and* $\langle T_{\mu\nu}^{partonic} \rangle_w$ *arises due to the existence of an OPE that is continued analytically*. It is thus misleading to refer to duality as an additional assumption.

Up to this point the discussion was quite generic. To specify it for s.l. B decays one chooses the current J_μ to be the weak charged current related to $b \to c$ or $b \to u$. As already noted in Sec. 1.1., the expansion parameter for inclusive s.l. decays is given by the energy release $\sim 1/(m_b - m_c)$ $[1/m_b]$ for $b \to c$ $[b \to u]$.

2.3.2. Duality violation and analytic continuation

One of the main applications of the heavy quark expansion is the reliable extraction of $|V_{cb}|$ and $|V_{ub}|$. One wants to be able to arrive at a meaningful estimate of the theoretical uncertainty in the values obtained. There are three obvious sources of theoretical errors:

1. unknown terms of higher order in α_s;
2. unknown terms of higher order in $1/m_Q$;
3. uncertainties in the input parameters α_s, m_Q and the expectation values of local operators which appear in the OPE.

Duality violations constitute additional uncertainties.They arise from the fact that at finite order in $1/m_Q$, the Euclidean OPE is insensitive to contributions of the type $e^{-m_Q/\mu}$, with μ denoting some hadronic scale. While such a term is probably innocuous for beauty, it needs not be for charm quarks. Furthermore, under analytic continuation these terms turn into potentially more dangerous oscillating terms of the form $\sin(m_Q/\mu)$.

Though there is not (yet) a full theory for duality and its violations, progress has come about in the last few years for the following reasons:

- the understanding of the physical origins of duality violations has been refined as due to
  - hadronic thresholds;

  - so-called 'distant cuts';
  - the suspect validity of $1/m_c$ expansions.
- The issues surrounding the exponentially small terms discussed above and their analytic continuation have been understood.
- There is an increasing array of field-theoretical toy models, chief among them the 't Hooft model, which is QCD in 1+1 dimensions in the limit of $N_c \to \infty$. It is solvable and thus allows an unequivocal comparison of the OPE result with the exact solution.
- For the analysis of $b \to c$ transitions the small-velocity (SV) expansion is a powerful tool [7].

Based on general expectations as well as on analysing the models one finds that indeed duality violations are described by highly power suppressed 'oscillating' terms of the form

$$T(m_Q) \sim \left(\frac{1}{m_Q}\right)^k \sin(m_Q/\mu) \tag{50}$$

for some integer power k. More generally one can state:

- Duality will not be exact at finite masses. It represents an approximation the accuracy of which will increase with the energy scales in a way that depends on the process in question.
- Limitations to duality can enter only in the form of an oscillating function of energy or m_Q (or have to be exponentially suppressed), i.e. duality violation cannot modify all decay rates in the same way.
- The OPE equally applies to s.l. as well as to non-leptonic decay rates. Likewise both widths are subject to duality violations. The difference here is quantitative rather than qualitative; at finite heavy quark masses corrections are generally expected to be larger in the non-leptonic widths. In particular, duality violations there can be boosted by the accidental nearby presence of a narrow hadronic resonance. Similar effects could arise in s.l. rates, but are expected to be highly suppressed there.
- It is not necessary to have a proliferation of decay channels to reach the onset of duality, either approximate or asymptotic. Instructive examples are provided by the SV kinematics in s.l. decays and by non-leptonic rates in the 't Hooft model. For example, in the SV limit, the ground-state doublet of D mesons alone saturates the inclusive s.l. decay rate and is dual to the partonic rate [83]. The point here is that the large energy release would allow a large number of states to contribute kinematically, but only two channels are actually allowed by the dynamics.

Putting everything together it has been estimated by the authors of Ref. [82] – that *duality violations in the integrated s.l. width of B mesons cannot exceed the fraction of a percent.* As such we do not envision it to ever become the limiting factor in extracting $|V_{cb}|$ and $|V_{ub}|$ since the uncertainties in the expression for the s.l. width due to fixed higher order contributions will remain larger than this level. The oscillatory nature of duality violating contributions is a main ingredient in this conclusion. It also shows that duality violations could become quite sizeable if an only partially integrated width – let alone a distribution – is considered. Generally, for distributions the expansion parameter is not the heavy mass, rather it is a quantity such as $1/[m_Q(1-x)]$ where x is e.g. the rescaled charged lepton energy of a s.l. decay. From Eq. (50) one would expect that contributions the form $\sin(m_Q[1-x]/\mu)/[m_Q(1-x)]^k$ would appear in differential distributions.

2.3.3. How can we check the validity of parton–hadron duality?

If in the future a discrepancy between the measured and predicted values for, say, a CP asymmetry in B decays is found, one has to check very diligently all ingredients upon which the prediction was based, in particular the values for $|V_{cb}|$ and $|V_{ub}|$, before one could make a credible claim to have uncovered

New Physics. This means one needs a measure for potential duality violations that is not based purely on theoretical arguments.

Most theoretical uncertainties do not have a statistical nature. As in the case of experimental systematics, the most convincing way to control them is to determine the same quantity in independent ways and analyse their consistency. The heavy quark expansions lend themselves naturally to such an approach since they allow the description of numerous decay rates in terms of a handful of basic parameters, namely quark masses and hadronic expectation values. Of course, such independent determinations of the same quantity only probe the overall theoretical control: by themselves they cannot tell whether a failure is due to unusually large higher order contributions or to a breakdown of duality.

The fact that both the inclusive and exclusive methods for extracting $|V_{cb}|$ and $|V_{ub}|$ yield consistent values (see Secs. 2.4.,2.5., 3., and 4.) is such a test. Theoretical corrections are nontrivial and essential for the agreement. As discussed in Sec. 2.2., the study of moments offers another important consistency check. In particular, we emphasize that the b quark mass extracted from the shape variables is consistent, within errors, with the one extracted from sum rules and lattice calculations (see Sec. 2.1.), and that the analyses of CLEO and DELPHI data, and those of the leptonic and hadronic moments point to very similar values for the kinetic energy parameter $\lambda_1 \sim -\mu_\pi^2$. This suggests that no anomalously large higher order corrections or unexpectedly sizeable duality violating contributions are present in the HQE used to described inclusive s.l. $b \to c$ decays. However, once again, we stress that these comparisons do not represent direct tests of duality.

2.3.4. Model based investigations of duality

It is desirable to study in more explicit detail how duality comes about, how it is approached and what its limitations are. This can be done in the context of exactly soluble field theories, in particular the 't Hooft model, which is QCD in 1+1 dimensions with the number of colours going to infinity [84]. There one finds duality to be achieved very quickly, i.e. after a mere handful of channels open up.

For detailed studies in 1+3 dimensions one is at present limited to the use of quark models employing certain types of potential. However, one has to handle these models with care, as they have sometimes led to confusion. In particular, it has been argued in Ref.[86] that within quark models one could have an $\mathcal{O}(1/m_Q)$ contribution to the ratio of inclusive to free quark total decay rate. Such terms are absent in the OPE, and therefore violate duality. The arguments presented in [86] and similar papers have been discussed in [82], where their internal flaws have been pointed out. One of the important lessons is that such models exhibit automatically the proper behaviour in the Shifman-Voloshin (SV) limit [7], where $\Lambda_{QCD} \ll \delta m = m_b - m_c \ll m_b$. In particular, they have to satisfy a set of sum rules. Once one realizes that such models are automatically in compliance with what we know to be true in QCD, it becomes clear that no $1/m_Q$ terms can appear [88,89,90]. Of particular importance in this context are the Bjorken sum rule for $\mathcal{O}(\frac{(\delta m)^2}{m_b^2})$ terms and the Voloshin sum rule for $\mathcal{O}(\frac{\delta m}{m_b})$ terms**. Other terms are suppressed by higher powers of $1/m_b$ or powers of $\Delta/\delta m$, Δ being the level spacing of $O(\Lambda_{QCD})$, *i.e.* the difference between the ground state and the first excited level. Once such models have been brought into compliance with what we know to be true in QCD – like the validity of the SV sum rules – then they can play a significant heuristic role in educating our intuition about the onset of duality.

In Ref. [90] a detailed study of the cancellations required for duality to hold have been performed using a harmonic oscillator (HO) potential. The interest of this model is that the truncation of states to the first band of orbital excitations (lowest D^{**}) becomes exact to the relevant order $1/m_b^2$, which allows us to perform a complete and explicit numerical or analytical calculation. Furthermore, this model is

**It also has been demonstrated explicitly that, contrary to what suggested in note 3 of Ref. [86], no term of $\mathcal{O}(\frac{\delta m}{m_b^2})$ exist in QCD [87].

close to the ones used in [86], so that one can check precisely the various statements made there. Using a constant for the leptonic interaction one finds in the harmonic oscillator model

$$R_{sl} = \frac{\Gamma_{inclusive}}{\Gamma_{free\ quark}} = 1 + \frac{3}{R^2 m_b^2}(\frac{1}{4} - \frac{\Delta}{\delta m}) + \text{smaller terms} \tag{51}$$

where $\Delta = \frac{1}{m_d R^2}$ is a model parameter containing the square of the harmonic oscillator radius R and the light-quark mass m_d. Note that the first term inside the parentheses originates from the kinetic energy operator. In fact, it can be proven [89] that for *regular* potentials the whole series, directly calculated in the model, is *exactly* the one given by OPE.

What is then the explanation of the apparent disagreement with [86]? First, there is a misunderstanding induced by the expression "$1/m_Q$ duality violation", used sometimes in a misleading way. Ref. [86] does not dispute that the OPE is basically right and that the equality with free quark decay is satisfied within the expected accuracy in the region of phase space where the energy release is large $(t_{max}^{1/2} - t^{1/2})/\Delta \gg 1$, i.e. where many states are kinematically allowed ($t = q^2$). This is certainly true when t is small. What may cause problems, according to [86], is only the region near t_{max} where this condition is not satisfied and large effects can be generated. According to the authors of [89], one can certainly produce effects which violate the equality with free quark over the region of phase space *where only the ground state is opened*, of relative order $1/m_Q$ if this "relative order " means that one compares to the corresponding free quark decay *over the same region* of phase space. But they object that such effects be related to the *total* free quark decay which is much larger. Indeed, such effects are not of order $1/m_Q$ with respect to the total free quark decay rate, but much smaller, suppressed by powers of $2\Delta/\delta m$ [89]. This suppression factor amounts, in the standard $1/m_Q$ expansion at fixed ratio of heavy masses, to further powers of the heavy mass, because then $\delta m \propto m_b$. Also, numerically, they are small since $2\Delta/\delta m$ is small.

The first example given by Isgur is that the decrease of the ground state contribution with decreasing t (or increasing $|\vec{q}|$) due to the form factor must be compensated by the increase of the excited states to maintain duality with free quarks. This is exactly guaranteed by the Bjorken sum rule in the heavy quark limit, but it is no longer exact at finite mass, because there is a region below the D^{**} threshold where only the ground state $D + D^*$ contribute. Quantitatively, the term pointed out in [86] with a constant leptonic interaction reads (the choice of this interaction is not crucial):

$$\frac{\delta\Gamma}{\Gamma_{free}} \simeq -\rho^2 \frac{\int_{(\delta m-\Delta)^2}^{(\delta m)^2} dt |\vec{q}| \frac{|\vec{q}|^2}{m_b^2}}{\int_0^{(\delta m)^2} dt |\vec{q}|} \tag{52}$$

where $|\vec{q}|^2 \simeq (\delta m)^2 - t$, $-\rho^2 \frac{|\vec{q}|^2}{m_b^2}$ describes the falloff of the ground state (ρ^2 is the slope of the Isgur-Wise function), and the integration limits are approximated to the desired accuracy. At the lower limit of the numerator integral $t = (\delta m - \Delta)^2$ this falloff attains its maximum, $-\rho^2 \frac{2\Delta\delta m}{m_b^2}$. This term is by itself the expression of a $1/m_Q$ term in the SV limit [86]. However, the real magnitude is much smaller because one must integrate over a limited phase space, while the integral of the free quark decay in the denominator extends over a much larger region [90]:

$$\frac{\delta\Gamma}{\Gamma_{free}} \simeq -\frac{3}{5}\rho^2 \frac{2\Delta\delta m}{m_b^2} \left(\frac{2\Delta}{\delta m}\right)^{3/2} = -\frac{3}{5}\frac{m_d \delta m}{m_b^2} \left(\frac{2\Delta}{\delta m}\right)^{3/2} \tag{53}$$

where $\rho^2\Delta = \frac{m_d}{2}$ in the HO model. Parametrically, this is suppressed with respect to $1/m_Q$ because of the factor $(\frac{2\Delta}{\delta m})^{3/2}$.

In another example relying on a model of two-body decay, Isgur [86] tries to take into account also the larger effect due to the $\frac{m_d \delta m}{m_b^2}$ terms present in *partial rates*. Such terms, which corresponds to

$1/m_Q$, are present *separately* in the various exclusive channels. For instance one has for the ratio of the ground state to the free quark decay rates:

$$R_{sl}^{(ground\ state)} = 1 + \frac{3}{2}\frac{m_d \delta m}{m_b^2} + ..., \tag{54}$$

but they cancel in the total decay rate. Then, if the kinematical situation is such that only the ground state is produced, the total ratio R_{sl} would depart from 1 by $\frac{\frac{3}{2} m_d \delta m}{m_b^2}$. However, this effect is for t above the D** threshold $(M_B - M_{D^{**}})^2$, i.e. in a limited region of phase space. Hence, taking the ratio of this effect to the total rate, one gets:

$$\frac{\delta\Gamma}{\Gamma_{free}} \simeq \frac{3}{2}\frac{m_d \delta m}{m_b^2}\frac{\int_{(\delta m-\Delta)^2}^{(\delta m)^2} dt|\vec{q}|}{\int_0^{(\delta m)^2} dt|\vec{q}|} \simeq \frac{3}{2}\frac{m_d \delta m}{m_b^2}\left(\frac{2\Delta}{\delta m}\right)^{3/2}, \tag{55}$$

which is once more parametrically smaller by the factor $(\frac{2\Delta}{\delta m})^{3/2}$.

In conclusion, both effects are not $\mathcal{O}(1/m_Q)$ but much smaller. Thus the model dependent investigations of possible duality violations do not hint at any effect beyond the OPE of full QCD. In particular, taking into account the sum rules valid in full QCD allows us to show explicitly the absence of contributions at order $1/m_Q$, which would be a gross violation of OPE or, likewise, of duality.

2.3.5. Conclusion

All we currently know from purely theoretical considerations indicates that duality violations should be safely below one percent in the s.l. branching ratio. This is likely to remain in the noise of theoretical uncertainties due to higher order perturbative and non-perturbative ($O(1/m_b^3)$ and higher) corrections. Hence we will not assign additional uncertainty to the extraction of $|V_{cb}|$ from possible duality violation in inclusive decays. As discussed above, this picture will be tested through an intense program of high precision measurements in the near future, and most notably by the study of different moments of the s.l. distributions – even separately in the decays of B_d, B^- and B_s mesons.

2.4. Review and future prospects for the inclusive determination of $|V_{cb}|$

The value of the CKM matrix element $|V_{cb}|$ can be obtained by comparing the measured value of the b-quark s.l. decay partial width with its prediction in the context of the OPE. Experimentally, this partial width is obtained by measuring the inclusive s.l. decay rate of B-hadrons and their lifetime(s). Present measurements are rather accurate and experimental uncertainties lead to a relative error of about 1% on $|V_{cb}|$. The main limitation for a precise determination of $|V_{cb}|$ comes from theory, as the expression for the s.l. decay width depends on several poorly known parameters that are introduced by perturbative and non-perturbative QCD effects. Only recently, as discussed in Sec. 2.2., some of the non-perturbative parameters describing corrections of order $\mathcal{O}(1/m_b)$, $\mathcal{O}(1/m_b^2)$, and $\mathcal{O}(1/m_b^3)$ have been constrained experimentally. As a result, not only has the accuracy on $|V_{cb}|$ improved, but also a large fraction of the previous systematic uncertainty has changed nature.

In the following, we briefly summarize the main ingredients of the evaluation of $|V_{cb}|$ from inclusive b s.l. decay measurements. As discussed in Sec. 2.3., a possible violation of parton-hadron duality can be legitimately neglected at the present level of accuracy, and we will not include it in our estimate of the error associated with $|V_{cb}|$.

2.4.1. Perturbative QCD corrections

Using the pole mass definition for quark masses, the first order QCD perturbative corrections to the s.l. b-decay width have been given in [67,92] and dominant second order (BLM) corrections have been

obtained in [91]; the subdominant two-loop corrections have been estimated in [94]. The s.l. width can be written as

$$\Gamma(b\to c\ell\overline{\nu}_\ell)=\frac{G_F^2 m_b^5|V_{cb}|^2\mathcal{A}_{ew}}{192\pi^3}F(z)\left\{1-\frac{\alpha_s(m_b)}{\pi}\frac{2}{3}f(z)-\frac{\alpha_s^2}{\pi^2}\left[\beta_0\chi^{\rm BLM}(z)+\chi_0(z)\right]\right\}. \quad (56)$$

In this expression:

- the phase space factor $F(z)=1-8z+8z^3-z^4-12z^2\ln z$, with $z=m_c^2/m_b^2$, accounts for the mass of the final quark, and both m_c and m_b are pole masses;
- $\beta_0=11-\frac{2}{3}n_f$, where n_f is the number of active flavours;
- $\mathcal{A}_{ew}\simeq 1+2\frac{\alpha}{\pi}\ln\frac{m_Z}{m_b}$ and corresponds to the electroweak correction, cfr. Eq. (107) below;
- $f(x)=h(x)/F(x)$ with

$$\begin{aligned} h(x) &= -(1-x^2)\left(\frac{25}{4}-\frac{239}{3}x+\frac{25}{4}x^2\right)+x\ln x\left(20+90x-\frac{4}{3}x^2+\frac{17}{3}x^3\right)\\ &\quad +x^2\ln^2 x(36+x^2)+(1-x^2)\left(\frac{17}{3}-\frac{64}{3}x+\frac{17}{3}x^2\right)\ln(1-x)\\ &\quad -4(1+30x^2+x^4)\ln x\ln(1-x)-(1+16x^2+x^4)\left[6Li_2(x)-\pi^2\right]\\ &\quad -32x^{3/2}(1+x)\left[\pi^2-4Li_2(\sqrt{x})+4Li_2(-\sqrt{x})-2\ln x\ln\frac{1-\sqrt{x}}{1+\sqrt{x}}\right] \end{aligned} \quad (57)$$

  Numerical values for $f(x)$ can be found in [93] and are reported in Table 3.15.

$\frac{m_c}{m_b}$	0.	0.1	0.2	0.3	0.4	0.5	0.6	0.7	0.8	0.9	1
$f(\frac{m_c^2}{m_b^2})$	3.62	3.25	2.84	2.50	2.23	2.01	1.83	1.70	1.59	1.53	1.50

Table 3.15: *Values of $f(x)$ for several values of m_c/m_b.*

- $\chi^{\rm BLM}$, corresponding to the BLM corrections, is equal to 1.68 for $m_c/m_b=0.3$;
- χ_0, corresponding to the non-BLM corrections, is equal to -1.4 ± 0.4 for $m_c/m_b=0.3$.

The convergence of the perturbative series in Eq. (56) appears problematic. It has been demonstrated that this expansion can be much better controlled – within a few % – using a properly normalized short-distance mass [95,20]. This is the case, for instance, of the kinetic running mass* defined in Eq. (17). Replacing in Eq. (56) the pole quark masses by kinetic running masses through Eq. (17) and expanding in α_s, one obtains:

$$\Gamma(b\to c\ell\overline{\nu}_\ell)=\frac{G_F^2 m_b(\mu)^5|V_{cb}|^2\mathcal{A}_{ew}}{192\pi^3}F(z(\mu))\left[1+a_1(\mu)\frac{\alpha_s(m_b)}{\pi}+a_2(\mu)\left(\frac{\alpha_s(m_b)}{\pi}\right)^2\right], \quad (58)$$

where $z(\mu)=m_c^2(\mu)/m_b^2(\mu)$. A typical value for μ is 1 GeV. The explicit expressions for $a_{1,2}(\mu)$ can be found in [98,97].

2.4.2. Non-perturbative QCD corrections

Non-perturbative corrections in the OPE start at second order in $1/m_Q$ [2]. Including those of $O(1/m_b^2)$ [1,2] and $O(1/m_b^3)$ [63], and changing the scale at which α_s is evaluated to an arbitrary value q, Eq. (58)

*Other definitions for quark masses can be adopted, which do not suffer from problems attached to the pole mass definition, see Sec. 2.1.

becomes:

$$\Gamma(b\to c\ell\overline{\nu}_\ell)=\frac{G_F^2 m_b(\mu)^5|V_{cb}|^2\mathcal{A}_{ew}}{192\pi^3}\quad\left[1+b_1(\mu)\frac{\alpha_s(q)}{\pi}+b_2(\mu,q)\left(\frac{\alpha_s(q)}{\pi}\right)^2\right]\left\{F(z(\mu))\left(1-\frac{\mu_\pi^2}{2m_b^2(\mu)}\right)\right.$$
$$\left.-G(z(\mu))\frac{1}{2m_b^2(\mu)}\left(\mu_G^2-\frac{\rho_{LS}^3}{m_b(\mu)}\right)+H(z(\mu))\frac{\rho_D^3}{6m_b^3(\mu)}\right\}\qquad(59)$$

where $b_1(\mu)=a_1(\mu)$ and $b_2(\mu,q)=a_2(\mu)+a_1(\mu)\frac{\beta_0}{2}\ln\frac{q}{m_b}$, and where we have introduced the functions ($z=(m_c/m_b)^2$)

$$G(z)=3-8z+24z^2-24z^3+5z^4+12z^2\ln z,$$
$$H(z)=77-88z+24z^2-8z^3+5z^4+12(4+3z^2)\ln z.$$

A very recent analysis [97] contains a comprehensive discussion of all the aspects of the Γ_{sl} calculation and several improvements. In particular, it includes BLM corrections to all orders in the scheme with running kinetic masses and non-perturbative parameters. The effect of the resummed BLM corrections is small, 0.1% of the s.l. width, if compared to the perturbative corrections calculated in Eq. (59) at $q=m_b$. Ref. [97] also discusses the role played by four-quark operators containing a pair of charm quark fields in the higher orders of the OPE. These operators give in principle $O(1/m_b^3)$ contributions that are not necessarily negligible and require further study.

In the quark pole mass approach, quark masses are usually re-expressed in terms of heavy hadron masses, using the HQET relation of Eq. (37): the corresponding expression for the s.l. width can be found in [58] and is quoted below for completeness:

$$\Gamma(b\to c\ell\overline{\nu}_\ell)=\frac{G_F^2\overline{M}_B^5|V_{cb}|^2}{192\pi^3}0.3689\ \left[1-1.54\frac{\alpha_s}{\pi}-1.43\beta_0\frac{\alpha_s^2}{\pi^2}-1.648\frac{\overline{\Lambda}}{\overline{M}_B}\left(1-0.87\frac{\alpha_s}{\pi}\right)\right.$$
$$-0.946\frac{\overline{\Lambda}^2}{\overline{M}_B^2}-3.185\frac{\lambda_1}{\overline{M}_B^2}+0.02\frac{\lambda_2}{\overline{M}_B^2}-0.298\frac{\overline{\Lambda}^3}{\overline{M}_B^3}-3.28\frac{\overline{\Lambda}\lambda_1}{\overline{M}_B^3}$$
$$+10.47\frac{\overline{\Lambda}\lambda_2}{\overline{M}_B^3}-6.153\frac{\rho_1}{\overline{M}_B^3}+7.482\frac{\rho_2}{\overline{M}_B^3}-7.4\frac{\mathcal{T}_1}{\overline{M}_B^3}+1.491\frac{\mathcal{T}_2}{\overline{M}_B^3}$$
$$\left.-10.41\frac{\mathcal{T}_3}{\overline{M}_B^3}-7.482\frac{\mathcal{T}_4}{\overline{M}_B^3}+\mathcal{O}\left(\frac{1}{\overline{M}_B^4}\right)\right]\qquad(60)$$

In this equation, $\overline{M}_B=\frac{M_B+3M_{B^*}}{4}=5.313$ GeV and the corresponding value for charmed mesons is taken to be equal to 1.975 GeV. The relations between the parameters used in the two formalisms have been recalled in Eq. (39). The value of μ_G^2 is strongly constrained by the mass splitting between B^* and B mesons, for instance one finds $\mu_G^2(1\text{ GeV})=0.35^{+0.03}_{-0.02}$ GeV^2 [72]. For the other non-perturbative parameters one has to rely on theoretical estimates. Alternately, they can be constrained by measuring other observables: as explained in Sec. 2.2., the moments of differential distributions in b-hadron s.l. decays and the moments of the photon energy distribution in $b\to s\gamma$ decays depend on the same parameters that enter the $|V_{cb}|$ determination. Measurements of these quantities can therefore be used to determine the OPE parameters and to verify the overall consistency of the formalism.

2.4.3. $|V_{cb}|$ determination

The value for $|V_{cb}|$ is obtained by comparing the theoretical and experimental determinations of the inclusive s.l. decay partial width:

$$\Gamma_{sl}|_{th}=\text{BR}_{sl}|_{exp}\times\tau_b|_{exp}\qquad(61)$$

In PDG2000 [99], the uncertainty attached to $|V_{cb}|$ was of $O(5\%)$ and was dominated by the theoretical uncertainty related to the heavy quark parameters. Using the analysis of the first hadronic moment and

the first moment of the photon energy distribution in $b \to s\gamma$ decays mentioned in Sec. 2.2., together with Eq. (60), CLEO has obtained [58]:

$$|V_{cb}| = 40.4 \times (1 \pm 0.022|_{exp} \pm 0.012|_{\overline{\Lambda},\lambda_1} \pm 0.020|_{th}) \times 10^{-3} \tag{62}$$

The first uncertainty corresponds to the experimental measurements of the s.l. branching fraction, of the B^0_d and B^+ fractions as obtained by CLEO, and of the B^0_d and B^+ lifetimes given in PDG2000. The second uncertainty corresponds to the errors on $\overline{\Lambda}$ and λ_1 in the analysis of the moments. The last uncertainty corresponds to the remaining theoretical error coming from contributions of $\mathcal{O}(1/m_b^3)$ and higher order perturbative corrections, estimated from the uncertainty on the scale at which α_s has to be evaluated [†]. It appears that the corresponding variation of $\alpha_s = 0.22 \pm 0.05$ gives the largest contribution (± 0.017). Remaining contributions to the theory error have been obtained by varying the values of parameters contributing at $\mathcal{O}(1/m_b^3)$ within $\pm(0.5)^3$ GeV^3, a rather arbitrary range, based only on naive dimensional analysis.

CLEO's result on $|V_{cb}|$ was improved, at the Workshop, mainly by using all experimental measurements on b-hadron s.l. branching fraction and lifetime [101]. Recent experimental results, made available at the ICHEP 2002 Conference in Amsterdam, and obtained by the LEP experiments [102], by BaBar [103] and by BELLE [104] have been combined [105], including previous measurements of these quantities given in [106]:

$$\begin{aligned}
\Gamma_{sl}|_{\Upsilon(4S)}(b \to X_c \ell^- \overline{\nu}_\ell) &= 0.431 \times (1 \pm 0.019 \pm 0.016) \times 10^{-10}\ \mathrm{MeV} \\
\Gamma_{sl}|_{LEP}(b \to X_c \ell^- \overline{\nu}_\ell) &= 0.438 \times (1 \pm 0.024 \pm 0.015) \times 10^{-10}\ \mathrm{MeV} \\
\Gamma_{sl}|_{Average}(b \to X_c \ell^- \overline{\nu}_\ell) &= 0.434 \times (1 \pm 0.018) \times 10^{-10}\ \mathrm{MeV}
\end{aligned} \tag{63}$$

In these expressions the second contribution to the errors corresponds to uncertainties in the decay modelling and in the subtraction of the $b \to u\ell^-\overline{\nu}_\ell$ component. Using the above result, the corresponding uncertainty in Eq. (62) can be reduced by about a factor two. Keeping the same values for the two remaining uncertainties and correcting for the slightly different central values of BR_{sl} and τ_b, one finds

$$|V_{cb}| = 40.7 \times (1 \pm 0.010|_{exp} \pm 0.012|_{\overline{\Lambda},\lambda_1} \pm 0.020|_{th}) \times 10^{-3} \tag{64}$$

This approach was adopted to obtain the value of $|V_{cb}|$ quoted in the corresponding mini-review [107] of PDG2002 [106][‡]. However, the result quoted in the main CKM section of the PDG2002, $|V_{cb}| = (41.2 \pm 2.0) \times 10^{-3}$, does not take into account this progress, and still assigns a large uncertainty of 2.0×10^{-3}, which is meant to account for possible parton-hadron duality violation.

As summarized in Sec. 2.2., progress has been achieved soon after the Workshop both on theoretical and experimental aspects of the $|V_{cb}|$ determination. On the theoretical side, the moments of the s.l. distributions have been studied using schemes that avoid the problems related to the pole mass [64,65,71]. The inclusion of higher order moments has been reconsidered in [71,65] and, as we have seen, some of the corresponding measurements have been used in these analyses. On the experimental side, new measurements of moments have been presented by BaBar [78], CLEO [75,77], and DELPHI [59].

The analysis of [65] employs first, second, and truncated moments to fit the values of the $\overline{\Lambda}$, λ_1 parameters and obtain constraints on $\mathcal{O}(1/m_b^3)$ contributions. Four different definitions of the heavy quark masses have also been considered. A consistent picture for inclusive b-hadron s.l. decays is obtained when theoretical uncertainties are taken into account, especially if the BaBar preliminary data [78] are excluded. Using the average given in Eq. (63), the result of [65] for $|V_{cb}|$ in the 1S scheme is

$$|V_{cb}| = (41.2 \pm 0.9) \times 10^{-3}. \tag{65}$$

[†] In that analysis the range is taken to be $[m_b/2,\ 2m_b]$.

[‡] In PDG2002, the value given in the corresponding mini-review for $|V_{cb}| = (40.4 \pm 0.5 \pm 0.5 \pm 0.8) \times 10^{-3}$ is slightly different as it depends on the values of experimental results available at that time.

In the analysis of Ref. [71], which is based on DELPHI data and includes third order moments, the low-scale running mass approach is used to extract μ_π^2 and the two parameters contributing at order $\mathcal{O}(1/m_b^3)$. Neither the moments nor $|V_{cb}|$ are actually sensitive to ρ_{LS}^3. The other parameter appearing at this order, $\rho_D^3 = (0.05 \pm 0.05)\ \mathrm{GeV}^3$, is found to be in good agreement with some theoretical expectation (about 0.1 GeV^3 [72]). In the low-scale running mass scheme the uncertainty related to the scale at which α_s is computed has also been reduced with respect to the pole mass analysis. Employing the average s.l. width given in Eq. (63), the result of Ref. [71] is

$$|V_{cb}| = 41.7 \times (1 \pm 0.010|_{exp} \pm 0.015|_{m_b, m_c, \mu_\pi^2, \mu_G^2, \rho_D^3, \rho_{LS}^3} \pm 0.010|_{pert\ QCD} \pm 0.010|_{th}) \times 10^{-3}. \quad (66)$$

The last two uncertainties in this equation are theoretical and correspond to the scale ambiguity for α_s and to possible contributions from $\mathcal{O}(1/m_b^4)$ terms for which an upper limit corresponding to the contribution of the previous order term has been used. The above estimate of the overall theoretical error agrees well with that of [97].

All the results presented in this Section are preliminary. They indicate a promising future for the approach where all non-perturbative parameters, up to order $\mathcal{O}(1/m_b^3)$, are experimentally constrained. Only the preliminary BaBar analysis [78] does not seem to fit the picture: it seems difficult to reconcile the dependence of BaBar first hadronic moment on the lepton momentum cut with the other measurements in the context of the OPE. Although a high lepton momentum cut could in principle spoil the convergence of the power expansion, this point definitely needs to be fully understood.

2.4.4. Prospects

Impressive improvements have been obtained in the determination of $|V_{cb}|$ from inclusive b-hadron s.l. decay measurements during and just after this Workshop. The moments in inclusive s.l. and radiative decays have been studied in new theoretical frameworks. Preliminary analyses of recent experimental measurements of such moments indicate that all parameters contributing to $\mathcal{O}(1/m_b^3)$ included can be constrained by experiment. The results for $|V_{cb}|$ in Eqs. (65) and (66) are very similar. We can adopt a central value given by their average with a 2.3% accuracy:

$$\boxed{|V_{cb}| = 41.4 \cdot (1 \pm 0.018|_{exp} \pm 0.014|_{th}) \times 10^{-3}\ .} \quad (67)$$

in which the largest fraction of the uncertainty depends on experimental measurements. These analyses have to be confirmed, as most of them correspond to preliminary results, and the possible discrepancy raised by BaBar data has to be investigated, especially with respect to the impact of the lepton energy cut, by lowering the cut as much as possible. If the present picture remains valid, more effort has to be invested in the control of remaining theoretical errors, namely $i)$ the uncertainty related to the truncation of the perturbative QCD expansion and $ii)$ the importance of four-quark operators containing the charm quark and of $\mathcal{O}(1/m_b^n),\ n \geq 4$ corrections.

2.5. Review and future prospects for the inclusive determination of $|V_{ub}|$

The charmless s.l. decay channel $b \to u\ell\bar{\nu}$ can in principle provide a clean determination of $|V_{ub}|$ along the lines of that of $|V_{cb}|$. The main problem is the large background from $b \to c\ell\bar{\nu}$ decay, which has a rate about 60 times higher than that for the charmless s.l. decay. The experimental cuts necessary to distinguish the $b \to u$ from the $b \to c$ transitions enhance the sensitivity to the non-perturbative aspects of the decay, like the Fermi motion of the b quark inside the B meson, and complicate the theoretical interpretation of the measurement.

The inclusive decay rate $\mathrm{B} \to X_u\ell\bar{\nu}$ is calculated using the OPE. At leading order, the decay rate is given by the parton model decay rate. As we have seen, non-perturbative corrections are suppressed by at least two powers of $1/m_b$ and to $O(1/m_b^2)$ they are parameterized by the two universal matrix elements

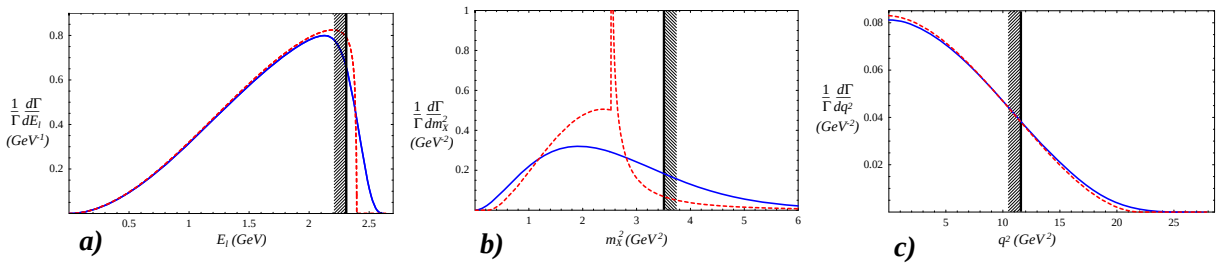

Fig. 3.5: *The distribution of the three main discriminating variables in inclusive* $\mathrm{B} \to X_u \ell \bar{\nu}$ *analyses: lepton energy* E_ℓ *(left), hadronic invariant mass* M_X^2 *(center) and di-lepton invariant mass* q^2 *(right), as given by* $O(\alpha_s)$ *parton level decay (dashed curves), and including the Fermi motion model (solid curves) with typical parameters. The vertical line marks the cut necessary to eliminate the* $b \to c$ *transitions in each case.*

μ_π^2 and μ_G^2 (or λ_1 and λ_2), see Sec. 1.1. At $O(1/m_b^3)$, the Darwin term ρ_D^3 reduces $\Gamma(\mathrm{B} \to l\nu X_u)$ by 1 - 2 %. Perturbative corrections are known through order α_s^2 [108]. All this allows to relate the total inclusive decay rate directly to $|V_{ub}|$ [109]

$$|V_{ub}| = 0.0040 \times (1 \pm 0.03|_{m_b} \pm 0.025|_{QCD}) \left(\frac{\mathrm{BR}(\mathrm{B} \to l\nu X_u)}{0.0016}\right)^{\frac{1}{2}} \left(\frac{1.55 \text{ ps}}{\tau_B}\right)^{\frac{1}{2}} \qquad (68)$$

where in the second error both perturbative and non-perturbative uncertainties are included. The uncertainty due to the b mass assumes $\delta m_b \sim 60$ MeV and can easily be rescaled to accommodate the error in Eq. (26). The errors reported in Eq. (68) are very similar to those given in [25]. In fact, despite the use of slightly different inputs, and of different formalisms, the results of Refs. [109] and [25] are remarkably consistent, their central values differing by only 1.7%. Information from the moments of the s.l. distributions is unlikely to decrease significantly the overall uncertainty in Eq. (68).

The large background from $\mathrm{B} \to X_c \ell \bar{\nu}$ makes the direct measurement of the inclusive rate a very challenging task. In principle, there are several methods to suppress this background and all of them restrict the phase space region where the decay rate is measured. Hence, great care must be taken to ensure that the OPE is valid in the relevant phase space region.

There are three main kinematical cuts which separate the $b \to u\ell\bar{\nu}$ signal from the $b \to c\ell\bar{\nu}$ background:

1. A cut on the lepton energy $E_\ell > (M_B^2 - M_D^2)/2M_B$ [110]
2. A cut on the hadronic invariant mass $M_X < M_D$ [111]
3. A cut on the leptonic invariant mass $q^2 > M_B^2 - M_D^2$ [112]

These cuts correspond to about 10%, 80% and 20% respectively of the signal selected. The simplest kinematical discriminator for $b \to u$ versus $b \to c$ is the endpoint in the ℓ inclusive spectrum, where the first evidence for $|V_{ub}| \neq 0$ was seen [110]. However, in this case the remaining phase space is characterized by $\Delta E_\ell = M_D^2/2M_B = 320$ MeV $\sim \Lambda_{QCD}$. Because of this cut on the lepton energy, the selected hadronic system has large energy and small invariant mass, and is placed in a kinematic region where the OPE is not expected to converge. Measurements done using this method have given [110] $|V_{ub}|/|V_{cb}| = (0.08 \pm 0.02)$, where the 25% error is dominated by the theoretical uncertainty.

In the original analyses [110] several models [113,114] were used to estimate the rate at the endpoint. In fact, the exact fraction of signal decays selected depends strongly on a *shape function*, as illustrated in Fig. 3.5, where the spectrum in the parton model is compared to the one including the structure function. Physically, the *shape or structure function* (sometimes also called light-cone distribution function) encodes the Fermi motion of the b quark inside the B meson, which is inherently

non-perturbative. To estimate the effect of the structure function on the rate measured in the endpoint region, several models for the shape function have been constructed. They are constrained by the values of the first few moments of the shape function, which are related to physical quantities like m_b and $\mu_\pi^2 \sim -\lambda_1$ [115–117]. The model dependence of the measurement can be reduced by noting that the shape function, like the Fermi motion inside the meson, is a universal property of the B meson, independent of the decay process. Consequently, the shape function can in principle be extracted from a different $\mathrm{heavy} \to \mathrm{light}$ process and then employed in the inclusive $\mathrm{B} \to X_u \ell \bar{\nu}$ decay [116–118]. The best way is to use the $\mathrm{B} \to X_s \gamma$ decay. At leading order in $1/m_b$ and α_s, the photon spectrum in the radiative decay is proportional to the light cone distribution function. This strategy for determining $|V_{ub}|$ has three main drawbacks:

- The b quark distribution function is the same in $\mathrm{B} \to l\nu X_u$ and $\mathrm{B} \to \gamma X_s$ only at leading order in $1/m_b$ and in α_s; perturbative QCD corrections complicate its extraction [119,120];
- There are process specific corrections of order $1/m_b$ which still need to be evaluated reliably. In Ref. [121] it is argued that these corrections could be quite sizeable. Even after a precise measurement of the photon spectrum there are unknown and not-calculable contributions $\sim \mathcal{O}(1/m_b)$ in $\mathrm{B} \to l\nu X_u$ which could spoil the accurate extraction of $|V_{ub}|$. It has also been pointed out [122] that there are contributions of dimension six operators, suppressed by $1/m_b^3$, but enhanced by a phase space factor of $16\pi^2$. They arise from so called *weak annihilation* (WA) contributions, and their total contribution survives any cut used to reject the $b \to c\ell\nu$ background. The size of WA contributions is hard to estimate, as very little is known about the values of the relevant four-quark operator matrix elements. They could in principle be constrained by a comparison of B^0 and $\mathrm{B}^\pm$ decay rates. While their impact on the integrated width is modest ($\lesssim 2\%$), in the endpoint region WA terms could give effects of up to 20% [123]. This conclusion, however, is challenged in [124], according to which the uncertainty induced by subleading shape functions is safely below 10%, for lepton energy cuts $E_\ell \leq 2.2$ GeV. See also [118].
- Finally, the endpoint region represents such a narrow slice of the phase space that may be vulnerable to violations of *local* parton-hadron duality.

The first analysis combining $\mathrm{B} \to l\nu X_u$ and $\mathrm{B} \to \gamma X_s$ was performed by CLEO [125]. To account for the distortion of the endpoint spectrum due to the motion of the B mesons, the initial state radiation and the experimental resolution, CLEO fit for the observed data using a theoretical momentum spectrum to model these distortions. They find

$$|\mathrm{V_{ub}}| = (4.12 \pm 0.34 \pm 0.44 \pm 0.23 \pm 0.24) \times 10^{-3}$$

in the lepton momentum range 2.2–2.6 GeV/c. Here the first error combines statistical and experimental uncertainty on the measured rate, the second error is the uncertainty on the fraction of leptons within the acceptance, derived from the uncertainty in the $b \to s\gamma$ shape function, the third error is the theoretical uncertainty on the extraction of $|V_{ub}|$ from the total rate, the fourth error is an estimate of the uncertainty that results from the unknown power corrections in applying the $b \to s\gamma$ shape function to $b \to u\ell\nu$. To evaluate this last uncertainty, the parameters of the shape function are varied by the expected order of the corrections: $\Lambda_{QCD}/M_B \approx 10\%$. Clearly, this sets only the *scale* of that uncertainty.

In principle, the hadronic recoil mass provides the single most efficient kinematical discriminator against the $b \to c\ell\nu$ background. The $b \to c\ell\nu$ background is separated from the signal imposing $M_X < M_D$. After this cut, more than 80% of the signal survives. However, due to the experimental resolution, the $b \to c\ell\nu$ transitions contaminate the $M_X < M_D$ region, and therefore either the cut is lowered, or a different strategy has to be employed. When the cut on the hadronic recoil mass is used, the main theoretical issue arises from the knowledge of the fraction of $b \to u\ell\nu$ events with M_X below a given cut-off mass, M_{cut}:

$$\Phi_{SL}(M_{\mathrm{cut}}) \equiv \frac{1}{\Gamma(B \to l\nu X_u)} \int_0^{M_{\mathrm{cut}}} dM_X \frac{d\Gamma}{dM_X}$$

where $\Phi(0) = 0$ and $\Phi(M_B) = 1$. The M_X spectrum is in fact sensitive to the values of the HQE parameters m_b, μ_π^2, etc. It also depends on the heavy quark shape function, although the dependence is weaker than for the lepton energy in the endpoint region. To set the scale of the problem: a very rough estimate for $\Phi_{SL}(1.7\ \mathrm{GeV})$ lies between 0.55 and 0.9; i.e. a measurement of $\Phi_{SL}(1.7\ \mathrm{GeV})$ yields a value for $|V_{ub}|$ with *at most* a $\pm 12\%$ uncertainty, and possibly less. The actual uncertainty in realistic experimental analyses has been estimated by the experimental collaborations. Since a cut on the hadronic invariant mass allows for a much larger portion of the decay rate to survive, the uncertainties from weak annihilation contributions are safely below the 5% level. The subleading shape functions contributions can in this case be analysed using the same method as in [121]. A preliminary discussion can be found in [118].

The above observations motivated an intense effort to measure $|V_{ub}|$ using inclusive analyses at LEP, where B hadrons are produced with a large and variable momentum and in most of the cases the B decay products are contained into narrow jets in $Z^0 \to b\bar{b}$ events. These characteristics make the LEP measurements complementary to the ones at the $\Upsilon(4S)$. All four LEP experiments have provided a measurement of $|V_{ub}|$ using inclusive methods, although the actual procedures differ significantly.

DELPHI [126] perform an inclusive reconstruction of the hadronic mass of the system emitted together with the lepton in the B hadron decay. The B s.l. sample is split into $b \to u\ell\nu$ enriched and depleted samples based on the separation between tertiary and secondary vertices (taking advantage of the finite charm lifetime) and on the presence of tagged kaons in the final state. The mass of the hadronic system M_X is used to subdivide further the sample into a $b \to X_u\ell\nu$–favoured region ($M_X < 1.6$ GeV) and a $b \to X_c\ell\nu$–dominated region. The signal is extracted from a simultaneous fit to the number of decays classified according to the four different categories and the distributions of the lepton energy in the reconstructed B rest frame.

The leptonic invariant mass, $q^2 = (p_\ell + p_\nu)^2$, can also suppress the $b \to c$ background [112]. This cut allows to measure $|V_{ub}|$ without requiring knowledge of the structure function of the B meson (see Fig. 3.5c). The acceptance of this cut on q^2 can be calculated using the usual local OPE. Depending on the value of the cut, the fraction of selected signal events can range between 10 and 20%, but the theoretical uncertainty on $|V_{ub}|$, dominated by higher order power corrections, can range from 15% for $q^2_{\mathrm{cut}} = M_B^2 - M_D^2 = 11.6\,\mathrm{GeV}^2$ to 25% for $q^2_{\mathrm{cut}} = 14\,\mathrm{GeV}^2$ (see also [127]). The q^2 method allows to measure $|V_{ub}|$, albeit with larger uncertainties than when one combines the lepton energy or the hadron invariant mass cut with data from $\mathrm{B} \to X_s\gamma$ decay.

Recently, a strategy relying on the combination of q^2 and M_X cuts has been proposed [128]. The M_X cut is used to reject the charm background, while the q^2 cut is used to eliminate the high energy, low invariant mass region. Rejecting the region at small q^2 reduces the impact of the shape function in the M_X analysis. Strong interaction effects on M_X are maximal there due to the significant recoil [128]. Imposing, for instance, $q^2 \geq 0.35 m_b^2$ eliminates the impact of the primordial Fermi motion encoded in $M_X < 1.7$ GeV events. Up to 50% of all $\mathrm{B} \to X_u\ell\bar{\nu}$ events survive this cut, making possible to measure $|V_{ub}|$ with uncertainties safely below the 10% level.

CLEO has presented the first experimental attempt to implement this method [129]. The analysis is based on a full fit to $q^2/(E_\ell + E_\nu)^2$, M_X and $\cos\theta_{W\ell}$. Models are needed to extract the sample composition and to relate the regions of higher sensitivity and theoretically safer to the inclusive charmless s.l. branching fraction. However, imposing these additional cuts has drawbacks. The overall energy scale governing the intrinsic hardness of the reaction gets smaller since it is driven at large q^2 by $m_b - \sqrt{q^2}$ rather than m_b. This enhances the impact of higher-order contributions which are not calculated, like in the case of the direct cut on q^2. Furthermore, cutting simultaneously on M_X and q^2 decreases the fraction of the full width retained in the sample, and exposes the calculation to violations of duality. Finally, the cut on q^2 removes the possibility to incorporate in full the constraints on the spectrum which follow from the properties of the shape function, because it dissolves the connection between the M_X spectrum and the shape function.

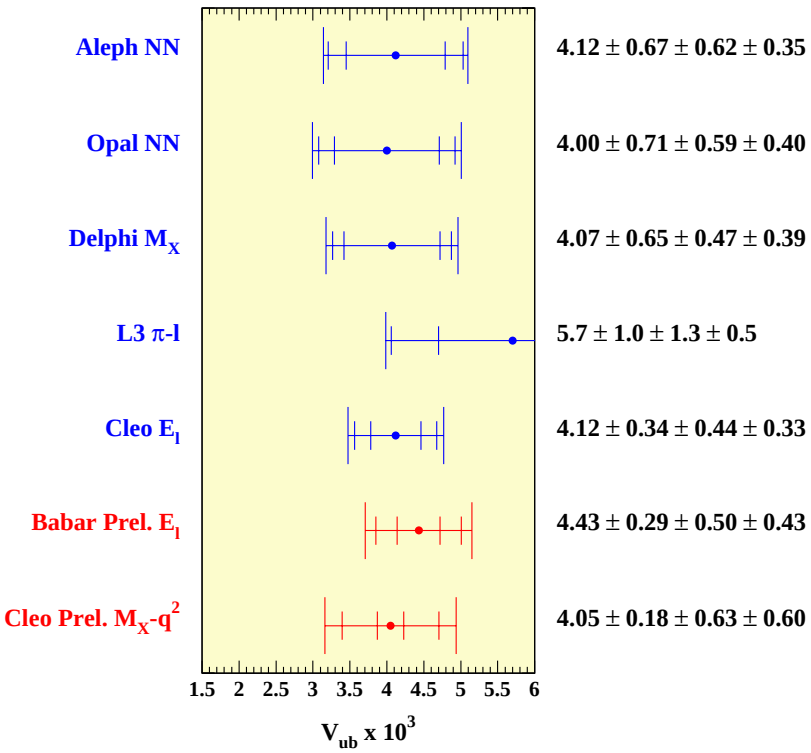

Fig. 3.6: *Summary of the inclusive determinations of* $|V_{ub}|$.

Yet another approach has been followed by the ALEPH and OPAL collaborations in their analyses [130]. They use neural networks, which input a large number of kinematic variables (20 in ALEPH, 7 in OPAL) to discriminate between the $b \to c\ell\nu$ and the $b \to u\ell\nu$ decays. In both experiments, the signal is extracted from a fit to the network output, restricted to a region enriched in signal events. The observation of s.l. $b \to u\ell\nu$ decays at LEP has been very challenging. These analyses pioneered new approaches for extracting $|V_{ub}|$. Their main drawback is the S/B ratio, that requires the control of the background level to better than 5% . Concerns, discussed within the community, include the modelling of the uncertainties on the non-D and D* components of the background from B decays, the modelling of the $\mathrm{B_s}$ and b-baryon s.l. decays and the estimation of the $b \to u\ell\nu$ modelling uncertainties due to the uneven sampling of the decay phase space.

Since tight selections are needed to extract the signal, the effects of these experimental cuts trimming the inclusive distributions must be understood. In particular, it is important to make sure the the inclusive analyses are probing the selected phase space in an even and uniform way. Neural network analyses bias the phase space toward the region of large E_ℓ and low M_X, where the signal-to-background ratio is larger. The uncertainty quoted by ALEPH accounts for the range of models tested. In this case, it would be desirable to test more unbiased methods. DELPHI, on the other hand, has shown that the M_X analysis has a reasonably uniform sensitivity in the M_X-E_ℓ plane and a recent CLEO analysis, repeated for different sets of M_X-q^2 selections, finds results compatible with LEP.

Finally, L3 applies a sequential cut analysis using the kinematics of the lepton and of the leading hadron in the same jet for discrimination of the signal events [131]. The uncertainty (see Fig. 3.6) is larger than in other analyses, mainly because the result depends on a few exclusive final states only.

All the analyses discussed in this Section have an individual accuracy of about 15% and, as can be seen in Fig. 3.6, their central values agree within that uncertainty. One can distinguish two sets of inclusive determinations of $|V_{ub}|$ which rely on roughly the same theoretical assumptions and are extracted within the same OPE framework. The LEP inclusive results have been averaged accounting for correlated systematics. The uncertainty of the CLEO determination from the lepton end-point and the

$b \to s\gamma$ spectrum can be re-expressed in a way corresponding to that used for the LEP averaging. The results read

$$\boxed{\begin{array}{l} |V_{ub}|^{incl}_{LEP} = [4.09^{+0.36\,+0.42\,+0.24}_{-0.39\,-0.47\,-0.26} \pm 0.21] \times 10^{-3}, \\ |V_{ub}|^{incl}_{CLEO} = [4.08 \pm 0.44 \pm 0.27 \pm 0.33 \pm 0.21] \times 10^{-3}, \end{array}} \tag{69}$$

where the first error corresponds to statistical and experimental systematics, the second to the dominant $b \to c$ background, the third to $b \to u$ modelling, and the last one to the relation between $|V_{ub}|$ and the branching fraction, see Eq. (68). A first exercise aimed at understanding the relationship between the different sources of systematics in these determinations and to obtain a global average was started at the workshop. A conservative approach consists in taking the systematic uncertainties as fully correlated. This combined result has a total uncertainty of $\pm 14\%$ and is used in Chapter 5 (see Table 5.1). However, the uncertainties are only partly correlated and more precise measurements are becoming available: once the systematics and their correlation are better understood there is room for considerable improvement.

As the B factories start focusing on the inclusive measurements of $|V_{ub}|$, there is potential for considerable progress. A more precise evaluation of the $b \to s\gamma$ photon spectrum will lead to a more precise effective shape function and we now have several methods to employ it efficiently in the extraction of $|V_{ub}|$. A recent proposal [132], for instance, uses the s.l. differential distribution in M_X/E_X together with the $b \to s\gamma$ photon spectrum to build a short distance ratio from which $|V_{ub}|/|V_{cb}|$ can be extracted, testing at the same time some of the underlying assumptions. The use of event samples with one fully reconstructed B will reduce the contamination from $b \to c\ell\bar{\nu}$ decays in the reconstruction of the hadronic recoil mass and of q^2 and will allow for useful cross-checks [133]. Hence, experimental uncertainties should be reduced. If the various methods will give consistent central values while their precision improves, we will be confident that theoretical uncertainties are not biasing $|V_{ub}|$ beyond the level of precision which has been reached in the individual measurements.

3. Exclusive determination of $|V_{cb}|$

As we have seen in the previous section, inclusive $b \to c$ semileptonic (s.l.) decay rates have a solid description via the OPE. Exclusive s.l. decays have a similarly solid description in terms of heavy-quark effective theory (HQET). The main difference is that the non-perturbative unknowns in the inclusive rates can be determined from experimental measurements, while those arising in exclusive rates must be calculated. Thus, there is a major theoretical challenge here as non-perturbative QCD calculations have to performed. Experimentally, the D and D* mesons have to be reconstructed using several decay channels, to gain in statistics, and the signal has to be isolated from higher excited states. Moreover, the theory is under best control at the kinematic endpoint, where the rate vanishes. Consequently, not only must the differential decay rate be measured, it also must be extrapolated to the endpoint. Despite these experimental difficulties, and given the ongoing progress in lattice QCD, these channels provide a valuable cross-check at present and hold considerable promise for the future.

The exclusive determination of $|V_{cb}|$ is obtained by studying $\mathrm{B} \to \mathrm{D}^*\ell\nu$ and $\mathrm{B} \to \mathrm{D}\ell\nu$ decays, where ℓ stands for either e or μ. The differential rates for these decays are given by

$$\begin{aligned} \frac{d\Gamma(\mathrm{B} \to \mathrm{D}^*\ell\nu)}{dw} &= \frac{G_\mu^2 |V_{cb}|^2}{48\pi^3} \eta_{\mathrm{EW}}^2 \, (M_B - M_{D^*})^2 \, M_{D^*}^3 (w^2-1)^{1/2} (w+1)^2 \\ &\quad \times \left[1 + \frac{4w}{w+1} \, \frac{1 - 2w\, r_* + r_*^2}{(1-r_*)^2} \right] |\mathcal{F}(w)|^2 \,, \end{aligned} \tag{70}$$

$$\frac{d\Gamma(\mathrm{B} \to \mathrm{D}\ell\nu)}{dw} = \frac{G_\mu^2 |V_{cb}|^2}{48\pi^3} \eta_{\mathrm{EW}}^2 \, (M_B + M_D)^2 \, M_D^3 (w^2-1)^{3/2} |\mathcal{G}(w)|^2 \,, \tag{71}$$

where $w = v_B \cdot v_{D^{(*)}}$ is the product of the velocities of the initial and final mesons, and $r_* = M_{D^*}/M_B$. The velocity transfer is related to the momentum q transferred to the leptons by $q^2 = M_B^2 - 2wM_BM_{D^{(*)}} + M_{D^{(*)}}^2$, and it lies in the range $1 \le w < (M_B^2 + M_{D^{(*)}}^2)/2M_BM_{D^{(*)}}$. Electroweak radiative corrections introduce the muon decay constant $G_\mu = 1.1664 \times 10^{-5}$ GeV^{-2} (instead of G_F) and the factor $\eta_{\rm EW}^2$ (see Sec. 3.4.).

In the heavy-quark limit, the form factors $\mathcal{F}(w)$ and $\mathcal{G}(w)$ coincide with the Isgur-Wise function $\xi(w)$, which describes the long-distance physics associated with the light degrees of freedom in the heavy mesons [8,9]. This function is normalized to unity at zero recoil, corresponding to $w = 1$. There are corrections to heavy-quark limit from short distances, which can be calculated in perturbation theory in $\alpha_s(\sqrt{m_c m_b})$. There are also corrections from long distances, which are suppressed by powers of the heavy quark masses. The separation of the two sets of contributions can be achieved with HQET, which is reviewed, for example, in [12,13]. The calculation of the small corrections to this limit is explained below in Secs. 3.2. and 3.3. With a satisfactory calculation of these corrections, $|V_{cb}|$ can be determined accurately by extrapolating the differential decay rates to $w = 1$, yielding $|V_{cb}|\mathcal{F}(1)$ and $|V_{cb}|\mathcal{G}(1)$. Uncertainties associated with this extrapolation can be reduced using model-independent constraints on the shape of the form factors, derived with dispersive methods. These techniques are briefly reviewed in Sec. 3.1.

At present $\mathrm{B} \to \mathrm{D}^*\ell\nu$ transitions yield a more precise value of $|V_{cb}|$ than $\mathrm{B} \to \mathrm{D}\ell\nu$. The statistics are three times higher. More importantly, phase space suppresses $\mathrm{B} \to \mathrm{D}^*\ell\nu$ by only $(w-1)^{1/2}$, but $\mathrm{B} \to \mathrm{D}\ell\nu$ by $(w-1)^{3/2}$. Finally, the theoretical calculation of $\mathcal{F}(1)$ is under better control than that of $\mathcal{G}(1)$. Nevertheless, $\mathrm{B} \to \mathrm{D}\ell\nu$ provides a useful check. For example, $|V_{cb}|$ drops out of the (experimental) ratio $|V_{cb}|\mathcal{F}(1)/|V_{cb}|\mathcal{G}(1)$, which can be used to test the theoretical calculations.

3.1. Theory-guided extrapolation in w

Dispersive methods allow the derivation of rigorous, model-independent constraints on the form factors in exclusive s.l. or radiative decays. The derivation is based on first principles: the analyticity properties of two-point functions of local current operators and the positivity of the corresponding hadronic spectral functions. Analyticity relates integrals of these spectral functions to the behaviour of the two-point functions in the deep Euclidean region, where they can be calculated using the operator product expansion. Positivity guarantees that the contributions of the states of interest to these spectral functions are bounded from above. Constraints on the relevant form factors are then derived, given the latter's analyticity properties. The beauty of these techniques is that the bounds can be improved with information about the form factors, such as their value or derivatives at different kinematic points, or their phase along various cuts. These techniques also have the advantage that the constraints they yield are optimal for any given input.

Here we focus on the application of these methods to $\mathrm{B} \to \mathrm{D}^{(*)}\ell\nu$ decays. The first such application was carried out in [136], where three-parameter descriptions of the corresponding differential decay rates were presented. In [137], it was shown how a judicious change of variables can be used to reduce the number of parameters. The most recent analyses [138,139] take two-loop and non-perturbative corrections to the relevant two-point correlators into account and make use of heavy-quark spin symmetry in the ground-state doublets $(\mathrm{B}, \mathrm{B}^*)$ and $(\mathrm{D}, \mathrm{D}^*)$. Ref. [139] uses spin symmetry more extensively, and accounts for the dominant $1/m_Q$ and radiative corrections. The results are one-parameter descriptions of the form factors $\mathcal{G}(w)$ and $A_1(w) = \mathcal{F}(w)/\mathcal{K}(w)$, with $\mathcal{K}(w)$ defined below in Eq. (73), that are accurate to better than 2% over the full kinematic range.

In the case of $\mathrm{B} \to \mathrm{D}^*\ell\nu$ transitions, it is convenient to constrain the form factor $A_1(w)$ instead of $\mathcal{F}(w)$ in order to avoid large, kinematically enhanced corrections to the heavy-quark limit. This yields

for $\mathcal{F}(w)$ [139]:

$$\frac{\mathcal{F}(w)}{\mathcal{F}(1)} \approx \mathcal{K}(w)\left\{1 - 8\rho^2_{A_1} z + (53.\rho^2_{A_1} - 15.)z^2 - (231.\rho^2_{A_1} - 91.)z^3\right\}\,, \tag{72}$$

with z given in Eq. (76) and where the only parameter, the slope parameter $\rho^2_{A_1}$ of $A_1(w)$ at zero recoil, is constrained by the dispersive bounds to lie in the interval $-0.14 < \rho^2_{A_1} < 1.54$. This constraint on $\rho^2_{A_1}$ is somewhat weaker than the one derived from the inclusive heavy-quark sum rules of Bjorken [143] and Voloshin [144] which require $0.4 \leq \rho^2_{A_1} \leq 1.3$ once $O(\alpha_s)$ corrections have been included [145]. A stronger lower bound has been derived by Uraltsev [146]. This is to be compared with the world experimental average $\rho^2_{A_1} = 1.50 \pm 0.13$ given in Sec. 3.6.1.

In Eq. (72), the function $\mathcal{K}(w)$ is

$$\mathcal{K}(w)^2 = \frac{2\,\dfrac{1 - 2wr_* + r_*^2}{(1-r_*)^2}\left[1 + \dfrac{w-1}{w+1}\,R_1(w)^2\right] + \left[1 + \dfrac{w-1}{1-r_*}\Big(1 - R_2(w)\Big)\right]^2}{1 + \dfrac{4w}{w+1}\,\dfrac{1 - 2wr_* + r_*^2}{(1-r_*)^2}}, \tag{73}$$

where r_* is given after Eq. (71), and $R_1(w)$ and $R_2(w)$ describe corrections to the heavy-quark limit. They are usually expanded in Taylor series around $w = 1$. Using QCD sum rules [140,141,142] one finds [139]

$$\begin{aligned} R_1(w) &\approx 1.27 - 0.12(w-1) + 0.05(w-1)^2\,, \\ R_2(w) &\approx 0.80 + 0.11(w-1) - 0.06(w-1)^2\,. \end{aligned} \tag{74}$$

The sum-rule calculation is supported by measurements reported by the CLEO Collaboration [188], $R_1(1) = 1.18 \pm 0.30 \pm 0.12$ and $R_2(1) = 0.71 \pm 0.22 \pm 0.07$. These values are obtained assuming that $R_1(w)$ and $R_2(w)$ are constant in w and that $A_1(w)$ is linear in w. CLEO also find that $R_1(1)$ and $R_2(1)$ are not sensitive either to the form of $A_1(w)$ or the w dependence of the form factors, consistent with the mild w dependence in Eq. (74). Note that the extractions of $|V_{cb}|$ by CLEO and BELLE discussed in Sec. 3.6.1. use CLEO's measurements of $R_1(1)$ and $R_2(1)$.

For $\mathrm{B} \to \mathrm{D}\ell\nu$ decays, the parametrization of [139] is

$$\frac{\mathcal{G}(w)}{\mathcal{G}(1)} \approx 1 - 8\rho^2_{\mathcal{G}} z + (51.\rho^2_{\mathcal{G}} - 10.)z^2 - (252.\rho^2_{\mathcal{G}} - 84.)z^3\,, \tag{75}$$

with

$$z = \frac{\sqrt{w+1} - \sqrt{2}}{\sqrt{w+1} + \sqrt{2}}\,, \tag{76}$$

and where the only parameter, the slope parameter $\rho^2_{\mathcal{G}}$ at zero recoil is constrained by the dispersive bounds to lie in the interval $-0.17 < \rho^2_{\mathcal{G}} < 1.51$ which can be compared with the world experimental average $\rho^2_{\mathcal{G}} = 1.19 \pm 0.19$ given in Sec. 3.6.2.

It is interesting to note that heavy quark symmetry breaking in the difference of the slope and curvature parameters of the form factors $\mathcal{F}(w)$ and $\mathcal{G}(w)$, together with measurements of the ratios R_1 and R_2 may strongly constrain the calculations which determine $\mathcal{F}(1)$ and $\mathcal{G}(1)$ [189]. More importantly, a better knowledge of the slope parameters will reduce the error on $|V_{cb}|$, because of the large correlation between the two parameters [189] (see Fig. 3.8).

3.2. Theoretical calculations of the form factor $\mathcal{F}(1)$ for $B \to D^* \ell\nu$ decays

The zero-recoil form factor $\mathcal{F}(1)$ must be calculated non-perturbatively in QCD. At zero recoil ($w = 1$), all $B \to D^* \ell\nu$ form factors but h_{A_1} are suppressed by phase space, and

$$\mathcal{F}(1) = h_{A_1}(1) = \langle D^*(v)|A^\mu|\overline{B}(v)\rangle, \tag{77}$$

where A^μ is the $b \to c$ axial vector current. Thus, the theoretical information needed is contained in one relatively simple hadronic matrix element, which heavy-quark symmetry [7,8,9] requires to be close to unity. Heavy-quark *spin* symmetry would imply $\langle D^*(v)|A^\mu|\overline{B}(v)\rangle = \langle D(v)|V^\mu|\overline{B}(v)\rangle$, where V^μ is the $b \to c$ vector current. If, in addition, heavy-quark *flavor* symmetry is used, these amplitudes can be equated to $\langle B(v)|V^\mu|\overline{B}(v)\rangle$. The last matrix element simply counts the number of b quarks in a $\overline{B}$ meson and is, hence, exactly 1. Deviations from the symmetry limit arise at short distances, from the exchange of gluons with $m_c < k < m_b$, and also at long distances. Short-distance corrections are suppressed by powers of $\alpha_s(\sqrt{m_c m_b})$, and long-distance corrections are suppressed by powers of the heavy-quark masses. The heavy-quark symmetries also require the corrections of order $1/m_Q$ to vanish, a result known as Luke's theorem [147]. In summary, thanks to heavy-quark symmetry, uncertainties from treating the long-distance, non-perturbative QCD are suppressed by a factor of order $(\bar{\Lambda}/2m_c)^2 \sim 5\%$, where $\bar{\Lambda} \sim 500$MeV is the contribution of the light degrees of freedom to the mass of the mesons. Owing to these constraints from heavy-quark symmetry, the exclusive technique is sometimes called model-independent [134], but in practice model dependence could appear at order $1/m_c^2$, through estimates of the deviation of $h_{A_1}(1)$ from 1.

To date three methods have been used to estimate $h_{A_1}(1) - 1$. One approach starts with a rigorous inequality relating the zero-recoil form factor to a spectral sum over excited states [148,21]. Here some contributions can be measured by moments of the inclusive s.l. decay spectrum (cf. Sec. 2.4.), but others can be estimated only qualitatively. The other two methods both start with HQET to separate long- and short-distance contributions [149]. The short-distance contributions are calculated in perturbative QCD. The long-distance contributions are intrinsically non-perturbative. Several years ago they were estimated in a non-relativistic quark model [149,135]. More recently, the HQET technique has been adapted to lattice gauge theory [150,151], and an explicit calculation, in the so-called quenched approximation, has appeared [152].

The three methods all quote an uncertainty on $\mathcal{F}(1)$, and hence $|V_{cb}|$, of around 4%. The errors arising in the sum rule and the quark model calculations are difficult to quantify and do not appear to be reducible. In the lattice gauge theory calculations, there are several ways to reduce the error, notably by removing the quenched approximation and in improving the matching of lattice gauge theory to HQET and continuum QCD. It is conceivable that one could reduce the uncertainty to the percent level over the next few years.

3.2.1. Sum rule method

Here the main result of a sum rule that puts a rigorous bound on $h_{A_1}(1)$ is quoted. For a lucid and brief derivation, the reader may consult a classic review of the heavy-quark expansion [153]. Based on the optical theorem and the operator-product expansion, one can show that

$$|h_{A_1}(1)|^2 + \frac{1}{2\pi}\int_0 d\epsilon\, w(\epsilon) = 1 - \Delta_{1/m^2} - \Delta_{1/m^3} \tag{78}$$

where $\epsilon = E - M_{D^*}$ is the relative excitation energy of higher resonances and non-resonant $D\pi$ states with $J^{PC} = 1^{-+}$, and $w(\epsilon)$ is a structure function for the vector channel. The contributions Δ_{1/m^n} describe corrections to the axial vector current for finite-mass quarks. The excitation integral is related to finite-mass corrections to the bound-state wave functions—hence the "sum" over excited states. The Δ_{1/m^n} and the excitation integral are positive, so Eq. (78) implies $|h_{A_1}(1)| < 1$.

Let first consider the excitation integral. For $\epsilon \gg \bar{\Lambda}$, the hadronic states are dual to quark-gluon states. Introducing a scale μ to separate this short-distance part from the long-distance part (which must be treated non-perturbatively), one writes

$$\frac{1}{2\pi}\int_0 d\epsilon\, w(\epsilon) = \frac{1}{2\pi}\int_0^\mu d\epsilon\, w(\epsilon) + [1-\eta_A^2(\mu)]. \tag{79}$$

Here the short-distance quantity $\eta_A(\mu)$ lumps together the short-distance ($\epsilon > \mu$) contribution. Then, rearranging Eq. (78),

$$h_{A_1}(1) = \eta_A(\mu) - \frac{1}{2}\Delta_{1/m^2} - \frac{1}{2}\Delta_{1/m^3} - \frac{1}{4\pi}\int_0^\mu d\epsilon\, w(\epsilon) \tag{80}$$

and $\eta_A(\mu)$ is computed perturbatively (to two loops [154]). The other contributions arise from long distances and must be taken from other considerations. There is a good handle on the second term on the right-hand side of Eq. (80), namely,

$$\Delta_{1/m^2} = \frac{\mu_G^2}{3m_c^2} + \frac{\mu_\pi^2(\mu)-\mu_G^2}{4}\left(\frac{1}{m_c^2} + \frac{2/3}{m_c m_b} + \frac{1}{m_b^2}\right), \tag{81}$$

where μ_G^2 and $\mu_\pi^2(\mu)$ are matrix elements of the chromomagnetic energy and kinetic energy (of the b quark) in the $\overline{\rm B}$ meson. Note that the kinetic energy μ_π^2 depends on the scale μ. Apart from subtleties of renormalization conventions, μ_G^2 and $\mu_\pi^2(\mu)$ are related to the quantities λ_2 and λ_1, given in the discussion of inclusive s.l. decays. Ignoring this subtlety for the moment, $\mu_G^2 = 3\lambda_2 = 3(M_{B^*}^2 - M_B^2)/4$ and $\mu_\pi^2 = -\lambda_1$. The last term in Eq. (80), from higher hadronic excitations, is unconstrained by data.

To make a numerical determination, one must choose a conventional value for the separation scale to μ, usually 1 GeV. The choice of μ alters $\eta_A(\mu)$ and $\mu_\pi^2(\mu)$, as well as the excitation integral, in ways that can be computed in perturbative QCD. A recent review [4] of the heavy quark expansion takes

$$\frac{1}{4\pi}\int_0^{1\ {\rm GeV}} d\epsilon\, w(\epsilon) = 0.5 \pm 0.5, \tag{82}$$

but emphasises that this is a heuristic estimate. Ref. [4] found $h_{A_1}(1) = 0.89 \pm 0.04$, using a then-current value of μ_π^2. With CLEO's analysis of moments of the inclusive s.l. decay spectrum in hand, one can convert that determination of λ_1 to a determination of $\mu_\pi^2(1\ {\rm GeV})$. The updated sum-rule becomes [4]

$$\mathcal{F}(1) = h_{A_1}(1) = 0.900 \pm 0.015 \pm 0.025 \pm 0.025, \tag{83}$$

where the uncertainties are, respectively, from the two-loop calculation of $\eta_A(1\ {\rm GeV})$, the excitation integral [*i.e.*, Eq. (82)], and an estimate of Δ_{1/m^3} based on dimensional analysis. The uncertainty from $\eta_A(\mu)$ could be reduced, in principle, with a three-loop calculation, but it is already smaller than the other two, which appear to be irreducible.

3.2.2. HQET-based methods

The main drawback of the sum rule method is that the excitation integral is not well constrained. Using HQET one can characterize it in more detail. Based on heavy-quark symmetry one can write

$$h_{A_1}(1) = \eta_A\left[1 + \delta_{1/m^2} + \delta_{1/m^3}\right] \tag{84}$$

where η_A is a short-distance coefficient, which is discussed in more detail below. Heavy-quark symmetry implies the normalization of the first term in brackets [8,9] and the absence of a correction $\delta_{1/m}$ of

order $1/m_Q$ [147]. The corrections δ_{1/m^n} of order $1/m_Q^n$ contain long-distance matrix elements. Simply from enumerating possible terms at second and third order, they have the structure

$$\delta_{1/m^2} = -\frac{\ell_V}{(2m_c)^2} + \frac{2\ell_A}{(2m_c)(2m_b)} - \frac{\ell_P}{(2m_b)^2}, \tag{85}$$

$$\delta_{1/m^3} = -\frac{\ell_V^{(3)}}{(2m_c)^3} + \frac{\ell_A^{(3)}\Sigma}{(2m_c)(2m_b)} + \frac{\ell_D^{(3)}\Delta}{(2m_c)(2m_b)} - \frac{\ell_P^{(3)}}{(2m_b)^3}, \tag{86}$$

where $\Sigma = 1/(2m_c) + 1/(2m_b)$ and $\Delta = 1/(2m_c) - 1/(2m_b)$.

HQET is a systematic method for separating out the long- and short-distance corrections to the symmetry limit, making efficient use of the constraints of heavy-quark symmetry. It provides a detailed description of the ℓs [149,158], of the form

$$\ell_X = \sum_i c_i(\mu)\mathcal{M}_i(\mu), \tag{87}$$

where the $c_i(\mu)$ are short-distance coefficients and the $\mathcal{M}_i(\mu)$ matrix elements defined in the effective field theory. The scale μ is now the renormalization scale of HQET. Some contributions on the right-hand side come from the $1/m_Q$ expansion of the physical B and D^* mesons and others from the expansion of the axial vector current. The latter coincide with the λ_1 and λ_2 (or μ_π^2 and μ_G^2) terms in Eq. (81). The long-distance corrections of the states are, in Eq. (80), contained in $\int_0^\mu d\epsilon w(\epsilon)$.

It is well-known that intermediate quantities defined in effective field theories depend on the renormalization scheme, but physical quantities do not. We dwell on it briefly here, for reasons that will become clear below. At one-loop level, the short-distance coefficient is

$$\eta_A(c) = 1 + \frac{4}{3}\frac{\alpha_s}{4\pi}\left[3\frac{m_b+m_c}{m_b-m_c}\ln\frac{m_b}{m_c} - 8\right] + \frac{4}{3}\frac{\alpha_s}{4\pi}c\mu^2\left(\Delta^2 + 2\Sigma^2\right) \tag{88}$$

where the constant c is characteristic of the scheme for renormalizing operators in HQET. In minimal subtraction schemes $c = 0$, whereas the energy cutoff in Eq. (79) implies $c = 4/3$ (cf. Eq. (19)). Similarly, the scheme (and μ) dependence of the ℓs is, to order α_s,

$$\ell_V(c) = \ell_V(0) + \frac{4}{3}\frac{\alpha_s}{4\pi}3c\mu^2, \tag{89}$$

$$\ell_A(c) = \ell_A(0) - \frac{4}{3}\frac{\alpha_s}{4\pi}\,c\mu^2, \tag{90}$$

$$\ell_P(c) = \ell_P(0) + \frac{4}{3}\frac{\alpha_s}{4\pi}3c\mu^2. \tag{91}$$

Combining the above formulae, one can check that the scheme dependence drops out of $h_{A_1}(1)$.

As long as one is careful to keep track of the scheme, it does not matter which is used. For many purposes it is simplest to define all operator insertions in minimal subtraction, for which $c = 0$. This is not a problem, as long as one knows how to calculate the ℓs in the same scheme. (For example, the $-\lambda_1$ and μ_π^2 are defined by the same HQET matrix element, renormalized such that $c = 0$ and $4/3$, respectively.)

The HQET formalism does not provide numerical estimates for the ℓs: that requires a non-perturbative approach to QCD. The first estimates [149,135] used the non-relativistic quark model, which, though not QCD, can be a useful guide and tends to yield rather small δ_{1/m^2}. The more recent of these estimates [135] takes δ_{1/m^2} to be -0.055 ± 0.025, and relies on sum rule constraints. Combining it with the two-loop calculation of η_A [155,156], one obtains

$$\mathcal{F}(1) = h_{A_1}(1) = 0.907 \pm 0.007 \pm 0.025 \pm 0.017, \tag{92}$$

where the quoted uncertainties [135,155] are from perturbation theory, errors in the quark model estimate of the $1/m_Q^2$ terms, and the omission of $1/m_Q^3$ terms. Uncertainties from α_s and the quark masses are not included. This result does not pay close attention to the scheme dependence mentioned above, because it uses the standard ($c = 0$) result for η_A, corresponding to a minimal subtraction definition of the matrix elements in Eq. (87). The quark model, on the other hand, presumably yields the ℓs in some other scheme (with unknown $c \neq 0$). In that case, Eq. (92) over- or undercounts the contribution at the interface of long and short distances. Moreover, we note that estimates of the perturbative error based on BLM resummation [157,66] are larger than in Eq. (92).

Now let us turn to the recent lattice calculation of $h_{A_1}(1)$. A direct calculation of the matrix element $\langle \mathrm{D}^*|A^\mu|\mathrm{B}\rangle$ in Eq. (77) would be straightforward, but not interesting: similar matrix elements like $\langle 0|A^\mu|\mathrm{B}\rangle$ and $\langle \pi|V^\mu|\mathrm{B}\rangle$ have 15–20% errors [159]. One must involve heavy-quark symmetry from the outset: if one can focus on $h_{A_1} - 1$, there is a chance of success, because a 20% error on $h_{A_1} - 1$ is interesting. The key here is to observe that lattice gauge theory with Wilson fermions has the same heavy-quark symmetries as continuum QCD, for all $m_Q a$ [160]. Consequently, one can build up a description of lattice gauge theory using HQET, with the same logic and structure as above [150,151,161]. In this description the ℓs in Eqs. (85) and (86) are the same as for continuum QCD, apart from lattice effects on the light quarks and gluons. Discretization effects of the heavy quark appear at short distances, where perturbation theory can be used. Thus, the principal change from the usual application of HQET is in the short-distance coefficients.

To calculate the ℓs in lattice gauge theory, one needs some quantities with small statistical and normalization errors, whose heavy-quark expansion contains the ℓs. Work on $\mathrm{B} \to \mathrm{D}$ form factors [162] showed that certain ratios have the desired low level of uncertainty. For the problem at hand one needs

$$\frac{\langle \mathrm{D}|\bar{c}\gamma^4 b|\mathrm{B}\rangle\langle \mathrm{B}|\bar{b}\gamma^4 c|\mathrm{D}\rangle}{\langle \mathrm{D}|\bar{c}\gamma^4 c|\mathrm{D}\rangle\langle \mathrm{B}|\bar{b}\gamma^4 b|\mathrm{B}\rangle} = \left\{\eta_V^{\mathrm{lat}}\left[1 - \ell_P \Delta^2 - \ell_P^{(3)}\Delta^2\Sigma\right]\right\}^2, \tag{93}$$

$$\frac{\langle \mathrm{D}^*|\bar{c}\gamma^4 b|\mathrm{B}^*\rangle\langle \mathrm{B}^*|\bar{b}\gamma^4 c|\mathrm{D}^*\rangle}{\langle \mathrm{D}^*|\bar{c}\gamma^4 c|\mathrm{D}^*\rangle\langle \mathrm{B}^*|\bar{b}\gamma^4 b|\mathrm{B}^*\rangle} = \left\{\eta_V^{\mathrm{lat}}\left[1 - \ell_V \Delta^2 - \ell_V^{(3)}\Delta^2\Sigma\right]\right\}^2, \tag{94}$$

$$\frac{\langle \mathrm{D}^*|\bar{c}\gamma^j\gamma_5 b|\mathrm{B}\rangle\langle \mathrm{B}^*|\bar{b}\gamma^j\gamma_5 c|\mathrm{D}\rangle}{\langle \mathrm{D}^*|\bar{c}\gamma^j\gamma_5 c|\mathrm{D}\rangle\langle \mathrm{B}^*|\bar{b}\gamma^j\gamma_5 b|\mathrm{B}\rangle} = \left\{\check{\eta}_A^{\mathrm{lat}}\left[1 - \ell_A \Delta^2 - \ell_A^{(3)}\Delta^2\Sigma\right]\right\}^2. \tag{95}$$

For lattice gauge theory, the heavy-quark expansions in Eqs. (93)–(95) have been derived in Ref. [150], leaning heavily on Refs. [149,158]. One-loop perturbation theory for η_V^{lat} and $\check{\eta}_A^{\mathrm{lat}}$ is in Ref. [151]. Thus, these ratios yield all three terms in δ_{1/m^2} and three of four terms in δ_{1/m^3} (including the largest, $\ell_V^{(3)}/(2m_c)^3$).

The method then proceeds as follows. First, one computes the ratios on the left-hand sides of Eqs. (93)–(95) with standard techniques of lattice gauge theory, for many combinations of the heavy quark masses. Meanwhile one calculates the short-distance coefficients η_V^{lat} and $\check{\eta}_A^{\mathrm{lat}}$ in perturbation theory. Then, one fits the numerical data to the HQET description, obtaining the ℓs as fit parameters. One can then combine these results with the perturbative calculation of η_A to obtain $h_{A_1}(1)$. The scheme mismatch that arises with the quark model calculation of the ℓs is absent here, as long as one uses the same scheme to calculate η_V^{lat} and $\check{\eta}_A^{\mathrm{lat}}$ on the one hand, and η_A on the other.

As expected, ℓ_V is the largest of the $1/m_Q^2$ matrix elements. Because of the fit, the value of ℓ_V is highly correlated with that of $\ell_V^{(3)}$, but the physical combination is better determined.

Matching uncertainties arise here, as it is usually the case with HQET. In Ref. [152] they are of order α_s^2, $\alpha_s \cdot (\bar{\Lambda}/m_c)^2$, and $(\bar{\Lambda}/m_Q)^3$. These can be improved in the future through higher-order matching calculations. Another uncertainty comes from the dependence of the ratios on the light spectator quark, whose mass lies in the range $0.4 \leq m_q/m_s \leq 1$. There turns out to be a slight linear dependence on m_q, whose main effect is to increase the statistical error. In addition, there is a pion loop contribution [164] that is mistreated in the quenched approximation [165]. The omission of this effect is treated

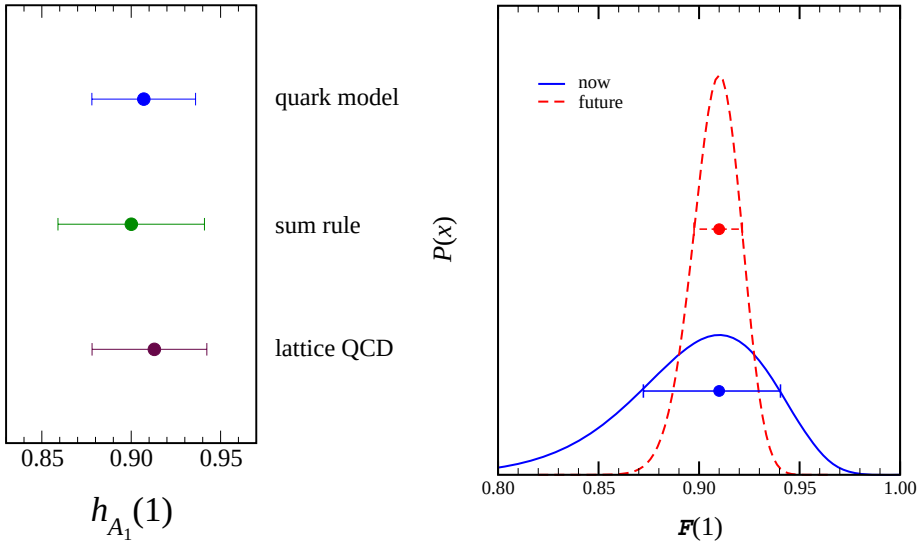

Fig. 3.7: *(a) Comparison of methods for $\mathcal{F}(1)$. Note that the result labelled "quark model" actually uses sum rule constraints. (b) Model likelihood function for $\mathcal{F}(1)$, now and with projected smaller errors in the future.*

as a systematic error. After reconstituting $h_{A_1}(1)$ [152]

$$\mathcal{F}(1) = h_{A_1}(1) = 0.913^{+0.024}_{-0.017} \pm 0.016^{+0.003+0.000+0.006}_{-0.014-0.016-0.014}, \tag{96}$$

where the uncertainties stem, respectively, from statistics and fitting, HQET matching, lattice spacing dependence, the chiral extrapolation, and the effect of the quenched approximation.

3.2.3. Comparison and summary

In Fig. 3.7(a) we compare the three results for $\mathcal{F}(1)$ from Eqs. (83), (92), and (96). All are compatible with

$$\mathcal{F}(1) = 0.91^{+0.03}_{-0.04} \tag{97}$$

The agreement is remarkable, even when one considers that all rely on heavy-quark symmetry (and, so, compute the deviation from 1), and all compute the short-distance part in perturbation theory (roughly half of the deviation). It is worth recalling the defects of the techniques. The quark model omits some dynamics (more than the quenched approximation in lattice QCD), and it is not clear that it gives the ℓs in the same scheme as η_A. The sum rule has an incalculable contribution from excitations with $(M - M_{D^*})^2 < \mu^2$, which can only be estimated. The present lattice result is in the quenched approximation, but errors associated with quenching can, in this case, be estimated and are given in the last two error bars in Eq. (96).

When using Eq. (97) in a global fit to the CKM matrix, one should appreciate the quality of the theoretical information. A flat distribution based on Eq. (97) would be incorrect: the three methods agree well and, more significantly, part of the uncertainty in Eq. (96) is statistical, and other uncertainties are under some control. Also, one cannot rule out a tail for lower values, $\mathcal{F}(1) < 0.87$; they are just unexpected. Finally, we know that $\mathcal{F}(1) \leq 1$ from the sum rule in Eq. (78). A simple function that captures these features is the Poisson distribution (for $x > 0$)

$$P(x) = N x^7 e^{-7x}, \quad x = \frac{1 - \mathcal{F}(1)}{0.090}, \tag{98}$$

where N normalizes the distribution. This distribution differs slightly from a synopsis of the lattice result [163]. The most probable value has been shifted from 0.913 to 0.910, mindful of the central value

from the sum rule. [The average based on Eq. (98) is 0.90.] Future work with lattice gauge theory could reduce the uncertainty by a factor of 3, with unquenched calculations to reduce several of the systematic errors, higher-order HQET matching to reduce the others, and higher statistics to reduce the statistical errors. Fig. 3.7(b) sketches how the resulting distribution would look. Recent developments [168] in the treatment of systematic errors (except quenching) will allow lattice calculations to provide a distribution that directly reflects statistical and systematic uncertainties, instead of a schematic distribution as in Eq. (98).

3.3. Theoretical calculations of the form factor $\mathcal{G}(1)$ for $\mathrm{B} \to \mathrm{D}\ell\nu$ decays

The form factor $\mathcal{G}(W)$ for $\mathrm{B} \to \mathrm{D}\ell\nu$ is given by

$$\mathcal{G}(w) = h_+(w) - \frac{M_B - M_D}{M_B + M_D} h_-(w), \tag{99}$$

where the form factors $h_\pm(w)$ are defined by

$$\langle \mathrm{D}(v')|V^\mu|\mathrm{B}(v)\rangle = \sqrt{M_B M_D}\left[(v'+v)^\mu h_+(w) - (v'-v)^\mu h_-(w)\right]. \tag{100}$$

Even at zero-recoil both form factors remain. With HQET one can derive expressions analogous to Eq. (84). Neglecting contributions of order α_s/m_Q^n, one finds [149,158,150],

$$h_+(1) = \eta_V \left[1 - \left(\frac{1}{2m_c} - \frac{1}{2m_b}\right)^2 \ell_P\right], \tag{101}$$

$$h_-(1) = \beta_V + \left(\frac{1}{2m_c} - \frac{1}{2m_b}\right)\Lambda_- + \left(\frac{1}{(2m_c)^2} - \frac{1}{(2m_b)^2}\right)\ell_-, \tag{102}$$

where β_V is of order α_s. Like the ℓs above, Λ_- and ℓ_- are (combinations of) matrix elements of HQET. They must be obtained by a non-perturbative method. Note that the matrix element ℓ_P appearing in $h_+(1)$ is the same as in $\mathcal{F}(1)$.

Luke's theorem, applied to $\mathrm{B} \to \mathrm{D}\ell\nu$, explains why there is no $1/m_Q$ term in $h_+(1)$. The other form factor $h_-(1)$ is not protected by Luke's theorem, and, unfortunately, it appears in $\mathcal{G}$ even at zero recoil [134]. Moreover, although some constraint might be obtained from sum rules, there is presently no useful bound analogous to that implied by Eq. (78). In conclusion, there is less theoretical control over $\mathcal{G}(1) - 1$ than $\mathcal{F}(1) - 1$.

There are several calculations of $\mathcal{G}(1)$. Using the quark model, Scora and Isgur find [166]

$$\mathcal{G}(1) = 1.03 \pm 0.07. \tag{103}$$

As mentioned above for $\mathcal{F}(1)$, the quark model presumably has a problem with scheme dependence, though it may be a useful guide. There have been a few calculations of ℓ_P, Λ_-, and ℓ_- with QCD sum rules. Including the full α_s^2 correction and using the sum-rule results of [142], one finds [167]:

$$\mathcal{G}(1) = 1.02 \pm 0.08. \tag{104}$$

Although this result is based on QCD, it is unlikely that the error bar can be reduced further. Finally, Hashimoto *et al.* have used lattice QCD and a strategy similar to that for $\mathcal{F}(1)$, which homes in on $\mathcal{G}(1) - 1$. They find [162]

$$\mathcal{G}(1) = 1.058^{+0.021}_{-0.017}, \tag{105}$$

where errors from statistics, tuning of heavy quark masses, and omitted radiative corrections have been added in quadrature. One should also expect some uncertainty from the quenched approximation, perhaps 15–20% of $\mathcal{G}(1) - 1$. Unlike the calculation of by $\mathcal{F}(1)$ by the same group [152], here the dependence on the lattice spacing was not studied. These issues could be cleared up, by completing calculations

of (lattice) radiative corrections needed to improve the calculation of $h_-(1)$, and then carrying out the Monte Carlo calculation of $h_-(1)$ at several lattice spacings.

In conclusion, the status of the theoretical calculations of $\mathcal{G}(1)$ is less satisfactory than for $\mathcal{F}(1)$. We believe that

$$\mathcal{G}(1) = 1.04 \pm 0.06 \tag{106}$$

fairly summarizes the present theoretical knowledge of $\mathcal{G}(1)$.

3.4. Electroweak corrections

For completeness, we close with a brief summary of electroweak corrections to exclusive s.l. decays. Some of these effects are shared by the radiative corrections to muon decay, and that is why the muon decay constant G_μ appears in Eqs. (70) and (71).Another effect is simply radiation of photons from the outgoing charged lepton, which could be important in semi-electronic decays, if the experimental acceptance is non-uniform in the electron's energy. A complete treatment is not available, but an adequate prescription is given in Ref. [169]. If the decaying B meson is electrically neutral, one must multiply the right-hand side of Eq. (71) with a factor [170] $1 + \alpha\pi$ to account for the Coulomb attraction of the outgoing charged lepton and charged D^*. This corresponds to a shift in $|V_{cb}|$ of about 1%.

There are also virtual corrections from diagrams with W and Z bosons. The leading parts of these effects are enhanced by the large logarithm $\ln(M_Z/M_B)$, which arise from distances much shorter than the QCD scale, and their net effect is the factor $\eta_{\rm EW}^2$ in Eq. (71). One finds [171]

$$\eta_{\rm EW} = 1 + \frac{\alpha}{\pi}\ln(m_Z/\mu) \tag{107}$$

where the scale μ separates weak and strong effects. It is natural to set $\mu = M_B$, in which case $\eta_{\rm EW} = 1.0066$. Should the accuracy of the QCD form factor $\mathcal{F}$ fall below 1%, it might be necessary to go beyond the leading log description of Eq. (107), but that could require the introduction of new form factors besides $\mathcal{F}$, so a general treatment is difficult.

3.5. Semileptonic B decays to a hadronic system heavier than D or D*

Semileptonic B decays into p-wave charm mesons are the most important sources of background polluting the measurement of the $\mathrm{B} \to \mathrm{D}^*\ell\nu$ decay rate. The hadronic system heavier than $\mathrm{D}^{(*)}$ is commonly identified as 'D^{**}'.

In infinite quark mass limit, hadrons containing a single heavy quark can be classified by their total spin J and by the angular momentum j of their light degree of freedom. In this limit, heavy quark mesons come in degenerate doublets with total spin $J = j \pm \frac{1}{2}$. Therefore, the four charm meson states 'D^{**}' corresponding to the angular momentum $l = 1$ are classified in two doublets: $\mathrm{D}_0, \mathrm{D}^*{}_1$ with $j = \frac{1}{2}$ and $J^P = (0^+, 1^+)$, and $\mathrm{D}_1, \mathrm{D}^*{}_2$ with $j = \frac{3}{2}$ and $J^P = (1^+, 2^+)$. Both D_1 and $\mathrm{D}^*{}_2$ are narrow states ($\Gamma \simeq 20$ MeV). This small width is a consequence of their strong decay proceeding through d-wave transitions. The resonances of the other doublet are expected to be rather broad, as they decay through s-wave pion emission.

The existence of the narrow resonant states is well established [106] and a signal for a broad resonance has been seen by CLEO [177], but the decay characteristics of these states in b-hadron s.l. decays have large uncertainties. The average of ALEPH [178], CLEO [179] and DELPHI [181] narrow state branching fractions show that the ratio

$$R_{**} = \frac{\mathcal{B}(\overline{\mathrm{B}} \to \mathrm{D}_2^*\ell\bar{\nu})}{\mathcal{B}(\overline{\mathrm{B}} \to \mathrm{D}_1\ell\bar{\nu})} \tag{108}$$

is smaller than one (< 0.6 at 95% C.L.[182]), in disagreement with HQET calculations where an infinite quark mass is assumed [183], but in agreement with calculations which take into account finite quark mass corrections [184].

To estimate the 'D^{**}', the LEP experiments use the treatment of narrow D^{**} proposed in [184] which accounts for $\mathcal{O}(1/m_c)$ corrections. Ref. [184] provides several possible approximations of the 'D^{**}' form factors, that depend on five different expansion schemes (A, A_{inf}, B_{inf}, B_1, B_2) and on three input parameters ($\eta_{ke}, t_{h1}, z_{h1}$).

Each proposed scheme is tested with the relevant input parameters varied over a range consistent with the experimental limit on R_{**}. The $\mathcal{F}(1)V_{cb}$ analysis is repeated for each allowed point of the scan and the systematic error is the maximal difference from the central value obtained in this way. Non-resonant terms may not be modelled correctly in this approach.

3.6. Review and future prospects for the exclusive determination of $|V_{cb}|$

3.6.1. $|V_{cb}|$ from $B \to D^* \ell\nu$ decays

The decay $B \to D^* \ell\nu$ has been studied in experiments performed at the $\Upsilon(4S)$ center of mass energy and at the Z^0 center of mass energy at LEP. At the $\Upsilon(4S)$, experiments have the advantage that the w resolution is good. However, they have more limited statistics near $w = 1$ in the decay $\overline{B}^0 \to D^{*+}\ell^-\bar{\nu}_\ell$, because of the lower reconstruction efficiency of the slow pion, from the $D^{*+} \to \pi^+ D^0$ decay. The decay $B^- \to D^{*0}\ell^-\bar{\nu}_\ell$ is not affected by this problem and CLEO [172] uses both channels. In addition, kinematic constraints enable $\Upsilon(4S)$ experiments to identify the final state without a large contamination from the poorly known s.l. B decays to 'D^{**}'. At LEP, B's are produced with a large momentum (about 30 GeV on average). This makes the determination of w dependent upon the neutrino four-momentum reconstruction, thus giving a relatively poor resolution and limited physics background rejection capabilities. The advantage that LEP experiments have is an efficiency which is only mildly dependent upon w.

Experiments determine the product $(\mathcal{F}(1) \cdot |V_{cb}|)^2$ by fitting the measured $d\Gamma/dw$ distribution. Measurements at the $\Upsilon(4S)$ have been performed by CLEO [172] and BELLE [173]. At LEP data are available from ALEPH [175], DELPHI [174] and OPAL [176]. At LEP, the dominant source of systematic error is the uncertainty on the contribution to $d\Gamma/dw$ from s.l. $B \to D^{**}$ decays. The "D^{**}" includes both narrow orbitally excited charmed meson and non-resonant or broad species. The treatment of the "D^{**}" spectra is described in 3.5., while branching ratios of the processes which affect the value of $|V_{cb}|$ are taken from [182].

experiment	$\mathcal{F}(1)\lvert V_{\rm cb}\rvert$ ($\times 10^3$)	$\rho^2_{A_1}$	$\rm Corr_{stat}$	References
ALEPH published	31.9± 1.8± 1.9	0.31± 0.17± 0.08	92%	[175]
ALEPH update	31.5± 2.1± 1.3	0.58± 0.25± 0.11	94%	[182]
DELPHI	35.5± 1.4± 2.4	1.34± 0.14± 0.23	94%	[174]
OPAL	37.1± 1.0± 2.0	1.21± 0.12± 0.20	90%	[176]
BELLE	35.8± 1.9± 1.8	1.45± 0.16± 0.20	90%	[173]
CLEO	43.1± 1.3± 1.8	1.61± 0.09± 0.21	86%	[172]

Table 3.16: *Experimental results as published by the collaborations. LEP numbers use theoretical predictions for R_1 and R_2. The published ALEPH result is obtained using a linear fit and the old ISGW model [114] for D^{**}. The updated ALEPH numbers (used in our average) are obtained using the same fit parameterization and D^{**} models as the other LEP experiments [185]. The BELLE result listed in the Table uses R_1 and R_2 from CLEO data.*

Parameter	Value	Reference
$\mathrm{R_b} = \Gamma(Z \to b\bar{b})/\Gamma(Z \to had)$	(21.64 $\pm$ 0.07)%	[180]
$\mathrm{f_d} = \mathcal{B}(b \to \mathrm{B}_d)$	(40.0 $\pm$1.1)%	[186]
$\tau(\mathrm{B}^0)$	(1.54 $\pm$ 0.015) ps	[187]
${x_E}^{LEP} = E(\mathrm{B\ meson})/\sqrt{\mathrm{s}}$	0.702 $\pm$ 0.008	[180]
$\mathcal{B}(\mathrm{D}^{*+} \to \mathrm{D}^0\pi^+)$	(67.7 $\pm$ 0.5) %	[106]
$\mathrm{R_1}$	1.18 ± 0.32	[188]
$\mathrm{R_2}$	0.71 ± 0.23	[188]
$\mathcal{B}(\bar{\mathrm{B}} \to \tau\bar{\nu}_\tau \mathrm{D}_s^+)$	(1.27 $\pm$ 0.21)%	[182]
$\mathcal{B}(\mathrm{B}^- \to \mathrm{D}^{*+}\pi^-\ell\bar{\nu})$	(1.29$\pm$0.16) %	[182]
$\mathcal{B}(\bar{\mathrm{B}}^0_\mathrm{d} \to \mathrm{D}^{*+}\pi^0\ell\bar{\nu})$	(0.61 ± 0.08)%	[182]
$\mathcal{B}(\mathrm{B}_s \to \mathrm{D}^{\star+}\mathrm{K}\ell\bar{\nu})$	(0.65 ± 0.23)%	[182]

Table 3.17: *Values of the most relevant parameters affecting the measurement of $|V_{cb}|$. The three D^{**} production rates are fully correlated.*

Table 3.16 summarizes all published data as quoted in the original papers. To combine the published data, the central values and the errors of $\mathcal{F}(1)|V_{cb}|$ and $\rho^2_{A_1}$ are re-scaled to the same set of input parameters. These common inputs are listed in Table 3.17. The $\mathcal{F}(1)|V_{cb}|$ values used for obtaining an average are extracted with the parametrization of Eq. (72), taking on the experimental determinations of the vector and axial form factor ratios R_1 and R_2 [188]. The LEP data, which originally used theoretical values for these ratios, are re-scaled accordingly [185]. Table 3.18 summarizes the corrected data. The averaging procedure [185] takes into account statistical and systematic correlations between $\mathcal{F}(1)|V_{cb}|$ and $\rho^2_{A_1}$. Averaging the measurements in Table 1, we get:

$$\mathcal{F}(1)|V_{cb}| = (38.3 \pm 1.0) \times 10^{-3}$$

and

$$\rho^2_{A_1} = 1.5 \pm 0.13$$

with a confidence level [§] of 5.1%. The error ellipses for the corrected measurements and for the world average are shown in Fig. 3.8.

The main contributions to the systematic error in $\mathcal{F}(1)|V_{cb}|$ are from the uncertainty on the $\mathrm{B} \to \mathrm{D}^{**}\ell\nu$ shape and on $\mathcal{B}(b \to \mathrm{B}_d)$ (0.57×10^{-3}), fully correlated among the LEP experiments, the branching fraction of D and D* decays (0.4×10^{-3}), fully correlated among all the experiments, and the slow pion reconstruction from BELLE and CLEO (0.28×10^{-3}), which are uncorrelated. The main contribution to the systematic error on $\rho^2_{A_1}$ is from the uncertainties in the CLEO's measurement of $\mathrm{R_1}$ and $\mathrm{R_2}$ (0.12), fully correlated among experiments. Because of the large contribution of this uncertainty to the non-diagonal terms of the covariance matrix, the averaged $\rho^2_{A_1}$ is higher than one would naively expect. This situation will improve substantially in the next few years through a better determination of R_1 and R_2, using the higher statistics samples being accumulated at the B-factories, as well as through the full exploration of the s.l. B decays to D^{**}.

Using $\mathcal{F}(1) = 0.91 \pm 0.04$, as given in Sec. 3.2. but with a symmetrized error, one gets

$$\boxed{|V_{cb}| = (42.1 \pm 1.1_{exp} \pm 1.9_{th}) \times 10^{-3}.} \qquad (109)$$

[§] The χ^2 per degree of freedom is less than 2, and we do not scale the error.

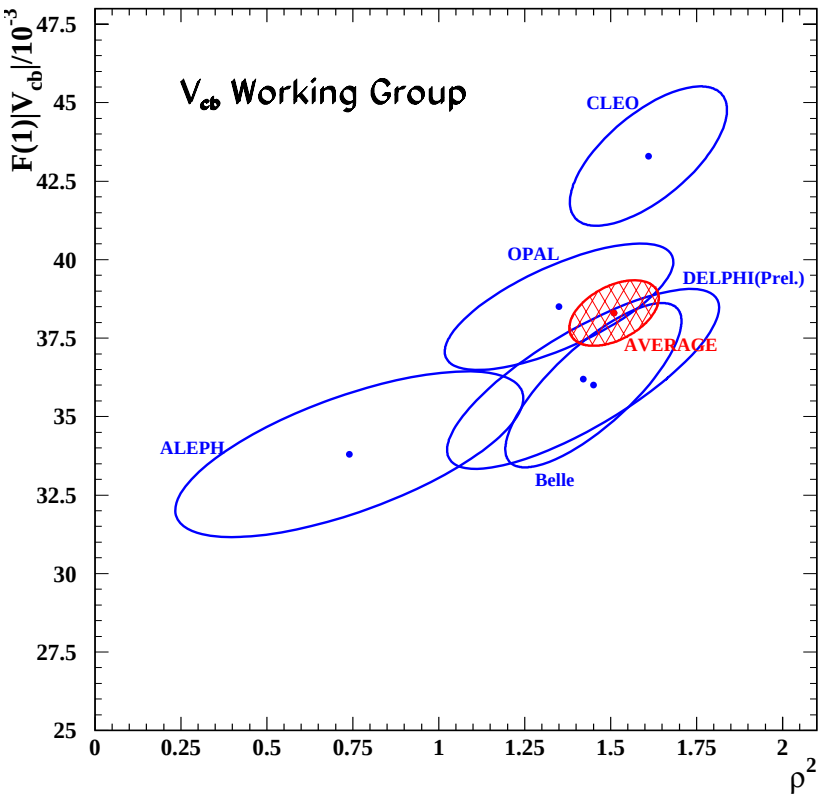

Fig. 3.8: *The error ellipses for the corrected measurements and world average for $\mathcal{F}(1)|V_{cb}|$ vs $\rho^2_{A_1}$. The ellipses correspond to a 39% C.L.*

experiment	$\mathcal{F}(1)\lvert V_{\rm cb}\rvert$ $(\times 10^{-3})$	$\rho^2_{A_1}$	$\rm Corr_{stat}$
ALEPH	33.8± 2.1± 1.6	0.74± 0.25± 0.41	94%
DELPHI	36.1± 1.4± 2.5	1.42± 0.14± 0.37	94%
OPAL	38.5± 0.9± 1.8	1.35± 0.12± 0.31	89%
BELLE	36.0± 1.9± 1.8	1.45± 0.16± 0.20	90%
CLEO	43.3± 1.3± 1.8	1.61± 0.09± 0.21	86%
World average	38.3 ± 0.5± 0.9	1.51± 0.05± 0.12	86%

Table 3.18: *Experimental results after the correction to common inputs and world average. The LEP numbers are corrected to use R_1 and R_2 from CLEO data. $\rho^2_{A_1}$ is the slope parameter as defined in Eq. (72) at zero recoil.*

experiment	$\mathcal{G}(1)\|V_{cb}\|(\times 10^{-3})$	$\rho^2_{\mathcal{G}}$	References
Published values			
ALEPH	31.1± 9.9± 8.6	0.20± 0.98± 0.50	[175]
BELLE	41.1± 4.4± 5.2	1.12± 0.22± 0.14	[190]
CLEO	44.4± 5.8± 3.7	1.27± 1.25± 0.14	[191]
Scaled values			
ALEPH	37.7± 9.9± 6.5	0.90 ± 0.98± 0.38	
BELLE	41.2± 4.4± 5.1	1.12± 0.22± 0.14	
CLEO	44.6± 5.8± 3.5	1.27± 0.25± 0.14	
World average	41.3 ± 2.9± 2.7	1.19± 0.15± 0.12	

Table 3.19: *Experimental results before and after the correction to common inputs and world average. $\rho^2_{\mathcal{G}}$ is the slope parameter as defined in Eq. (75).*

The dominant error is theoretical, but there are good prospects to reduce it through improvements in lattice QCD calculations, particularly removing the quenched approximation.

3.6.2. $|V_{cb}|$ from $\mathrm{B} \to \mathrm{D}\ell\nu$ decays

The strategy to extract $|V_{cb}|\mathcal{G}(1)$ is identical to that used for $|V_{cb}|\mathcal{F}(1)$ in $\mathrm{B} \to \mathrm{D}\ell\nu$ decays. As discussed above, theoretical estimates of $\mathcal{G}(1)$ are not, at this time, as accurate. This channel is much more challenging also from the experimental point of view because $d\Gamma_D/dw$ is more heavily suppressed near $w = 1$ than $d\Gamma_{D^*}/dw$, due to the helicity mismatch between initial and final states, and because it is hard to isolate from the dominant background, $\mathrm{B} \to \mathrm{D}^*\ell\nu$, as well as from fake D-ℓ combinations. Thus, the extraction of $|V_{cb}|$ from this channel is less precise than the one from the $\mathrm{B} \to \mathrm{D}^*\ell\nu$ decay. Nevertheless, the $\mathrm{B} \to \mathrm{D}\ell\nu$ channel provides a consistency check.

BELLE [190] and ALEPH [175] have studied the $\overline{\mathrm{B}}^0 \to \mathrm{D}^+\ell^-\bar{\nu}$ channel, while CLEO [191] has studied both $\mathrm{B}^+ \to \mathrm{D}^0\ell^+\bar{\nu}$ and $\overline{\mathrm{B}}^0 \to \mathrm{D}^+\ell^-\bar{\nu}$ decays. The parametrization used in these studies for the extrapolation to zero recoil is that of Eq. (75). The published results are shown in Table 3.19, together with the results scaled to common inputs. Averaging the latter according to the procedure of [185], we get $\mathcal{G}(1)|V_{cb}| = (41.3 \pm 4.0) \times 10^{-3}$ and $\rho^2_{\mathcal{G}} = 1.19 \pm 0.19$, where $\rho^2_{\mathcal{G}}$ is the slope parameter of $\mathcal{G}(w)$ at zero recoil.

Using $\mathcal{G}(1) = 1.00 \pm 0.07$, as given in Sec. 3.3., we get

$$|V_{cb}| = (41.3 \pm 4.0_{exp} \pm 2.9_{theo}) \times 10^{-3}, \tag{110}$$

consistent with Eq. (109) from $\mathrm{B} \to \mathrm{D}^*\ell\nu$ decay, but with an uncertainty about twice as large.

Since $|V_{cb}|$ drops out of the measured ratio $\mathcal{G}(w)/\mathcal{F}(w)$, this can be compared to theoretical calculations independently of their basis. In the heavy-quark limit, both form factors are given by the same function of w. A precise measurement of their ratio would provide information about the size of symmetry-breaking corrections away from zero recoil. Some experiments have also looked at the differential decay rate distribution to extract the ratio $\mathcal{G}(w)/\mathcal{F}(w)$. However, data are not precise enough to measure the symmetry-breaking corrections away from zero recoil. From the measured values of $\mathcal{G}(1)|V_{cb}|$ and $\mathcal{F}(1)|V_{cb}|$, we get $\mathcal{G}(1)/\mathcal{F}(1) = 1.08 \pm 0.09$, consistent with the form factor values that we used.

4. Exclusive determination of $|V_{ub}|$

As seen in Sec. 2.5., $|V_{ub}|$ can be measured from the inclusive $b \to ul\nu$ rate — blind to the particular decay mode. Such measurements require, however, that kinematic selections be made to discriminate against the dominant $b \to cl\nu$ background. This introduces additional theoretical uncertainties that can be significant.

An alternative route to measure $|V_{ub}|$ is the exclusive reconstruction of particular $b \to ul\nu$ final states. Experimentally this provides some extra kinematical constraints for background suppression, and theoretically the uncertainties are of a different nature. The extraction of $|V_{ub}|$ is complicated by the fact that the quarks are not free, but bound inside mesons. The probability that the final state quarks will form a given meson is described by form factors. And unlike exclusive $b \to cl\nu$ decays, heavy quark symmetry does not help to normalize these form factors at particular kinematic points. A variety of calculations of these form factors exists, based on lattice QCD, QCD sum rules, perturbative QCD, or quark models. At present, none of these methods allows for a fully model-independent determination of $|V_{ub}|$, though lattice calculations should, in time, provide a means to reach this goal. It is thus very important to obtain a consistent measurement of $|V_{ub}|$ with both the inclusive and exclusive approach and also to find consistent results for the various exclusive modes. The simplest mode theoretically is $\mathrm{B} \to \pi l\nu$, since a description of its rate involves only one form factor in the limit of vanishing lepton mass, instead of the three required for vector final states.

The differential rate for $\mathrm{B}^0 \to \pi^- l^+ \nu$ decays ($l = e$ or μ) is given by

$$\frac{1}{|V_{ub}|^2}\frac{d\Gamma}{dq^2} = \frac{G_F^2}{24\pi^3}\left[(v\cdot k)^2 - m_\pi^2\right]^{3/2} |f_{B\pi}^+(q^2)|^2, \tag{111}$$

where the form factor $f_{B\pi}^+(q^2)$ is defined through

$$\langle \pi^-(k)|\bar{b}\gamma^\mu u|\mathrm{B}^0(p)\rangle = f_{B\pi}^+(q^2)\left[(p+k)^\mu - \frac{M_B^2 - m_\pi^2}{q^2}q^\mu\right] + f_{B\pi}^0(q^2)\frac{M_B^2 - m_\pi^2}{q^2}q^\mu, \tag{112}$$

with q^2 the momentum transfer squared, $q^2 = (p-k)^2 = M_B^2 + m_\pi^2 - 2M_B v\cdot k$, and $p = M_B v$. In the s.l. domain, q^2 takes values in the range from 0 to $q^2_{\rm max} \equiv (M_B - m_\pi)^2$ which corresponds to $v\cdot k$ varying from $M_B/2 + m_\pi^2/(2M_B)$ to m_π. The form factor $f_{B\pi}^0(q^2)$ does not contribute to the rate in the limit of vanishing lepton mass.

4.1. Lattice QCD determinations of semileptonic heavy-to-light form factors

Lattice QCD simulations potentially provide a means of calculating heavy-to-light decay form factors from first principles¶. These calculations are model independent in the sense that they are based on approximations of QCD that can be systematically improved to arbitrarily high accuracy. In practice, however, all calculations to date have been performed in the quenched approximation, where the effect of sea quarks is treated as a mean field. This introduces a systematic error that is difficult to estimate *a priori*, though experience shows that for many hadronic quantities, the deviations induced by the quenched approximation are in the 10 to 15% range.

Besides the quenched approximation, which will be lifted (at least partially) in the near future, there are two major practical limitations in the lattice calculation of heavy-to-light form factors. One is that the spatial momenta of the initial and final state hadrons are restricted to be less than about 2 GeV, to avoid large discretization errors. The other is that light-quark masses are much larger than their physical value and the corresponding "pion" mass is $m_\pi \gtrsim$ 400 MeV, so that an extrapolation to the physical light quarks is needed (the so-called chiral extrapolation). As a result, the available region for $\vec{q}$ is limited to values above about $q^2_{\rm max}/2$.

¶ An introductory, though slightly dated, review of some of the subjects covered in this section can be found in [192]

4.1.1. Results for $\mathrm{B}^0 \to \pi^- l^+ \nu$ form factors

In addition to the extrapolations in light-quark mass, an understanding of the dependence of the form factors on heavy-quark mass is necessary. For both these purposes, the HQET motivated form factors [202] $f_1(v\cdot k)$ and $f_2(v\cdot k)$ are useful. They are related to the form factors $f^+_{B\pi}$ and $f^0_{B\pi}$ of Eq. (112) through

$$f^+_{B\pi}(q^2) = \sqrt{M_B}\left\{\frac{f_2(v\cdot k)}{v\cdot k}+\frac{f_1(v\cdot k)}{M_B}\right\}, \tag{113}$$

$$f^0_{B\pi}(q^2) = \frac{2}{\sqrt{M_B}}\frac{M_B^2}{M_B^2-m_\pi^2}\left\{[f_1(v\cdot k)+f_2(v\cdot k)] - \frac{v\cdot k}{M_B}\left[f_1(v\cdot k)+\frac{m_\pi^2}{(v\cdot k)^2}f_2(v\cdot k)\right]\right\}. \tag{114}$$

The HQET form factors are defined such that the heavy quark scaling with $M_B \to \infty$ is manifest, namely, $f_{1,2}(v\cdot k)$ become independent of M_B up to logarithms coming from the renormalization of the heavy-light current. The corrections due to finite M_B are then described as a power series in $1/M_B$. At leading order in the $1/M_B$ expansion, $f^+_{B\pi}(q^2)$ is proportional to $f_2(v\cdot k)$, while $f^0_{B\pi}(q^2)$ is proportional to a linear combination $f_1(v\cdot k)+f_2(v\cdot k)$. Thus, the heavy quark scaling of $f^+_{B\pi}(q^2)$ and $f^0_{B\pi}(q^2)$ is given by,

$$f^+_{B\pi}(q^2) \sim \sqrt{M_B}, \tag{115}$$

$$f^0_{B\pi}(q^2) \sim \frac{1}{\sqrt{M_B}}, \tag{116}$$

for fixed $v\cdot k$, up to logarithms and $1/M_B$ corrections.

Recently four major lattice groups, UKQCD [193], APE [194], Fermilab [195], and JLQCD [196], have performed quenched calculations of $\mathrm{B}\to\pi l\nu$ form factors. The UKQCD [193] and APE [194] collaborations use non-perturbatively $O(a)$-improved Wilson fermions [197,198,199]) and treat heavy quarks relativistically. In this formalism, the leading discretization errors induced by the heavy-quark mass, m_Q, are reduced from am_Q to $(am_Q)^2$, with a the lattice spacing. To keep these errors under control with the lattice spacing $a \sim 1/2.7\,\mathrm{GeV}$ available to them, they have to perform the calculations for heavy-quark masses in the neighborhood of the charm-quark mass and extrapolate to the bottom. The drawback of this approach is that the extrapolation can be significant and that discretization errors may be amplified if this extrapolation is performed before a continuum limit is taken. The Fermilab group [195], on the other hand, uses a formalism for heavy quarks in which correlation functions computed with Wilson-type fermions are reinterpreted using HQET [160,161]. In this way, they can reach both the charm and bottom quarks without extrapolation, and they investigate the discretization errors using three lattice spacings (β = 6.1, 5.9 and 5.7) covering $1/a \sim$ 1.2–2.6 GeV. The JLQCD collaboration [196] employs a lattice NRQCD action [200,201] for heavy quarks so that the bottom quark mass is covered by interpolation, and the calculation is done on a coarse lattice, $1/a \sim$ 1.6 GeV (β = 5.9). Both the Fermilab and NRQCD approach are based on expansions of QCD in powers of $1/m_Q$ and precision calculations at the physical b-quark mass require the inclusion of corrections proportional to powers of $1/m_b$ which can be difficult to compute accurately. In the case of NRQCD, one is also confronted with the fact that the continuum limit cannot be taken. All groups use an $O(a)$-improved Wilson action [197] for light quarks. Fig. 3.9 shows a comparison of recent results for the $\mathrm{B}^0 \to \pi^- l^+ \nu$ form factors $f^+_{B\pi}(q^2)$ and $f^0_{B\pi}(q^2)$ from the four groups [193,194,195,196]. For convenience, the values of these form factors are also reported in Table 3.20. The lattice results are available only for the large q^2 region (13 GeV$^2 \gtrsim q^2 \gtrsim$ 23 GeV^2) corresponding to small spatial momenta of the initial B and final pion.

Good agreement is found amongst the different groups for $f^+_{B\pi}(q^2)$, while the results for $f^0_{B\pi}(q^2)$ show a slight disagreement. To assess where these differences may come from and, more generally, to estimate systematic errors, the heavy and light quark extrapolations, which form a core part of the underlying analysis, are now briefly reviewed.

Ref.	q^2 [GeV^2]	$f^0_{B\pi}(q^2)$	$f^+_{B\pi}(q^2)$	$1/\|V_{ub}\|^2 d\Gamma/dq^2$ [ps^{-1}GeV^{-2}]
APE	13.6	$0.46(7)^{+5}_{-8}$	$0.70(9)^{+10}_{-3}$	$0.33(9)^{+\ 9}_{-\ 3}$
APE	15.0	$0.49(7)^{+6}_{-8}$	$0.79(10)^{+10}_{-4}$	$0.31(8)^{+\ 8}_{-\ 3}$
APE	16.4	$0.54(6)^{+5}_{-9}$	$0.90(10)^{+10}_{-4}$	$0.28(6)^{+\ 6}_{-\ 3}$
UKQCD	16.7	$0.57^{+6\ +5}_{-6\ -20}$	$0.9^{+1\ +2}_{-2\ -1}$	$0.29^{+10\ +11}_{-\ 9\ -\ 6}$
FNAL	17.23	$0.64^{+\ 9+10}_{-\ 3-10}$	$1.13^{+24+17}_{-\ 9-17}$	$0.35^{+15}_{-\ 6}(11)$
JLQCD	17.79	0.407(92)	1.03(22)	0.25(11)
APE	17.9	$0.59(6)^{+4}_{-10}$	$1.05(11)^{+10}_{-6}$	$0.25(5)^{+\ 5}_{-\ 3}$
UKQCD	18.1	$0.61^{+6\ +6}_{-6\ -19}$	$1.1^{+2\ +2}_{-2\ -1}$	$0.27^{+8\ +11}_{-7\ -\ 1}$
FNAL	18.27	$0.70^{+\ 9+11}_{-\ 4-11}$	$1.36^{+23+20}_{-\ 9-20}$	$0.37^{+13}_{-\ 5}(11)$
JLQCD	18.29	0.421(92)	1.09(21)	0.240(94)
JLQCD	18.80	0.435(98)	1.16(21)	0.231(84)
APE	19.3	$0.64(6)^{+4}_{-10}$	$1.25(13)^{+9}_{-8}$	$0.22(5)^{+\ 3}_{-\ 3}$
JLQCD	19.30	0.45(11)	1.24(21)	0.221(76)
FNAL	19.31	$0.76^{+10+11}_{-\ 4-11}$	$1.59^{+21+24}_{-\ 7-24}$	$0.36^{+10}_{-\ 3}(11)$
UKQCD	19.5	$0.66^{+5\ +6}_{-5\ -17}$	$1.4^{+2\ +3}_{-2\ -1}$	$0.25^{+7\ +11}_{-6\ -\ 1}$
JLQCD	19.81	0.47(12)	1.33(22)	0.210(71)
JLQCD	20.31	0.49(13)	1.43(24)	0.199(68)
FNAL	20.35	$0.83^{+10+12}_{-\ 4-12}$	$1.72^{+18+26}_{-\ 8-26}$	$0.28^{+\ 6}_{-\ 3}(9)$
APE	20.7	$0.71(6)^{+3}_{-10}$	$1.53(17)^{+8}_{-11}$	$0.19(4)^{+\ 2}_{-\ 3}$
JLQCD	20.82	0.51(14)	1.54(27)	0.187(66)
UKQCD	20.9	$0.72^{+5\ +6}_{-4\ -14}$	$1.8^{+2\ +4}_{-2\ -1}$	$0.23^{+6\ +11}_{-5\ -\ 1}$
FNAL	21.38	$0.89^{+10+13}_{-\ 4-13}$	1.84^{+20+27}_{-14-27}	$0.20^{+\ 4}_{-\ 3}(6)$
APE	22.1	$0.80(6)^{+1}_{-12}$	$1.96(23)^{+6}_{-18}$	$0.16(4)^{+\ 1}_{-\ 3}$
FNAL	22.41	$0.95^{+12+14}_{-\ 3-14}$	1.96^{+24+29}_{-20-29}	$0.13^{+\ 3}_{-\ 3}(4)$
FNAL	23.41	$1.00^{+13+15}_{-\ 3-15}$	2.10^{+29+32}_{-25-32}	$0.09^{+\ 2}_{-\ 2}(2)$

Table 3.20: Form factors and differential rate for $B^0 \to \pi^- l\nu$ decays from UKQCD [193], APE [194], FNAL [195] and JLQCD [196]. The first set of errors is statistical and the second, systematic. In the case of JLQCD, these two sets of errors were combined quadratically.

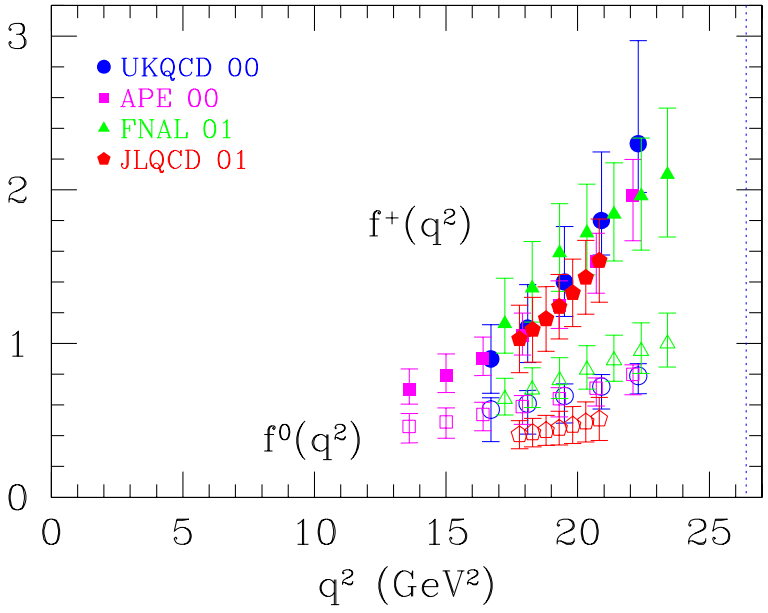

Fig. 3.9: *Recent lattice results for* $\mathrm{B}^0 \to \pi^- l^+ \nu$ *form factors* $f^+_{B\pi}(q^2)$ *and* $f^0_{B\pi}(q^2)$. *Statistical and systematic errors are added in quadrature.*

Heavy quark scaling

At a fixed value of $v \cdot k$, the $1/M_B$ dependences of the form factors $f^+_{B\pi}(q^2)/\sqrt{M_B}$ and $f^0_{B\pi}(q^2)\sqrt{M_B}$ from JLQCD are compared to those of APE [194] in Fig. 3.10. Both collaborations agree that there is no significant $1/M_B$ dependence in $f^+_{B\pi}(q^2)/\sqrt{M_B}$. For $f^0_{B\pi}(q^2)\sqrt{M_B}$, on the other hand, the APE [194] result has a significant slope, which is also supported by the Fermilab result [195] (not shown in the plot), while JLQCD do not see such dependence. The reason for this disagreement is not clear, but it partly explains the smaller value of $f^0_{B\pi}(q^2)$ of JLQCD data in Fig. 3.9.

Chiral extrapolation

The chiral extrapolation of the HQET form factors $f_1(v \cdot k) + f_2(v \cdot k)$ and $f_2(v \cdot k)$ is demonstrated in Fig. 3.11. This extrapolation is performed at fixed $v \cdot k$ by fitting the form factors to a power series in the light quark mass, as suggested in [193]. No attempt is made to account for chiral logarithms because they are not correctly reproduced in the quenched theory [206,207]. The figure shows that the extrapolation is insignificant for $f_2(v \cdot k)$ (or $f^+_{B\pi}(q^2)$), while a large extrapolation is involved in $f_1(v \cdot k) + f_2(v \cdot k)$ (or $f^0_{B\pi}(q^2)$).

Summary of current status

The current status of quenched lattice calculations of the $\mathrm{B} \to \pi l \nu$ form factors may be summarized as follows:

- The physical form factor $f^+_{B\pi}(q^2)$ has small $1/M_B$ corrections in the range of recoils explored. As a result, neither the extrapolation from the charm-quark-mass region (in the UKQCD and APE results) nor the truncation of the $1/M_B$ expansion (in the Fermilab and JLQCD results) is a dominant source of systematic error. $f^0_{B\pi}(q^2)$ is more sensitive to $1/M_B$ corrections, and the agreement among different groups is poorer.
- The form factor $f^+_{B\pi}(q^2)$ is relatively insensitive to light-quark mass, and simple polynomial chiral extrapolations are stable. This is not the case for $f^0_{B\pi}(q^2)$, which displays significant light-quark-mass dependence.
- The agreement amongst the four groups for $f^+_{B\pi}(q^2)$ as shown in Fig. 3.9 is remarkable, because

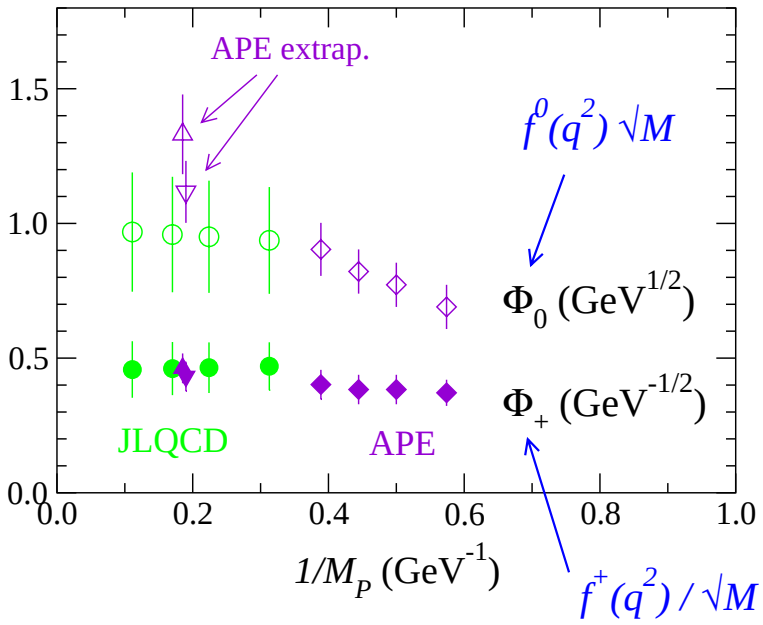

Fig. 3.10: $1/M_B$ *scaling of the form factors* $f^+_{B\pi}(q^2)/\sqrt{M_B}$ *(filled symbols) and* $f^0_{B\pi}(q^2)\sqrt{M_B}$ *(open symbols) at fixed* $v\cdot k \sim 0.95$ GeV. *Data from APE [194] (diamonds) and JLQCD [196] (circles).*

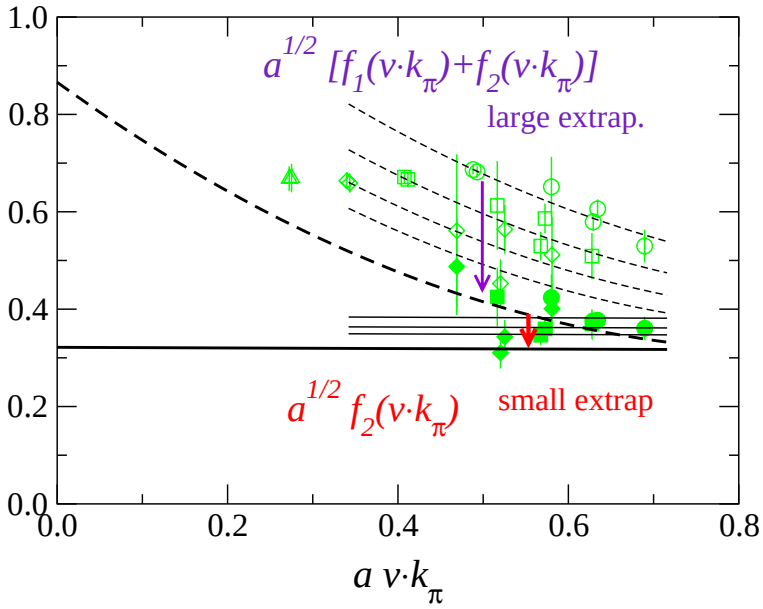

Fig. 3.11: *The chiral extrapolation of the HQET form factors* $f_1(v\cdot k)+f_2(v\cdot k)$ *(open symbols) and* $f_2(v\cdot k)$ *(filled symbols) is indicated by the vertical, downward-pointing arrows. Data from JLQCD [196].*

the groups use different methods for modelling the b quark, for matching the lattice current to the continuum one, for performing chiral extrapolations, *etc.* This agreement is probably due to the fact that this form factor is relatively insensitive to heavy- and light-quark masses, as long as $q^2_{\rm max}$ is not approached too closely.

These observations allow us to conclude that the systematic error is under control at the level of accuracy shown in Fig. 3.9.

On the other hand, the lattice calculations reviewed have important drawbacks:

- They are performed in the quenched approximation.
- The available lattice results are restricted to the large q^2 region. They may be used to predict the partially integrated decay rate, but predictions for the total decay rate usually introduce some model dependence.
- For the physical form factor $f^+_{B\pi}(q^2)$, the current error is of order 20% for all groups and a significant reduction in error will be challenging.

Strategies for determining $|V_{ub}|$

With the quenched lattice results for $\mathrm{B}^0 \to \pi^- l^+ \nu$ decays presented above, the only unknown in the expression of Eq. (111) for the differential decay rate is $|V_{ub}|$. To illustrate this point, the results of the four collaborations for this rate are reproduced in Table 3.20. It is clear, then, that $|V_{ub}|$ can be determined without assumptions about the q^2 dependence of form factors, once experiments measure the differential or partially integrated rate in the range of q^2 values reached in these calculations. Future lattice calculations in full, unquenched QCD will permit completely model-independent determinations of $|V_{ub}|$.

The total rate or the differential rate closer to $q^2 = 0$ can also be used to extract $|V_{ub}|$, but then an extrapolation becomes necessary. This extrapolation usually introduces model dependence and the resulting $|V_{ub}|$ thus inherits a systematic error that is difficult to quantify.

Pole dominance models suggest the following momentum dependence for the form factors,

$$f^i_{B\pi}(q^2) = \frac{f_{B\pi}(0)}{(1 - q^2/M_i^2)^{n_i}}, \tag{117}$$

where $i = +,\ 0$, n_i is an integer exponent and the kinematical constraint $f^+_{B\pi}(0) = f^0_{B\pi}(0)$ has already been imposed. Combining this with the HQS scaling relations of Eq. (115) implies $n_+ = n_0 + 1$. Light-cone sum rule scaling further suggests $n_0 = 1$ [211] [‖]. Another pole/dipole parametrization for $f^0_{B\pi}$ and $f^+_{B\pi}$, which accounts for the B^* pole in $f^+_{B\pi}$ correctly, has been suggested by Becirevic and Kaidalov (BK) [241]:

$$\begin{aligned} f^+_{B\pi}(q^2) &= \frac{f_{B\pi}(0)}{(1 - q^2/m^2_{B^\star})(1 - \alpha q^2/m^2_{B^\star})} \\ f^0_{B\pi}(q^2) &= \frac{f_{B\pi}(0)}{(1 - q^2/\beta m^2_{B^\star})}. \end{aligned} \tag{118}$$

Fitting this parametrization to the results of each of the four collaborations yields the results summarized in Table 3.21. Though uncertainties are still quite large, consistency amongst the various lattice predictions, as well as with the LCSR result, is good.

Using the results of these fits, UKQCD [193] and APE [194], obtain the following total rate:

$$\Gamma(\mathrm{B}^0 \to \pi^- l^+ \nu)/|V_{\rm ub}|^2 = \begin{cases} 9^{+3+3}_{-2-4}\ \mathrm{ps}^{-1} & \text{UKQCD [193]} \\ 7.0 \pm 2.9\ \mathrm{ps}^{-1} & \text{APE [194]} \end{cases}, \tag{119}$$

[‖] Pole/dipole behaviour for $f^0_{B\pi}$ and $f^+_{B\pi}$ was also suggested in [212].

Ref.	$f_{B\pi}(0)$	α	β
UKQCD M-I[193]	0.30^{+6+4}_{-5-9}	0.46^{+9+37}_{-10-5}	1.27^{+14+4}_{-11-12}
APE M-II [194]	$0.28(6)^{+5}_{-5}$	$0.45(17)^{+6}_{-13}$	$1.20(13)^{+15}$
APE M-I [194]	$0.26(5)^{+4}_{-4}$	$0.40(15)^{+9}_{-9}$	$1.22(14)^{+15}$
FNAL M-I[195]	0.33^{+2}_{-3}	0.34^{+9}_{-3}	1.31^{+3}_{-9}
JLQCD M-II[196]	0.23^{+4}_{-3}	0.58^{+12}_{-9}	1.28^{+12}_{-20}
LCSR [213]	0.28(5)	0.32^{+21}_{-7}	

Table 3.21: Results of fits of the lattice results from the four groups to the BK parametrization of Eq. (118). In the results of UKQCD and APE, the second set of uncertainties corresponds to systematic errors. Method I (M-I) consists in first extrapolating the form factors obtained from the simulation in light-quark mass, heavy-quark mass etc. and then fitting to the BK parametrization. Method II (M-II) corresponds to first fitting the BK parametrization to the form factors obtained from the simulation, before any chiral, heavy-quark, ... extrapolations, and then peforming the extrapolations on the fit parameters. The row entitled LCSR corresponds to a fit to light-cone sum rule results.

where the first error in the UKQCD result is statistical and the second is the systematic error, which includes the difference between the parametrizations of Eqs. (117) and (118). In the APE result, where a fit to the pole/dipole parametrization is not considered, the error includes statistical and systematic errors summed in quadrature. Nevertheless, because of the model dependence of these results, a larger systematic error cannot be excluded.

4.1.2. Future directions

In the following we discuss the directions that should be explored in the near future to improve the accuracy in the determination of $|V_{ub}|$.

Extension toward lower q^2

As already discussed, it is not straightforward to extend lattice calculations of heavy-to-light form factors to the low q^2 region, though finer lattices will eventually get us there. Extrapolations to lower q^2 values can be performed using models which incorporate many of the known constraints on the form factors, but this introduces a model dependence which is difficult to quantify. It has been proposed, however, to use dispersion relations together with lattice data to obtain model-independent bounds for the form factors over the entire q^2 range [208,209,137]. These techniques are based on the same ingredients as those used to constrain the shape of the form factors for $\mathrm{B} \to \mathrm{D}^{(*)} l\nu$ decays, briefly presented in Sec. 3.1., though details of the implementation are quite different. An example is shown in Fig. 3.12. The bounds in that figure were obtained using the lattice results for $\mathrm{B} \to \pi l\nu$ form factors from [210], the most complete set available at the time.

Since then lattice calculations have improved significantly and it would be interesting to derive new bounds by combining modern lattice results for the form factors with the techniques developed in [209]. It may also be advantageous to take into account additional constraints on the form factors. Furthermore, other ways of extending the range of lattice calculations to lower values of q^2 should be investigated.

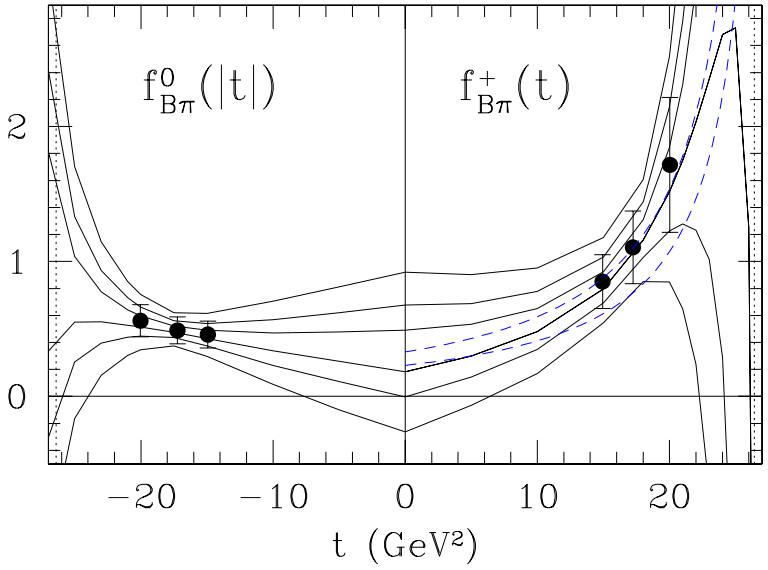

Fig. 3.12: *Dispersive bounds for $f_0(|t|)$ and $f_+(t)$ in $\mathrm{B}^0 \to \pi^- \ell^+ \nu$ decays [209]. The points are the lattice results of [210] with added systematic errors. The pairs of fine curves are, from the outermost to the innermost, the 95%, 70% and 30% bounds, where percentages represent the likelihood that the form factor take a value between the corresponding pair of curves at the given t. The dashed curves are the LCSR results of Eq. (129) [213]. Comparable results are given in Eq. (130) [235].*

Unquenching

Lattice calculations have to be performed with dynamical sea quarks to yield truly model independent results. Some groups already have gauge configurations for two flavours of sea quarks with degenerate masses $\gtrsim m_s/2$ (instead of the two very light u and d quarks and the lightish s quark found in nature). The study of B meson decays on these backgrounds presents no conceptual difficulty.

In practice, however, the chiral extrapolations required to reach the u and d quark masses may be rather delicate as it is not clear that the light-quark masses used in the simulations are light enough to be sensitive to the so-called chiral logarithms which are expected to dominate the small mass behaviour of many physical quantities (see e.g. [214–217] for recent discussions). It will be very important to control this light-quark-mass behaviour to obtain accuracies better than 10%.

Using $\mathrm{D} \to \pi \mathrm{l} \nu$ decays to improve predictions for $\mathrm{B} \to \pi \mathrm{l} \nu$ form factors

In the heavy charm and bottom limit, heavy quark symmetry relates the $\mathrm{B} \to \pi \mathrm{l} \nu$ form factors to $\mathrm{D} \to \pi \mathrm{l} \nu$. Burdman *et al.* [202] proposed to consider the ratio

$$\left.\frac{d\Gamma(\mathrm{B}^0 \to \pi^- l^+ \nu)/d(v\cdot k)}{d\Gamma(\mathrm{D}^0 \to \pi^- l^+ \nu)/d(v\cdot k)}\right|_{\text{same } v\cdot k} = \left|\frac{V_{ub}}{V_{cd}}\right|^2 \left(\frac{M_B}{M_D}\right)^2 \left|\frac{f^+_{B\pi}/\sqrt{M_B}}{f^+_{D\pi}/\sqrt{M_D}}\right|^2 , \tag{120}$$

from which one may extract the ratio of CKM matrix elements $|V_{ub}/V_{cd}|$. In view of the high-precision measurements of D decays promised by CLEO-*c*, such an approach to determining $|V_{ub}|$ is becoming increasingly relevant.

It is convenient to factorize the nearest pole contribution to $f^+_{B\pi}(q^2)$, which is expected to dominate the q^2 behaviour of this form factor in the heavy-quark limit, at least close to zero recoil. Thus, the breaking of heavy quark symmetry may be parametrized as

$$\frac{f^+_{B\pi}/\sqrt{M_B}}{f^+_{D\pi}/\sqrt{M_D}} = \frac{v\cdot k + \Delta_D}{v\cdot k + \Delta_B} R_{BD}(v\cdot k), \tag{121}$$

where $\Delta_{B,D} \equiv m_{B^*,D^*} - m_{B,D}$ and $(R_{BD}(v\cdot k)-1)$ describes the $1/M_{D,B}$ corrections to be calculated on the lattice. The question then becomes whether $R_{BD}(v\cdot k)$ can be calculated more accurately on the lattice than $f^+_{B\pi}(q^2)$. The answer is "yes" as a number of uncertainties are expected to cancel in the ratio. It is also encouraging that the heavy-quark-mass dependence of $f_2(v\cdot k)$ appears to be mild, as discussed previously.

To reach a level of 5% accuracy or better, the systematic errors associated with the heavy quark have to be under good control for both charm and bottom quarks. These errors should also be as similar as possible in the two regimes in order for them to cancel effectively. For these reasons, the relativistic and Fermilab approaches seem to be preferable to the use of NRQCD. Indeed, NRQCD involves an expansion of QCD in powers of $1/(am_Q)$ which requires either the inclusion of high-orders or coarse lattices ($a^{-1} \ll m_Q$) when m_Q approaches the charm mass. High orders are difficult to implement in practice and coarse lattices imply large discretization errors.

To reach such levels of accuracy, it is also important to study carefully the extent to which uncertainties associated with the chiral extrapolation of the form factors and with the presence of chiral logarithms cancel in the ratio of bottom to charm amplitudes.

B to vector meson semileptonic decays

The rate for $\mathrm{B} \to \rho l\nu$ is less strongly suppressed kinematically near $q^2_{\rm max}$ than is the rate for $\mathrm{B} \to \pi l\nu$ and it is larger overall. Thus, the number of events will be larger in the region where the lattice can compute the relevant matrix elements reliably. In [218], the UKQCD collaboration suggested that $|V_{ub}|$ be obtained directly from a fit to the differential decay rate around $q^2_{\rm max}$, with the overall normalization of this rate, up to a factor of $|V_{ub}|^2$, determined using lattice results. With their lattice results, such a measurement would allow an extraction of $|V_{ub}|$ with a 10% statistical and a 12% systematic error coming from theory. [**] A first measurement of this differential rate has actually already been performed by CLEO [219].

Very recently, two lattice collaborations (UKQCD [222] and SPQcdR [223]) have begun revisiting $\mathrm{B} \to \rho l\nu$ decays. Their calculations are performed in the quenched approximation and results are still preliminary. Shown in Fig. 3.13 are the four independent form factors required to describe the $\mathrm{B} \to \rho$ s.l. matrix elements, as obtained by SPQcdR [223] at two values of the lattice spacing. Also shown are results from light-cone sum rule calculations [228] which are expected to be reliable for lower values of q^2. These sum rule results look like very natural extensions of the form factors obtained on the finer lattice. Combining the LCSR results for $q^2 \le 10\,\mathrm{GeV}^2$ with the results on the finer lattice for $q^2 > 10\,\mathrm{GeV}^2$ yields $\Gamma(\mathrm{B}^0 \to \rho^- l\nu) = (19 \pm 4)|V_{ub}|^2\,\mathrm{ps}^{-1}$ [223]. It will be interesting to see what the calculations of [222,223] give for the differential rate above $10\,\mathrm{GeV}^2$ once they are finalized.

As was the case for $\mathrm{B} \to \pi l\nu$ decays, derivation of the full q^2 dependence of the form factors from lattice data involves a large extrapolation from $q^2 > 10\,\mathrm{GeV}^2$ all the way down to $q^2 = 0$. Here, the use of dispersion relations is complicated by the singularity structure of the relevant correlation functions and form factors. There exist, however, lattice-constrained parametrizations of $\mathrm{B} \to \rho l\nu$ form factors, which are consistent with lattice results and heavy-quark scaling relations at large q^2, and with kinematic constraints and light-cone sum rule scaling at $q^2 = 0$ [211]. These parametrizations provide simple, few-parameter descriptions of s.l. form factors. [††] However, at values of the recoil for which there are not lattice results (i.e. low q^2), they are not predictions of (quenched) QCD.

[**] Other early lattice work on $\mathrm{B} \to \rho l\nu$ can be found in [220,221].

[††] Away from $q^2 = 0$, these parametrizations are actually not fully consistent with the large-recoil symmetry relations derived in [212] amongst the soft contributions to the relevant form factors. For completeness, let us mention that the α_s corrections to these symmetry relations were calculated in [224] and corrections in powers of $1/m_b$ were investigated in [225,226,227]

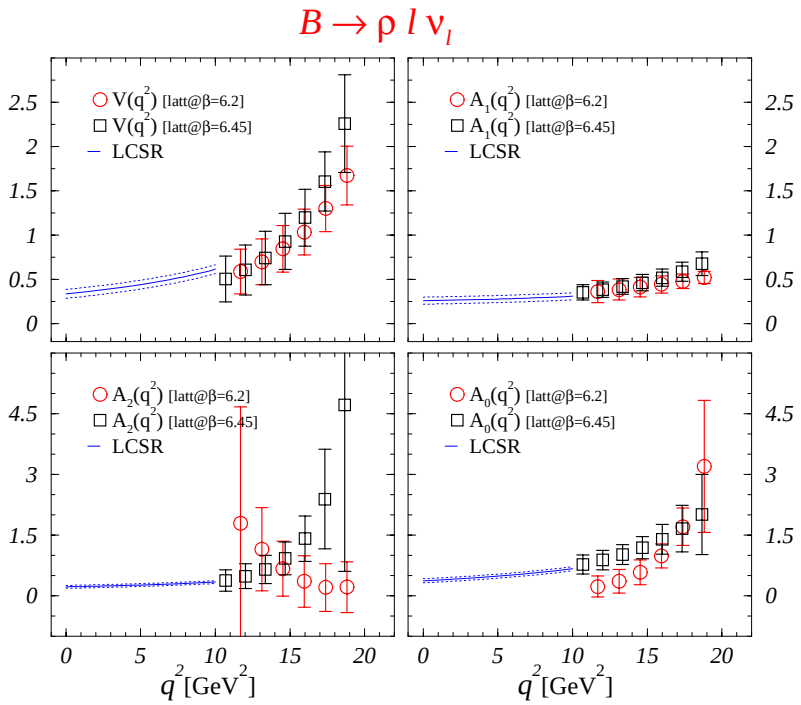

Fig. 3.13: *Example of quenched lattice results for* $\mathrm{B} \to \rho l \nu$ *form factors plotted as a function of* q^2 *[223]. These results were obtained at two values of the inverse lattice spacing* $1/a = 3.7\,\mathrm{GeV}$ *and* $2.7\,\mathrm{GeV}$*, corresponding to bare couplings values* $\beta = 6.45$ *and* 6.2 *respectively. Also shown at low* q^2 *are the light-cone sum rule results of [228].*

4.1.3. Summary

Four groups have recently performed quenched lattice calculations of $\mathrm{B} \to \pi l \nu$ form factors for $q^2 \gtrsim 12\ \mathrm{GeV}^2$ and their results agree. Agreement is best for $f_{B\pi}^+$ which determines the rate for these decays in the limit of vanishing lepton mass. The error on this form factor is of order 20%. The main sources of remaining systematic errors are quenching and light-quark-mass extrapolations for all the groups, and heavy-quark-mass extrapolations, discretization, and perturbative matching, depending on the group.

A substantial reduction in the error (i.e. below 10%) will be difficult to achieve solely in lattice QCD. This is where the use of ratios of s.l. B and D rates, such as the one given in Eq. (120), could be very helpful.

There is still a substantial number of improvements to be made to present calculations. The list includes unquenching, the use of dispersive bounds or other means of extending the kinematic reach of lattice calculations, the determination of ratios of s.l. B and D rates, and more investigations of $\mathrm{B} \to \rho l \nu$ decays.

4.2. Heavy-to-light form factors from light-cone sum rules

The QCD light-cone sum rules (LCSR) [230,231] provide estimates of various heavy-to-light transition form factors. In particular, $\mathrm{B} \to P, V$ form factors ($P = \pi, \mathrm{K}$ and $V = \rho, \mathrm{K}^*, \phi$) have been calculated at small and intermediate momentum transfers, typically at $0 < q^2 \leq m_b^2 - 2m_b\Lambda_{QCD}$. The upper part of this interval overlaps with the region accessible to the lattice calculations of the same form factors, allowing one to compare the results of two methods. In what follows we will concentrate on the LCSR prediction for the $\mathrm{B} \to \pi$ form factor $f_{B\pi}^+$ [232–234]. Its accuracy has been recently improved in Ref. [235]. For the LCSR $\mathrm{B} \to V$ form factors we refer to the NLO calculation in Ref. [228] and to the resulting parametrization in Ref. [236].

The LCSR approach to calculate $f^+_{B\pi}$ employs a specially designed theoretical object, the vacuum-to-pion correlation function

$$F_\mu(p,q) = i\int d^4x e^{iqx}\langle\pi^+(p)|\, T\{\bar{u}\gamma_\mu b(x), m_b\bar{b}i\gamma_5 d(0)\}\,|0\rangle = F((p+q)^2,q^2)p_\mu + O(q_\mu)\,, \quad (122)$$

where the $b\to u$ weak current is correlated with the quark current which has the B meson quantum numbers, and $p^2 = m_\pi^2$. Writing down the dispersion relation for the invariant amplitude F:

$$F((p+q)^2,q^2) = \frac{2f_B f^+_{B\pi}(q^2)M_B^2}{M_B^2-(p+q)^2} + \sum_{B_h}\frac{2f_{B_h}f^+_{B_h\pi}(q^2)m^2_{B_h}}{m^2_{B_h}-(p+q)^2}\,, \quad (123)$$

one represents the correlation function (122) in terms of hadronic degrees of freedom in the B channel. The ground-state contribution in Eq. (123) contains a product of the B meson decay constant f_B and the form factor $f^+_{B\pi}(q^2)$ we are interested in, whereas the sum over B_h accounts for the contributions of excited and continuum B states.

The dispersion relation is then matched to the result of QCD calculation of $F((p+q)^2,q^2)$ at large virtualities, that is, at $|\,(p+q)^2-m_b^2\,|\gg\Lambda^2_{QCD}$ and $q^2\ll m_b^2$. In this region the operator-product expansion (OPE) near the light-cone $x^2=0$ is employed:

$$F((p+q)^2,q^2) = \sum_{t=2,3,4}\int Du_i\sum_{k=0,1}\left(\frac{\alpha_s}{\pi}\right)^k T_k^{(t)}((p+q)^2,q^2,u_i,m_b,\mu)\varphi_\pi^{(t)}(u_i,\mu)\,. \quad (124)$$

This generic expression is a convolution of calculable short-distance coefficient functions $T_k^{(t)}$ and universal pion light-cone distribution amplitudes (DA) $\varphi_\pi^{(t)}(u_i,\mu)$ of twist t. Here, m_b is the one-loop b-quark pole mass, μ is the factorization scale and the integration goes over the pion momentum fractions $u_i = u_1,u_2,...$ distributed among quarks and gluons, so that $Du_i \equiv du_1du_2...\delta(1-\sum_i u_i)$. In particular, $\varphi_\pi^{(2)}(u_1,u_2,\mu) = f_\pi\varphi_\pi(u,\mu)$, $(u_1=u, u_2=1-u)$ where φ_π is the lowest twist 2, quark-antiquark pion DA normalized to unity:

$$\varphi_\pi(u,\mu) = 6u(1-u)\left(1+\sum_n a_{2n}(\mu)C_{2n}^{3/2}(2u-1)\right)\,. \quad (125)$$

In the above, C_{2n} are Gegenbauer polynomials and the oefficients $a_n(\mu)$, that are suppressed logarithmically at large μ, determine the deviation of $\varphi_\pi(u)$ from its asymptotic form. Importantly, the contributions to Eq. (124) corresponding to higher twist and/or higher multiplicity pion DA are suppressed by inverse powers of the b-quark virtuality $(m_b^2-(p+q)^2)$, allowing one to retain a few low twist contributions in this expansion. Furthermore, one uses quark-hadron duality to approximate the sum over B_h in Eq. (123) by a dispersion integral over the quark-gluon spectral density, introducing a threshold parameter s_0^B. The final step involves a Borel transformation $(p+q)^2\to M^2$, where the scale of the Borel parameter M^2 reflects the characteristic virtuality at which the correlation function is calculated.

The resulting sum rule relation obtained by matching Eqs. (123) and (124) can be cast in the following form:

$$f_B f^+_{B\pi}(q^2) = \frac{1}{M_B^2}\exp\left(\frac{M_B^2}{M^2}\right)\sum_{t=2,3,4}\sum_{k=0,1}\left(\frac{\alpha_s}{\pi}\right)^k \mathcal{F}_k^{(t)}(q^2,M^2;m_b,s_0^B,\mu;\{\text{DA}\}^{(t)})\,, \quad (126)$$

where the double expansion (in twists and in α_s) and the dependence on the relevant parameters are made explicit. In particular, $\{DA\}^{(t)}$ denotes the non-perturbative normalization constant and non-asymptotic coefficients for each given twist component, e.g., for φ_π: $\{DA\}^{(2)} = \{f_\pi, a_i\}$. The sum rule (126) includes all zeroth order in α_s, twist 2,3,4 contributions containing quark-antiquark and quark-antiquark-gluon DA of the pion. The perturbative expansion has NLO accuracy, including the $O(\alpha_s)$ corrections

to the twist 2 [233] and twist 3 coefficient functions, the latter recently calculated in Ref. [235]. More details on the derivation of LCSR (126) and the explicit expressions can be found in the review papers [237–239].

For the B meson decay constant entering LCSR (126) one usually employs the conventional SVZ sum rule [46] for the two-point correlator of $\bar{b}i\gamma_5 q$ currents with $O(\alpha_s)$ accuracy (a recent update of this sum rule [240] is discussed in Chapter 4 of the present document):

$$f_B = \sum_{d=0,3\div 6} \sum_{k=0,1} \left(\frac{\alpha_s}{\pi}\right)^k C_k^{(d)}(\overline{M}^2, m_b, s_0^B, \mu)\langle 0|\Omega_d(\mu)|0\rangle\,, \tag{127}$$

where the expansion contains the perturbative term with dimension $d = 0$ ($\Omega_0 = 1$), and, at $d \geq 3$, goes over condensates, the vacuum averages of operators $\Omega_d = \bar{q}q, G^a_{\mu\nu}G^{a\mu\nu}, ...$, multiplied by calculable short-distance coefficients $C_k^{(d)}$. The Borel parameter $\overline{M}$ is correlated with M. The LCSR prediction for the $\mathrm{B} \to \pi$ form factor is finally obtained dividing Eq. (126) by Eq. (127):

$$f^+_{B\pi}(q^2) = (f_B f^+_{B\pi}(q^2))_{LCSR}/(f_B)_{2ptSR}\,. \tag{128}$$

In order to demonstrate that the expansion in both twist and α_s in this relation works well, we present the approximate percentage of various contributions to the resulting form factor (128):

twist	DA	LO	$O(\alpha_s)$ NLO
2	$\bar{q}q$	~ 50 %	~ 5%
3	$\bar{q}q$	~ 40 %	~ 1%
4	$\bar{q}q$	~ 5 %	-
3+4	$\bar{q}qG$		

The input parameters used in the numerical analysis of the sum rules (126) and (127) have a limited accuracy. The theoretical uncertainty is estimated by varying these inputs within the allowed regions and adding up linearly the separate uncertainties induced by these variations in the numerical prediction for $f^+_{B\pi}$. The resulting total uncertainties are given below, together with the parametrizations of the form factor. A detailed theoretical error analysis can be found in Ref. [213]. To summarize it briefly, one source of uncertainty is the value of the b-quark one-loop pole mass. The two most recent LCSR analyses use $m_b = 4.7 \pm 0.1$ GeV [213] and $m_b = 4.6 \pm 0.1$ GeV [235]. In both studies, the threshold s_0^B is not an independent parameter, being determined by stabilizing f_B calculated from Eq. (127) at a given b-quark mass. The uncertainty induced by varying the factorization scale μ (adopted simultaneously as the normalization scale for α_s) is very small, firstly, because the NLO approximation is implemented for both dominant twist 2 and 3 terms, and, secondly, because the relatively large $O(\alpha_s)$ corrections to the twist 2 contribution and to the f_B sum rule cancel in the ratio (128). Another source of uncertainty is our limited knowledge of the non-asymptotic part in the pion DA (determined by the coefficients a_{2n} and the analogous coefficients in twist 3,4 DA). In Ref. [213] these coefficients were varied from a certain non-asymptotic ansatz of DA (motivated by QCD sum rules) to purely asymptotic DA. Such a substantial variation covers the existing constraints on non-asymptotic coefficients obtained from LCSR for pion form factors. The latter constraints have been used in Ref. [235]. In fact, LCSR involve integration over normalized DA, therefore it is natural that the results only moderately depend on the non-asymptotic coefficients. Finally, to assess the reliability of the LCSR procedure one has to comment on the use of quark-hadron duality, which is the most sensitive point in the sum rule approach. We expect that the sensitivity to the duality approximation is substantially reduced: 1) by restricting the Borel parameter at not too large values and 2) by dividing out the f_B sum rule which depends on the same threshold. The fact that the QCD sum rule prediction for f_B (see Chapter 4 and [240]) is in a good agreement with the lattice results indicates that quark-hadron duality is indeed valid in the B channel.

For a convenient use in the experimental analysis, the LCSR results for $\mathrm{B} \to \pi$ form factor are usually fitted to simple parametrizations. One of them, suggested in Ref. [213] employs the ansatz [241] based on the dispersion relation for $f^+_{B\pi}(q^2)$. The latter is fitted to the LCSR predictions for $f^+_{B\pi}$ in its validity region $0 < q^2 \leq 14 - 16$ GeV^2. For the B*-pole term the B$^*B\pi$ coupling [242] is determined from the same correlation function (124). The result is:

$$f^+_{B\pi}(q^2) = \frac{0.23 \div 0.33}{(1 - q^2/M^2_{B^*})(1 - \alpha_{B\pi} q^2/M^2_{B^*})} \,. \tag{129}$$

where the values of the slope parameter correlated with the lower and upper limits of the interval for $f^+_{B\pi}(0)$ are almost equal: $\alpha_{B\pi} = 0.39 \div 0.38$. A different parametrization was suggested recently in Ref. [235]:

$$\begin{aligned} f^+_{B\pi}(q^2) \quad &= \frac{0.26 \pm 0.06 \pm 0.05}{1 - a(q^2/M^2_B) + b(q^2/M^2_B)^2}, \quad q^2 < q^2_0, \\ &= \frac{c}{1 - q^2/M^2_{B^*}}, \quad q^2 > q^2_0 \,, \end{aligned} \tag{130}$$

where the LCSR result is extrapolated to large q^2 using the B*-pole form. In Eq. (130) the ranges of fitted parameters, $a = 2.34 \div 1.76$, $b = 1.77 \div 0.87$, $c = 0.384 \div 0.523$, and $q^2_0 = 14.3 \div 18.5$ GeV^2, are correlated with the first error in $f^+_{B\pi}(0)$, whereas the second error is attributed to the uncertainty of the quark-hadron duality approximation. Note that all values within the uncertainty intervals in Eqs. (129) and (130) have to be considered as equally acceptable theoretical predictions, without any "preferred central value". The numerical differences between the form factors (129) and (130) are smaller than the estimated uncertainties and are caused by slightly different inputs and by the small $O(\alpha_s)$ correction to the twist 3 term taken into account in Eq. (130) but not in Eq. (129) (where an additional uncertainty was attributed to this missing correction).

Having at hand the form factor, one can predict the $\mathrm{B} \to \pi l \nu$ decay distribution using Eq. (111), as is shown in Fig. 3.14 in the case of the form factor (129). The corresponding integrated s.l. width is

$$\Gamma(\mathrm{B}^0 \to \pi^- \mathrm{l}^+ \nu) = (7.3 \pm 2.5) |\mathrm{V_{ub}}|^2 \mathrm{ps}^{-1} \,, \tag{131}$$

where the indicated error is mainly caused by the uncertainty of $f^+_{B\pi}(0)$, whereas the uncertainty of the form factor shape is insignificant. This prediction [213] was recently used by BELLE in their preliminary analysis of $\mathrm{B} \to \pi l \nu$ decay (see Sec. 4.3.1.). A similar estimate of $|V_{ub}|$ was obtained in Ref. [213] using the older CLEO measurement [245] of the $\mathrm{B} \to \pi l \nu$ width.

The advantage of LCSR is that one can easily switch from the $\mathrm{B} \to \pi$ to $\mathrm{D} \to \pi$ form factor replacing b quark by c quark in the underlying correlation function (124). The LCSR prediction for $f^+_{D\pi}$ obtained in Ref. [213] and parametrized in the form analogous to Eq. (129) yields a D*-pole dominance:

$$f^+_{D\pi} = \frac{0.65 \pm 0.11}{1 - q^2/m^2_{D^*}} \,, \tag{132}$$

at $0 < q^2 < (M_D - m_\pi)^2$. The corresponding s.l. width $\Gamma(\mathrm{D}^0 \to \pi^- e^+ \nu_e)/|V_{cd}|^2 = 0.13 \pm 0.05$ ps^{-1} calculated with the known value of $|V_{cd}|$ is, within errors, in agreement with the experimental number 0.174 ± 0.032 ps^{-1} [106]. To make this comparison more decisive it would be very important to have new, more accurate measurements of the decay distribution and integrated width of $\mathrm{D}^0 \to \pi^- e^+ \nu_e$.

Are further improvements of the LCSR result for $f^+_{B\pi}$ and $f^+_{D\pi}$ possible? As we have seen, the accuracy of OPE for the correlation function is quite sufficient. The $O(\alpha_s^2)$ level recently achieved in the sum rule for f_B [240] is certainly not an immediate task for LCSR, being also technically very difficult. More important is to improve the accuracy of the input parameters by 1) narrowing the interval of the b quark mass and 2) gaining a better control over the parameters of pion DA. For the latter, in particular,

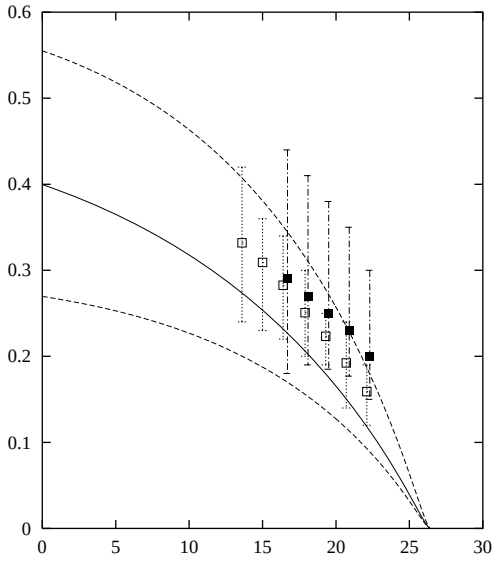

Fig. 3.14: *LCSR prediction for the* $\mathrm{B} \to \pi l\nu$ *decay distribution [213] at the nominal values of inputs (solid), with the interval of theoretical uncertainties (dashed), compared with some of the recent lattice calculations taken from Refs. [243] (solid points) and [194] (open points).*

one needs more precise data on pion form factors, especially on $\gamma^*\gamma \to \pi^0$ (the latter form factor can in principle be measured at the same e^+e^- B-factories) and, eventually, lattice QCD simulations of $\varphi_\pi(u)$ and other DA. A better control over duality approximation in the B and D channels can be achieved if radially excited B and D states are accurately identified with their masses and widths. Optimistically, one may hope to reduce the overall uncertainty of the LCSR prediction for $f^+_{B\pi}$ and other heavy-to-light form factors to the level of $\pm 10\%$, which is a natural limit for any QCD sum rule prediction.

In conclusion, we emphasize that, in addition to providing estimates of the form factors, LCSR help in understanding important physical aspects of the heavy-to-light transitions. First of all, LCSR allow to *quantitatively* assess the role of the soft (end-point) vs hard (perturbative gluon exchange) contributions to the form factors, because both contributions are taken into account in this approach. Secondly, using LCSR one is able to predict [231] the $m_b \to \infty$ limit, $f^+_{B\pi}(0) \sim 1/m_b^{3/2}$, which is used in some lattice extrapolations. Last but not least, LCSR can be expanded in powers of $1/m_b$ and $1/E_\pi$ assessing the size of $1/m_b$ and $1/E$ corrections to various relations predicted in effective theories for heavy-to-light decays.

4.3. Review and future prospects for the exclusive determination of $|V_{ub}|$

4.3.1. Measurements of $BR(\mathrm{B} \to \pi\ell\nu)$

The first exclusive measurement of the mode $\mathrm{B} \to \pi\ell\nu$ was presented by the CLEO collaboration in 1996 [245]. The neutrino momentum is inferred from the missing momentum in the event, using the hermeticity of the detector. Events with multiple charged leptons or a non-zero total charge are rejected, resulting in a reduced efficiency in favour of an improved neutrino momentum resolution. Isospin relations for the relative partial width are used to combine the B^+ and B^0 modes. A fit is performed using the variables $M_{cand} = \sqrt{E^2_{\mathrm{beam}} - |\vec{p}_\nu + \vec{p}_\ell + \vec{p}_{\rho,\omega,\pi}|^2}$ and $\Delta E = (E_{\rho,\omega,\pi} + E_\ell + |\vec{p}_{\mathrm{miss}}|c) - E_{\mathrm{beam}}$, where E_{beam} is the well known beam energy. The modes $\mathrm{B} \to \rho\ell\nu$ (with ρ^0 and ρ^-) and $\mathrm{B} \to \omega\ell\nu$ are also included in the fit because of cross-feed between these modes and $\mathrm{B} \to \pi\ell\nu$. The ρ (ω) mode uses the invariant two (three) π mass in the fit to distinguish better between resonant and non-resonant final states. Backgrounds from continuum processes are subtracted using off-resonance data. The shape of

the five signal contributions, the $b \to c$, and $b \to u$ backgrounds are provided by Monte Carlo simulation. The final results for the branching ratio and $|V_{ub}|$ are obtained by averaging over four separate form factor calculations: two quark models (ISGW2 [246] and Melikhov [247]), a model by Wirbel Stech and Bauer [248], and a hybrid model that uses a dispersion-relation-based calculation of the $\pi\ell\nu$ form factor [249] and combines lattice calculation of the $\rho\ell\nu$ form factors [250] with predicted $\rho\ell\nu$ form factor relations [251]. The dominant systematic uncertainties arise from uncertainties in the detector simulation and modelling of the $b \to u\ell\nu$ backgrounds. The result using 2.66 fb^{-1} on resonance data is

$$\mathcal{B}(\mathrm{B}^0 \to \pi^- e^+ \nu) = (1.8 \pm 0.4 \pm 0.3 \pm 0.2) \times 10^{-4}\,, \text{ and} \quad (133)$$

$$|V_{ub}| = (3.3 \pm 0.2\,^{+0.3}_{-0.4} \pm 0.78) \times 10^{-3}\,. \quad (134)$$

The errors given are statistical, systematic, and theoretical, in the order shown. Note that the above value of $|V_{ub}|$ is extracted using both the π and ρ modes. At ICHEP 2002 BELLE presented a preliminary result using 60 fb^{-1} on-peak and 9 fb^{-1} off-peak data [253]. Results are quoted for the UKQCD model [211]

$$\mathcal{B}(\mathrm{B}^0 \to \pi^- e^+ \nu) = (1.35 \pm 0.11 \pm 0.21) \times 10^{-4}\,, \text{ and} \quad (135)$$

$$|V_{ub}| = (3.11 \pm 0.13 \pm 0.24 \pm 0.56) \times 10^{-3} \quad (136)$$

and for the LCSR model [213]

$$\mathcal{B}(\mathrm{B}^0 \to \pi^- e^+ \nu) = (1.31 \pm 0.11 \pm 0.20) \times 10^{-4}\,, \text{ and} \quad (137)$$

$$|V_{ub}| = (3.58 \pm 0.15 \pm 0.28 \pm 0.63) \times 10^{-3}\,. \quad (138)$$

The CLEO collaboration submitted a preliminary updated analysis [257] to ICHEP 2002 based on 9.7×10^6 B$\overline{\mathrm{B}}$ pairs. In addition to more data compared to Ref. [245], the analysis has been improved in several ways: the signal rate is measured differentially in three q^2 regions so as to minimize modelling uncertainties arising from the q^2 dependence of the form factors (this is the first time this has been done in the $\mathrm{B} \to \pi\ell\nu$ mode); minimum requirements on the signal charged lepton momentum were lowered for both the pseudoscalar and vector modes, thereby increasing the acceptance and also reducing the model dependence; and the $X_u\ell\nu$ feed-down modelling included a simulation of the inclusive process using a parton-level calculation by De Fazio and Neubert [258], its non-perturbative parameters measured in the CLEO analysis of the $\mathrm{B} \to X_s\gamma$ photon energy spectrum [117,74], with the ISGW2 [246] model used to describe a set of expected resonant states[‡‡]. The preliminary CLEO result [257] for the branching fraction was

$$\mathcal{B}(\mathrm{B}^0 \to \pi^- e^+ \nu) = (1.376 \pm 0.180\,^{+0.116}_{-0.135} \pm 0.008 \pm 0.102 \pm 0.021) \times 10^{-4}, \quad (139)$$

where the uncertainties are statistical, experimental systematic, and the estimated uncertainties from the $\pi\ell\nu$ form factor, the $\rho\ell\nu$ form factors, and from modelling the other $\mathrm{B} \to X_u\ell\nu$ feed-down decays, respectively. By extracting rates independently in three separate q^2 ranges, the CLEO analysis demonstrated a significant reduction in the model dependence due to efficiency variations as a function of q^2.

In a preliminary effort to reduce the impact of theoretical uncertainties on the form factor normalization, the CLEO collaboration [257] used q^2-dependent partial branching fractions to extract $|V_{ub}|$ using a $\pi\ell\nu$ form factor from light cone sum rules in the range $q^2 < 16$ GeV^2 and from lattice QCD calculations above this range to obtain the averaged preliminary result

$$|V_{ub}| = (3.32 \pm 0.21 \pm {}^{+0.17}_{-0.19} \pm {}^{+0.55}_{-0.39} \pm 0.12 \pm 0.07) \times 10^{-3}, \quad (140)$$

where the uncertainties represent the same quantities defined in the branching-fraction expression above. In addition, by performing simple χ^2 fits of $|V_{ub}|$ across the three q^2 ranges with a given form factor model, the CLEO method can discriminate between competing form factor model shapes on the basis of χ^2 probabilities in the fits to the data. The CLEO technique has been used, for example, to demonstrate that the ISGW2 [246] model is likely to be unreliable for the extraction of $|V_{ub}|$ from the $\pi\ell\nu$ mode.

[‡‡]Note that the inclusive rate is reduced to allow for that portion of the total rate that is treated exclusively by the ISGW2 model.

4.3.2. Measurements of $BR(\mathrm{B} \to \rho\ell\nu)$

Analyses that are optimized for the modes $\mathrm{B} \to \rho\ell\nu$ were performed by CLEO [219] and BaBar [254]. BELLE also presented a preliminary result at ICHEP 2002 [255]. Again the modes $\mathrm{B}^+ \to \rho^0\ell^+\nu$, $\mathrm{B}^0 \to \rho^-\ell^+\nu$, $\mathrm{B}^+ \to \omega\ell^+\nu$, $\mathrm{B}^+ \to \pi^0\ell^+\nu$, and $\mathrm{B}^0 \to \pi^-\ell^+\nu$ (with $\rho^0 \to \pi^+\pi^-$, $\rho^- \to \pi^0\pi^-$, and $\omega \to \pi^0\pi^+\pi^-$) are fully reconstructed, the inclusion of charge conjugate decays is implied throughout. The neutrino momentum is inferred from the missing momentum in the event. The selection is somewhat looser than for the other analysis (see above), resulting in a higher efficiency but decreased ΔE resolution. Off-resonance data, taken below the $\Upsilon(4S)$ resonance, are used for continuum subtraction. The shape of the five signal contributions, the $b \to c$, and $b \to u$ background are provided by Monte Carlo simulation. A fit with the two variables $M_{\pi\pi(\pi)}$ and ΔE is performed, simultaneously for the five decay modes and for two (for CLEO three) lepton-energy regions. $M_{\pi\pi(\pi)}$ is the invariant hadronic mass of the ρ (ω) meson and ΔE is the difference between the reconstructed and the expected B meson energy, $\Delta E \equiv E_{\rho,\omega,\pi} + E_\ell + |\vec{p}_{\mathrm{miss}}|c - E_{\mathrm{beam}}$. These analyses are most sensitive for lepton energies above 2.3 GeV, below that backgrounds from $b \to c\ell\nu$ decays dominate. Isospin and quark model relations are again used to couple the B^+ and B^0 and ρ and ω modes. The dominant systematic uncertainties arise from uncertainties in the detector simulation and modelling of the $b \to u\ell\nu$ backgrounds.

The CLEO and BaBar analyses obtain their results for the branching ratio and $|V_{ub}|$ by averaging over five separate form factor calculations: two quark models (ISGW2 [246] and Beyer/Melikhov [256]), a lattice calculation (UKQCD [211]), a model based on light cone sum rules (LCSR [228]), and a calculation based on heavy quark and $SU(3)$ symmetries by Ligeti and Wise [259]. CLEO published the result [219]

$$\mathcal{B}(\mathrm{B}^0 \to \rho^-\, e^+\, \nu) = (2.69 \pm 0.41\, ^{+0.35}_{-0.40} \pm 0.50) \times 10^{-4}\,, \text{and} \quad (141)$$

$$|V_{ub}| = (3.23 \pm 0.24\, ^{+0.23}_{-0.26} \pm 0.58) \times 10^{-3}\,. \quad (142)$$

BaBar uses 50.5 fb^{-1} on resonance and 8.7 fb^{-1} off-resonance data and obtains the preliminary result [254]

$$\mathcal{B}(\mathrm{B}^0 \to \rho^-\, e^+\, \nu) = (3.39 \pm 0.44 \pm 0.52 \pm 0.60) \times 10^{-4}\,, \text{and} \quad (143)$$

$$|V_{ub}| = (3.69 \pm 0.23 \pm 0.27\, ^{+0.40}_{-0.59}) \times 10^{-3}\,. \quad (144)$$

BELLE quotes preliminary results only for the ISGW2 model (without theoretical error) using 29 fb^{-1} on resonance and 3 fb^{-1} off-resonance data

$$\mathcal{B}(\mathrm{B}^+ \to \rho^0\ell^+\nu) = (1.44 \pm 0.18 \pm 0.23) \times 10^{-4}\,, \text{and} \quad (145)$$

$$|V_{ub}| = (3.50 \pm 0.20 \pm 0.28) \times 10^{-3}\,. \quad (146)$$

Another result was obtained by CLEO earlier (this analysis was described in the previous Section [245])

$$\mathcal{B}(\mathrm{B}^0 \to \rho^-\, e^+\, \nu) = (2.5 \pm 0.4\, ^{+0.5}_{-0.7} \pm 0.5) \times 10^{-4}\,, \text{and} \quad (147)$$

$$|V_{ub}| = (3.3 \pm 0.2\, ^{+0.3}_{-0.4} \pm 0.78) \times 10^{-3} \text{ (as in Eq. 134).}$$

Note that the above value of $|V_{ub}|$ is extracted using both the π and ρ modes. CLEO quotes the following average result for the two analyses that were presented in Refs. [245,219]:

$$|V_{ub}| = (3.25 \pm 0.14\, ^{+0.21}_{-0.29} \pm 0.55) \times 10^{-3}\,. \quad (148)$$

More recently, the CLEO collaboration has presented a preliminary analysis [257] that uses the neutrino-reconstruction technique to reconstruct the modes $\mathrm{B} \to \rho\ \ell\ \nu$ in a self-consistent way along with the other experimentally accessible $b \to u\ \ell\ \nu$ exclusive modes. Whereas the analyses described in Refs. [219,254,255] are principally sensitive to the lepton endpoint region above 2.3 GeV, the improved CLEO measurement [257] imposes a charged-lepton momentum criterion of 1.5 GeV/c with a view to reducing the dominating theoretical uncertainties. Due to the large uncertainties in $\rho\ell\nu$ from modelling the simulated feed-down $\mathrm{B} \to X_u\ell\nu$ backgrounds, at the time of ICHEP 2002 the $\rho\ell\nu$ mode was not used by CLEO to determine a preliminary $|V_{ub}|$ value.

4.3.3. *Measurements of $BR(\mathrm{B} \to \omega\ell\nu)$*

A first preliminary result was presented at ICHEP 2002 by the BELLE collaboration [260]. The analysis uses electrons with $E > 2.2$ GeV and is based on 60 fb^{-1} on resonance and 6 fb^{-1} off-resonance data. Events are selected by requiring that the missing mass is consistent with zero ($M^2_{\rm miss} < 3.0\ {\rm GeV}/c^2$), and that the Dalitz amplitude is 75% of its maximum amplitude ($A = |p_{\pi^+} \times p_{\pi^-}| > 0.75 \times A_{\rm max}$). After subtraction of all backgrounds, 59 ± 15 signal events remain. The dominant systematic error is the background estimation (18%). The preliminary result using the ISGW2 form factors is

$$\mathcal{B}(\mathrm{B}^+ \to \omega e^+ \nu) = (1.4 \pm 0.4 \pm 0.3) \times 10^{-4}\,. \tag{149}$$

No value for $|V_{ub}|$ is given for this analysis.

4.3.4. *Measurements of $BR(\mathrm{B} \to \eta\ell\nu)$*

As in the case of the $\mathrm{B} \to \pi\ell\nu$ mode, the decay $\eta\ell\nu$ is described by only one form factor; however, the extraction of $|V_{ub}|$ is complicated by the $\eta - \eta'$ mixing. Experimentally, the η has a clear signal and, due to its large mass, one can study the region of low η momenta, where lattice calculations are most reliable. $\mathrm{B} \to \eta\ell\nu$ decays can be related via Heavy Quark Symmetry to $\mathrm{D} \to \eta\ell\nu$. It is envisioned that future measurements of the latter mode by CLEO-c can be used to calibrate the lattice calculations, and the B-factories can then use the calibrated lattice to measure $\mathrm{B} \to \eta\ell\nu$. A first preliminary result using approximately 9.7×10^6 $\mathrm{B\overline{B}}$ events was presented at DPF 2002 by the CLEO collaboration [261]:

$$\mathcal{B}(\mathrm{B}^+ \to \eta\ell^+\nu) = (0.39^{+0.18+0.09}_{-0.16-0.08}) \times 10^{-4}\,. \tag{150}$$

The separate CLEO global exclusive study [257], submitted to ICHEP 2002, also found evidence for the mode $\mathrm{B}^+ \to \eta\ell^+\nu$ with a significance of 2.5σ. No value for $|V_{ub}|$ was determined from these analyses.

4.3.5. *Summary*

Several mature measurements of the channels $\mathrm{B} \to \pi\ell\nu$ and $\mathrm{B} \to \rho\ell\nu$ exist and can be used to extract the value of $|V_{ub}|$. That these results are limited by the large theoretical uncertainties on the heavy-to-light form factor shapes and normalizations renders the exclusive approaches important to help clarify the non-perturbative QCD aspect of these decays, besides providing an alternative avenue to $|V_{ub}|$. With larger data samples, increased experimental acceptances, and improvements in our understanding of the background processes, the competing form factor models and calculations can now begin to be tested through shape-sensitive comparisons with data. A summary of some of the results is shown in Fig. 3.15. For the BELLE $\mathrm{B} \to \pi\ell\nu$ result the average of the two form factor model results is shown.

A combined value (the last row in Fig. 3.15) has been calculated as weighted average of the combined CLEO result, the BaBar $\mathrm{B} \to \rho e\nu$ result and BELLE's $\mathrm{B} \to \pi\ell\nu$ result. The weights are determined by the statistical error added in quadrature with the uncorrelated part of the systematic uncertainty. We assume that the systematic uncertainty is composed quadratically out of an uncorrelated part and a correlated part of about equal size, where the correlated part arises mainly from the modelling of the $b \to u$ feed-down background. The experimental error of the combined value includes this correlated contribution. The relative theoretical error is similar for all measurements; we take the one from the BaBar measurement. The result is

$$\boxed{|V_{ub}|_{excl} = (3.38 \ \pm \ 0.24_{exp\ {}^{+0.37}_{-0.54\ th}}) \ \times \ 10^{-3}\,.} \tag{151}$$

5. B hadron lifetimes and lifetime differences

Beside the direct determination of inclusive and exclusive s.l. decay widths, there are several other measurements of B meson properties which are instrumental in testing some of the theoretical tools (OPE,

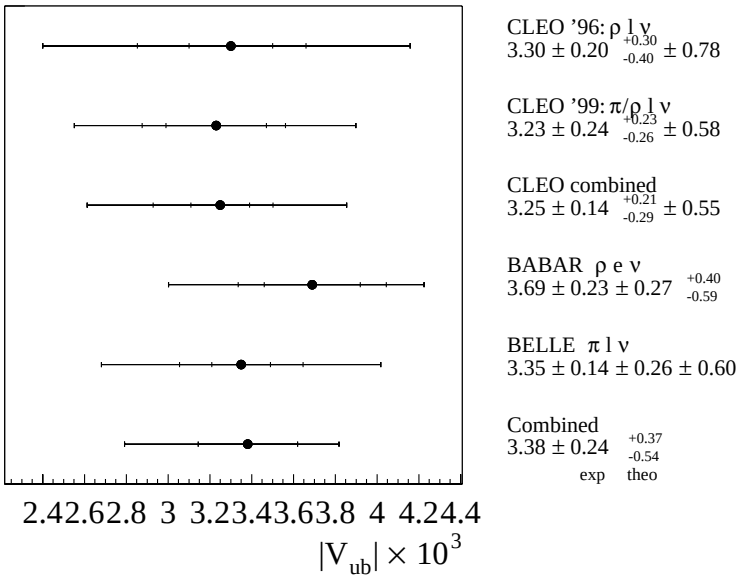

Fig. 3.15: *Current s.l. exclusive measurements of $|V_{ub}|$. The combined value is explained in the text.*

HQET, and lattice QCD) and are relevant in the precision determination of the CKM parameters. For instance, a precise evaluation of ΔM_d from the measurement of the time integrated $\mathrm{B}^0_d - \overline{\mathrm{B}}^0_d$ oscillation rate requires an accurate measurement of the $\overline{\mathrm{B}}^0_d$ meson lifetime. The accuracy of the $\overline{\mathrm{B}}^0_d$ lifetime and of the lifetime ratio of charged to neutral mesons are also a source of uncertainty in the extraction of $|V_{cb}|$ with the exclusive method. Measurements of B lifetimes test the decay dynamics, giving important information on non-perturbative QCD effects induced by the spectator quark(s). Decay rates are expressed using the OPE formalism, as an expansion in Λ_{QCD}/m_Q. Spectator effects contribute at $O(1/m_Q^3)$ and non-perturbative contributions can be reliably evaluated, at least in principle, using lattice QCD calculations.

Since the start of the data taking at LEP/SLC/Tevatron, an intense activity has been devoted to studies of inclusive and exclusive B hadron lifetimes. Most of the exclusive lifetime measurements are based on the reconstruction of the beauty hadron proper time by determining its decay length and momentum. The most accurate measurements are based on inclusive or partial reconstructions (such as topological reconstruction of B decay vertex and determination of its charge or reconstruction of $\mathrm{B} \to \mathrm{D}^{(*)}\ell^+\nu X$). These techniques exploit the kinematics offered by e^+e^- colliders at energies around the Z^0 peak, and also by hadron colliders, and the excellent tracking capabilities of the detectors. The accuracy of the results for B_d and B_u mesons, where the samples of candidates are larger, are dominated by systematics, including backgrounds, b-quark fragmentation, branching fractions and modelling of the detector response. In the case of B_s and Λ_b, the uncertainty is still statistical dominated. Final averages of the results obtained are given in Table 3.22 [262]. The averages for the B^0_d and B^+ lifetimes include also the recent very precise measurements by the B factories [263]. Fig. 3.16 gives the ratios of different B hadron lifetimes, compared with theory predictions (dark yellow bands). The achieved experimental precision of the hadron lifetimes – from a fraction of percent to a few percent – is quite remarkable. The phenomenological interpretation of these results in terms of exclusive lifetime ratios is discussed extensively in Sec 5.6.

The longer lifetime of charged B mesons as compared to the neutral ones has been established at 5σ level. The B^0_d and B^0_s lifetimes are found to be equal within a $\simeq$4% accuracy. The lifetimes of b-baryons appear to be shorter than those of B^0_d mesons. Although this is in qualitative agreement with

B Hadrons	Lifetime [ps]
$\tau(b)$	1.573 ± 0.007 (0.4 %)
$\tau(\mathrm{B}_d^0)$	1.540 ± 0.014 (0.9 %)
$\tau(\mathrm{B}^+)$	1.656 ± 0.014 (0.8 %)
$\tau(\mathrm{B}_s^0)$	1.461 ± 0.057 (3.9 %)
$\tau(\Lambda_b^0)$	1.208 ± 0.051 (4.2 %)

$\tau(\mathrm{B}_u^+)/\tau(\mathrm{B}_d^0) = 1.073 \pm 0.014$

$\tau(\mathrm{B}_s^0)/\tau(\mathrm{B}_d^0) = 0.949 \pm 0.038$

$\tau(\Lambda_b^0)/\tau(\mathrm{B}_d^0) = 0.798 \pm 0.052$

$\tau(b\,\mathrm{baryon})/\tau(\mathrm{B}_d^0) = 0.784 \pm 0.034$

Table 3.22: *Summary of B hadron lifetime results provided by the Lifetime Working Group [262].*

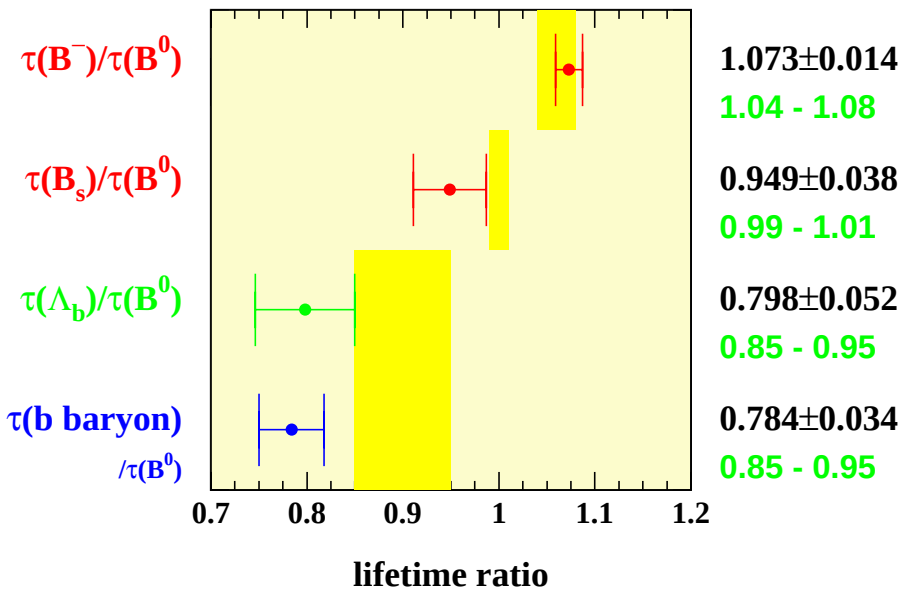

Fig. 3.16: *Ratios of exclusive B hadrons lifetimes [262], compared with the theoretical predictions given in Secs. 5.1. and 5.6. and shown by the dark yellow bands.*

expectations, the magnitude of the lifetime ratio of beauty baryons to mesons has been the subject of intense scrutiny, both by experiments and theorists, in view of a possible discrepancy. Indeed, recent calculations of higher order terms have improved the agreement of b baryon lifetime predictions with the present experimental results. The most precise determinations of the b baryon lifetimes come from two classes of partially reconstructed decays. The first has a Λ_c^+ baryon exclusively reconstructed in association with a lepton of opposite charge. The second uses more inclusive final states, where the enrichment in beauty baryons is obtained by requiring a proton or a Λ^0 to be tagged together with a lepton in the decay. These measurements are affected by uncertainties related to the Λ_b polarization and to poorly known beauty baryon fragmentation functions and decay properties.

Accessing the lifetime differences $\Delta\Gamma_s$ offers also an independent possibility of constraining the CKM unitarity triangle. This quantity is sensitive to a combination of CKM parameters very similar to the one entering ΔM_s (see Eq. (162) below), and an upper bound on $\Delta\Gamma_s$ translates in a upper bound on ΔM_s. With future accurate determinations, this method can therefore provide, in conjunction with the determination of ΔM_d, an extra constraint on the $\bar{\rho}$ and $\bar{\eta}$ parameters.

In the Standard Model the width difference $(\Delta\Gamma/\Gamma)$ of B_s mesons is expected to be rather large and within the reach of experiment in the near future. Recent experimental studies already provide an interesting bound on this quantity as will be detailed in Sec. 5.5. On the other hand, the two mass eigenstates of the neutral B_d system have in the SM only slightly different lifetimes. This is because the difference in the lifetimes is CKM-suppressed with respect to that in the B_s system. A rough estimate leads to $\frac{\Delta\Gamma_d}{\Gamma_d} \sim \frac{\Delta\Gamma_s}{\Gamma_s} \cdot \lambda^2 \approx 0.5\%$, where $\Delta\Gamma_s/\Gamma_s \approx 15\%$ [264,265].

5.1. Theoretical description of the width difference of B_s mesons

The starting point in the study of beauty hadron lifetimes is the construction of the effective weak Hamiltonian for the $\Delta B = 1$ transitions, which is obtained after integrating out the heavy degrees of freedom of the W and Z^0-bosons and of the top quark.

Neglecting the Cabibbo suppressed contribution of $b \to u$ transitions and terms proportional to $|V_{td}|/|V_{ts}|$ ($\sim \lambda$) in the penguin sector, the $\Delta B = 1$ effective Hamiltonian can be written as (cf. Eq. (26) of Chapter 1)

$$\mathcal{H}_{\rm eff}^{\Delta B=1} = \frac{G_F}{\sqrt{2}} V_{cb}^* \sum_i C_i(\mu) Q_i + h.c. \tag{152}$$

The explicit expressions for the various operators can be found e.g. in [266]. The Wilson coefficients $C_i(\mu)$ in the effective Hamiltonian contain the information about the physics at short distances (large energies) and are obtained by matching the full (Standard Model) and the effective theory ($\mathcal{H}_{\rm eff}^{\Delta B=1}$) at the scale $\mu \simeq M_W$. This matching, as well as the evolution from M_W to the typical scale $\mu \simeq m_b$, are known at the next-to-leading order (NLO) in perturbation theory [266].

Through the optical theorem, the width difference of B_s mesons can be related to the absorptive part of the forward scattering amplitude

$$\Delta\Gamma_{\mathrm{B}_s} = -\frac{1}{M_{\mathrm{B}_s}} \mathrm{Im} \langle \bar{\mathrm{B}}_s | \mathcal{T} | \mathrm{B}_s \rangle \,, \tag{153}$$

where the transition operator $\mathcal{T}$ is written as

$$\mathcal{T} = i \int d^4x \; T \left(\mathcal{H}_{eff}^{\Delta B=1}(x) \mathcal{H}_{eff}^{\Delta B=1}(0) \right) \,, \tag{154}$$

in terms of the $\Delta B = 1$ effective Hamiltonian.

Because of the large mass of the b-quark, it is possible to construct an OPE for the transition operator $\mathcal{T}$, which results in a sum of local operators of increasing dimension. The contributions of higher dimensional operators are suppressed by higher powers of the b-quark mass. In the case of the width

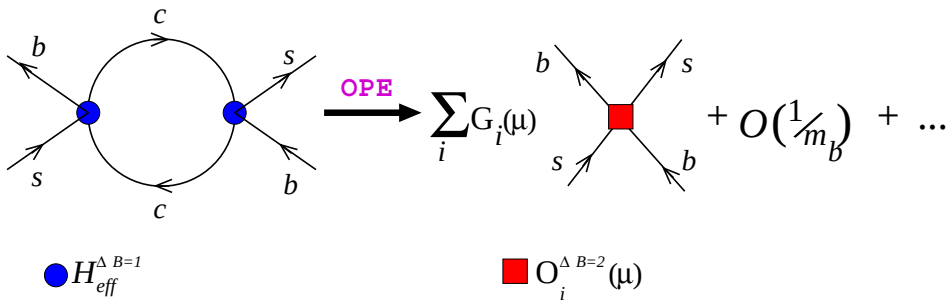

Fig. 3.17: *Heavy quark expansion: the non-local T-product of the l.h.s. (with the doubly inserted $\mathcal{H}_{eff}^{\Delta B=1}$) is expanded in the series in $1/m_b$, each coefficient being the sum of local $\Delta B = 2$ operators.*

difference $(\Delta\Gamma/\Gamma)_{B_s}$, the leading term in the expansion is parametrically of order $16\pi^2(\Lambda_{\rm QCD}/m_b)^3$. The result of this second OPE, which is illustrated in Fig. 3.17, reads

$$\Delta\Gamma_{\rm B_s} = \frac{G_F^2 m_b^2}{12\pi M_{\rm B_s}} |V_{cb}^* V_{cs}|^2 \left\{ G_1(\mu)\langle \bar{\rm B}_s|O_1(\mu)|{\rm B}_s\rangle + G_2(\mu)\langle \bar{\rm B}_s|O_2(\mu)|{\rm B}_s\rangle + \delta_{1/m_b} \right\}, \qquad (155)$$

where the $\Delta B = 2$ operators on the r.h.s. are

$$\begin{aligned} O_1 &= \bar{b}\gamma_\mu(1-\gamma_5)s\;\bar{b}\gamma_\mu(1-\gamma_5)s\,, \\ O_2 &= \bar{b}(1-\gamma_5)s\;\bar{b}(1-\gamma_5)s\,, \end{aligned} \qquad (156)$$

where a sum over repeated colour indices (i, j) is understood; δ_{1/m_b} contains the $1/m_b$ correction [267]. Contributions proportional to $1/m_b^n$ $(n \geq 2)$ are neglected. The short distance physics effects (above the scale μ) are now encoded in the coefficient functions $G_{1,2}(\mu)$ which are combinations of the $\Delta B = 1$ Wilson coefficients.

The NLO corrections to the coefficients $G_{1,2}$ have been computed in Ref. [264]. They are large ($\sim 35\%$) and their inclusion is important. The long distance QCD dynamics is described in Eq. (155) by the matrix elements of the local operators O_1 and O_2, which are parametrized as

$$\langle \bar{\rm B}_s|O_1(\mu)|{\rm B}_s\rangle = \frac{8}{3} F_{\rm B_s}^2 M_{\rm B_s}^2 B_1(\mu)\,, \qquad \langle \bar{\rm B}_s|O_2(\mu)|{\rm B}_s\rangle = -\frac{5}{3}\left(\frac{F_{\rm B_s} M_{\rm B_s}^2}{m_b(\mu)+m_s(\mu)}\right)^2 B_2(\mu)\,, \quad (157)$$

where the B-parameters are equal to unity in the vacuum saturation approximation (VSA). To measure the deviations from the VSA one should also include the non-factorizable (non-perturbative) QCD effects. For such a computation a suitable framework is provided by the lattice QCD simulations. In principle, the lattice QCD approach allows the fully non-perturbative estimate of the hadronic quantities to an arbitrary accuracy. In practice, however, several approximations need to be made which, besides the statistical, introduce also a systematic uncertainty in the final results. The steady progress in increasing the computational power, combined with various theoretical improvements, helps reducing ever more systematic uncertainties. Various approximate treatments of the heavy quark on the lattice, and thus various ways to compute the B-parameters of Eq. (157), have been used:

- HQET: After discretizing the HQET lagrangian (to make it tractable for a lattice study), the matrix elements of Eq. (157) were computed in Ref. [268], but only in the static limit ($m_b \to \infty$).
- NRQCD: A step beyond the static limit has been made in Ref. [269], where the $1/m_b$-corrections to the NRQCD lagrangian have been included, as well as a large part of $1/m_b$-corrections to the

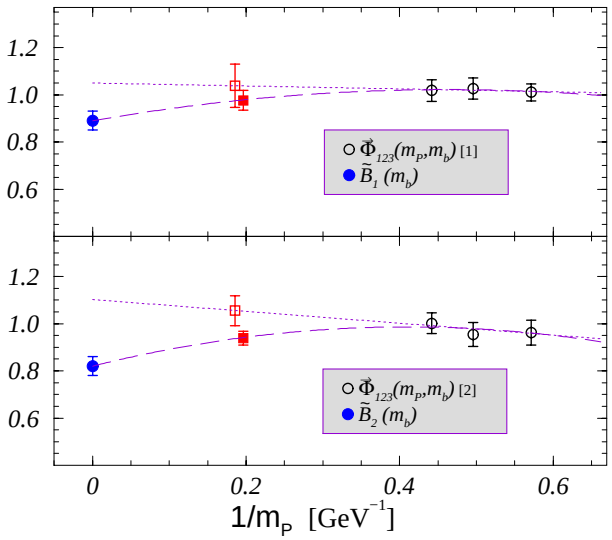

Fig. 3.18: *The lattice determination of $B_1(m_b)$ and $B_2(m_b)$ obtained in QCD with three heavy–light mesons m_P are combined with the static HQET result, $m_P \to \infty$. The result of the linear extrapolation to $1/M_{\mathrm{B}_s}$ is marked by the empty squares, whereas the interpolation is denoted by the filled squares.*

matrix elements of the four-fermion operators. It is important to note, however, that discretization errors associated with the light degrees of freedom cannot be reduced by taking a continuum limit, $a \to 0$, since the NRQCD expansion requires $a \sim 1/m_Q$. Instead, these errors are reduced by including higher and higher dimension operators whose coefficients are adjusted to improve the discretization. Such a procedure is difficult to carry out beyond terms of $O(a)$ and one must therefore show that the residual discretization and $1/m_b$ power-correction effects are small at finite a [270].

- Relativistic approach: The matrix elements were computed [271] by using an $O(a)$-improved action in the region of masses close to the charm quark and then extrapolated to the b-quark sector by using the heavy quark scaling laws. However, this extrapolation can be significant and discretization errors will be amplified to varying degrees depending on the quantity studied, if it is performed before a continuum limit is taken. A discussion of this amplification in the context of neutral B meson mixing can be found in [272].

As of now, none of the above approaches is accurate enough on its own and all of them should be used to check the consistency of the obtained results.

A more accurate determination of the B-parameters relevant for $(\Delta\Gamma/\Gamma)_{B_s}$ has been recently obtained in Ref. [273]. To reduce the systematics of the heavy quark extrapolation, the results obtained in the static limit of the HQET [268] were combined with those of Ref. [271], where lattice QCD is employed for three mesons of masses in the region of D_s-mesons. As a result, one actually *interpolates* to the mass of the B_s-meson. This interpolation is shown in Fig. 3.18. The resulting values from Ref. [273], in the $\overline{\mathrm{MS}}$(NDR) scheme of Ref. [264], are

$$B_1(m_b) = 0.87(2)(5)\ , \qquad B_2(m_b) = 0.84(2)(4)\ , \tag{158}$$

where the first errors are statistical and the second include various sources of systematics. An important remark is that the above results are obtained in the quenched approximation ($n_f = 0$), and the systematic error due to quenching could not be estimated. The effect of the inclusion of the dynamical quarks has been studied within the NRQCD approach. The authors of Ref. [274] conclude that the B-parameters are

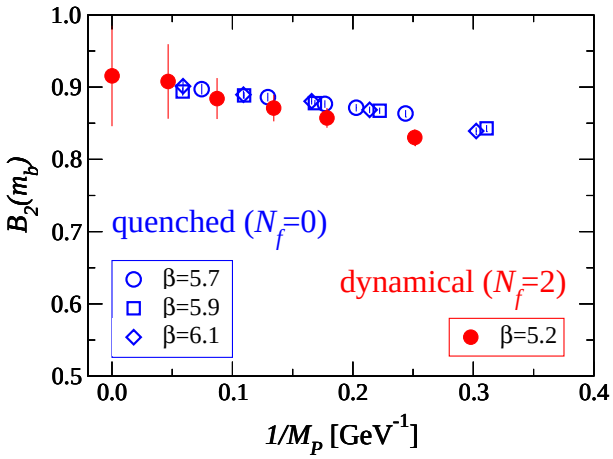

Fig. 3.19: *Results of the JLQCD collaboration [274], showing that the effects of quenching are negligible.*

essentially insensitive to the change from $n_f = 0$ to $n_f = 2$ (see Fig. 3.19). From their (high statistics) unquenched simulation, they quote

$$\begin{aligned} B_1(m_b)_{(n_f=2)} &= 0.83(3)(8)\ , \qquad B_2(m_b)_{(n_f=2)} = 0.84(6)(8)\ , \\ B_1(m_b)_{(n_f=0)} &= 0.86(2)(5)\ , \qquad B_2(m_b)_{(n_f=0)} = 0.85(1)(5)\ , \end{aligned} \tag{159}$$

where, for comparison, we also display their most recent results obtained in the quenched approximation [275]. The results of the two lattice approaches (Eqs. (158) and (159)) are in good agreement.

The theoretical estimate of $(\Delta\Gamma/\Gamma)_{\mathrm{B}_s}$ is obtained by combining the lattice calculations of the matrix elements with the Wilson coefficients. To that purpose two different formulas have been proposed which are both derived from Eq. (155):

- In Ref. [264] the width difference has been normalized by using the s.l. branching ratio $BR(\mathrm{B}_d \to X\ell\nu_\ell)$ which is experimentally determined. In this way one obtains the expression

$$\left(\frac{\Delta\Gamma}{\Gamma}\right)_{\mathrm{B}_s} = \frac{128\pi^2 BR(\mathrm{B_d} \to \mathrm{X}\ell\nu_\ell)}{3\, m_b^3\, g_{SL}\, \eta_{QCD}} |V_{cs}|^2 F_{\mathrm{B}_s}^2 M_{\mathrm{B}_s}\, \mathcal{M}\,, \tag{160}$$

  where

$$\mathcal{M} = G_1(z) B_1(m_b) + \frac{5}{8} \frac{M_{\mathrm{B}_s}^2}{\left(m_b(m_b) + m_s(m_b)\right)^2} G_2(z) B_2(m_b) + \tilde{\delta}_{1/m}\,, \tag{161}$$

  with $z = m_c^2/m_b^2$, and the phase space factor $g_{SL} = F(z)$ and $\eta_{QCD} = 1 - \frac{2}{3}\frac{\alpha_s}{\pi} f(z)$ are given in Sec. 2.4.

- One can also use the measured mass difference in the B_d neutral meson system to write [271]:

$$\left(\frac{\Delta\Gamma}{\Gamma}\right)_{\mathrm{B}_s} = \frac{4\pi}{3}\frac{m_b^2}{M_W^2}\left|\frac{V_{cb}V_{cs}}{V_{td}V_{tb}}\right|^2 \left(\tau_{\mathrm{B}_s} \Delta M_{B_d} \frac{M_{\mathrm{B}_s}}{M_{B_d}}\right)^{(\mathrm{exp})} \frac{B_1(m_b)\xi^2}{\eta_B(m_b) S_0(x_t)}\, \mathcal{M}\,, \tag{162}$$

  where ξ is defined as $\xi = (F_{\mathrm{B}_s}\sqrt{\hat{B}_{\mathrm{B}_s}})/(f_{B_d}\sqrt{\hat{B}_{B_d}})$, and $S_0(x_t)$ is defined in Sec. 1.1. of Chapter 4.

From the point of view of the hadronic parameters, the advantage of the second formula is that it is expressed in terms of the ratio ξ, in the evaluation of which many systematic uncertainties of the lattice

calculations cancel. The estimate of ξ, however, is affected by an uncertainty due to the chiral extrapolation, which comes from the fact that in present lattice calculation it is not possible to simulate directly quark masses smaller than $\sim m_s/2$. Therefore an extrapolation to the physical d-quark mass is necessary. The first formula, instead, is expressed in terms of the decay constant F_{B_s} whose determination does not require a chiral extrapolation. However, other systematic uncertainties may be important in this case such as those coming from the value of the absolute lattice scale (inverse lattice spacing), the renormalization of the axial current and $1/m_b$-corrections.

In the numerical analysis, to derive a prediction for $(\Delta\Gamma/\Gamma)_{B_s}$, we use the values of parameters listed in Table 3.23. Notice that in the error for ξ the uncertainty due to the chiral extrapolation is quoted separately (second error).

Parameter	*Value and error*	*Parameter*	*Value and error*
$\alpha_s(m_b)$	0.22	m_t	165 ± 5 GeV
M_W	80.41 GeV	m_b	4.26 ± 0.09 GeV
M_{B_d}	5.28 GeV	m_c/m_b	0.28 ± 0.02
M_{B_s}	5.37 GeV	m_s	105 ± 25 MeV
τ_{B_s}	$1.461 \pm 0.057\, ps$	$\eta_B(m_b)$	0.85 ± 0.02
$\lvert V_{cb}\rvert$	0.0395 ± 0.0017	F_{B_s}	238 ± 31 MeV
$\lvert V_{ts}\rvert$	0.0386 ± 0.0013	ξ	$1.24 \pm 0.03 \pm 0.06$
$\lvert V_{cs}\rvert$	0.9756 ± 0.0005	$B_1(m_b)$	0.86 ± 0.06
$\lvert V_{td}\rvert$	0.0080 ± 0.0005	$B_2(m_b)$	0.84 ± 0.05
ΔM_{B_d}	$0.503 \pm 0.006\, ps^{-1}$	$G(z)$	0.030 ± 0.007
$BR(\mathrm{B}_d \to X l \nu_l)$	$10.6 \pm 0.3\%$	$G_S(z)$	0.88 ± 0.14

Table 3.23: *Average and errors of the main parameters used in the numerical analysis. When the error is negligible it has been omitted. The heavy-quark masses (m_t, m_b and m_c) are the $\overline{\mathrm{MS}}$ masses renormalized at their own values, e.g. $m_t = m_t^{\overline{\mathrm{MS}}}(m_t^{\overline{\mathrm{MS}}})$. The strange quark mass, $m_s = m_s^{\overline{\mathrm{MS}}}(\mu = 2\,GeV)$, is renormalized in $\overline{\mathrm{MS}}$ at the scale $\mu = 2$ GeV. The value for F_{B_s} and ξ are taken from Ref. [217].*

The value of the b-quark mass deserves a more detailed discussion. The *b-pole* mass, which corresponds at the NNLO to the $\overline{MS}$ mass $m_b = 4.26$ GeV quoted in Table 3.23, is $m_b^{pole} = 4.86$ GeV. Since the formulae for $(\Delta\Gamma/\Gamma)_{B_s}$ have been derived only at the NLO, however, it may be questionable whether to use $m_b^{pole} = 4.86$ GeV or $m_b^{pole} = 4.64$ GeV, corresponding to $m_b \simeq 4.26$ GeV at the NLO. That difference is very important for the value of $\tilde{\delta}_{1/m}$ which, computed in the VSA, varies between -0.4 and -0.6. In addition, a first principle non-perturbative estimates of the matrix elements entering the quantity $\tilde{\delta}_{1/m}$ is still lacking. For this reason we include $\pm 30\%$ of uncertainty in the estimate of$\tilde{\delta}_{1/m}$ stemming from the use of the VSA. We finally obtain the predictions:

$$\left(\frac{\Delta\Gamma}{\Gamma}\right)^{Eq.\ (160)}_{\mathrm{B}_s} = (8.5 \pm 2.8) \times 10^{-2}\,, \qquad \left(\frac{\Delta\Gamma}{\Gamma}\right)^{Eq.\ (162)}_{\mathrm{B}_s} = (9.0 \pm 2.8) \times 10^{-2}\,. \tag{163}$$

In Fig. 3.20 we show the corresponding probability distribution functions (pdf).

We see that the results obtained with the two formulas are in good agreement. From the pdfs we observe that $(\Delta\Gamma/\Gamma)_{B_s}$ can span a very large range of values, say between 0.03 and 0.15: the theoretical

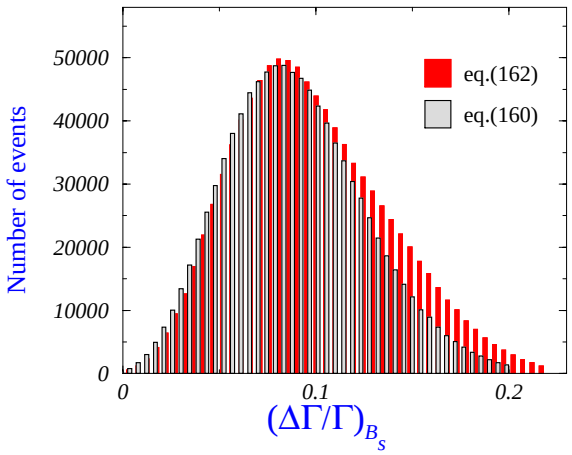

Fig. 3.20: *Probability density function (pdf) for* $(\Delta\Gamma/\Gamma)_{B_s}$ *using the formulas 160 and 162. The pdf corresponding to the smaller value is the one obtained with Eq. (160).*

uncertainty on this quantity is large. The main source of uncertainty, besides the assumption of local quark-hadron duality, comes from the $1/m_b$ corrections parameterized by $\tilde{\delta}_{1/m}$. That uncertainty is enhanced by a rather large cancellation between the leading contributions (first two terms of Eq. (161)) and it is very difficult to reduce, since it would require the non-perturbative estimate of many dimension-7, $\Delta B = 2$, operators. Such a calculation is very challenging and most probably beyond the present capability of the lattice QCD approach. Given the present theoretical uncertainty on $(\Delta\Gamma/\Gamma)_{\mathrm{B}_s}$ it is unlikely that signals of physics beyond the Standard Model may be detected from the measurement of this quantity.

5.2. Width difference of B_d mesons

The phenomenology of $\Delta\Gamma_d$ has been mostly neglected so far, in contrast to the lifetime difference in the B_s system, because the present data fall so short of the needed accuracy. However, in the prospect of experiments with high time resolution and large statistics, its study will become relevant. In fact, it may affect a precise determination of the CKM phase β, and it also provides several opportunities for detecting New Physics.

The width difference $\Delta\Gamma_d/\Gamma_d$ has been estimated in [276] including the $1/m_b$ contribution and part of the NLO QCD corrections. Adding the latter corrections decreases the value of $\Delta\Gamma_d/\Gamma_d$ computed at the leading order by a factor of almost 2. This yields

$$\Delta\Gamma_d/\Gamma_d = (2.6^{+1.2}_{-1.6}) \times 10^{-3}\,. \tag{164}$$

Using another expansion of the partial NLO QCD corrections proposed in [277], one gets

$$\Delta\Gamma_d/\Gamma_d = (3.0^{+0.9}_{-1.4}) \times 10^{-3}\,, \tag{165}$$

where preliminary values for the bag factors from the JLQCD collaboration [278] are used. The contributions to the error (in units of 10^{-3}) are ± 0.1 each from the uncertainties in the values of the CKM parameters and the parameter $x_d = (\Delta M_d/\Gamma)_d$, ± 0.5 each from the bag parameters and the mass of the b quark, ± 0.3 from the assumption of naive factorization made for the $1/m_b$ matrix elements, and $^{+0.5}_{-1.2}$ from the scale dependence. The error due to the missing terms in the NLO contribution is estimated to be ± 0.8 in the calculation of Eq. (164). Although it is reduced in the calculation of Eq. (165), a complete NLO calculation is definitely desirable for a more reliable result.

5.3. Relation between $\sin(2\beta)$ and $\Delta\Gamma_d$

The time-dependent CP asymmetry measured through the 'gold-plated' mode $\mathrm{B}_d \to J/\psi \mathrm{K}_\mathrm{S}$ is

$$\mathcal{A}_{CP} = \frac{\Gamma[\overline{\mathrm{B}}_d(t) \to J/\psi \mathrm{K}_S] - \Gamma[\mathrm{B}_d(t) \to J/\psi \mathrm{K}_S]}{\Gamma[\overline{\mathrm{B}}_d(t) \to J/\psi \mathrm{K}_S] + \Gamma[\mathrm{B}_d(t) \to J/\psi \mathrm{K}_S]} \approx \sin(\Delta M_d t)\sin(2\beta) \ , \tag{166}$$

which is valid when the lifetime difference, the direct CP violation, and the mixing in the neutral K mesons are neglected. As the accuracy of this measurement increases, the corrections due to these factors will need to be taken into account. Using the effective parameter $\bar{\epsilon}$ that absorbs several small effects and uncertainties, including penguin contributions (see [276] for a precise definition), and keeping only linear terms in that effective parameter, the asymmetry becomes

$$\begin{aligned} \mathcal{A}_{CP} \ &= \ \sin(\Delta M_d t)\sin(2\beta)\left[1 - \sinh\left(\frac{\Delta\Gamma_d t}{2}\right)\cos(2\beta)\right] \\ &\quad +2\mathrm{Re}(\bar{\epsilon})\left[-1 + \sin^2(2\beta)\sin^2(\Delta M_d t) - \cos(\Delta M_d t)\right] \\ &\quad +2\mathrm{Im}(\bar{\epsilon})\cos(2\beta)\sin(\Delta M_d t) \ . \end{aligned} \tag{167}$$

The first term represents the standard approximation of Eq. (166) together with the correction due to the lifetime difference $\Delta\Gamma_d$. The other terms include corrections due to CP violation in the B–$\bar{\mathrm{B}}$ and K–$\bar{\mathrm{K}}$ mixings.

Future experiments aim to measure β with an accuracy of 0.005 [279]. The corrections due to $\bar{\epsilon}$ and $\Delta\Gamma_d$ will become a large fraction of the systematic error. This error can be reduced by a simultaneous fit of $\sin(2\beta), \Delta\Gamma_d$ and $\bar{\epsilon}$. The BaBar Collaboration gives a bound on the coefficient of $\cos(\Delta M_d t)$ in Eq. (168), where other correction terms are neglected [280]. When measurements will become accurate enough to really constrain the $\cos(\Delta M_d t)$ term, all the other terms in Eq. (168) would also be measurable. In this case, the complete expression for $\mathcal{A}_{CP}$ needs to be used.

5.4. New Physics signals

The lifetime difference in neutral B mesons can be written in the form

$$\Delta\Gamma_q = -2|\Gamma_{21}|_q \cos(\Theta_q - \Phi_q) \ , \tag{168}$$

where $\Theta_q \equiv \mathrm{Arg}(\Gamma_{21})_q, \Phi_q \equiv \mathrm{Arg}(M_{21})_q$, and $q \in \{d, s\}$ (see Sec. 1.2.). In the B_s system, the new physics effects can only decrease the value of $\Delta\Gamma_s$ with respect to the SM [281]. In the B_d system, an upper bound for $\Delta\Gamma_d$ can be given, depending on the additional assumption of three-generation CKM unitarity:

$$\Delta\Gamma_d \leq \frac{\Delta\Gamma_d(\mathrm{SM})}{\cos[\mathrm{Arg}(1+\delta f)]} \ , \tag{169}$$

where δf depends on hadronic matrix elements. The bound in Eq. (169) can be calculated up to higher order corrections. In [276], $|\mathrm{Arg}(1+\delta f)| < 0.6$, so that $\Delta\Gamma_d < 1.2\ \Delta\Gamma_d(\mathrm{SM})$. A violation of this bound would indicate a violation of the unitarity of 3×3 CKM matrix. A complete NLO calculation would provide a stronger bound.

The ratio of two effective lifetimes can be used to measure the quantity $\Delta\Gamma_{obs(d)} \equiv \cos(2\beta)\Delta\Gamma_d/\Gamma_d$ (see Sec. 5.5.3.). In the presence of new physics, this quantity is in fact (see Eq. (168))

$$\Delta\Gamma_{obs(d)} = -2(|\Gamma_{21}|_d/\Gamma_d)\cos(\Phi_d)\cos(\Theta_d - \Phi_d), \tag{170}$$

where in the Standard Model

$$\Delta\Gamma_{obs(d)}(\mathrm{SM}) = 2(|\Gamma_{21}|_d/\Gamma_d)\cos(2\beta)\cos[\mathrm{Arg}(1+\delta f)] \tag{171}$$

is predicted to be positive. New physics is not expected to affect Θ_d, but it may affect Φ_d in such a way that $\cos(\Phi_d)\cos(\Theta_d - \Phi_d)$ changes sign. A negative sign of $\Delta\Gamma_{obs(d)}$ would therefore be a clear signal for New Physics. The time-dependent asymmetry in $J/\psi \mathrm{K}_S$ (or $J/\psi K_L$) measures $\mathcal{A}_{CP} = -\sin(\Delta M_d t)\sin(\Phi_d)$, where $\Phi_d = -2\beta$ in the SM. The measurement of $\sin(\Phi_d)$ still allows for a discrete ambiguity $\Phi_d \leftrightarrow \pi - \Phi_d$. If Θ_d can be determined independently of the mixing in the B_d system, then the measurement of $\Delta\Gamma_{obs(d)}$ will in principle resolve the discrete ambiguity.

In conclusion, the measurement of $\Delta\Gamma_d$ and related quantities should become possible in a near future, providing further important informations on the flavour sector of the SM.

5.5. Experimental review and future prospects for $\Delta\Gamma$ measurements

The width difference $\Delta\Gamma_s = \Gamma_{long} - \Gamma_{short}$ can be extracted from lifetime measurements of B_s decays. A first method is based on a double exponential lifetime fit to samples of events containing mixtures of CP eigenstates, like s.l. or $\mathrm{D_s}$-hadron B_s decays. A second approach consists in isolating samples of a single CP eigenstate, such as $\mathrm{B}_s \to J/\psi\phi$. The former method has a quadratic sensitivity to $\Delta\Gamma_s$, whereas the latter has a linear dependence and suffers from a much reduced statistics. A third method has been also proposed [299] and consists in measuring the branching fraction $\mathrm{B_s} \to \mathrm{D}_s^{(*)+}\mathrm{D}_s^{(*)-}$. More details on the different analyses performed are given in the following.

L3 [300] and DELPHI [301] use inclusively reconstructed $\mathrm{B_s}$ and $\mathrm{B}_s \to \mathrm{D}_s l\nu X$ events, respectively. If those sample are fitted assuming a single exponential lifetime, then, assuming $\frac{\Delta\Gamma_s}{\Gamma_s}$ is small, the measured lifetime is given by:

$$\tau_{\mathrm{B}_s^{incl.}} = \frac{1}{\Gamma_s}\frac{1}{1-\left(\frac{\Delta\Gamma_s}{2\Gamma_s}\right)^2}\ (\mathrm{incl.\,B}_s) \qquad ; \qquad \tau_{\mathrm{B}_s^{semi.}} = \frac{1}{\Gamma_s}\frac{1+\left(\frac{\Delta\Gamma_s}{2\Gamma_s}\right)^2}{1-\left(\frac{\Delta\Gamma_s}{2\Gamma_s}\right)^2}\ (\mathrm{B}_s \to \mathrm{D}_s l\nu X) \qquad (172)$$

The single lifetime fit is thus more sensitive to the effect of $\Delta\Gamma$ in the s.l. case than in the fully inclusive one. The same method is used for the $\mathrm{B_s}$ world average lifetime (recomputed without the DELPHI measurement [302]) obtained by using only the s.l. decays. The technique of reconstructing only decays at defined CP has been exploited by ALEPH, DELPHI and CDF. ALEPH [299], reconstructs the decay $\mathrm{B_s} \to \mathrm{D_s}^{(*)+}\mathrm{D_s}^{(*)-} \to \phi\phi\mathrm{X}$ which is predominantly CP even. The proper time dependence of the $\mathrm{B_s^0}$ component is a simple exponential and the lifetime is related to $\Delta\Gamma_s$ via

$$\frac{\Delta\Gamma_\mathrm{s}}{\Gamma_\mathrm{s}} = 2\left(\frac{1}{\Gamma_\mathrm{s}}\frac{1}{\tau_{\mathrm{B_s^{short}}}} - 1\right). \qquad (173)$$

Another method consists in using the branching fraction, $\mathrm{BR}(\mathrm{B_s} \to \mathrm{D_s}^{(*)+}\mathrm{D_s}^{(*)-})$. Under several theoretical assumptions [303]

$$BR(\mathrm{B}_s \to \mathrm{D}_s^{(*)+}\mathrm{D}_s^{(*)-}) = \frac{\Delta\Gamma_s}{\Gamma_s\left(1+\frac{\Delta\Gamma_s}{2\Gamma_s}\right)}. \qquad (174)$$

This is the only constraint on $\frac{\Delta\Gamma_\mathrm{s}}{\Gamma_s}$ which does not rely on the measurement of the $\mathrm{B_s^0}(\mathrm{B}_d^0)$ lifetime. DELPHI [304] uses a sample of $\mathrm{B_s} \to \mathrm{D_s} - \mathrm{hadron}$, which is expected to have an increased CP-even component as the contribution due to $\mathrm{D}_s^{(*)+}\mathrm{D}_s^{(*)-}$ events is enhanced by selection criteria. CDF [305] reconstructs $\mathrm{B}_s \to J/\psi\phi$ with $J/\psi \to \mu^+\mu^-$ and $\phi \to \mathrm{K^+K^-}$ where the CP even component is equal to 0.84 ± 0.16 obtained by combining CLEO [306] measurement of CP even fraction in $\mathrm{B_d} \to \mathrm{J}/\psi\mathrm{K}^{*0}$ and possible $SU(3)$ symmetry correction. The results, summarized in Table 3.24, are combined following the procedure described in [307]. The log-likelihood of each measurement are summed and normalized with respect to its minimum. Two measurements are excluded from the average for different reasons:

Experiment	B_s decays	$\Delta\Gamma_s/\Gamma_s$
DELPHI	$B_s \to D_s l\nu X$	< 0.47
Other s.l.	$B_s \to D_s l\nu X$	< 0.31
ALEPH	$B_s \to \phi\phi X$	$0.43^{+0.81}_{-0.48}$
ALEPH (BR method)	$B_s \to \phi\phi X$	$0.26^{+0.30}_{-0.15}$
DELPHI	$B_s \to D_s - \text{hadron}$	< 0.70
CDF	$B_s \to J/\psi\phi$	$0.36^{+0.50}_{-0.42}$

Table 3.24: *Summary of the available measurements on $\Delta\Gamma_s/\Gamma_s$ used to calculate the limit.*

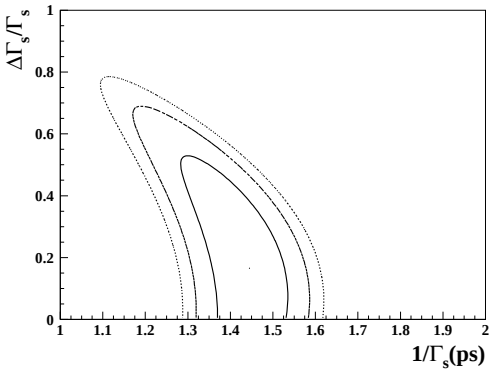

Fig. 3.21: 65%, 95% *and* 99% *C. L. contours of negative log-likelihood in the τ_{B_s}, $\Delta\Gamma_s/\Gamma_s$ plane.*

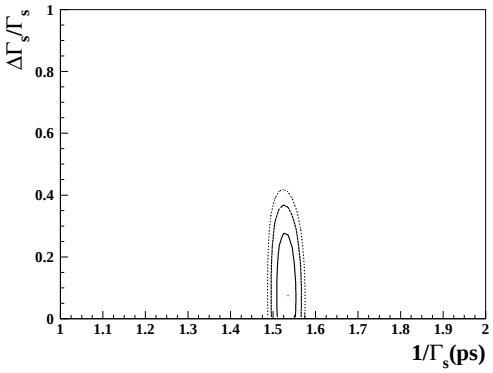

Fig. 3.22: *Same as Fig. 3.21 with the constraint $1/\Gamma_s = \tau_{B_d}$.*

- L3 inclusive analysis: the likelihood is not available and it cannot be reconstructed from the numerical result;
- ALEPH branching ratio analysis: the theoretical assumptions in Eq. (174) are controversial and the systematic error due to these assumptions has not been estimated.

The 65%, 95% and 99% confidence level contours are shown in Fig. 3.21. The result is

$$\Delta\Gamma_s/\Gamma_s = 0.16^{+0.15}_{-0.16}$$
$$\Delta\Gamma_s/\Gamma_s < 0.54 \text{ at } 95\% \text{ C.L.}$$

In order to improve the limit the constraint $1/\Gamma_s = \tau_{B_d}$ can be imposed. This is well motivated theoretically, as the total widths of the B_s^0 and the B_d^0 mesons are expected to be equal within less than 1% (see Fig. 3.16) and that $\Delta\Gamma_{B_d}$ is expected to be small. It results in:

$$\Delta\Gamma_s/\Gamma_s = 0.07^{+0.09}_{-0.07}$$
$$\Delta\Gamma_s/\Gamma_s < 0.29 \text{ at } 95\% \text{ C.L.}$$

The relative confidence level contours plot is shown in Fig. 3.22.

5.5.1. Prospects for Tevatron experiments

CDF measured the $B_s \to J/\psi\,\phi$ lifetime [308] and polarization [309] separately. In the future the idea is to combine these two measurements by fitting both the lifetime and the transversity angle*. The use of the transversity allows to separate the CP even from the CP odd component. A study has been performed, by assuming similar performances as those achieved during Run I (mass resolution, background fractions, etc.) and improved proper time resolution ($18\ \mu$m). With an integrated luminosity of 2 fb^{-1}, corresponding to about 4000 events, an accuracy on $\Delta\Gamma_s/\Gamma_s$ of 5% could be reached †. Using the same integrated luminosity and the impact parameter trigger [310], CDF could expect to reconstruct 2500 $B_s \to D_s^+ D_s^-$ events, with a signal-to-noise ratio of 1:1.5. Using this sample the lifetime of the short component can be measured with an error of 0.044 ps, which corresponds to $\sigma\left(\Delta\Gamma_s/\Gamma_s\right) = 0.06$. The $D_s\pi$ and $D_s 3\pi$ decays could be also used. Those events are flavour-specific, thus they correspond to well defined mixtures of B_s^{short} and B_s^{long}. By using $\sim 75,000$ events $1/\Gamma_s$ can be measured with an error of 0.007 ps. Combining together the flavour specific measurement and the $D_s^+ D_s^-$ analysis, CDF can reach an error $\sigma\left(\Delta\Gamma_s/\Gamma_s\right) = 0.04$.

DØ has based its studies of B_s lifetime difference measurements on its strong dimuon trigger and the extensive coverage of the calorimeter and the muon detector. It is expected that approximately 7000 $B_s \to J/\psi\,\phi$ events will be reconstructed with an integrated luminosity of 2 fb^{-1}. The sensitivity of the measurements depends on two parameters: (a) the fraction of the CP-even component of the $J/\psi\,\phi$ final state‡, and (b) the CP-violating phase ϕ in the mixing of the B_s system§. The methods discussed here invoke utilization of CP eigenstates, therefore an angular analysis is needed to disentangle the admixture of CP-even and CP-odd contributions.

The $J/\psi\,\phi$ channel can be exploited in two ways:

- by comparison of the CP-eigenstate lifetimes: the sensitivity in this measurement is proportional to $\Delta\Gamma_s\,\cos\phi = \Delta\Gamma_{CP}\,\cos^2\phi$.
- by comparison of a CP-eigenstate lifetime to that of a "50-50" admixture, *e.g.*: $\Delta\Gamma_s = 2\,\cos\phi \times [\Gamma(B_s^{\mathrm{CP\ even}}) - \Gamma(B_s^{\mathrm{CP}\ 50-50})]$. About 1000 events of the $B_s \to D_s\,\pi$ decay will be used for the extraction of $\Gamma(B_s^{\mathrm{CP}\ 50-50})$.

Additional decay channels may include $B_s \to J/\psi\,\eta$ and $J/\psi\,\eta'$ (both being CP-even states). Combining all modes, DØ can achieve a measurement on $\Delta\Gamma_s\,/\Gamma_s$ with precision between $\sigma = 0.04$ ($\mathrm{CP_{even}} = 100\%$) and $\sigma = 0.07$ ($\mathrm{CP_{even}} = 50\%$)

BTEV studied their $\Delta\Gamma_s/\Gamma_s$ reach in three different scenarios. Assuming a $b\bar{b}$ cross section of $100\ \mu$b, the number of expected events, using 2 fb^{-1} of integrated luminosity, are:

1. 91700 $B_s \to D_s\,\pi$
2. 1700 $B_s \to J/\psi\,\eta$ and 6400 $B_s \to J/\psi\,\eta\prime$, where $\tau_{B_s^{short}} = 1/\Gamma_s^{short}$ is measurable;
3. 41400 $B_s \to J/\psi\,\phi$ where the lifetime, $\tau_x = 1/\Gamma_s^x$, is a mixture of a Γ_s^{short} and a Γ_s^{long} components.

The analysis details are discussed in [277]. The results are summarised in Table 3.25, obtained under the assumption that $\Delta\Gamma_s/\Gamma_s = 0.15$.

*The transversity angle is defined as the angle between the μ^+ and the z axis in the rest frame of the J/ψ, where the z axis is orthogonal to the plane defined by the ϕ and K^+ direction.

†In this results it is assumed that the CP_{even} fraction is 0.77 ± 0.19. If $\mathrm{CP}_{even} = 0.5(1)$, the error becomes $\sigma\left(\Delta\Gamma_s/\Gamma_s\right) = 0.08\,(0.035)$.

‡The $\mathrm{CP_{even}}$ fraction has been measured by CDF in Run-I: (77±19)%.

§The CP-violating phase, defined by $\alpha_{CP}(B_s \to J/\psi\,\phi) \sim \sin\phi$, is expected to be small in the Standard Model.

Decay Modes Used	Error on $\Delta\Gamma_s/\Gamma_s$		
Integrated Luminosity in fb^{-1}	2	10	20
$D_s\pi$, $J/\psi\eta^{(\prime)}$	0.0273	0.0135	0.0081
$D_s\pi$, $J/\psi\phi$	0.0349	0.0158	0.0082
$D_s\pi$, $J/\psi\eta^{(\prime)}$,$J/\psi\phi$	0.0216	0.0095	0.0067

Table 3.25: *Projection for statistical error on $\Delta\Gamma_s/\Gamma_s$ which can be obtained by the BTeV experiment.*

	LHCb	ATLAS	CMS
$\sigma(\frac{\Delta\Gamma_s}{\Gamma_s})/\frac{\Delta\Gamma_s}{\Gamma_s}$	8.4%	11.3%	7.5%
$\sigma(\frac{\Delta\Gamma_s}{\Gamma_s})$	0.013	0.017	0.011
$\sigma(\Gamma_s)/\Gamma_s$	0.6%	0.7%	0.5%
$\sigma(A_{\|\|})/A_{\|\|}$	0.7%	0.8%	0.6%
$\sigma(A_\perp)/A_\perp$	2%	3%	2%
ϕ_s ($x_s = 20$)	0.02	0.03	0.014
ϕ_s ($x_s = 40$)	0.03	0.05	0.03

Table 3.26: *Expected statistical uncertainties on $B_s^0 \to J/\psi\phi$ parameters for each experiment under the assumptions presented in the text. The value $\frac{\Delta\Gamma_s}{\Gamma_s} = 0.15$ is used as input to the fit.*

5.5.2. Prospects for LHC experiments

The LHC experiments have investigated the measurement of $\Delta\Gamma_s$ in the exclusive $B_s^0 \to J/\psi\phi$ decay following the studies done in [312]. In these analyses, $\Delta\Gamma_s$ and Γ_s are fitted simultaneously with the weak phase $\phi_s = arg(V_{cs}^* V_{cb}/V_{cs}V_{cb}^*)$ and the two helicity amplitude values, $A_{||}$ and $A_\perp$, while the mixing parameter $x_s = \Delta m_s/\Gamma$ is assumed to be known and kept fixed. The results summarised in Table 3.26 correspond to 3 (5) years running at a luminosity of $10^{33}cm^{-2}s^{-1}(2\cdot 10^{32}cm^{-2}s^{-1})$ for ATLAS and CMS (LCHb).

5.5.3. Measurement of $\Delta\Gamma_d/\Gamma_d$

In the case of $\Delta\Gamma_d/\Gamma_d$, the time resolution is no longer a limiting factor in the accuracy of lifetime measurements. At present, the only experimental limit comes from DELPHI [311], which has been obtained by fitting a sample of inclusive B decays to determine the mass difference ΔM_d without neglecting the $\Delta\Gamma_d$ term. At 90% C.L. $\Delta\Gamma_d/\Gamma_d < 0.20$. Given the large number of B_d produced at LHC and the proposed super B factories, it should be possible to measure $\Delta\Gamma_d/\Gamma_d \sim 0.5\%$. Using the time evolution of a single final state, however, is not sufficient as the time measurements of the decay of an untagged B_d to a single final state can only be sensitive to quadratic terms in $\Delta\Gamma_d/\Gamma_d$, [276]. This problem can be circumvented by combining the information from two different decay modes or by using angular distributions. It is then possible to have observables linear in $\Delta\Gamma_d/\Gamma_d$, which can provide $\Delta\Gamma_d/\Gamma_d \sim 0.5\%$. A viable option, perhaps the most efficient among those in [276], is to compare the measurements of the *average untagged lifetimes* of the s.l. decay mode τ_{SL} and of the CP-specific decay modes $\tau_{CP_\pm}$. The ratio between the two lifetimes is

$$\frac{\tau_{SL}}{\tau_{CP\pm}} = 1 \pm \frac{\cos(2\beta)}{2}\frac{\Delta\Gamma_d}{\Gamma_d} + \mathcal{O}\left[(\Delta\Gamma_d/\Gamma_d)^2\right] \quad . \tag{175}$$

The measurement of these two lifetimes will give a value of $|\Delta\Gamma_d|$, since $|\cos(2\beta)|$ will already be known with good accuracy by that time.

The LHC expects about 7×10^5 events of $J/\psi \mathrm{K}_S$ per year, whereas the number of s.l. decays at LHCb alone that will be directly useful in the lifetime measurements is expected to exceed 10^6 per year. The s.l. data sample may be further increased by including self-tagging decay modes, such as $\mathrm{D}_s^{(*)+}\mathrm{D}^{(*)-}$.

At hadronic machines, the $\mathrm{B}_d/\overline{\mathrm{B}}_d$ production asymmetry may be a stumbling block for the determination of the average untagged lifetimes. This drawback is obviously absent at the B factories. There, the most promising approach is to constrain $\Delta\Gamma_d/\Gamma_d$ by using $\Upsilon(4\mathrm{S})$ events where one B meson is fully reconstructed in a CP-specific decay mode, and the decay point of the second B meson is reconstructed using an inclusive technique that relies predominantly on s.l. and other self-tagging modes. For these events, only the *signed* difference of proper decay-times, $\Delta t = t_{\mathrm{CP}} - t_{\mathrm{tag}}$, i.e. not the decay times themselves, can be inferred since the production point cannot be reconstructed. The average value of Δt is given by

$$\langle \Delta t \rangle = \eta_{\mathrm{CP}} \cos(2\beta)\, \tau_{\mathrm{B}_d} \frac{\Delta\Gamma_d}{\Gamma_d} + \mathcal{O}\left[(\Delta\Gamma_d/\Gamma_d)^3\right] \tag{176}$$

where η_{CP} denotes the CP eigenvalue of the CP-specific final state considered. The BaBar potential has been studied using $J/\psi\, \mathrm{K}_S$ and similar charmonium final states. The expected statistical precision on $\Delta\Gamma_d/\Gamma_d$ is determined using the B reconstruction efficiencies and the experimental Δt resolution determined from BaBar's first data. From extrapolations based on published BaBar measurements of τ_{B_d} and $\sin(2\beta)$, the precision on τ_{B_d} and $\cos(2\beta)$ is expected to improve at the same time as the precision on $\langle \Delta t \rangle$, and to remain good enough to turn the $\langle \Delta t \rangle$ measurement into an evaluation of $\Delta\Gamma_d/\Gamma_d$. Using $\tau_{\mathrm{B}_d} = 1.55$ ps, $\sin(2\beta) = 0.6$ and 30 fb^{-1} of data one gets: $\sigma\left(\Delta\Gamma_d/\Gamma_d\right) = 0.073$. Using 300 fb^{-1} of data $\sigma\left(\Delta\Gamma_d/\Gamma_d\right) = 0.023$ is expected, and for 500 fb^{-1} $\sigma\left(\Delta\Gamma_d/\Gamma_d\right) = 0.018$.
At super B factories, 50 ab^{-1} of data may be obtained. A statistical precision at the 0.2 % level could be achieved. Strategies to reduce the systematic uncertainties to this level have not yet been studied in detail.

5.6. Theoretical description of b-hadron lifetimes and comparison with experiment

The same theoretical tools used to study $(\Delta\Gamma/\Gamma)_{B_s}$ in Sec. 5.1. can also be applied to describe the lifetime ratios of hadrons containing a b-quark, such as $\tau(\mathrm{B}_u)/\tau(\mathrm{B}_d)$, $\tau(\mathrm{B}_s)/\tau(\mathrm{B}_d)$, $\tau(\Lambda_b)/\tau(\mathrm{B}_d)$. The leading contributions in the heavy quark expansion (HQE) are represented, in the present case, by the dimension-3 operator $\bar{b}b$ ($\mathcal{O}(1)$) and the dimension-5 operator $\bar{b}\sigma_{\mu\nu}G^{\mu\nu}b$ ($\mathcal{O}(1/m_b^2)$). The first term in the expansion reproduces the predictions of the naïve quark spectator model. At this order, the hadronic decay is described in terms of the free b-quark decay, and the lifetime ratios of beauty hadrons are all predicted to be unity. The leading corrections, of $\mathcal{O}(1/m_b^2)$, describe the soft interactions of the spectator quark(s) inside the hadron, but give a small contribution ($\lesssim 2\%$) to the lifetime ratios.

The large lifetime difference of beauty hadrons which has been observed experimentally can be explained by considering hard spectator effects, that appear at $\mathcal{O}(1/m_b^3)$. Although suppressed by an additional power of $1/m_b$, these effects are enhanced with respect to the leading contributions by a phase-space factor of $16\pi^2$, being $2 \to 2$ processes instead of $1 \to 3$ decays (see Fig. 3.23). As in the case of the OPE for $(\Delta\Gamma/\Gamma)_{B_s}$, the starting point to describe the beauty hadron lifetimes is the effective $\Delta B = 1$ weak Hamiltonian, which enter the transition operator

$$\mathcal{T} = i \int d^4x\, T\left(\mathcal{H}_{\mathrm{eff}}^{\Delta B=1}(x)\mathcal{H}_{\mathrm{eff}}^{\Delta B=1}(0)\right) . \tag{177}$$

From the forward matrix elements of this operator, and using the optical theorem, one computes the

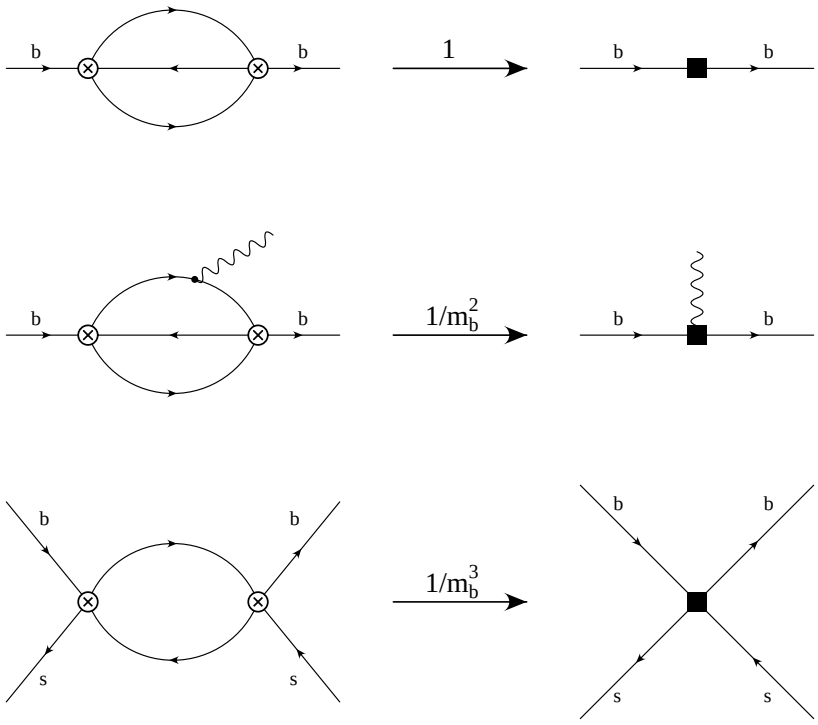

Fig. 3.23: *Examples of LO contributions to the transition operator $\mathcal{T}$ (left) and to the corresponding local operator (right). The crossed circles represent the insertions of the $\Delta B = 1$ effective Hamiltonian. The black squares represent the insertion of a $\Delta B = 0$ operator.*

inclusive decay width of a hadron H_b containing a b quark

$$\Gamma(H_b) = \frac{1}{M_{H_b}} \mathrm{Im} \langle H_b | \mathcal{T} | H_b \rangle \,. \tag{178}$$

The result of the HQE, in this case, is expressed in terms of matrix elements of $\Delta B = 0$ operators and it is given by

$$\Gamma(H_b) = \frac{G_F^2 |V_{cb}|^2 m_b^5}{192\pi^3} \left[c^{(3)} \frac{\langle H_b | \bar{b} b | H_b \rangle}{2M_{H_b}} + c^{(5)} \frac{g_s}{m_b^2} \frac{\langle H_b | \bar{b} \sigma_{\mu\nu} G^{\mu\nu} b | H_b \rangle}{2M_{H_b}} + \frac{96\pi^2}{m_b^3} \sum_k c_k^{(6)} \frac{\langle H_b | O_k^{(6)} | H_b \rangle}{2M_{H_b}} \right], \tag{179}$$

where we have included all contributions up to $\mathcal{O}(1/m_b^2)$ and those $1/m_b^3$ corrections which are enhanced by the phase-space factor $16\pi^2$. The complete list of the dimension-6 operators $O_k^{(6)}$, which represent the contribution of hard spectator effects, includes

$$\begin{array}{ll} \mathcal{O}_1^q = (\bar{b}\, q)_{V-A} \, (\bar{q}\, b)_{V-A} \,, & \mathcal{O}_2^q = (\bar{b}\, q)_{S-P} \, (\bar{q}\, b)_{S+P} \,, \\ \mathcal{O}_3^q = (\bar{b}\, t^a q)_{V-A} \, (\bar{q}\, t^a b)_{V-A} \,, & \mathcal{O}_4^q = (\bar{b}\, t^a q)_{S-P} \, (\bar{q}\, t^a b)_{S+P} \,, \end{array} \tag{180}$$

with $q = u, d, s, c$, and the penguin operator

$$\mathcal{O}_P = (\bar{b} t^a b)_V \sum_{q=u,d,s,c} (\bar{q} t^a q)_V \,. \tag{181}$$

It is important to emphasize that the symbols b and $\bar{b}$ in the operators (180,181) denote the heavy quark field HQET. The reason is that renormalized operators, in QCD, mix with operators of lower dimension,

with coefficients proportional to powers of the b-quark mass. Therefore, the dimensional ordering of the HQE, based on the assumption that contributions of higher dimensional operators are suppressed by increasing powers of the b-quark mass, would be lost in this case. In order to implement the expansion, the matrix elements of the local operators should be cut-off at a scale smaller than the b-quark mass, which is naturally realized in the HQET. The HQE can be expressed in terms of QCD operators in those cases in which, because of their specific quantum numbers, these operators cannot mix with lower lower dimensional operators. This is the case, for instance, for the leading contributions in the HQE of $(\Delta\Gamma/\Gamma)_{B_s}$ and of the lifetime ratio $\tau(\mathrm{B}_u)/\tau(\mathrm{B}_d)$.

The Wilson coefficients $c^{(3)}$ and $c^{(5)}$ in Eq. (179) have been computed at the LO in Ref. [282], while the NLO corrections to $c^{(3)}$ have been evaluated in [92,283–285]. The NLO corrections to $c^{(5)}$ are still unknown, but their impact on the lifetime ratio is expected to be negligible. The coefficient functions $c_k^{(6)}$ of the current-current operators of dimension-6 have been computed at the LO in Refs. [286–288]. At this order the coefficient of the penguin operator $c_P^{(6)}$ vanishes. The NLO correction to $c_k^{(6)}$ for the operators $\mathcal{O}_k^q$ with $q = u, d$ has been recently completed in Refs. [289,290], and extended to $q = s$ in Ref. [289]. A complete list of these coefficients, calculated at NLO in the NDR-$\overline{\mathrm{MS}}$ scheme of Ref. [291], is given in Table 3.27. The operators containing the valence charm quark ($q = c$ in Eq. (180)) are expected to give a negligible contribution to the non-charmed hadron decay rates. The calculation of the NLO corrections to these coefficient functions, as well as the NLO calculation of the coefficient function of the penguin operator, have not been performed yet.

q	u	d	s
c_1^q	$-0.29^{+0.02}_{-0.04}$	$-0.03^{-0.01}_{+0.01}$	$-0.03^{-0.01}_{+0.01}$
c_2^q	$-0.02^{-0.01}_{+0.01}$	$0.03^{+0.01}_{-0.02}$	$0.04^{+0.00}_{-0.02}$
c_3^q	$2.37^{+0.12}_{-0.10}$	$-0.68^{-0.01}_{+0.01}$	$-0.58^{-0.00}_{+0.01}$
c_4^q	$-0.05^{-0.01}_{+0.00}$	$0.68^{-0.00}_{+0.00}$	$0.65^{-0.00}_{+0.00}$

Table 3.27: *Wilson coefficients $c_k^q(\mu_0)$ computed in the HQET, at NLO, at the scale $\mu_0 = m_b$. The coefficients also have a residual dependence on the renormalization scale μ_1 of the $\Delta B = 1$ operators, which is a NNLO effect. The uncertainty due to the variation of the scale μ_1 is reflected in the error bars (central values are obtained by using $\mu_1 = m_b$, upper error for $\mu_1 = m_b/2$ and the lower one for $\mu_1 = 2\,m_b$). In the evaluation we take $m_c/m_b = 0.28$. All the coefficients remain unchanged under the variation of $m_c/m_b = 0.28 \pm 0.02$ except for c_3^q, which changes by about 2%.*

The matrix elements of dimension-3 and dimension-5 operators, appearing in Eq. (179), can be expressed in terms of the HQET parameters $\mu_\pi^2(H_b)$ and $\mu_G^2(H_b)$ as

$$\begin{aligned}
\langle H_b|\bar{b}b|H_b\rangle &= 2M_{H_b}\left(1 - \frac{\mu_\pi^2(H_b) - \mu_G^2(H_b)}{2m_b^2} + \mathcal{O}(1/m_b^3)\right), \\
\langle H_b|\bar{b}g_s\sigma_{\mu\nu}G^{\mu\nu}b|H_b\rangle &= 2M_{H_b}\left(2\mu_G^2(H_b) + \mathcal{O}(1/m_b)\right).
\end{aligned} \tag{182}$$

Using these expansions in the lifetime ratio of two beauty hadrons one finds

$$\begin{aligned}
\frac{\tau(H_b)}{\tau(H_b')} &= 1 + \frac{\mu_\pi^2(H_b) - \mu_\pi^2(H_b')}{2m_b^2} - \left(\frac{1}{2} + \frac{2c^{(5)}}{c^{(3)}}\right)\frac{\mu_G^2(H_b) - \mu_G^2(H_b')}{m_b^2} \\
&\quad - \frac{96\pi^2}{m_b^3\, c^{(3)}}\sum_k c_k^{(6)}\left(\frac{\langle H_b'|O_k^{(6)}|H_b\rangle}{2M_{H_b}} - \frac{\langle H_b'|O_k^{(6)}|H_b'\rangle}{2M_{H_b'}}\right).
\end{aligned} \tag{183}$$

From the heavy hadron spectroscopy one obtains $\mu_\pi^2(\Lambda_b) - \mu_\pi^2(\mathrm{B}) \approx 0.01(3)$ GeV^2 and $\mu_\pi^2(\Lambda_b) - \mu_\pi^2(\mathrm{B}) \approx 0$. Therefore the impact of the second term in the above formula is completely negligible. On the other hand, $\mu_G^2(\mathrm{B}_q) = 3(M_{\mathrm{B}_q^*}^2 - M_{\mathrm{B}_q}^2)/4$, which gives $\mu_G^2(\mathrm{B}_{u,d}) \approx 0.36$ GeV^2, $\mu_G^2(\mathrm{B}_s) \approx 0.38$ GeV^2, while $\mu_G^2(\Lambda_b) = 0$. Therefore, only in the case $\tau(\Lambda_b)/\tau(\mathrm{B}_d)$, the third term gives a contribution that is visibly different from zero. By using $(1/2 + 2c^{(5)}/c^{(3)}) = -1.10(4)$, we thus obtain

$$\frac{\tau(\mathrm{B}^+)}{\tau(\mathrm{B}_d)} = 1.00 - \Delta_{\mathrm{spec}}^{\mathrm{B}^+}\,, \quad \frac{\tau(\mathrm{B}_s)}{\tau(\mathrm{B}_d)} = 1.00 - \Delta_{\mathrm{spec}}^{\mathrm{B}_s}\,, \quad \frac{\tau(\Lambda_b)}{\tau(\mathrm{B}_d)} = 0.98(1) - \Delta_{\mathrm{spec}}^{\Lambda}\,, \tag{184}$$

where the $\Delta_{\mathrm{spec}}^{H_b}$ represent the $1/m_b^3$ contributions of hard spectator effects (second line in Eq. (183)).

The comparison of Eq. (184) with the experimental results given in Table 3.28 shows that without inclusion of the spectator effects the experimental values could not be explained.

	Theory Prediction	World Average
$\frac{\tau(\mathrm{B}^+)}{\tau(\mathrm{B}_d)}$	1.06±0.02	1.073±0.014
$\frac{\tau(\mathrm{B}_s)}{\tau(\mathrm{B}_d)}$	1.00±0.01	0.949±0.038
$\frac{\tau(\Lambda_b)}{\tau(\mathrm{B}_d)}$	0.90±0.05	0.798±0.052

Table 3.28: *Comparison of theoretical expectations and experimental results for the ratios of exclusive lifetimes.*

Beside the coefficient functions presented in Table 3.27, the essential ingredients entering the corrections $\Delta_{\mathrm{spec}}^{H_b}$ are the hadronic matrix elements. We follow [292] and parameterize the B meson matrix elements as follows

$$\begin{aligned}
&\frac{\langle \mathrm{B}_q|\mathcal{O}_1^q|\mathrm{B}_q\rangle}{2M_{\mathrm{B}_q}} = \frac{F_{\mathrm{B}_q}^2 M_{\mathrm{B}_q}}{2}\,(B_1^q + \delta_1^{qq})\,, \quad
\frac{\langle \mathrm{B}_q|\mathcal{O}_3^q|\mathrm{B}_q\rangle}{2M_{\mathrm{B}_q}} = \frac{F_{\mathrm{B}_q}^2 M_{\mathrm{B}_q}}{2}\,(\varepsilon_1^q + \delta_3^{qq})\,,\\
&\frac{\langle \mathrm{B}_q|\mathcal{O}_2^q|\mathrm{B}_q\rangle}{2M_{\mathrm{B}_q}} = \frac{F_{\mathrm{B}_q}^2 M_{\mathrm{B}_q}}{2}\,(B_2^q + \delta_2^{qq})\,, \quad
\frac{\langle \mathrm{B}_q|\mathcal{O}_4^q|\mathrm{B}_q\rangle}{2M_{\mathrm{B}_q}} = \frac{F_{\mathrm{B}_q}^2 M_{\mathrm{B}_q}}{2}\,(\varepsilon_2^q + \delta_4^{qq})\,,\\
&\frac{\langle \mathrm{B}_q|\mathcal{O}_k^{q'}|\mathrm{B}_q\rangle}{2M_{\mathrm{B}_q}} = \frac{F_{\mathrm{B}_q}^2 M_{\mathrm{B}_q}}{2}\,\delta_k^{q'q} \quad , \qquad
\frac{\langle \mathrm{B}_q|\mathcal{O}_P|\mathrm{B}_q\rangle}{2M_{\mathrm{B}_q}} = \frac{F_B^2 M_B}{2}\,P^q\,.
\end{aligned} \tag{185}$$

where the parameters δ_k^{qq} are defined as the $\delta_k^{qq'}$ in the limit of degenerate quark masses ($m_q = m_{q'}$). For the Λ_b baryon we define

$$\begin{aligned}
&\frac{\langle \Lambda_b|\mathcal{O}_1^q|\Lambda_b\rangle}{2M_{\Lambda_b}} = \frac{F_B^2 M_B}{2}\left(L_1 + \delta_1^{\Lambda q}\right) \quad \text{for } q = u,d\,,\\
&\frac{\langle \Lambda_b|\mathcal{O}_3^q|\Lambda_b\rangle}{2M_{\Lambda_b}} = \frac{F_B^2 M_B}{2}\left(L_2 + \delta_2^{\Lambda q}\right) \quad \text{for } q = u,d\,,\\
&\frac{\langle \Lambda_b|\mathcal{O}_1^q|\Lambda_b\rangle}{2M_{\Lambda_b}} = \frac{F_B^2 M_B}{2}\,\delta_1^{\Lambda q} \quad \text{for } q = s,c\,,\\
&\frac{\langle \Lambda_b|\mathcal{O}_3^q|\Lambda_b\rangle}{2M_{\Lambda_b}} = \frac{F_B^2 M_B}{2}\,\delta_2^{\Lambda q} \quad \text{for } q = s,c\,,\\
&\frac{\langle \Lambda_b|\mathcal{O}_P|\Lambda_b\rangle}{2M_{\Lambda_b}} = \frac{F_B^2 M_B}{2}\,P^{\Lambda}\,.
\end{aligned} \tag{186}$$

In addition, in the case of Λ_b, the following relation holds up to $1/m_b$ corrections:

$$\langle\Lambda_b|\mathcal{O}_1^q|\Lambda_b\rangle = -2\,\langle\Lambda_b|\mathcal{O}_2^q|\Lambda_b\rangle\,, \quad \langle\Lambda_b|\mathcal{O}_3^q|\Lambda_b\rangle = -2\,\langle\Lambda_b|\mathcal{O}_4^q|\Lambda_b\rangle\,. \tag{187}$$

In Eqs.(185) and (186), $B_{1,2}$, $L_{1,2}$ and $\varepsilon_{1,2}$ are the "standard" bag parameters, introduced in Ref. [286]. Those parameters have already been computed in both the lattice QCD and QCD sum rule approaches. The parameters δ_k have been introduced in Ref. [292] to account for the corresponding penguin contractions. A non-perturbative lattice calculation of the δ_k parameters is possible, in principle. However, the difficult problem of subtractions of power-divergences has prevented their calculation.

In terms of parameters introduced above, the spectator contributions to the lifetime ratios, $\Delta_{\rm spec}^{H_b}$, are expressed in the form

$$\begin{aligned}
\Delta_{\rm spec}^{B^+} &= 48\pi^2\,\frac{F_B^2 M_B}{m_b^3 c^{(3)}}\,\sum_{k=1}^{4}\left(c_k^u - c_k^d\right)\mathcal{B}_k^d\,,\\
\Delta_{\rm spec}^{\rm B_s} &= 48\pi^2\,\frac{F_B^2 M_B}{m_b^3 c^{(3)}}\,\left\{\sum_{k=1}^{4}\Big[r\,c_k^s\,\mathcal{B}_k^s - c_k^d\,\mathcal{B}_k^d + \left(c_k^u + c_k^d\right)\left(r\,\delta_k^{ds} - \delta_k^{dd}\right) + \right.\\
&\qquad \left. c_k^s\left(r\,\delta_k^{ss} - \delta_k^{sd}\right) + c_k^c\left(r\,\delta_k^{cs} - \delta_k^{cd}\right)\Big] + c_P\left(rP^s - P^d\right)\right\}\,, \qquad (188)\\
\Delta_{\rm spec}^{\Lambda} &= 48\pi^2\,\frac{F_B^2 M_B}{m_b^3 c^{(3)}}\,\left\{\sum_{k=1}^{4}\Big[\left(c_k^u + c_k^d\right)\mathcal{L}_k^\Lambda - c_k^d\,\mathcal{B}_k^d + \left(c_k^u + c_k^d\right)\left(\delta_k^{\Lambda d} - \delta_k^{dd}\right) + \right.\\
&\qquad \left. c_k^s\left(\delta_k^{\Lambda s} - \delta_k^{sd}\right) + c_k^c\left(\delta_k^{\Lambda c} - \delta_k^{cd}\right)\Big] + c_P\left(P^\Lambda - P^d\right)\right\}\,.
\end{aligned}$$

where r denotes the ratio $(F_{\rm B_s}^2 M_{\rm B_s})/(F_B^2 M_B)$ and, in order to simplify the notation, we have defined the vectors of parameters

$$\begin{aligned}
\vec{\mathcal{B}}^q &= \{B_1^q, B_2^q, \varepsilon_1^q, \varepsilon_1^q\}\,,\\
\vec{\mathcal{L}} &= \{L_1, -L_1/2, L_2, -L_2/2\}\,,\\
\vec{\delta}^{\Lambda q} &= \{\delta_1^{\Lambda q}, -\delta_1^{\Lambda q}/2, \delta_2^{\Lambda q}, -\delta_2^{\Lambda q}/2\}\,.
\end{aligned} \tag{189}$$

An important result of Eq. (188) is that, because of the $SU(2)$ symmetry, the non-valence (δs) and penguin (Ps) contributions cancel out in the expressions of the lifetime ratio $\tau(\rm B_u)/\tau(\rm B_d)$. Thus, the theoretical prediction of this ratio is at present the most accurate, since it depends only on the non-perturbative parameters actually computed by current lattice calculations. The prediction of the ratio $\tau(\Lambda_b)/\tau(\rm B_d)$, instead, is affected by both the uncertainties on the values of the δ and P parameters, and by the unknown expressions of the Wilson coefficients c_k^c and c_P at the NLO. For the ratio $\tau(\rm B_s)/\tau(\rm B_d)$ the same uncertainties exist, although their effect is expected to be smaller, since the contributions of non-valence and penguin operators cancel, in this case, in the limit of exact $SU(3)$ symmetry.

In the numerical analysis of the ratios $\tau(\rm B_s)/\tau(\rm B_d)$ and $\tau(\Lambda_b)/\tau(\rm B_d)$, we will neglect the non-valence and penguin contributions (*i.e.* we set all $\delta = P = 0$). The non-valence contributions vanish in the VSA, and present phenomenological estimates indicate that the corresponding matrix elements are suppressed, with respect to the valence contributions, by at least one order of magnitude [293,294]. On the other hand, the matrix elements of the penguin operators are not expected to be smaller than those of the valence operators. Since the coefficient function c_P vanishes at the LO, this contribution is expected to have the size of a typical NLO corrections. Thus, from a theoretical point of view, a quantitative evaluation of the non-valence and penguin operator matrix elements would be of the greatest interest to improve the determination of the Λ_B lifetime.

By neglecting the non valence and penguin contributions, and using for the Wilson coefficients the NLO results collected in Table 3.27, one obtains from Eq. (188) the following expressions

$$\begin{aligned}
\Delta^{B^+}_{\rm spec} &= -0.06(2)\, B_1^d - 0.010(3)\, B_2^d + 0.7(2)\, \varepsilon_1^d - 0.18(5)\, \varepsilon_2^d \,, \\
\Delta^{\rm B_s}_{\rm spec} &= -0.010(2)\, B_1^s + 0.011(3)\, B_2^s - 0.16(4)\, \varepsilon_1^s + 0.18(5)\, \varepsilon_2^s \\
&\quad + 0.008(2)\, B_1^d - 0.008(2)\, B_2^d + 0.16(4)\, \varepsilon_1^d - 0.16(4)\, \varepsilon_2^d \,, \qquad (190) \\
\Delta^{\Lambda}_{\rm spec} &= -0.08(2)\, L_1 + 0.33(8)\, L_2 \\
&\quad + 0.008(2)\, B_1^d - 0.008(2)\, B_2^d + 0.16(4)\, \varepsilon_1^d - 0.16(4)\, \varepsilon_2^d \,,
\end{aligned}$$

For the charm and bottom quark masses, and the B meson decay constants we have used the central values and errors given in Table 3.29. The strong coupling constant has been fixed at the value $\alpha_s(m_Z) = 0.118$. The parameter $c^{(3)}$ in Eq. (188) is a function of the ratio m_c^2/m_b^2, and such a dependence has been consistently taken into account in the numerical analysis and in the estimates of the errors. For the range of masses given in Table 3.29, $c^{(3)}$ varies in the interval $c^{(3)} = 3.4 \div 4.2$ [285].

$B_1^d = 1.2 \pm 0.2$	$B_1^s = 1.0 \pm 0.2$
$B_2^d = 0.9 \pm 0.1$	$B_2^s = 0.8 \pm 0.1$
$\varepsilon_1^d = 0.04 \pm 0.01$	$\varepsilon_1^s = 0.03 \pm 0.01$
$\varepsilon_2^d = 0.04 \pm 0.01$	$\varepsilon_2^s = 0.03 \pm 0.01$
$L_1 = -0.2 \pm 0.1$	$L_2 = 0.2 \pm 0.1$
$m_b = 4.8 \pm 0.1$ GeV	$m_b - m_c = 3.40 \pm 0.06$ GeV
$F_B = 200 \pm 25$ MeV	$F_{\rm B_s}/F_B = 1.16 \pm 0.04$

Table 3.29: *Central values and standard deviations of the input parameters used in the numerical analysis. The values of m_b and m_c refer to the pole mass definitions of these quantities.*

As discussed before, for the ratio $\tau(\rm B_u)/\tau(\rm B_d)$ the HQE can be also expressed in terms of operators defined in QCD. The corresponding coefficient functions can be evaluated by using the matching between QCD and HQET computed, at the NLO, in Ref. [292]. In this way, one obtains the expression

$$\Delta^{B^+}_{\rm spec} = -0.05(1)\, \bar{B}_1^d - 0.007(2)\, \bar{B}_2^d + 0.7(2)\, \bar{\varepsilon}_1^d - 0.15(4)\, \bar{\varepsilon}_2^d \qquad (191)$$

where the $\bar{B}$ and $\bar{\varepsilon}$ parameters are now defined in terms of matrix elements of QCD operators.

The errors quoted on the coefficients in Eq. (190) are strongly correlated, since they originate from the theoretical uncertainties on the same set of input parameters. For this reason, in order to evaluate the lifetime ratios, we have performed a Bayesian statistical analysis by implementing a short Monte Carlo calculation. The input parameters have been extracted with flat distributions, assuming as central values and standard deviations the values given in Table 3.29. The results for the B-parameters are based on the lattice determinations of Refs. [295,297] ¶. We have included in the errors an estimate of the uncertainties not taken into account in the original papers. The QCD results for the B meson B-parameters of Ref. [297] have been converted to HQET at the NLO [292]‖. The contributions of all the δ and P parameters have been neglected. In this way we obtain the final NLO predictions for the

¶ For recent estimates of these matrix elements based on QCD sum rules, see Refs. [298].

‖ With respect to [292], we use for the B meson B-parameters the results updated in [297].

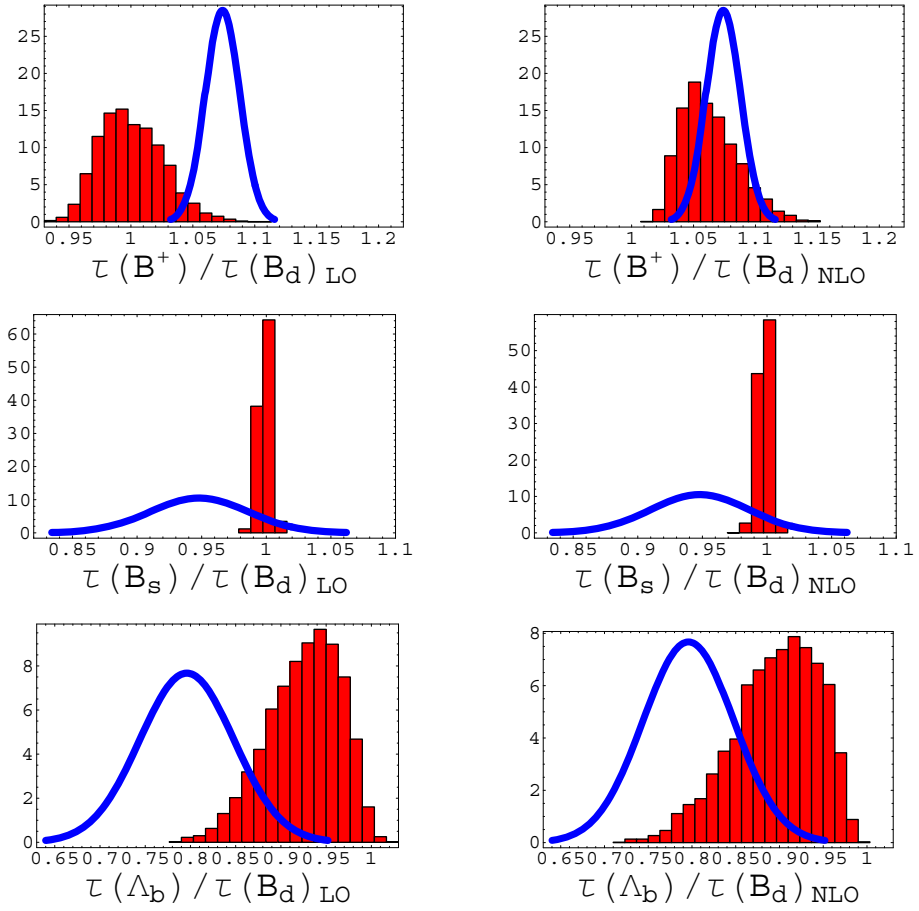

Fig. 3.24: *Theoretical (histogram) vs experimental (solid line) distributions of lifetime ratios. The theoretical predictions are shown at the LO (left) and NLO (right).*

lifetimes ratios summarised in Table 3.28. The central values and uncertainties correspond to the average and the standard deviation of the theoretical distributions, shown in Fig. 3.24, together with those from the experimental determinations. The uncertainty coming from the residual scale dependence represents less than 20% of the quoted errors.

With the inclusion of the NLO corrections, the theoretical prediction for the ratio $\tau(\mathrm{B}_u)/\tau(\mathrm{B}_d)$ is in good agreement with the experimental measurement, also summarised in Table 3.28. The agreement is also good for the ratio $\tau(\mathrm{B}_s)/\tau(\mathrm{B}_d)$, with the difference between theoretical predictions and experimental determinations below 1σ. A possible mismatch between the predicted and measured values for the ratio $\tau(\Lambda_b)/\tau(\mathrm{B}_d)$ has been much debated in past years. Interpretation in terms of a breakdown of the HQE framework and the appearance of a signal of quark-hadron duality violation have been claimed. The inclusion of higher order terms seems to reestablish a compatibility between predictions of the beauty baryon lifetime with the present experimental determinations. However, this issue will require further scrutiny in view of new, more precise results expected from the Tevatron Run II and from the fact that the theoretical predictions are less accurate in this case, since a reliable estimate of the contribution of the non-valence and penguin operators are not yet available.

5.7. Future prospects for b-hadron lifetime measurements

The B factories are now providing new, accurate determinations of the lifetimes of the B_d^0 and B^+ meson, which could decrease the relative error on to (0.4-0.5)%. Results from the Tevatron Run II are eagerly expected, since will provide precise measurements of the B_s^0 and Λ_b lifetimes and also results for the Ξ_b, Ω_b and the B_c beauty hadrons. Further improvements are then expected from the LHC experiments, with special regard to B_s^0 and baryon lifetimes.

CDF evaluated the lifetimes measurement capabilities exploiting separately the leptonic and the hadronic decay channels. The leptonic decays considered are only to $J/\psi \rightarrow \mu\mu$, this means exclusive decays. The uncertainties shown in Table 3.30 are only statistical and are obtained by scaling by a factor 50 the Run I measurements. The systematic uncertainty is expected to be the same order as that for the Run I analyses, at the level of 1%. Since in Run I there were no measurements based on hadronic decays, the Run II estimations had to be based on Monte Carlo simulations. The major interest is in measuring the B_s and Λ_b lifetime and the expected statistical errors are quoted in Table 3.30. With these measurements the $\mathrm{B}_s/\mathrm{B}^0$ lifetime ratio to will have an uncertainty of $\sim 0.5\%$, which is of the same order of the predicted deviation from unity. Λ_b baryons, reconstructed in the $\Lambda_c\pi$, $pD^0\pi$, $p\pi$ and pK decay channels, will allow a stringent test for the theoretical predictions of the lifetime ratio of Λ_b to B^0 if the signal to noise ratio of 1 can be obtained.

$\sigma\left(c\tau\right)/c\tau$	$\mathrm{B}^{\pm}$	B_d^0	B_s^0	Λ_b
Run II leptonic triggers	0.6%	0.6%	2%	3%
Run II hadronic trigger			0.5%	0.8%

Table 3.30: *CDF lifetime statistical error projections with leptonic and hadronic triggers for 2 fb*$^{-}1$ *of data. The systematic uncertainty is expected to be at the level of* 1%.

The DØ experiment has concentrated its studies on the projection for the Λ_b lifetime measurement. The preferred decay is $J/\psi\Lambda^0$ with $J/\psi \rightarrow \mu\mu$ and $\Lambda^0 \rightarrow p\pi^-$. In 2 fb^{-1} the expected number of reconstructed events is of order of 15,000, corresponding to a relative lifetime accuracy of 9%.

At LHC, lifetime measurements of different B hadron species will be based on even larger statistics, collected in individual exclusive channels. ATLAS [313,314] has performed a simulation for studying the statistical precision on the Λ_b^0 lifetime using the $\Lambda_\mathrm{b}^0 \rightarrow \Lambda^0\,\mathrm{J}/\psi$ decay channel. In three years of running at $10^{33} cm^{-2} s^{-1}$ luminosity, 75000 $\Lambda_\mathrm{b}^0 \rightarrow \Lambda^0\,\mathrm{J}/\psi$ signal decays can be reconstructed (with 1500 background events, mostly J/ψ paired to a primary Λ^0). Considering a proper time resolution of 0.073 ps, the estimated relative uncertainty on the Λ_b^0 lifetime is 0.3%.

References

[1] J. Chay, H. Georgi, and B. Grinstein, Phys. Lett. B **247** (1990) 399; M. Voloshin and M. Shifman, Sov. J. Nucl. Phys. **41** (1985) 120; A.V. Manohar and M.B. Wise, Phys. Rev. D **49** (1994) 1310; B. Blok *et al.*, Phys. Rev. D **49** (1994) 3356.

[2] I.I. Bigi *et al.*, Phys. Lett. B **293** (1992) 430; Phys. Lett. B **297** (1993) 477 (E); Phys. Rev. Lett. **71** (1993) 496.

[3] A.V. Manohar and M.B. Wise, Cambridge Monogr. Part. Phys. Nucl. Phys. Cosmol. **10** (2000) 1; I.I. Bigi, M.A. Shifman, N.G. Uraltsev, Ann. Rev. Nucl. Part. Sci. **47** (1997) 591 [hep-ph/9703290]; Z. Ligeti, eConf **C020805** (2002) L02 [hep-ph/0302031].

[4] N.G. Uraltsev, in *At the Frontier of Particle Physics: Handbook of QCD*, edited by M. Shifman (World Scientific, Singapore, 2001) [hep-ph/0010328].

[5] E.V. Shuryak, Phys. Lett. B **93** (1980) 134; E.V. Shuryak, Nucl. Phys. B **198** (1982) 83;
J.E. Paschalis and G.J. Gounaris, Nucl. Phys. B **222** (1983) 473;
F.E. Close, G.J. Gounaris and J.E. Paschalis, Phys. Lett. B **149** (1984) 209;
S. Nussinov and W. Wetzel, Phys. Rev. D **36** (1987) 130.

[6] M.A. Shifman and M.B. Voloshin, Sov. J. Nucl. Phys. **45** (1987) 292 [Yad. Fiz. **45** (1987) 463].

[7] M.A. Shifman and M.B. Voloshin, Sov. J. Nucl. Phys. **47** (1988) 511 [Yad. Fiz. **47** (1988) 801].

[8] N. Isgur and M.B. Wise, Phys. Lett. B **232** (1989) 113.

[9] N. Isgur and M.B. Wise, Phys. Lett. B **237** (1990) 527.

[10] E. Eichten and F. Feinberg, Phys. Rev. D **23** (1981) 2724; W.E. Caswell and G.P. Lepage, Phys. Lett. B **167** (1986) 437; E. Eichten, Nucl. Phys. B Proc. Suppl. **4** (1988) 170; G.P. Lepage and B.A. Thacker, Nucl. Phys. B Proc. Suppl. **4** (1988) 199; H.D. Politzer and M.B. Wise, Phys. Lett. B **206** (1988) 681 and Phys. Lett. B **208** (1988) 504; E. Eichten and B. Hill, Phys. Lett. B **240** (1990) 193 and Phys. Lett. B **243** (1990) 427; B. Grinstein, Nucl. Phys. B **339** (1990) 253; H. Georgi, Phys. Lett. B **240** (1990) 447; A.F. Falk, H. Georgi, B. Grinstein and M.B. Wise, Nucl. Phys. B **343** (1990) 1; A.F. Falk, B. Grinstein and M.E. Luke, Nucl. Phys. B **357** (1991) 185; T. Mannel, W. Roberts and Z. Ryzak, Nucl. Phys. B **368** (1992) 204; J.G. Körner and G. Thompson, Phys. Lett. B **264** (1991) 185; S. Balk, J.G. Körner and D. Pirjol, Nucl. Phys. B **428** (1994) 499 [hep-ph/9307230].

[11] J.M. Flynn and N. Isgur, J. Phys. G **18** (1992) 1627 [hep-ph/9207223].

[12] M. Neubert, Phys. Rept. **245** (1994) 259 [hep-ph/9306320].

[13] M. Neubert, hep-ph/0001334.

[14] A.H. Hoang, hep-ph/0204299;
A. X. El-Khadra and M. Luke, Ann. Rev. Nucl. Part. Sci. **52** (2002) 201 [hep-ph/0208114].

[15] R. Tarrach, Nucl. Phys. B **183** (1981) 384;
A.S. Kronfeld, Phys. Rev. D **58** (1998) 051501 [hep-ph/9805215];
P. Gambino and P.A. Grassi, Phys. Rev. D **62** (2000) 076002 [hep-ph/9907254].

[16] I.I. Bigi, M.A. Shifman, N.G. Uraltsev and A.I. Vainshtein, Phys. Rev. D **50** (1994) 2234 [hep-ph/9402360]; M. Beneke and V.M. Braun, Nucl. Phys. B **426** (1994) 301 [hep-ph/9402364].

[17] N. Gray, D.J. Broadhurst, W. Grafe and K. Schilcher, Z. Phys. C **48** (1990) 673.

[18] K. Melnikov and T. v. Ritbergen, Phys. Lett. B **482** (2000) 99 [hep-ph/9912391];
K.G. Chetyrkin and M. Steinhauser, Nucl. Phys. B **573** (2000) 617 [hep-ph/9911434].

[19] A.H. Hoang *et al.*, Eur. Phys. J. direct C **3** (2000) 1 [hep-ph/0001286].

[20] I.I. Bigi, M.A. Shifman, N.G. Uraltsev and A.I. Vainshtein, Phys. Rev. D **56** (1997) 4017 [hep-ph/9704245].

[21] I.I. Bigi, M.A. Shifman, N.G. Uraltsev and A.I. Vainshtein, Phys. Rev. D **52** (1995) 196 [hep-ph/9405410].

[22] A. Czarnecki, K. Melnikov and N.G. Uraltsev, Phys. Rev. Lett. **80** (1998) 3189 [hep-ph/9708372].

[23] M. Beneke, Phys. Lett. B **434** (1998) 115 [hep-ph/9804241].

[24] Y. Schroder, Phys. Lett. B **447** (1999) 321 [hep-ph/9812205].
M. Peter, Phys. Rev. Lett. **78** (1997) 602 [hep-ph/9610209].

[25] A.H. Hoang, Z. Ligeti and A.V. Manohar, Phys. Rev. Lett. **82** (1999) 277 [hep-ph/9809423]; Phys. Rev. D **59** (1999) 074017 [hep-ph/9811239].

[26] A.H. Hoang and T. Teubner, Phys. Rev. D **60** (1999) 114027 [hep-ph/9904468].

[27] A. Pineda, JHEP **0106** (2001) 022 [hep-ph/0105008].

[28] V.A. Novikov, *et al.*, Phys. Rev. Lett. **38** (1977) 626 [Erratum-ibid. **38** (1977) 791];
L.J. Reinders, H. Rubinstein and S. Yazaki, Phys. Rept. **127** (1985) 1.

[29] M.B. Voloshin, Int. J. Mod. Phys. A **10** (1995) 2865 [hep-ph/9502224].

[30] J.H. Kühn, A.A. Penin and A.A. Pivovarov, Nucl. Phys. B **534** (1998) 356 [hep-ph/9801356].

[31] A.A. Penin and A.A. Pivovarov, Phys. Lett. B **435** (1998) 413 [hep-ph/9803363]; Nucl. Phys. B **549** (1999) 217 [hep-ph/9807421].

[32] A.H. Hoang, Phys. Rev. D **59** (1999) 014039 [hep-ph/9803454].

[33] K. Melnikov and A. Yelkhovsky, Phys. Rev. D **59** (1999) 114009 [hep-ph/9805270].

[34] M. Jamin and A. Pich, Nucl. Phys. Proc. Suppl. **74** (1999) 300 [hep-ph/9810259].

[35] A.H. Hoang, Phys. Rev. D **61** (2000) 034005 [hep-ph/9905550].

[36] M. Beneke and A. Signer, Phys. Lett. B **471** (1999) 233 [hep-ph/9906475].

[37] A.H. Hoang, hep-ph/0008102.

[38] J.H. Kuhn and M. Steinhauser, Nucl. Phys. B **619** (2001) 588 [Erratum-ibid. B **640** (2002) 415] [hep-ph/0109084].

[39] J. Erler and M. x. Luo, Phys. Lett. B **558** (2003) 125 [hep-ph/0207114].

[40] M. Eidemuller, hep-ph/0207237.

[41] J. Bordes, J. Penarrocha and K. Schilcher, hep-ph/0212083.

[42] A.H. Hoang and G. Corcella, Phys. Lett. B **554** (2003) 133 [hep-ph/0212297].

[43] A. Pineda and F.J. Yndurain, Phys. Rev. D **58** (1998) 094022 [hep-ph/9711287].

[44] A.H. Hoang, Nucl. Phys. Proc. Suppl. **86** (2000) 512 [hep-ph/9909356].

[45] N. Brambilla, Y. Sumino and A. Vairo, Phys. Rev. D **65** (2002) 034001 [hep-ph/0108084].

[46] M. A. Shifman, A. I. Vainshtein and V. I. Zakharov, Nucl. Phys. B **147** (1979) 385 and 448.

[47] M. Eidemuller and M. Jamin, Phys. Lett. B **498** (2001) 203 [hep-ph/0010334];
J. Penarrocha and K. Schilcher, Phys. Lett. B **515** (2001) 291 [hep-ph/0105222].

[48] G. Martinelli, *et al.*, Nucl. Phys. B **445** (1995) 81 [hep-lat/9411010].

[49] K. Jansen *et al.*, Phys. Lett. B **372** (1996) 275 [hep-lat/9512009].

[50] D. Becirevic, V. Lubicz and G. Martinelli, Phys. Lett. B **524** (2002) 115 [hep-ph/0107124].

[51] J. Rolf and S. Sint [ALPHA Collaboration], JHEP **0212** (2002) 007 [hep-ph/0209255].

[52] C.T. Davies *et al.*, Phys. Rev. Lett. **73** (1994) 2654 [hep-lat/9404012].

[53] V. Gimenez, L. Giusti, G. Martinelli and F. Rapuano, JHEP **0003** (2000) 018 [hep-lat/0002007].

[54] G. Martinelli and C.T. Sachrajda, Nucl. Phys. B **559** (1999) 429 [hep-lat/9812001].

[55] S. Collins, hep-lat/0009040.

[56] F. Di Renzo and L. Scorzato, JHEP **0102** (2001) 020 [hep-lat/0012011].

[57] J. Heitger and R. Sommer [ALPHA Collaboration], Nucl. Phys. Proc. Suppl. **106** (2002) 358 [hep-lat/0110016]; R. Sommer, hep-lat/0209162.

[58] D. Cronin-Hennessy *et al.* [CLEO Collaboration], Phys. Rev. Lett. **87** (2001) 251808 [hep-ex/0108033].

[59] D. Bloch *et al.* [DELPHI Collaboration], DELPHI 2002-070-CONF 604;
M. Battaglia *et al.* [DELPHI Collaboration], DELPHI 2002-071-CONF-605;
M. Calvi, hep-ex/0210046.

[60] B. Aubert *et al.* [BaBar Collaboration], hep-ex/0207184.

[61] M. Gremm, A. Kapustin, Z. Ligeti and M.B. Wise, Phys. Rev. Lett. **77** (1996) 20 [hep-ph/9603314].

[62] M.B. Voloshin, Phys. Rev. D **51** (1995) 4934 [hep-ph/9411296].

[63] M. Gremm and A. Kapustin, Phys. Rev. D **55** (1997) 6924 [hep-ph/9603448].

[64] C.W. Bauer and M. Trott, Phys. Rev. D **67** (2003) 014021 [hep-ph/0205039].

[65] C.W. Bauer *et al.*, Phys. Rev. D **67** (2003) 054012 [hep-ph/0210027].

[66] N.G. Uraltsev, Nucl. Phys. B **491** (1997) 303.

[67] M. Jezabek and J.H. Kuhn, Nucl. Phys. B **320** (1989) 20;
A. Czarnecki, M. Jezabek and J.H. Kuhn, Acta Phys. Polon. B **20** (1989) 961;
A. Czarnecki and M. Jezabek, Nucl. Phys. B **427** (1994) 3 [hep-ph/9402326].

[68] M. Gremm and I. Stewart, Phys. Rev. D **55** (1997) 1226 [hep-ph/9609341].

[69] A.F. Falk, M.E. Luke and M.J. Savage, Phys. Rev. D **53** (1996) 2491 [hep-ph/9507284].

[70] A.F. Falk and M.E. Luke, Phys. Rev. D **57** (1998) 424 [hep-ph/9708327].

[71] M. Battaglia *et al.*, Phys. Lett. B **556** (2003) 41 [hep-ph/0210319].

[72] N.G. Uraltsev, Phys. Lett. B **545** (2002) 337 [hep-ph/0111166].

[73] A.S. Kronfeld and J.N. Simone, Phys. Lett. B **490** (2000) 228 [Erratum-ibid. B **495** (2000) 441] [hep-ph/0006345].

[74] S. Chen *et al.* [CLEO Collaboration], Phys. Rev. Lett. **87**, 251807 (2001).

[75] R. Briere *et al.* [CLEO Collaboration], CLEO-CONF-02-10, hep-ex/0209024.

[76] A.H. Hoang, Nucl. Phys. B, Proc. Suppl. **86** (2000) 512 [hep-ph/9909356]; A.H. Hoang and A.V. Manohar, Phys. Lett. B **483** (2000) 94 [hep-ph/9911461]; hep-ph/0008102; hep-ph/0102292.

[77] A.H. Mahmood *et al.* [CLEO Collaboration], CLNS 02/1810, CLEO 02-16, hep-ex/0212051.

[78] B. Aubert *et al.* [BaBar Collaboration], hep-ex/0207084.

[79] E.C. Poggio, H.R. Quinn and S. Weinberg, Phys. Rev. D **13** (1976) 1958.

[80] M. Greco, G. Penso and Y. Srivastava, Phys. Rev. D **21** (1980) 2520.

[81] M.A. Shifman, "Quark-hadron duality," in B. Ioffe Festschrift 'At the Frontier of Particle Physics / Handbook of QCD', ed. M. Shifman (World Scientific, Singapore, 2001), [hep-ph/0009131].

[82] I.I. Bigi and N.G. Uraltsev, Int. J. Mod. Phys. A **16** (2001) 5201 [hep-ph/0106346].

[83] C.G. Boyd, B. Grinstein and A.V. Manohar, Phys. Rev. D **54** (1996) 2081 [hep-ph/9511233].

[84] R.F. Lebed, N.G. Uraltsev, Phys. Rev. D **62** (2000) 094011 [hep-ph/0006346], and refs. therein.

[85] J. Chay, H. Georgi, B. Grinstein, Phys. Lett. B **247** (1990) 339.

[86] N. Isgur, Phys. Lett. B **448** (1999) 111 [hep-ph/9811377].

[87] A. Le Yaouanc, *et al.*, Phys. Lett. B **480** (2000) 119 [hep-ph/0003087].

[88] A. Le Yaouanc *et al.*, Phys. Rev. D **62** (2000) 074007 [hep-ph/0004246].

[89] A. Le Yaouanc *et al.*, Phys. Lett. B **517** (2001) 135 [hep-ph/010333].

[90] A. Le Yaouanc *et al.*, Phys. Lett. B **488** (2000) 153 [hep-ph/0005039].

[91] M. Luke, M.J. Savage and M.B. Wise, Phys. Lett. B **345** (1995) 301.

[92] Y. Nir, Phys. Lett. B **221** (1989) 184.

[93] N. Cabibbo and L. Maiani, Phys. Lett. B **79** (1978) 109; the original QED calculation is published in R.E. Behrends *et al.*, Phys. Rev. **101** (1956) 866.

[94] A. Czarnecki and K. Melnikov, Phys. Rev. D **59** (1998) 014036.

[95] N.G. Uraltsev, Int. J. Mod. Phys. A **11** (1996) 513.

[96] M. Voloshin and M. Shifman, Sov. J. Nucl. Phys. **41** (1985) 120;
J. Chay, H. Georgi and B. Grinstein, Phys. Lett. B **247** (1990) 399.

[97] D. Benson, I.I. Bigi, Th. Mannel, and N.G. Uraltsev, hep-ph/0302262.

[98] N.G. Uraltsev, Mod. Phys. Lett. A **17** (2002) 2317 [hep-ph/0210413].

[99] D.E. Groom *et al.*, Eur. Phys. J. C **15** (2000) 1.

[100] J. Bartelt *et al.* [CLEO Collaboration], CLEO CONF 98-21.

[101] Thorsten Brandt computed the average of b-hadron semileptonic partial width inclusive measurements available for the Workshop.

[102] The LEP Electroweak Working Group, *http://lepewwg.web.cern.ch/LEPEWWG/*,
CERN-EP-2001-098 and hep-ex/0112021.

[103] B. Aubert *et al.* [BaBar Collaboration], hep-ex/0208018.

[104] K. Abe *et al.* [BELLE Collaboration], hep-ex/0208033.

[105] The LEP Vcb Working group, see *http://lepvcb.web.cern.ch/LEPVCB/*.

[106] K. Hagiwara *et al.*, Phys. Rev. D **66** (2002) 010001.

[107] M. Artuso and E. Barberio, hep-ph/0205163 (a shorter version has been included in [106] as a minireview on $|V_{cb}|$).

[108] T. van Ritbergen, Phys. Lett. B **454** (1999) 353 [hep-ph/9903226].

[109] N.G. Uraltsev, Int. J. Mod. Phys. A **14** (1999) 4641 [hep-ph/9905520].

[110] R. Fulton *et al.* [CLEO Collaboration], Phys. Rev. Lett. **64** (1990) 16;
J. Bartelt *et al.* [CLEO Collaboration], Phys. Rev. Lett. **71** (1993) 411;
H. Albrecht *et al.* [ARGUS Collaboration], Phys. Lett. B **255** (1991) 297.

[111] V.D. Barger, C.S. Kim and R.J. Phillips, Phys. Lett. B **251** (1990) 629;
A.F. Falk, Z. Ligeti and M.B. Wise, Phys. Lett. B **406** (1997) 225;
R.D. Dikeman and N.G. Uraltsev, Nucl. Phys. B **509** (1998) 378;
I.I. Bigi, R.D. Dikeman and N.G. Uraltsev, Eur. Phys. J. C **4** (1998) 453.

[112] C.W. Bauer, Z. Ligeti and M.E. Luke, Phys. Lett. B **479** (2000) 395 [hep-ph/0002161].

[113] G. Altarelli, *et al.*, Nucl. Phys. B **208** (1982) 365;
M. Wirbel, B. Stech, M. Bauer, Zeit. Phys. C **29** (1985) 637.

[114] N. Isgur *et al.*, Phys. Rev. D **39** (1989) 799.

[115] M. Neubert, Phys. Rev. D **49** (1994) 3392;
T. Mannel and M. Neubert, Phys. Rev. D **50** (1994) 2037.

[116] I.I. Bigi, M.A. Shifman, N.G. Uraltsev and A.I. Vainshtein, Int. J. Mod. Phys. A **9** (1994) 2467 [hep-ph/9312359].

[117] M. Neubert, Phys. Rev. D **49** (1994) 4623; A.L. Kagan and M. Neubert, Eur. Phys. J. C **7** (1999) 5 [hep-ph/9805303].

[118] I.I. Bigi and N.G. Uraltsev, Int. J. Mod. Phys. A **17** (2002) 4709 [hep-ph/0202175].

[119] U. Aglietti, Phys. Lett. B **515** (2001) 308 [hep-ph/0103002] and Nucl. Phys. B **610** (2001) 293 [hep-ph/0104020].

[120] A.K. Leibovich, I. Low and I.Z. Rothstein, Phys. Rev. D **61** (2000) 053006 [hep-ph/9909404].

[121] C.W. Bauer, M.E. Luke and T. Mannel, hep-ph/0102089 and Phys. Lett. B **543** (2002) 261 [hep-ph/0205150].

[122] I.I. Bigi and N.G. Uraltsev, Nucl. Phys. B **423** (1994) 33 [hep-ph/9310285];
M.B. Voloshin, Phys. Lett. B **515** (2001) 74 [hep-ph/0106040].

[123] A.K. Leibovich, Z. Ligeti and M.B. Wise, Phys. Lett. B **539** (2002) 242 [hep-ph/0205148].

[124] M. Neubert, Phys. Lett. B **543** (2002) 269 [hep-ph/0207002].

[125] A. Bornheim *et al.* [CLEO Collaboration], Phys. Rev. Lett. **88** (2002) 231803 [hep-ex/0202019].

[126] P. Abreu *et al.* [DELPHI Collaboration], Phys. Lett. B **478** (2000) 14.

[127] M. Neubert, JHEP **0007** (2000) 022 [hep-ph/0006068].

[128] C.W. Bauer, Z. Ligeti and M.E. Luke, Phys. Rev. D **64** (2001) 113004 [hep-ph/0107074].

[129] A. Bornheim *et al.* [CLEO Collaboration], hep-ex/0207064.

[130] R. Barate *et al.* [ALEPH Collaboration], Eur. Phys. J. C **6** (1999) 555;
G. Abbiendi *et al.* [OPAL Collaboration], Eur. Phys. J. C **21** (2001) 399.

[131] M. Acciarri *et al.* [L3 Collaboration], Phys. Lett. B436, 174 (1998).

[132] U. Aglietti, M. Ciuchini and P. Gambino, Nucl. Phys. B **637** (2002) 427 [hep-ph/0204140].

[133] R.V. Kowalewski and S. Menke, Phys. Lett. B **541** (2002) 29 [hep-ex/0205038].

[134] M. Neubert, Phys. Lett. B **264** (1991) 455.

[135] M. Neubert, Phys. Lett. B **338** (1994) 84 [hep-ph/9408290].

[136] C.G. Boyd, B. Grinstein and R.F. Lebed, Nucl. Phys. B **461** (1996) 493 [hep-ph/9508211].

[137] C.G. Boyd and R.F. Lebed, Nucl. Phys. B **485** (1997) 275 [hep-ph/9512363].

[138] C.G. Boyd, B. Grinstein and R.F. Lebed, Phys. Rev. D **56** (1997) 6895 [hep-ph/9705252].

[139] I. Caprini, L. Lellouch and M. Neubert, factors," Nucl. Phys. B **530** (1998) 153 [hep-ph/9712417].

[140] M. Neubert, Z. Ligeti and Y. Nir, Phys. Lett. B **301** (1993) 101 [hep-ph/9209271].

[141] M. Neubert, Z. Ligeti and Y. Nir, Phys. Rev. D **47** (1993) 5060 [hep-ph/9212266].

[142] Z. Ligeti, Y. Nir and M. Neubert, Phys. Rev. D **49** (1994) 1302 [hep-ph/9305304].

[143] J. D. Bjorken, *in* Proceedings of the 4th Recontres de Physique de la Vallèe d'Aoste, La Thuille, Italy, 1990, ed. M. Greco (Editions Frontières, Gif-Sur-Yvette, 1990);
N. Isgur and M. B. Wise, Phys. Rev. D **43** (1991) 819.

[144] M.B. Voloshin, Phys. Rev. D **46** (1992) 3062.

[145] A.G. Grozin and G.P. Korchemsky, Phys. Rev. D **53** (1996) 1378;
C.G. Boyd, B. Grinstein, and A.V. Manohar, Phys. Rev. D **54** (1996) 2081;
C.G. Boyd, Z. Ligeti, I.Z. Rothstein, and M.B. Wise, Phys. Rev. D **55** (1997) 3027.

[146] N.G. Uraltsev, Phys. Lett. B **501** (2001) 86 [hep-ph/0011124].

[147] M.E. Luke, Phys. Lett. B **252** (1990) 447.

[148] M.A. Shifman, N.G. Uraltsev, and A.I. Vainshtein, Phys. Rev. D **51** (1995) 2217 [hep-ph/9405207]; [Erratum-ibid. **52** (1995) 3149].

[149] A.F. Falk and M. Neubert, Phys. Rev. D **47** (1993) 2965 [hep-ph/9209268].

[150] A.S. Kronfeld, Phys. Rev. D **62**, 014505 (2000) [hep-lat/0002008].

[151] J. Harada, *et al.*, Phys. Rev. D **65**, 094514 (2002) [hep-lat/0112045].

[152] S. Hashimoto, *et al.*, Phys. Rev. D **66** (2002) 014503 [hep-ph/0110253].

[153] I.I. Bigi, M.A. Shifman and N.G. Uraltsev, Annu. Rev. Nucl. Part. Sci. **47** (1997) 591 [hep-ph/9703290].

[154] A. Czarnecki, K. Melnikov and N.G. Uraltsev, Phys. Rev. D **57** (1998) 1769 [hep-ph/9706311].

[155] A. Czarnecki, Phys. Rev. Lett. **76** (1996) 4124 [hep-ph/9603261].

[156] A. Czarnecki and K. Melnikov, Nucl. Phys. B **505** (1997) 65 [hep-ph/9703277].

[157] N.G. Uraltsev, hep-ph/9804275.

[158] T. Mannel, Phys. Rev. D **50** (1994) 428 [hep-ph/9403249].

[159] S. Ryan, Nucl. Phys. B Proc. Suppl. **106** (2002) 86 [hep-lat/0111010].

[160] A.X. El-Khadra, A.S. Kronfeld, and P.B. Mackenzie, Phys. Rev. D **55** (1997) 3933 [hep-lat/9604004].

[161] J. Harada, *et al.*, Phys. Rev. D **65** (2002) 094513 [hep-lat/0112044].

[162] S. Hashimoto *et al.,* Phys. Rev. D **61** (2000) 014502 [hep-ph/9906376].

[163] A.S. Kronfeld, P.B. Mackenzie, J.N. Simone, S. Hashimoto and S.M. Ryan, in *Flavor Physics and CP Violation,* edited by R.G.C. Oldemann, hep-ph/0207122.

[164] L. Randall and M.B. Wise, Phys. Lett. B **303** (1993) 135;
M.J. Savage, Phys. Rev. D **65** (2002) 034014 [hep-ph/0109190].

[165] D. Arndt, hep-lat/0210019.

[166] D. Scora and N. Isgur, Phys. Rev. D **52** (1995) 2783.

[167] Z. Ligeti, hep-ph/9908432.

[168] G.P. Lepage, *et al.*, Nucl. Phys. B Proc. Suppl. **106** (2002) 12 [hep-lat/0110175];
C. Morningstar, *ibid.* **109** (2002) 185 [hep-lat/0112023].

[169] D. Atwood and W.J. Marciano, Phys. Rev. D **41** (1990) 1736.

[170] E.S. Ginsberg, Phys. Rev. **171** (1968) 1675; **174** (1968) 2169(E); **187** (1969) 2280(E).

[171] A. Sirlin, Nucl. Phys. B **196** (1982) 83.

[172] R.A. Briere *et al.* [CLEO Collaboration], Phys. Rev. Lett. **89** (2002) 81803; [hep-ex/0203032].

[173] K. Abe *et al.* [BELLE Collaboration], Phys. Lett. B **526** (2002) 247; [hep-ex/0111060].

[174] P. Abreu *et al.* [DELPHI Collaboration], Phys. Lett. B **510** (2001) 55 [hep-ex/0104026].

[175] D. Buskulic *et al.* [ALEPH Collaboration], Phys. Lett. B **935** (1997) 373.

[176] G. Abbiendi *et al.* [OPAL Collaboration], Phys. Lett. B **482** (2000) 15.

[177] S. Anderson *et al.* [CLEO Collaboration], Nucl.Phys. A **663** (2000) [hep-ex/9908009].

[178] D. Buskulic *et al.* [ALEPH Collaboration], Z. Phys. C **73** (1997) 601.

[179] A. Anastassov *et al.* [CLEO Collaboration], Phys. Rev. Lett. **80** (1998) 4127.

[180] LEP/SLD Electroweak Heavy Flavor Group, results presented at the Winter 2001 Conferences, see *http://lepewwg.web.cern.ch/LEPEWWG/heavy/*

[181] D. Block *et al.* [DELPHI Collaboration], contributed paper to ICHEP 2000, DELPHI 2000-106 Conf. 45.

[182] ALEPH, CDF, DELPHI, L3, OPAL, SLD, CERN-EP/2001-050.

[183] V. Morenas *et al.,* Phys. Rev. D **59** (1997) 5668 [hep-ph/9706265];
M.Q. Huang, C. Li and Y.B. Dai, Phys. Rev. D **61** (2000) 54010 [hep-ph/9909307].

[184] A.K. Leibovich, Z. Ligeti, I.W. Stewart, M.B. Wise Phys. Rev. D **57** (1998) 308 [hep-ph/9705467] and Phys. Rev. Lett. **78** (1997) 3995 [hep-ph/9703213].

[185] LEP V_{cb} Working Group, Internal Note, see *http://lepvcb.web.cern.ch/LEPVCB/*

[186] CDF, LEP, SLD B Oscillations Working Group, Internal Note, see *http://lepbosc.web.cern.ch/LEPBOSC/.*

[187] CDF, LEP, SLD B-hadron Lifetime Working Group, Internal Note, see *http://claires.home.cern.ch/claires/lepblife.html.*

[188] J.E. Duboscq *et al.* [CLEO Collaboration], Phys. Rev. Lett. **76** (1996) 3898.

[189] B. Grinstein and Z. Ligeti, Phys. Lett. B **526** (2002) 345 [hep-ph/0111392].

[190] K. Abe *et al.* [BELLE Collaboration], Phys. Lett. B **526** (2002) 258 [hep-ex/0111082].

[191] J. Bartelt *et al.* [CLEO Collaboration], Phys. Rev. Lett. **82** (1999) 3746.

[192] L. Lellouch, hep-ph/9912353.

[193] K.'C. Bowler *et al.* [UKQCD Collaboration], Phys. Lett. B **486** (2000) 111 [hep-lat/9911011].

[194] A. Abada *et al.*, V. Lubicz and F. Mescia, Nucl. Phys. B **619** (2001) 565 [hep-lat/0011065].

[195] A.X. El-Khadra *et al.*, Phys. Rev. D **64** (2001) 014502 [hep-ph/0101023].

[196] S. Aoki *et al.* [JLQCD Collaboration], Phys. Rev. D **64** (2001) 114505 [hep-lat/0106024].

[197] B. Sheikholeslami and R. Wohlert, Nucl. Phys. B **259** (1985) 572.

[198] M. Luscher, S. Sint, R. Sommer and P. Weisz, Nucl. Phys. B **478** (1996) 365 [hep-lat/9605038].

[199] M. Luscher, S. Sint, R. Sommer and H. Wittig, Nucl. Phys. B **491** (1997) 344 [hep-lat/9611015].

[200] B.A. Thacker and G.P. Lepage, Phys. Rev. D **43** (1991) 196.

[201] G.P. Lepage, *et al.*, Phys. Rev. D **46** (1992) 4052 [hep-lat/9205007].

[202] G. Burdman, Z. Ligeti, M. Neubert and Y. Nir, Phys. Rev. D **49** (1994) 2331 [hep-ph/9309272].

[203] G. Burdman and J.F. Donoghue, Phys. Lett. B **280** (1992) 287.

[204] M.B. Wise, Phys. Rev. D **45** (1992) 2188.

[205] T.M. Yan, *et al.*, Phys. Rev. D **46** (1992) 1148 [Erratum-ibid. D **55** (1997) 5851].

[206] D. Becirevic, S. Prelovsek and J. Zupan, Phys. Rev. D **67** (2003) 054010 [hep-lat/0210048].

[207] R. Fleischer, Phys. Lett. B **303** (1993) 147.

[208] C.G. Boyd, B. Grinstein and R.F. Lebed, Phys. Rev. Lett. **74** (1995) 4603 [hep-ph/9412324].

[209] L. Lellouch, Nucl. Phys. B **479** (1996) 353 [hep-ph/9509358].

[210] D.R. Burford, *et al.* [UKQCD Collaboration], Nucl. Phys. B **447** (1995) 425 [hep-lat/9503002].

[211] L. Del Debbio, *et al.* [UKQCD Collaboration], Phys. Lett. B **416** (1998) 392 [hep-lat/9708008].

[212] J. Charles, *et al.*, Phys. Rev. D **60** (1999) 014001 [hep-ph/9812358].

[213] A. Khodjamirian, *et al.*, Phys. Rev. D **62** (2000) 114002 [hep-ph/0001297].

[214] S. Dürr, DESY-02-121, hep-lat/0208051.

[215] C. Bernard, *et al.*, hep-lat/0209086.

[216] S. Hashimoto *et al.* [JLQCD Collaboration], hep-lat/0209091.

[217] L. Lellouch, plenary talk presented at ICHEP-2002, Amsterdam, July 2002, hep-ph/0211359.

[218] J. M. Flynn *et al.* [UKQCD Collaboration], Nucl. Phys. B **461** (1996) 327 [hep-ph/9506398].

[219] B.H. Behrens *et al.* [CLEO Collaboration], Phys. Rev. D **61** (2000) 052001 [hep-ex/9905056].

[220] A. Abada *et al.*, Nucl. Phys. B **416** (1994) 675 [hep-lat/9308007].

[221] C.R. Allton *et al.* [APE Collaboration], Phys. Lett. B **345** (1995) 513 [hep-lat/9411011].

[222] J. Gill [UKQCD Collaboration], Nucl. Phys. Proc. Suppl. **106** (2002) 391 [hep-lat/0109035].

[223] A. Abada, *et al.* [SPQcdR Collaboration], hep-lat/0209116.

[224] M. Beneke and T. Feldmann, Nucl. Phys. B **592** (2001) 3 [hep-ph/0008255].

[225] J. Chay and C. Kim, Phys. Rev. D **65** (2002) 114016 [hep-ph/0201197].

[226] C.W. Bauer, D. Pirjol and I.W. Stewart, Phys. Rev. D **66** (2002) 054005 [hep-ph/0205289].

[227] M. Beneke, *et al.*, Nucl. Phys. B **643** (2002) 431 [hep-ph/0206152].

[228] P. Ball and V.M. Braun, Phys. Rev. D **58** (1998) 094016 [hep-ph/9805422].

[229] N. Yamada *et al.* [JLQCD Collaboration], Nucl. Phys. Proc. Suppl. **106** (2002) 397 [hep-lat/0110087].

[230] I.I. Balitsky, V.M. Braun and A.V. Kolesnichenko, Nucl. Phys. B **312** (1989) 509;
V.M. Braun and I.E. Filyanov, Z. Phys. C **44** (1989) 157.

[231] V.L. Chernyak and I.R. Zhitnitsky, Nucl. Phys. B **345** (1990) 137.

[232] V.M. Belyaev, A. Khodjamirian and R. Rückl, Z. Phys. C **60** (1993) 349.

[233] A. Khodjamirian, R. Rückl, S. Weinzierl and O. Yakovlev, Phys. Lett. B **410** (1997) 275;
E. Bagan, P. Ball and V.M. Braun, Phys. Lett. B **417** (1998) 154.

[234] P. Ball, JHEP **9809** (1998) 005.

[235] P. Ball and R. Zwicky, JHEP **0110** (2001) 019 [hep-ph/0110115].

[236] A. Ali, P. Ball, L.T. Handoko and G. Hiller, Phys. Rev. D **61** (2000) 074024.

[237] A. Khodjamirian and R. Ruckl, in *Heavy Flavors*, 2nd edition, eds., A.J. Buras and M. Lindner, World Scientific (1998), p. 345, hep-ph/9801443.

[238] V.M. Braun, hep-ph/9911206.

[239] P. Colangelo and A. Khodjamirian, *Boris Ioffe Festschrift 'At the Frontier of Particle Physics; Handbook of QCD'*, ed. M. Shifman (World Scientific, Singapore, 2001), p.1495 [hep-ph/0010175].

[240] M. Jamin and B.O. Lange, Phys. Rev. D **65** (2002) 056005.

[241] D. Becirevic and A.B. Kaidalov, Phys. Lett. B **478** (2000) 417 [hep-ph/9904490].

[242] V.M. Belyaev, V.M. Braun, A. Khodjamirian and R. Ruckl, Phys. Rev. D **51** (1995) 6177 [hep-ph/9410280]; A. Khodjamirian, R. Ruckl, S. Weinzierl and O. Yakovlev, Phys. Lett. B **457** (1999) 245 [hep-ph/9903421].

[243] K.C. Bowler *et al.* [UKQCD Collaboration], Phys. Lett. B **486** (2000) 111.

[244] H. Ishino [Belle Collaboration], talk at XXXVII Rencontres de Moriond, March 2002.

[245] J.P. Alexander *et al.* [CLEO Collaboration], Phys. Rev. Lett. **77** (1996) 5000.

[246] D. Scora and N. Isgur, Phys. Rev. D **52** (1995) 2783.

[247] D. Melikhov, Phys. Rev. D **53** (1996) 2160.

[248] M. Wirbel, B. Stech and M. Bauer, Z. Phys. C **29** (1985) 637.

[249] G. Burdman and J. Kambor, Phys. Rev. D **55** (1997) 2817 [hep-ph/9602353].

[250] J.M. Flynn *et al.*, Nucl. Phys. B **461** (1996) 327.

[251] B. Stech, Phys. Lett. B **354** (1995) 447.

[252] BELLE Collaboration, BELLE-CONF 0124 (2001).

[253] BELLE Collaboration, see *http://www.ichep02.nl/Transparencies/CP/CP-1/CP-1-4.kwon.pdf*, ICHEP (2002).

[254] BaBar Collaboration, hep-ex/0207080.

[255] Y. Kwon [BELLE Collaboration], ICHEP CP-1-4 (2002).

[256] M. Beyer and D. Melikhov, Phys. Lett. B **436** (1998) 344.

[257] N. Adam *et al.* [CLEO Collaboration], CLEO-CONF/02-09, ICHEP02-ABS931.

[258] F. De Fazio and M. Neubert, JHEP **9906** (1999) 017.

[259] Z. Ligeti and M.B. Wise, Phys. Rev. D **53** (1996) 4937. .

[260] BELLE Collaboration, BELLE-CONF 02/42, ICHEP ABS 732.

[261] CLEO Collaboration, talk at DPF-2002, see *http://dpf2002.velopers.net/talks pdf/452talk.pdf.*

[262] LEP B Lifetime Working Group, see *http://lepbosc.web.cern.ch/LEPBOSC/lifetimes/ lepblife.html*

[263] B. Aubert *et al.* [BaBar Collaboration], Phys. Rev. Lett. **87** (2001) 201803;
K. Abe *et al.* [BELLE Collaboration], Phys. Rev. Lett. **88** (2002) 171801.

[264] M. Beneke *et al.*, Phys. Lett. B **459** (1999) 631 [hep-ph/9808385].

[265] M. Beneke and A. Lenz, J. Phys. G **G27** (2001) 1219 [hep-ph/0012222];
D. Becirevic, hep-ph/0110124 and refs. therein.

[266] A.J. Buras, M. Jamin, M.E. Lautenbacher and P.H. Weisz, Nucl. Phys. B **400** (1993) 37 [hep-ph/9211304]; A.J. Buras, M. Jamin and M.E. Lautenbacher, Nucl. Phys. B **400** (1993) 75 [hep-ph/9211321]; M. Ciuchini, E. Franco, G. Martinelli and L. Reina, Nucl. Phys. B **415** (1994) 403 [hep-ph/9304257].

[267] M. Beneke, G. Buchalla and I. Dunietz, Phys. Rev. D **54** (1996) 4419 [hep-ph/9605259].

[268] V. Gimenez and J. Reyes, Nucl. Phys. Proc. Suppl. **93** (2001) 95 [hep-lat/0009007].

[269] S. Hashimoto *et al.*, Phys. Rev. D **62** (2000) 114502 [hep-lat/0004022].

[270] S. Aoki *et al.* [JLQCD Collaboration], hep-lat/0208038.

[271] D. Becirevic *et al.*, Eur. Phys. J. C **18** (2000) 157 [hep-ph/0006135].

[272] L. Lellouch and C.J. Lin [UKQCD Collaboration], Phys. Rev. D **64** (2001) 094501 [hep-ph/0011086].

[273] D. Becirevic *et al.*, JHEP **0204** (2002) 025 [hep-lat/0110091].

[274] S. Hashimoto and N. Yamada [JLQCD Collaboration], hep-ph/0104080.

[275] S. Aoki *et al.* [JLQCD Collaboration], hep-lat/0208038.

[276] A.S. Dighe, *et al.*, Nucl. Phys. B **624** (2002) 377 [hep-ph/0109088] and hep-ph/0202070;
see also T. Hurth *et al.*, J. Phys. G **27** (2001) 1277 [hep-ph/0102159].

[277] K. Anikeev *et al.*, hep-ph/0201071.

[278] S. Hashimoto and N. Yamada [JLQCD Collaboration], hep-ph/0104080.

[279] P. Ball *et al.*, CERN-TH-2000-101, hep-ph/0003238.

[280] B. Aubert *et al.* [BaBar Collaboration], Phys. Rev. Lett. **87** (2001) 091801 [hep-ex/0107013].

[281] Y. Grossman, Phys. Lett. B **380** (1996) 99 [hep-ph/9603244].

[282] I.I. Bigi, N.G. Uraltsev and A.I. Vainshtein, Phys. Lett. B **293** (1992) 430; Erratum **297** (1993) 477 [hep-ph/9207214].

[283] Q. Ho-kim and X.-y. Pham, Phys. Lett. B **122** (1983) 297.

[284] E. Bagan, P. Ball, V.M. Braun and P. Gosdzinsky, Nucl. Phys. B **432** (1994) 3 [hep-ph/9408306].

[285] E. Bagan et al., Phys. Lett. B **342** (1995) 362; Erratum **374** (1996) 363 [hep-ph/9409440];
E. Bagan et al., Phys. Lett. B **351** (1995) 546 [hep-ph/9502338];
A.F. Falk et al., Phys. Lett. B **326** (1994) 145 [hep-ph/9401226].

[286] M. Neubert and C.T. Sachrajda, Nucl. Phys. B **483**, 339 (1997) [hep-ph/9603202].

[287] N.G. Uraltsev, Phys. Lett. B **376** (1996) 303 [hep-ph/9602324].

[288] M. Beneke and G. Buchalla, Phys. Rev. D **53** (1996) 4991 [hep-ph/9601249].

[289] E. Franco *et al.*, Nucl. Phys. B **633** (2002) 212 [hep-ph/0203089].

[290] M. Beneke *et al.*, hep-ph/0202106.

[291] V. Gimenez and J. Reyes, Nucl. Phys. B **545** (1999) 576 [hep-lat/9806023].

[292] M. Ciuchini, *et al.*, Nucl. Phys. B **625** (2002) 211 [hep-ph/0110375].

[293] V. Chernyak, Nucl. Phys. B **457** (1995) 96 [hep-ph/9503208].

[294] D. Pirjol and N.G. Uraltsev, Phys. Rev. D **59** (1999) 034012 [hep-ph/9805488].

[295] M. Di Pierro and C.T. Sachrajda [UKQCD Collaboration], Nucl. Phys. B **534** (1998) 373 [hep-lat/9805028].

[296] M. Di Pierro, C.T. Sachrajda and C. Michael [UKQCD Collaboration], Phys. Lett. B **468** (1999) 143 [hep-lat/9906031]; M. Di Pierro and C.T. Sachrajda [UKQCD Collaboration], Nucl. Phys. Proc. Suppl. **73** (1999) 384 [hep-lat/9809083].

[297] D. Becirevic, update of hep-ph/0110124 for the present work.

[298] P. Colangelo and F. De Fazio, Phys. Lett. B **387** (1996) 371 [hep-ph/9604425];
M.S. Baek, J. Lee, C. Liu and H.S. Song, Phys. Rev. D **57** (1998) 4091 [hep-ph/9709386];
H.Y. Cheng and K.C. Yang, Phys. Rev. D **59** (1999) 014011 [hep-ph/9805222];
C.S. Huang, C. Liu and S.L. Zhu, Phys. Rev. D **61** (2000) 054004 [hep-ph/9906300].

[299] ALEPH Collaboration, Phys. Lett. B **486** (2000) 286.

[300] L3 Collaboration, Phys. Lett. B **438** (1998) 417.

[301] DELPHI Collaboration, Eur. Phys. J. C **18** (2000) 229.

[302] ALEPH Collaboration, Phys. Lett. B **377** (1996) 205;
CDF Collaboration, Phys. Rev. D **59** (1999) 032004;
OPAL Collaboration, Phys. Lett. B **426** (1998) 161.

[303] R. Aleksan *et al.*, Phys. Lett. B **316** (1993) 567.

[304] DELPHI Collaboration, Eur. Phys. J. C **16** (2000) 555.

[305] CDF Collaboration, Phys. Rev. D **57** (1998) 5382.

[306] CLEO Collaboration, Phys. Rev. Lett. **79** (1997) 4533.

[307] ALEPH, CDF, DELPHI, L3, OPAL and SLD Collaborations, CERN-EP/2001-050.
See also *http://www.cern.ch/LEPBOSC.*

[308] CDF Collaboration, Phys. Rev. Lett. **77** (1996) 1945.

[309] CDF Collaboration, Phys. Rev. Lett. **75** (1995) 3068 and Phys. Rev. Lett. **85** (2000) 4668.

[310] W. Ashmanskas *et al.*, *Performance of the CDF Online Silicon Vertex Tracker* published in Proceedings of the 2001 IEEE Nuclear Science Symposium (NSS) and Medical Imaging Conference (MIC), San Diego, CA, November 2001.

[311] T. Allmendinger *et al.* [DELPHI Collaboration] DELPHI 2001-054 CONF 482.

[312] A. Dighe, I. Dunietz, H. Lipkin, J.L. Rosner, Phys. Lett. B **369** (1996) 144.

[313] M. Sevelda, PhD Thesis, Charles University of Prague, 1999.

[314] ATLAS TDR, CERN-LHCC-99-015.